The contribution of psychophysical spatial frequency channels to the discrimination of broadband contrast

Bruno Richard

A Thesis
In the Department
of
Psychology

Presented in Partial Fulfillment of the Requirements
For the Degree of
Doctor of Philosophy (Psychology) at
Concordia University
Montréal, Québec, Canada

October 2015

CONCORDIA UNIVERSITY
SCHOOL OF GRADUATE STUDIES

This is to certify that the thesis prepared

By: Bruno Richard

Entitled: The contribution of spatial frequency channels to the discrimination of broadband contrast

and submitted in partial fulfillment of the requirements for the degree of

Doctor of Philosophy (Psychology)

complies with the regulations of the University and meets the accepted standards with respect to originality and quality.

Signed by the final examining committee:

_____ Chair
Dr. B. Grohmann

_____ External Examiner
Dr. M.A. Webster

_____ External to Program
Dr. D. Howes

_____ Examiner
Dr. R. Gurnsey

_____ Thesis Co-Supervisor
Dr. A. Johnson

_____ Thesis Co-Supervisor
Dr. B. Hansen

Approved by: _____
Dr. K. Li, Graduate Program Director

October 22, 2015 _____
Dr. A. Roy, Dean, Faculty of Arts & Science

ABSTRACT

The contribution of psychophysical spatial frequency channels to the discrimination of broadband contrast

Bruno Richard, PhD
Concordia University, 2015

The design and function of the human visual system is thought to have been shaped by the environment and tasks humans have performed throughout evolution and experience. Thus, it is important to establish the association between the properties of natural scenes and the responses of the visual system to these features at a behaviourally relevant level (e.g., psychophysically). A relevant property of natural scenes - which human observers are sensitive to - is the slope of the orientation averaged Fourier amplitude spectrum (α). It characterizes the decrease in amplitude as a function of spatial frequency ($1/f^{\alpha}$), and has an average value of 1.0 (on logarithmic axes) in natural scenes. The process of detecting a change in α is thought to stem from the activity of one or more spatial frequency channels, but their exact contribution remains to be defined. The overarching goal of this dissertation was to assess the contribution of spatial frequency channels to the detection, and discrimination, of a change in α. We first set out to obtain psychophysical evidence that α discrimination thresholds were dependent on the spatial frequency content of noise stimuli with $1/f$ amplitude spectra. Our results showed that while all spatial frequency channels contribute to α discrimination, the channel(s) of most influence seem to correlate in peak spatial frequency to the dominant perceptual scale of the noise image. While the contribution of low spatial frequency channels discrimination of steep αs was evident from our data, the influence of higher spatial frequency channels to the discrimination of shallower αs was not. In an attempt to better isolate the role of high spatial frequency channels, we attempted to modulate their activity with trans-cranial Direct Current Stimulation (tDCS) and change α discrimination thresholds. However, while this technique is capable of modulating channels to alter contrast detection, we found tDCS to be an ill-suited technique to alter the response characteristics of channels under suprathreshold conditions (i.e., broadband noise discrimination). As a final effort to isolate the contribution of spatial frequency channels to the discrimination of broadband

contrast, we used a classification image paradigm to understand how different spatial frequencies contribute to the identification of a change in α. Interestingly, this method revealed task dependent contributions of spatial frequency channels to the discrimination of α. The identification of α is specific to α, in that increments and decrements in contrast in specific spatial frequency bands signal for particular αs, while the identification of a change in α (i.e., discrimination) was not specific to α. Regardless of the reference α, observers used an increment in contrast in low spatial frequency bands and decrement of contrast in higher spatial frequency bands to identify the odd stimulus. Taken together, these findings demonstrate that the discrimination of α is unspecific to α. Observers to rely on differences in contrast between low and high spatial frequency bands to detect a change in α, but may not be particularly tuned to certain α values as has previously been argued.

ACKNOWLEDGMENTS

A dissertation is a single authored work, but its completion would be impossible without the devotion and assistance of supervisors, advisors, family and friends. The following aims to acknowledge the most influential individuals that have contributed to this research project.

First and foremost, I cannot be grateful enough to my supervisor Dr. Aaron Johnson for the opportunity he awarded me to begin my graduate studies, and for his persistent assistance (in various forms) throughout the last nine years academic education (we almost made it to 10). I cannot thank him enough for the support, expertise, and of the utmost importance, his patience (as I have tried it multiple times). Dr. Aaron Johnson has been an excellent supervisor, a thoughtful advisor, and a wonderful friend.

Second, I must thank my co-supervisor, Dr. Bruce Hansen, who has truly been an inspirational presence throughout my academic education. The first of two theses I wrote during my undergraduate degree Concordia (the Johnson et al. 2011 study) was inspired by the work of Dr. Bruce Hansen. This thesis project ignited my interest in the study of the human visual system. I cannot thank you enough for the guidance and attention you have paid to my work, and for the valuable opportunities you have awarded me throughout the past few years.

I must also acknowledge the continued willingness to help of Dr. Rick Gurnsey. His role as an educator, and his attention to detail has played a fundamental part in my academic education. I am grateful he has agreed to be part of my dissertation committee. None of the experiments presented here would have been possible without the undergraduate students that have graciously volunteered their time. It takes a very special kind of person to discriminate noise patches, over and over again, for months. This is particularly true of Rebecca Birkett, who has been a valuable observer and outstanding research assistant.

The completion of my dissertation would have been impossible without the unconditional support of my parents. I cannot show sufficient gratitude to my mother, Carole Lesage, and my father, Christian Richard for emotional, financial, and gastronomic assistance they have awarded me for too long. I am also grateful to my

writing club colleagues, Gabrielle Roddy, Marie-Pierre Cossette, and Anne Almey, without whom I may have never met my deadline.

I must also acknowledge the financial assistance from the NSERC grant held by Dr. Aaron Johnson, and the graduate fellowship offered to me for this dissertation by FQRNT.

Last, but not certainly not least, I wish to dedicate this dissertation to my dog, Blitz, who has been a dear companion for the past fifteen and a half years of my life, and sadly, passed away a week prior to the submission of this work. You are dearly missed.

CONTRIBUTION OF AUTHORS

This dissertation consists of a general introduction, three experimental chapters (for a total of 7 experiments), and a general discussion. I wrote the general introduction and general discussion with feedback from my supervisor, Dr. Aaron Johnson, and co-supervisor Dr. Bruce Hansen. The contributions of Dr. Aaron Johnson, Dr. Bruce Hansen, Dr. Benjamin Thompson and myself to the co-authored experimental chapters are defined below.

Chapter 2: Size Matters: α Discrimination Thresholds are Influenced Most by Low Spatial Frequency Luminance Contrast when α is Equal to or Greater than the Natural Scene Average α

In collaboration with both Dr. Aaron Johnson and Dr. Bruce Hansen, I designed Experiment 2.1, and replicated the center-surround paradigm from the Johnson, Richard, Hansen, and Ellemberg (2011) study in Experiment 2.2. Dr. Bruce Hansen provided the original MATLAB code to generate the 1/*f* noise images used throughout this dissertation, and I altered the code according to the particular needs of an experiment. All participants were volunteer students in the laboratory, including myself, and I supervised the data collection process. I conducted all statistical analysis, and drafted the manuscript with feedback from Dr. Aaron Johnson and Dr. Bruce Hansen.

Chapter 3A: The Effects of tDCS Across the Spatial Frequencies and Orientations that Comprise the Contrast Sensitivity Function

This projected was conducted in the laboratory of Dr. Bruce Hansen at Colgate University. In collaboration with Dr. Bruce Hansen, Dr. Aaron Johnson, and Dr. Benjamin Thompson, I designed the experiments of Chapter 3A, and participated in data collection. Kristin Andres at Colgate University completed most of the data collection (8 of the 10 participants in the oblique orientation group, and all 10 participants in the horizontal orientation group came from Colgate University), while at Concordia University, both Rebecca Birkett and Yvette Esses assisted me with the data collection for the remaining two participants. I conducted all statistical analyses, and drafted the manuscript with feedback from Dr. Bruce Hansen, Dr. Aaron Johnson and Dr. Benjamin Thompson.

Chapter 3B: Does trans-Cranial Direct Current Stimulation (tDCS) Modify α Discrimination Thresholds?

Similar to Chapter 2, I designed the study of Chapter 3B in collaboration with Dr. Aaron Johnson and Dr. Bruce Hansen. Participants in this study were recruited from the Concordia Participant pool system, and I, in addition to Rebecca Birkett, Joella Matire, and Julian Rice, participated in the data collection. I conducted all statistical analyses and drafted the manuscript with feedback from Dr. Aaron Johnson and Dr. Bruce Hansen.

Chapter 4: The Task Dependent Contribution of Spatial Frequency Channels to the Perception of the α of Noise Images

With collaboration from Dr. Aaron Johnson and Dr. Bruce Hansen, I designed the experiments of Chapter 4 and received advice on the stimulus manipulation procedures from Dr. Andrew Haun. Participants in this study were undergraduate student volunteers. I conducted all statistical analyses and drafted the manuscript with feedback from Dr. Aaron Johnson and Dr. Bruce Hansen.

TABLE OF CONTENTS

LIST OF FIGURES

Figures in Chapter 1

Figures in Chapter 2

Figures in Chapter 3A

Figures in Chapter 3B

Figures in Chapter 4

Figures in Supplementary Materials of Chapter 3A

LIST OF TABLES

Tables in Chapter 2

Tables in Chapter 3A

Tables in Chapter 3B

Tables in Chapter 4

Tables in Supplementary Materials of Chapter 3A

LIST OF EQUATIONS

Equations in Chapter 1

Equations in Chapter 4

Equations in Supplementary Materials of Chapter 3A

Chapter 1

General Introduction

GENERAL INTRODUCTION

The environment that humans live in and the tasks they perform daily are thought to have shaped the design and function of our visual system through evolution and experience. Establishing the relationship between the features of natural scenes (i.e. real-world stimuli as opposed to synthetic stimuli), the responses that scene features evoke in humans, and how these features are encoded and used to perform daily tasks can advance our knowledge of human visual perception.

The early stages of visual processing (from the retina to the extra-striate cortex) operate through a series of distinct filter-like neuronal channels (or pathways) that detect different structural properties within an image (e.g., orientation, spatial frequency). Thus, at any moment in time, the complex light patterns from the environment that fall on the retina will stimulate numerous differently tuned channels, whose outputs will be weighted by the activity of other similarly and differently tuned channels. Visual processing, under natural stimulation, is thus the result of multiple interactions between channels, which can be excitatory or inhibitory (reviewed in Hansen, Haun, & Essock, 2008). However, in most studies on early visual processes, researchers have used dimensionally restricted (i.e., narrowband in spatial frequency and orientation) stimuli that activate only a subset of channels, whose tuning characteristics are matched to the properties of the stimulus (but see Goris, Wichmann, & Henning, 2009). While these studies have generated knowledge on the activity of small groups of channels that function in isolation, they do not reproduce the function and activity of these channels under naturalistic conditions. It has been posited that the function and underlying mechanisms of the early visual system are strongly tied to the properties of the environment it has developed in at the evolutionary, developmental, and behavioural timescales (Carandini et al., 2005; Field, 1987; Geisler, 2008; Hyvärinen, Hoyer, Hurri, & Gutmann, 2005; Hyvärinen, Hurri, & Hoyer, 2009; Olshausen & Field, 1996b, 1997, 2005; Olshausen & Lewicki, 2004; Simoncelli, 2003), and is therefore optimally suited to process stimuli it regularly encounters (e.g., natural - broadband - environments). Thus, the study of the visual system should be guided by an understanding of the statistical properties that describe natural scenes.

One of the most investigated representations of natural scenes is their Fourier amplitude spectra, which defines their autocorrelation property (e.g., their second order statistic; Olshausen & Field, 2000). All natural scenes have a Fourier amplitude spectra that fall as a function of

spatial frequency, at a rate of $1/f^{\alpha}$, where f is spatial frequency and α, on average, is 1.08 (Billock, 2000). It has been demonstrated that changing α in an image can alter psychophysical performance, which suggest that this property of natural scenes is relevant to the early processing stages of the visual system (Knill, Field, & Kersten, 1990; Párraga, Troscianko, & Tolhurst, 2000; Párraga et al., 2005; Tolhurst & Tadmor, 2000). However, a clear association between the response properties of spatial frequency channels - believed to underlie the detectability of a change in α - and psychophysical performance remains to be fully defined. The overarching goal of this dissertation was to identify a psychophysical mechanism responsible for encoding α and link it to the observed psychophysical performance of human observers on an α discrimination task. We aimed to bridge the gap in knowledge between the response properties of psychophysical channels in the early visual system to the second-order statistics of natural scenes and psychophysical performance.

Channels in the Early Visual System

The early stages of vision rely on functionally different neurons that operate like non-linear filters, in that they extract a narrow range of spatial frequency and orientation content from the retinal image (Bergen, Wilson, & Cowan, 1979; Blakemore & Campbell, 1969; Campbell & Robson, 1968; Campbell & Kulikowski, 1972; Carandini et al., 2005; De Valois, Albrecht, & Thorell, 1982; De Valois, Morgan, & Snodderly, 1974; Enroth-Cugell & Robson, 1966; Graham & Nachmias, 1971; Graham, 1989; Henning, Hertz, & Broadbent, 1974; Maffei & Fiorentini, 1973; Movshon, Thompson, & Tolhurst, 1978; Stromeyer & Julesz, 1972; Stromeyer & Klein, 1974; Wilson & Bergen, 1979; Wilson, McFarlane, & Phillips, 1983; Wörgötter & Koch, 1991). While physiological studies have direct access to the measurement of the responses characteristics of these neurons, psychophysical approaches must deal with the responses of the system as a whole. Therefore, psychophysical studies can demonstrate the existence of separate processing for a particular sub-range of stimulus features, but cannot identify the exact loci of this separate processing. Hence, the populations of neurons that show similar tuning to a particular stimulus dimension, and may therefore be responsible for the separate processing identified, are referred to as channels within the psychophysical literature (Braddick, Campbell, & Atkinson, 1978).

There are three main psychophysical approaches that have been used to define the properties of channels in the early visual system: selective adaptation (e.g., Blakemore &

Campbell, 1969), simultaneous masking (e.g., Campbell, Kulikowski, & Levinson, 1966), and subthreshold summation (e.g., Graham & Nachmias, 1971; Sachs, Nachmias, & Robson, 1971). Each method relies on the interactive effects of two stimuli on the detectability of a particular stimulus. In regards to the processing of spatial frequency content, these stimuli have typically been spatial periodic stimuli (e.g., sinusoidal gratings), with the experimental variables being the spatial frequency (in cycles/°) and the contrast of the sinusoid. The detectability of a sinusoidal grating varies according to its spatial frequency and contrast and peaks at or near of 4 cycles/° (when measured with sinusoidal gratings of a large spatial extent that is well localized in the Fourier domain; Peli et al., 1993). The idea of using sinusoids to stimulate channels stems from the Fourier series, which allows the description of any signal as the sum of sinusoidal components (Campbell & Robson, 1968; Peli, Arend, Young, & Goldstein, 1993; Smith, 2007). Indeed, early investigations on the encoding characteristics of the visual system defined them as a form of Fourier analysis. Specifically, it became evident that the early visual system decomposed the retinal input into an independent and linear subset of spatial frequency components (i.e., processed by multiple spatial frequency channels; Blakemore & Campbell, 1969; Campbell & Robson, 1968), a process similar to that of Fourier analysis.

The most referred to evidence for multi-channel models of spatial vision is that of the selective adaptation study of Blakemore & Campbell (1969). They found that prolonged exposure to a grating of a particular spatial frequency elevated contrast detection thresholds for that spatial frequency, while thresholds for other spatial frequencies remained unaffected. Tuned threshold elevation following adaptation could be obtained for spatial frequencies ranging between 3 and 20 cycles/°, and the bandwidth of threshold elevation was about 1.2 octaves full-width at half-height. According to Blakemore and Campbell (1969), this was an indication that the early visual system was composed of multiple, narrowly tuned, linear, and independent, spatial frequency channels, which served as a neural substrate for the Fourier analysis of visual pattern. Additional evidence for the independent processing of spatial frequency information came from a study conducted Campbell and Robson (1968). They demonstrated that the detectability of the square-wave grating, a waveform that results from the infinite sum of odd harmonic sinusoids, could be predicted by the detectability of one of its sinusoidal components (as they should under Fourier theory). Additionally, they found that the detectability of a square-wave grating was contained by contrast magnitude of its fundamental spatial frequency. That is,

the detectability of the square-wave did not change when additional harmonics were added to the grating until these harmonics reached their own detection thresholds (i.e., thresholds did not sum according to the presence of multiple spatial frequencies).

The discovery of multiple independent psychophysical channels served as initial evidence towards the definition of the early visual system as a Fourier analyzer. However, it was also crucial to demonstrate that the bandwidth of spatial frequency channels was sufficiently narrow to allow for a Fourier analysis. Initial attempts to define the bandwidth of channels suggested they were; estimates of bandwidth from subthreshold summation studies measured bandwidth of approximately 0.3 octaves (Braddick et al., 1978; Sachs et al., 1971). However, these were discordant with other estimates from channel bandwidth (see above), and subsequent studies demonstrated that the narrow bandwidth of channels identified with subthreshold summation was actually due to an artefact of the stimulus construction (Stromeyer & Klein, 1975). Indeed, follow-up investigations, which used masking paradigms to estimate the bandwidth of spatial frequency channels, showed their bandwidth to be significantly larger than those initially estimated, and variable across spatial frequency (Wilson et al., 1983; Wilson & Wilkinson, 1997). The bandwidth of a spatial frequency channel decreases as its preferred spatial frequency increases from about 2.5 octaves at low spatial frequencies to 1.25 octaves at high spatial frequencies (Wilson et al., 1983). These measurements corroborate those of single unit estimates of bandwidth (De Valois et al., 1982; Issa, Trepel, & Stryker, 2000; Tootell, Silverman, et al., 1988; Yu et al., 2010), and similar decreases in the bandwidth of channels as a function of increased spatial frequency was found in the orientation domain (30° at low spatial frequencies and 15° at high; Phillips & Wilson, 1984). That said, more recent investigations on the bandwidth of channels in both the orientation and spatial frequency domain have shown that psychophysical measurements of bandwidth with masking paradigms are subject to interactive effects generated by the mask on the responses of channels within the early visual cortex (Cass, Stuit, Bex, & Alais, 2009; Hansen & Hess, 2012; Meese & Holmes, 2010). Similar non-linear interactions between spatial frequency channels are also known to contribute to the measurement of channel bandwidth via selective adaptation (Abbonizio, Langley, & Clifford, 2002; Ross & Speed, 1991; Wilson & Humanski, 1993). Thus, channels extract information from the retinal image across a range of spatial frequencies and orientations. However, their interactive properties and larger bandwidth mean this process cannot be described as a Fourier analysis.

Instead, a fair amount of computing might be completed by non-linear interactions observed across spatial frequency channels (Wilson & Wilkinson, 1997).

The definition of a channel involves its independence. But, careful study of their response characteristics has demonstrated that channels can interact in a non-linear manner with both similarly and differently tuned channels (DeAngelis, Robson, Ohzawa, & Freeman, 1992; Henning et al., 1975; Legge & Foley, 1980; Meese & Hess, 2004; Meese & Holmes, 2010; Morrone, Burr, & Maffei, 1982; Olzak & Thomas, 1999; Petrov & Mckee, 2006; Polat & Sagi, 1993, 1994; Stromeyer & Julesz, 1972; Tolhurst & Barfield, 1978; Wilson & Wilkinson, 1997). These interactions are typically inhibitory in nature, in that the activity of a channel will inhibit that of a similarly or differently tuned channel, and have been well-defined by modern adaptation and masking psychophysical studies (Graham & Sutter, 1998; Graham & Sutter, 2000; Meese & Holmes, 2007; Meese, 2004; Petrov, Carandini, & McKee, 2005; Petrov & Mckee, 2006; Xing & Heeger, 2000). It is the work of Henning and colleagues (1975) that first suggested the existence of non-linear interactions between channels differently tuned in spatial frequency. They presented a contrast modulated stimulus with a carrier spatial frequency of 9.5 cycles/° contrast modulated by a spatial frequency of 1.9 cycles/°. They found that this pattern masked a grating with a spatial frequency of 1.9 cycles/°, even though the masking stimulus contained spatial frequency content 2 octaves above that of the target grating. That is, a carrier spatial frequency of 9.5 cycles/° contrast modulated by a spatial frequency of 1.9 cycles/° is equivalent to the sum of three gratings with spatial frequencies of 7.6, 9.5, and 11.4 cycles/°. As the distance between the masked stimulus and the lowest spatial frequency component of the mask (7.6 cycles/°) exceeds the bandwidth of any spatial frequency channel (De Valois et al., 1982; Stromeyer & Julesz, 1972; Stromeyer & Klein, 1975; Wilson et al., 1983), the resulting effect could only stem from differently tuned channel interactions.

Given this and other evidence, most models of spatial vision today encompass some form of non-linearity as a crucial component to convey useful information between different processing stages. This may be most easily demonstrated with Filter-Rectify-Filter modelling approaches, as they offer a simple definition of the non-linear neural responses to textures. The first stage within the model uses a bank of oriented filters who's output is rectified (either full-wave or half-wave) prior to being fed to a second bank of oriented filters with lower preferred spatial frequencies (Arsenault, Yoonessi, & Baker, 2011; Ellemberg, Allen, & Hess, 2006;

Graham, 2011; Johnson, Kingdom, & Baker, 2005; Schofield & Georgeson, 2003; Schofield, Rock, Sun, Jiang, & Georgeson, 2010). This model approach has been successfully implemented to explain results from a wide range of studies, including texture, luminance and contrast defined boundaries (Arsenault et al., 2011; Graham, 2011; Schofield & Georgeson, 2003; Schofield et al., 2010) and most recently, implemented to define neural responses to more complex, natural scene stimuli (Johnson & Baker, 2004; Johnson et al., 2005; Johnson, Prins, Kingdom, & Baker, 2007).

The original studies that have tried to define the functional properties of psychophysical spatial frequency channels relied heavily on the use of simple stimuli (e.g., sine-wave gratings), which are defined by a single spatial frequency and orientation (i.e., the stimuli are narrowband). While this method of channel analysis allowed for the study of channels in isolation, it offers an over-simplified view of channel function in more naturalistic, broadband environments (Dan, Atick, & Reid, 1996; David, Vinje, & Gallant, 2004; Hansen & Hess, 2012; Johnson & Baker, 2004; Kayser, Salazar, & Konig, 2003; Maldonado & Babul, 2007; Olshausen & Field, 1996b; Zetzsche & Röhrbein, 2001). Thus, psychophysical effects measured with stimuli that only activate a handful of channels cannot be representative of the non-linear interactions that may occur with more complex, broadband environments that activate multiple channels simultaneously. Additionally, the use of sinusoidal gratings to define channel behaviour offers little information as to why these channels behave or interact in the way they do. That is, the visual system has continuously been exposed to an environment that is spatially (and orientation) broadband and has therefore developed a coding scheme according to the properties of its broadband environment. An alternative approach may be to study the response characteristics of channels under broadband conditions, as they better represent the environments within which channels typically function. Thus, the study of spatial frequency channel function should include a study of the environment in which they developed.

Statistics of natural scenes

Individually, natural scenes are difficult to describe as they contain complex interactions of texture, color, motion, surface reflectance, and changes in illumination and contrast. However, scenes also display regularities that can be defined statistically (i.e., scenes described according to the probability distribution of the intensity of pixels within an image). Additionally, the statistical representation of natural scenes is known to be of relevance to the processes of the

early visual system (Burton & Moorhead, 1987; Geisler, 2008; Hyvärinen et al., 2009; Lee, Mumford, & Huang, 2012; Ruderman, 1994; Schwartz & Simoncelli, 2001; Simoncelli & Olshausen, 2001; Simoncelli, 2003; van der Schaaf & van Hateren, 1996). The simplest statistical property of natural scenes treats each position (or pixel) within an image independently. Therefore, a first-order statistic represents the information derived from an individual point within a probability density function of illumination (Doi & Lewicki, 2005; Hyvärinen et al., 2005, 2009; Yang, 2012). Single pixel statistics are thought to offer little information on interactive encoding processes, but have been shown to play an important role in the initial processing stages of the input stimulus (Atick & Redlich, 1992; Doi, Inui, Lee, Wachtler, & Sejnowski, 2003; D. L. Ruderman, Cronin, & Chiao, 1998).

The second-order statistics of natural scenes defines the correlation or covariance between two pixels across all locations and distances within an image. While these statistics may not carry information in regards to the particular structure within an image, they are never the less relevant to the encoding processes of the early visual system (Geisler, 2008; Graham & Field, 2007; Guyader, Chauvin, Peyrin, Hérault, & Marendaz, 2004; Simoncelli & Olshausen, 2001). There are different approaches to quantify the second-order statistic of natural images (e.g., Principle Component Analysis), but the most commonly used method is that of Fourier analysis (Hyvärinen et al., 2009). The fundamental result of a frequency-based representation of natural images is that their power spectrum falls off inversely to the square spatial frequency. It was television engineers that first discovered that the orientation averaged power (β), in images, falls by a rate of 2 as spatial frequency (measured in cycles per picture or cycles per degree) increases (Kretzmer, 1952). The power spectrum is the square of the Fourier amplitude spectrum, and therefore, in images, the amplitude spectrum falls inversely proportional to spatial frequency according to the following power law:

$$\text{Fourier Amplitude} = 1/f^{\alpha} \qquad \textbf{Equation 1.1}$$

with α, the exponent, which dictates the particular rate of descent (the slope of the amplitude spectrum). This means that the distribution of luminance contrast (the square of amplitude) across spatial frequency, in all natural images, can be represented according to a single parameter: α (Hyvärinen et al., 2009; D. L. Ruderman, 1994; Simoncelli, 2005; Wainwright & Simoncelli, 2000). **Figure 1.1-B** shows the 2D Fourier amplitude spectrum of the image (**Figure**

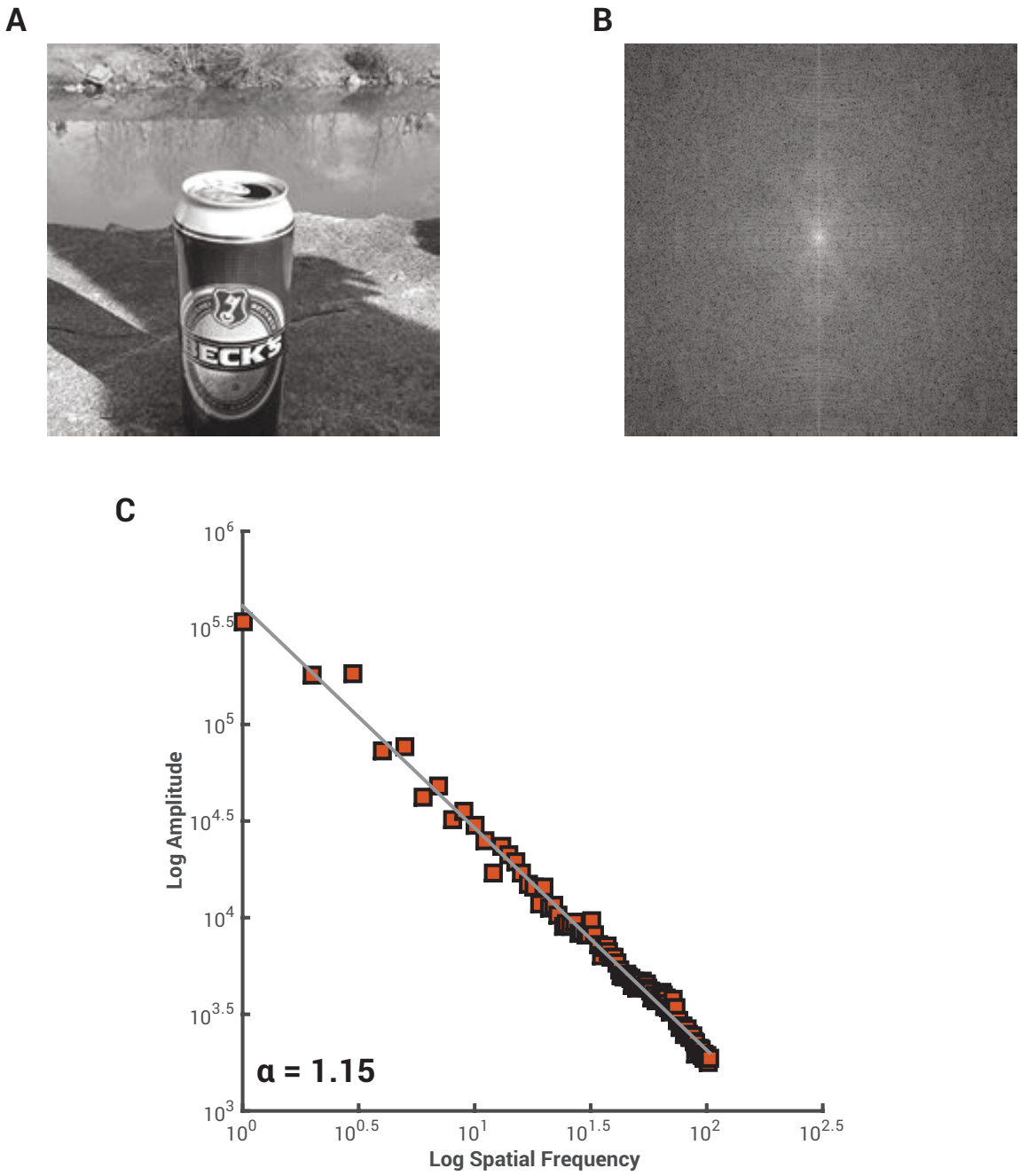

Figure 1.1 The Fourier representation of an image. **B** The 2D amplitude spectra of the image. **C** The orientation average amplitude spectrum of the image. Each square marker represents the log amplitude for a given log spatial frequency. The grey line is the line of best fit, which on logarithmic axes has a slope of 1.15.

1.1-A). It is clear from the 2D Fourier representation that most of the energy within the image is concentrated at the lower spatial frequencies and decreases as a function of increasing spatial frequency. The rate of descent of energy across spatial frequency is most easily calculated when amplitude is averaged over orientation and transformed into a 1D representation of the Fourier amplitude spectrum (**Figure 1.1-C).** On logarithmic axes (both spatial frequency and amplitude) the amplitude of the image falls at a rate of about $\alpha = 1.15$, which is close to the typical α observed in the natural environment of 1.08 (Billock, 2000; Burton & Moorhead, 1987; Field, 1987; Hansen & Essock, 2005; Ruderman, 1994; Tolhurst, Tadmor, & Chao, 1992; van der Schaaf & van Hateren, 1996).

While the orientation-averaged amplitude spectrum slope may not define the distribution of energy across both orientation and spatial frequency, which is important to visual processing (Hansen, Essock, Zheng, & DeFord, 2003; Hansen & Essock, 2005; Haun & Essock, 2010; Kim, Haun, & Essock, 2010), the value of α, in-of-itself, seems to carry some information on the general distribution of energy across scene categories. This is the premise of analyses of the distribution of αs in natural images, as the visual system is thought to be tuned, and potentially exploit, to the orientation-averaged slope of the amplitude spectrum of natural scenes. However, for this argument to hold, α must be somewhat representative of natural images. The exact α that may best represent the average natural scene has been of much debate, but it is generally agreed that it ranges between 0.6 and 1.6, with an average value of 1.08 (Billock, 2000; Field & Brady, 1997; Hansen & Essock, 2005). This range may be considered wide, but the distribution of αs across multiple images has been shown to narrow significantly, and have different modal tendencies, when the environment of the image is taken into consideration (Hansen & Essock, 2005). Specifically, αs for natural-only scenes peak in frequency within a range of [.90 .94], natural and man-made scenes peak within a range of [1.05 1.09], and man-made only peak within a range of [1.30 1.34].

The amplitude spectrum defines the distribution of amplitude (or luminance contrast for the power spectrum) across spatial frequency. The alignment of these spatial frequencies, and, therefore, the structural representation of an image, is carried by the phase spectrum in a spatial frequency-based representation of natural images. It is worth mentioning that when pit against one another, the phase spectrum is considered to be of more relevance than the amplitude spectrum to the definition of natural scenes (Bex & Makous, 2002; Gaspar & Rousselet, 2009;

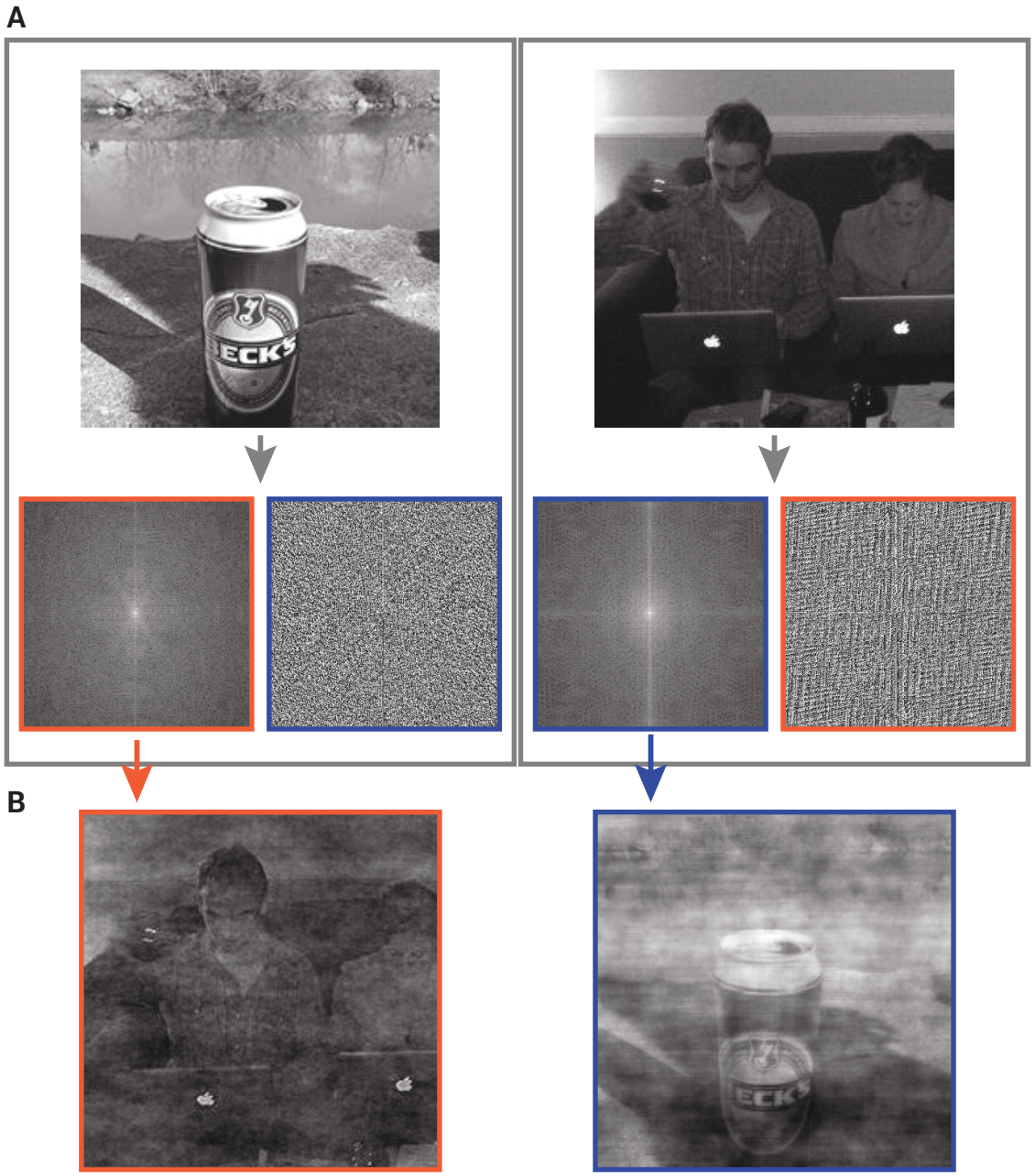

Figure 1.2. The relative contribution of both the amplitude spectrum and the phase spectrum of natural scenes to perception. **A** Two images, one of food, and one of a scientist consuming food for inspiration while programming, are separated into their respective amplitude and phase spectra. The images are then reconstructed and returned to the spatial domain, but the amplitude spectrum of each image is swapped. **B** The resulting image when the amplitude spectrum of the left image in **A** is reconstructed with the phase spectrum of the right image (RED). It is evident that the phase spectrum of the right image in **A** is the noticeable component of the altered image. This figure was inspired by Figure 5.16 in Hyvärinen et al. (2009).

Hansen & Hess, 2007; Hansen & Loschky, 2013; Hyvärinen et al., 2009; Wichmann, Braun, & Gegenfurtner, 2006). This can easily be demonstrated by swapping the amplitude and phase spectra of two images, and creating a new image with the amplitude spectrum of an image, and the phase spectrum of another image (see **Figure 1.2)**. The new image resembles the image from which the phase structure was taken. This is to be expected as natural scenes all have a $1/f^{\alpha}$ amplitude spectrum (Kretzmer, 1952). However, it is also evident that the new image contains discordant information and does not appear normal. Thus, while the 2D amplitude spectrum may not carry relevant information to the structure of an image, it is never the less a crucial component of the proper representation of images (Oliva & Torralba, 2001; Tadmor & Tolhurst, 1993; Torralba & Oliva, 2003).

The statistical representation of a single image can be defined by the combination of the Fourier phase and amplitude spectrum. However, the definition of multiple natural images is most easily accomplished with the orientation averaged amplitude spectrum slope as it can easily represent the distribution of luminance contrast across spatial frequency in multiple images. Additionally, it is likely that the human visual system has developed processes ideally suited to encode the type of environments it has encountered regularly (Barlow, 1961; Field, 1987; Graham, Chandler, & Field, 2006; Graham & Field, 2007; Simoncelli & Olshausen, 2001). Thus, the study of sensitivity to the orientation average amplitude spectrum slope of natural images may be indicative of the spatial frequency encoding processes employed by the human visual system, and thus, the study of spatial frequency channel behaviour within broadband environments (see Hansen and Essock (2005) for a discussion on the average representation of oriented content within natural scenes, and its contributions to the study of orientation dependent processes in the early visual system). There is indeed evidence that neural processes within the early visual system may function optimally under naturalistic stimulation condition, and we briefly review the literature below.

Neural adaptations to natural image statistics

There has been an accumulation of evidence towards demonstrating that cells, within the retina, the lateral geniculate nucleus (LGN), and striate cortex, respond "optimally" to images that contain statistical properties similar to those of natural stimuli (Atick, 1992; Coen-Cagli & Schwartz, 2013; Dan et al., 1996; David et al., 2004; Geisler, Najemnik, & Ing, 2009; Lörincz, Palotai, & Szirtes, 2012; Maldonado & Babul, 2007; Smyth, Willmore, Baker, Thompson, &

Tolhurst, 2003; Tolhurst, Smyth, & Thompson, 2009; Vinje & Gallant, 2000). It is important to mention that early studies on the neural representation of natural scenes searched for evidence of redundancy reduction, whereby redundant information (e.g., correlated pixels values) would be removed from the early neural code (Atick & Redlich, 1992; Atick, 1992; Barlow, 1961; Dan et al., 1996; Laughlin, 1987; Simoncelli & Olshausen, 2001). However, it is unclear if redundancy reduction is actually a coding scheme employed by the early visual system, as there is evidence that maintaining redundant information may be beneficial to the accurate coding of visual input (see Barlow, 2001).

Initial studies that experimentally tested for a potential coding scheme within the visual system tailored to the statistical properties of natural scenes relied on the demonstration that early visual responses were generated in accordance with an efficient code[1] (Atick & Redlich, 1992; Atick, 1992; Dan et al., 1996). This means that the spatial correlation of natural images (i.e., their second-order statistics) should effectively be removed by the early processing stages of vision. This work was initially conducted on the retinal ganglion cells (Atick & Redlich, 1992; Laughlin, 1987), and subsequently expanded to the LGN (Dan et al., 1996). Similar neurophysiological and modeling work has also been conducted to define the orientation and spatial frequency tuning of cells within striate cortex by maximizing the independence of neurons, which is the fundamental principle of the sparse coding algorithm and Independent Component Analysis (ICA; Baddeley et al., 1997; Bell & Sejnowski, 1997; Caywood, Willmore, & Tolhurst, 2004; Hancock, Baddeley, & Smith, 1992; Hyvärinen et al., 2005, 2009; Olshausen & Field, 1996a, 1996b, 1997; Olshausen & Lewicki, 2004; van Hateren & van der Schaaf, 1998). Maximizing a certain property of natural scenes in accordance with de-correlation (PCA) or independence (sparseness) has offered valuable insight into the receptive field properties of single cells in the early visual system. For example, Baddeley and colleagues (1997) demonstrated that the firing rate distributions of cells in cat V1 and in the monkey Inferior Temporal cortex (IT) are exponential under naturalistic stimulation, a sign that information may be transmitted in an optimal fashion, with a constraint on mean firing rate. However, it was later shown that the exponential shape of firing rate distributions was only correct under noise-free

[1] We only discuss representational efficiency here, with focus on the decorrelation of a correlated signal. The other forms of efficiency (metabolic and learning) are reviewed in Graham and Field (2007).

conditions, and that taking noise into consideration, and not optimality constraints, could account for the findings of Baddeley and colleagues (De Polavieja, 2002). Several studies have demonstrated that the visual system does show improved performance under naturalistic stimulation (for review: Simoncelli, 2003). However, as these studies were intended to measure the behaviour of single cells, they cannot clearly demonstrate how performance, at a psychophysical level, may be tied to, or affected by, the statistical properties of the natural environment.

Human psychophysical performance and the amplitude spectrum slope of natural scenes

A direct approach to evaluating how the performance of the visual system may vary according to natural versus unnatural conditions is to ask observers to perform a visual task on an image while modulating the α of the image. If performance is best when the α of the image is natural, then it can be argued that α contributes visual performance. For example, when the α of an image is unaltered (natural), performance on a morphing task, where an image is slowly morphed into a second different and unrelated image (Benson, 1994), is better than when their α is modulated to be steeper (α > natural value) or shallower (α < natural value; Párraga, Troscianko, & Tolhurst, 2000, 2005). These results suggest that the visual system is optimized to work within the natural αs of images it is exposed to. However, it is important to note that while morphing and manipulating the α of a natural image is an interesting approach to the measurement of perceptual performance, this artificial manipulation of α introduces noticeable and undesirable artefacts. When α is made steeper than its natural value the image is perceptually blurred while a shallower α will sharpen the images. However, naturally steep or naturally shallow αs do not appear blurred or sharp. This means that any performance change in this morphing sequence might not be indicative of optimal performance under naturalistic conditions, but instead reflect the difficulties induced by blurring or sharpening an image.

There are other psychophysical approaches that have demonstrated the tuning of early visual processes to α without the introduction of perceptual artefacts. For example, the α of a noise or natural image has been shown to have a large impact on the perception of single image components (Webster & Miyahara, 1997). Prolonged exposure to either natural scenes or $1/f$ noise images that varied in α shifts the peak in the contrast sensitivity function towards higher spatial frequencies and reduces contrast sensitivity to low spatial frequencies. These effects were similar when measured supra-threshold with a matching task (Webster & Miyahara, 1997).

Given that images with natural α have a significant amount of luminance contrast at low spatial, it is perhaps not surprising that low spatial frequency contrast sensitivity was most impaired. Interestingly, the shift in the peak of the CSF induced by adaptation varied according to α. No measurable effect on the peak of the CSF could be measured with an adaptor α = 0.0 (white noise with equal amounts of contrast at all spatial frequencies), while the peak of the CSF shifted towards higher spatial frequencies as α approximated 1.0 and returned to lower spatial frequencies as α exceeded 1.0 (following an inverted U-shape function). Thus, contrast sensitivity (and contrast matching) at low spatial frequencies is affected most by adaptation to broadband images, and the extent of adapted spatial frequencies will vary according to the particular α value of the image. Similar findings have also been reporting with masking paradigms, which have shown that the elevation of thresholds will vary according to the α of the mask (i.e., noise patterns modulated to have different αs). Broadband noise masks with an α = 1.0 generate significantly stronger masking effects – elevate thresholds most – on the detection of a Gabor pattern than broadband noise masks with shallower (α = 0.5) or steeper (α = 1.5) αs (Hansen & Hess, 2012). The variable masking strength of α extends to more complex target images, including natural scenes in a rapid scene categorization task (Hansen & Loschky, 2013; Loschky, Hansen, Sethi, & Pydimarri, 2010). Masks with αs similar to those of the target natural scene have larger masking effects than masks with dissimilar α, provided the α value of the target image is near 1.0 (Cass, Alais, Spehar, & Bex, 2009; Hansen & Loschky, 2013; Loschky et al., 2010).

Both adaptation and masking studies have clearly demonstrated that interactive visual processes are dependent upon the statistics of the image presented to observers (e.g., α). However, while these show the α of an image can influence visual processing, they do not necessarily define sensitivity to α. Questions in regards to the sensitivity of human observers to α have typically been answered by measuring the ability of human observers to detect, or discriminate, a change in α (Hansen & Hess, 2006; Johnson, Richard, Hansen, & Ellemberg, 2011; Knill, Field, & Kersten, 1990; Párraga & Tolhurst, 2000; Tadmor & Tolhurst, 1994; Thomson & Foster, 1997; Tolhurst & Tadmor, 1997). Knill and colleagues (1990) were the first to measure the ability of observers to discriminate a change in α between two noise images (referred to as 1/*f* noise for the remainder of the dissertation). They found α discrimination thresholds were lowest when the reference αs ranged between 1.4 and 1.8, which they argued

was the range human observers are tuned to. This may seem odd, given that these α values are well above the range measured in natural environments (αs = [0.8 1.0]; Billock, 2000). However, Tadmor and Tolhurst (1994) proposed that the findings of Knill and colleagues (1990) might be attributed to their use of noise images, as noise images are not truly representative of the content of natural scenes (they lack all structure). In order to verify hypothesis, Tadmor and Tolhurst (1994) measured α discrimination thresholds to natural images with a range of αs between [0.78 1.38] and noise images with comparable α values. They presented their images in a 3AFC task, whereby two images were set to a particular reference α (out of a possible 7) and the third with a slightly different α. Observers were asked to indicate which, within the set of three images, contained the odd α. For both natural and noise images, lowest α discrimination thresholds were found for steep αs, while observers' thresholds were highest for α values near 1.0 (the "typical" value of natural scenes; Billock, 2000). They argued that this was evidence for tuning of the visual system to an α of 1.0 and proposed that the high thresholds they measured were an indication of tolerance towards changes within the common range of α values. A high tolerance to changes in common αs, which could be due to an eye movement, blink or a shift in gaze, would have little impact on perceptual stability, and thus benefit the processing of natural scenes. One issue with the Tadmor and Tolhurst (1994) study was that they modulated the α of natural images in their discrimination paradigm, which as previously described, generates noticeable artefacts in the images that are absent when viewed with their original α. This brings to question how α discrimination thresholds may change according to the reference α when observers must discriminate against the true α of an image. While not the main goal of their study (they were mostly interested in measuring the impact of phase coherence on α discrimination), Thomson and Foster (1997) found, in a temporal 2AFC task, that α discrimination thresholds were highest when the natural image's α was near its natural α value (for all three reference αs used in the study - 0.7, 1.0, and 1.3). They argued against any tuning or tolerance of early visual processes to particular, or typical, αs.

A potential account for the discrepancies between studies on human sensitivity to α was brought forth by Hansen and Hess (2006). They proposed that methodological differences between previous studies, which include the size of the image patch presented, the use of $1/f$ noise versus natural images, and the retinal location of the stimulus presentation (fovea versus parafovea) might all be contributing factors to differences found in α discrimination thresholds.

They used a temporal version of the Odd-Man-Out procedure designed by Tadmor and Tolhurst (1994) to measure α discrimination thresholds with 1/*f* noise images and natural scenes (1° of visual angle is size) presented at fovea and parafoveal (the issue of stimulus size was not investigated in their study). They found that, regardless of retinal location tested, α discrimination thresholds were lowest for reference α values greater than 0.95 with natural images, and αs between 1.2 - 1.4 for 1/*f* noise. These results corroborated those of Knill and colleagues (1990). They also found a peak in thresholds at α = 0.8, which was most evident with measured with 1/*f* noise images and presented at parafovea, similar to the results of Tadmor and Tolhurst (1994). The findings of Hansen and Hess (2006) clarified certain discrepancies in previous studies on α discrimination, particularly in regards to visual resolution differences between the fovea and parafovea and α discrimination. In addition, they offer further evidence towards human sensitivity that is greatest for αs slightly steeper than those commonly observed in the natural environment, and high resilience for αs less than the typical observed value of 1.0.

Subsequent work on α discrimination has focused on refining our understanding of human observer sensitivity to α. It is known today that sensitivity to α is dependent on the observer's environmental experiences, and will only reach typical α discrimination threshold values around 10 years of age (Ellemberg, Hansen, & Johnson, 2012). Others have shown that α discrimination thresholds are subject to contextual interactions (Johnson et al., 2011). That is while most studies on human sensitivity to α have been conducted with small, localized stimuli that vary only in their α, image patches within a natural environments are never seen in isolation. This led Johnson and colleagues (2011) to ask if the tuning α may be altered by contextual cues. They used an Odd-Man-Out psychophysical paradigm identical to that of Hansen and Hess (2006) to estimate α discrimination thresholds for isolated broadband 1/*f* noise patches and noise patches with a surrounding 1/*f* noise annulus. The experimental manipulations included the reference α of the centre stimulus (0.4, 0.7, 1.0, 1.3, and 1.6), the α of the surround (0.7, 1.0, 1.3), and the distance between the centre and surround stimuli (0, 20, 40, and 60 arcmin). Oddly enough, average α discrimination thresholds for the centre stimulus alone condition were high and nearly identical for all reference α. Low α discrimination thresholds to steeper αs (1.2 – 1.4) were only found when the centre stimulus was circumscribed by a surround annulus. Additionally, the presence of a surround annulus had a facilitative effect on α discrimination thresholds, and this effect was not tuned to the α of the surround. However, α specific effects

were found on the persistence of the facilitation effect from the surround according to its distance from the centre. When the surround had a shallow α, the facilitative effects of the surround diminished as the distance increased, but for relatively steep surround αs (1.0 and 1.3) changes in the distance between the centre and the surround stimuli had little impact on facilitation. These findings indicate that, at least for steeper αs, discrimination may operate globally.

Spatial Vision Coding Mechanisms of Natural Images

In the preceding section, the questions of interest focused on if there is a particular range of α that human observers may perform best under and if this correlates with the tuning of the visual system to α. While there are caveats in the literature, it seems as though the human visual system is psychophysically tuned to natural images with α values near 1.0, and performs best when the α of an image has a value of 1.0. Given the association of tuning to α and performance, the next logical step was to ask how the processes of the early visual system might respond to images with 1/*f* amplitude spectra in order to determine the particular encoding mechanism. Early attempts to define, psychophysically, how observers discriminate between images that vary solely in α approached α discrimination as one of contrast discrimination (Tadmor & Tolhurst, 1994; Tolhurst & Tadmor, 1997). Thus, the detection of a change in α (i.e., α discrimination) was defined by the detectability of a change in contrast within a single spatial frequency band (or psychophysical channel).[2] Under narrowband conditions (e.g., sine-wave gratings), models of contrast discrimination are known to replicate human observer performance well (Baker, 2013; Foley & Legge, 1981; Goris, Wichmann, & Henning, 2009; Klein & Levi, 2009; Meese & Baker, 2011; Meese & Summers, 2007; Watson & Solomon, 1997; Wilson & Humanski, 1993; Wilson & Regan, 1984). Interestingly, even though contrast in broadband images is significantly more complex to describe (Adini et al., 2004; Brady & Field, 1995; Peli, 1990; Perna & Morrone, 2007), the α discrimination model proposed by Tadmor and Tolhurst (1994) explained α discrimination thresholds for reference α = 0.8 (and later on for α of 0.4, 0.8, 1.4 and 1.8; Tolhurst & Tadmor, 1997). They demonstrated that the magnitude of the change required to discriminate two noise images with different αs agreed with the amount of contrast change required to discriminate between simpler sinusoidal gratings at the appropriate spatial frequency

[2] We note that the term single-channel here, and for the remainder of the dissertation, is not used to signify a single-channel model of spatial vision. Instead, it refers to the detectability, or discriminability of a stimulus to be predominantly dictated by the activity of a single channel within an array of channels.

(Tolhurst & Tadmor, 1997). That is, the spatial frequency bands that contributed most to the discrimination of α varied according to the reference α. However, it has since been demonstrated that for broadband images, a non-squared contrast metric (e.g., Michelson Contrast, or band-limited contrast) is not an appropriate definition of contrast (Bex & Makous, 2002), nor the perceived contrast of natural images (Brady & Field, 1995; Field & Brady, 1997; Haun & Peli, 2013; McDonald & Tadmor, 2006). Furthermore, it is well established that the activity of a single spatial frequency channel is insufficient to define responses to stimuli that contain a significant amount of luminance contrast across multiple spatial frequencies (Bex, Solomon, & Dakin, 2009; DeAngelis et al., 1992; Elliott, Georgeson, & Webster, 2011; Hansen, Essock, Zheng, & DeFord, 2003; Hansen & Essock, 2005; Hansen, Haun, et al., 2008; Haun & Essock, 2010; Henning et al., 1975; Legge & Foley, 1980; Meese & Hess, 2004; Meese & Holmes, 2007, 2010; Morrone et al., 1982; Olman, Ugurbil, Schrater, & Kersten, 2004; Olzak & Thomas, 1999; Párraga & Tolhurst, 2000; Párraga et al., 2005; Polat & Sagi, 1993; Stromeyer & Klein, 1975; Stromeyer & Klein, 1974; Tajima & Okada, 2010; Webster & Miyahara, 1997; Wilson & Wilkinson, 1997). While Tolhurst and Tadmor (1997) agreed that the performance of observers on a slope discrimination task should not be defined solely by the activity of a single channel, they offered no alternative as to how the activity of multiple channels may pool, nor did they discuss how the activity of channels with other peak spatial frequencies may influence (e.g., normalized via contrast gain control; Foley, 1994; Heeger, 1992) the activity of the dominant channel they identified (i.e., the spatial frequency band accounting for most of the discriminability of the amplitude spectra). Multi-channel models (e.g., Rohaly, Ahumada, Jr., & Watson, 1997), which account for the interactive activity of multiple psychophysical spatial frequency channel (e.g., normalization), may offer a more plausible description of α discrimination.

One of the first attempts to define the perception of complex contrast patterns (e.g., broadband stimuli with $1/f$ spectra) according to the responses of multiple spatial frequency channels was developed by Field (1987). Field developed a model that measured the response characteristics of Gabor patterns (sinusoidal gratings windowed by a Gaussian envelope), with different orientation and spatial frequency selectivity, to six natural images. The tuning bandwidth (both spatial frequency and orientation) of the Gabor was varied according to various coding schemes in order to assess which may best represent the natural images. The optimal

spatial frequency bandwidth, defined as that which generated the largest signal to noise ratios, fell between 0.5 and 1.5 octaves, and subsequent modelling approaches that developed from the findings of Field (1987) have used constant, one-octave bandwidth filters to process the spatial frequency content of natural images (Brady & Field, 1995; Field & Brady, 1997). However, we note there is little evidence that spatial frequency channel bandwidth is constant in octaves over spatial frequency (De Valois, Albrecht, & Thorell, 1982; Foster, Gaska, Nagler, & Pollen, 1985; Wilson, McFarlane, & Phillips, 1983; Yu et al., 2010). While this modelling approach may not be biophysically valid, it nevertheless demonstrated that contrast in natural images could be well defined, and optimally transferred via a pool of spatial frequency channels with narrow tuning bandwidth. This model was further developed to define the perceived contrast of natural scenes according to the linearity and overall magnitude of filter responses to images with varying α (Brady & Field, 1995), and the magnitude of broadband masking effects on the perception of both narrowband and broadband stimuli (Hansen & Hess, 2012; Hansen & Loschky, 2013).

There have been other attempts to define the response characteristics of psychophysical spatial frequency channels under naturalistic conditions that have stemmed from the foundational work of Field (1987). The psychophysical results of the morphing task of Párraga et al. (2000) and Párraga et al. (2005) were well described by a multi-channel model of complex contrast detection. Párraga et al. (2005) used a spatial frequency channel model to estimate the visibility of differences between the test and reference images. This model measured the responses of several filters with one-octave spatial frequency bandwidth to contrast, similar to that of Field (1987), Brady and Field (1995), and Field and Brady (1997), but additionally pooled across spatial frequency in order to generate a response criterion for the comparison between the test and reference images. Their mulit-channel discrimination model performed better than a single-channel variant and an ideal-observer analysis. Additionally, their model explained differences in their morphing discrimination thresholds between observers, eccentricity, and picture sets. While the model generated by Párraga et al. (2005) did not explicitely try to predict α discrimination thresholds, it suggests that the discriminability of complex contrast patterns may be defined by the pooling of responses from multiple narrowly tuned spatial frequency channels. That said, they offered little towards the characteristics of spatial frequency pooling rules, which remain to be defined today (Haun & Essock, 2010; Haun & Peli, 2013; Rohaly et al., 1997).

Biologically plausible modelling approaches to the discrimination of α, inspired by the work of Field (1987), Brady and Field (1995), Field and Brady (1997), and Párraga et al. (2005), have demonstrated that the population activity of spatial frequency tuned neurons in striate cortex is related to the discriminability of images that vary solely in α (Tajima et al., 2010). Tajima and Okada (2010) developed a hypercolumn of neurons with varied spatial frequency tuning and used the pattern of activity within the hypercolumn to define the discriminability 1/*f* noise images. Their model performed well, and fit the α discrimination thresholds to both the foveal and parafoveal data of Hansen and Hess (2006) by only changing the spatial frequency tuning characteristics of cells; neurons with receptive fields located in fovea were modelled with a broader distribution of preferred spatial frequency, which extended to higher spatial frequencies those of the parafoveal neurons. Additionally, they found that implementing a normalization scheme, whereby the activity of individual cells within the hypercolumn were normalized by the total activity of cells within the hypercolumn generated, provided a better fit to the α discrimination thresholds of Hansen and Hess (2006) then when no normalization scheme was used. Their model extended the pre-existing filter models of α discrimination, and showed that a neurophysiologically plausible population response of cells tuned in spatial frequency, with normalization (Carandini, Heeger, & Movshon, 1997; Carandini & Heeger, 1994; Heeger, 1992; Nestares & Heeger, 1997), was well suited to define the discriminability of 1/*f* noise images. That said, their model contained a large number of free parameters (50), and while a necessity for biologically relevant models, their findings should be considered with this caveat in mind.

Most modelling approaches of α discrimination have defined discriminability according to the spatial frequency content of the stimulus and the corresponding responses of filters (or cells) tuned in spatial frequency to said content. However, direct psychophysical evidence for a spatial frequency dependent mechanism in the discrimination of α remains sparse. It is unclear if human observers asked to discriminate between images that vary in α utilize the spatial frequency content of the 1/*f* noise image in manner similar to that defined by these models. There is evidence that a spatial frequency dependent code, which adapts according to the reference α, is used by observers (Tolhurst & Tadmor, 1997). This study expanded on the band-limited contrast discrimination model developed by Tadmor and Tolhurst (1994) to the discrimination of αs (0.4, 0.8, 1.4 and 1.8) in addition to demonstrating the behavioural relevance of particular spatial

frequency bands to α discrimination. They found that observers relied on contrast within spatial frequency bands ranging between 2 and 10 cycles/° for reference α = 0.4, 1 and 4 cycles/° for reference α = 0.8, and 5-20 cycles/° for reference αs of 1.4 and 1.8. They then measured α discrimination thresholds when the α of the image was changed either within or outside the relevant spatial frequency band. When the change occurred inside the band, thresholds were unaltered as if the change had occurred across the entire spectrum. Thresholds were elevated when the change in α occurred outside the band, which indicated that observers changed the relevant spatial frequency band they normally used in order to complete the α discrimination task, and thus could not perform as well as they would when using the relevant band. While it is plausible human observers may rely more heavily on particular spatial frequency bands to detect a change in the α of an image, the modelling approach used by Tolhurst and Tadmor (1997) to define the relevant band suffered from similar caveats to those of single-channel models defined above (e.g., non-squared metric). Additionally, the bandwidth of the bands used in the psychophysical component of their study was unusually large, spanning over 2 octaves of spatial frequency content. While a bandwidth of two octaves may be representative of the bandwidth of channels at very low spatial frequencies, a band of 2 octaves will include multiple spatial frequency channels at higher spatial frequencies. It is therefore unclear which particular spatial frequency band, or if more than a single band, contributed to the change in α discrimination thresholds measured by Tolhurst and Tadmor (1997).

Overview of Experimental Chapters

As described in the above discussion, the perception of contrast in natural scenes is accomplished by a series of channels narrowly tuned for spatial frequency and orientation. How these channels may contribute to the discrimination of complex contrast patterns (e.g., the α of a noise or natural images) remains to be properly defined. Thus, the overarching goal of this dissertation was to assess the contribution of spatial frequency channels to the discrimination of α. We divided the goal of this dissertation into three sub-goals, which are defined below.

Chapter 2 served as a psychophysical demonstration that α discrimination thresholds are subject to the representation of spatial frequency content within an image. Specifically, we verified if α discrimination thresholds could be affected either by the representation of low spatial frequency luminance contrast, or low spatial frequency channel interactions, as is suggested by both psychophysical (Webster & Miyahara, 1997) and neurophysiological (Hansen,

Ellemberg, & Johnson, 2012; Hansen, Jacques, Johnson, & Ellemberg, 2011) evidence. We first measured how α discrimination thresholds may be affected by the representation of low spatial frequency luminance contrast with a simple manipulation of the size of 1/*f* noise images. An increase in stimulus size leads to an increased representation of low spatial frequency luminance contrast, and thus should lower thresholds if used by observers in an α discrimination task. Slope discrimination thresholds were measured with a 3-IFC "Odd-Man-Out" psychophysical procedure where observers were asked to identify, which of the first or third interval contained the stimulus with the odd α (the reference α was always presented in the second interval). This psychophysical method was used to estimate α discrimination thresholds for all experiments reported in this dissertation unless specified otherwise. In the second experiment of **Chapter 1**, we aimed to account for other factors that may lead to a decrease in thresholds when stimulus size in increased (e.g., summation of higher spatial frequency contrast) by measuring the contribution of low spatial frequency channels to α discrimination via a center-surround paradigm. This study replicated the original centre-surround experiment conducted by (Johnson et al., 2011), but increased the size of the gaps between the centre stimulus and the surround annulus to better target the influence of low spatial frequency channel interactions on α discrimination thresholds.

Chapter 3A and 3B implemented a relatively novel neuro-stimulation technique, trans-cranial Direct Current Stimulation (tDCS) as a tool to assess the contribution of spatial frequency channels to α discrimination more directly. The effects of tDCS on the activity of cells within the primary visual cortex are polarity specific. Anodal tDCS (current enters cortex) has been shown to have an overall excitatory effect on the activity of cells and facilitates performance, while cathodal tDCS (current exits cortex) has an inhibitory effect of cell activity, which inhibits performance (see Jacobson et al., 2012 for a meta-analytical review). While small in magnitude, the influence of tDCS suffices to elicit measurable changes in the behaviour of observers. Thus, the polarity specific effects of tDCS render it a useful tool to modulate the perceptual state of human observers. However, it is important to note that these effects are only robust when tDCS is applied over motor cortex (where it has been most widely studied; Nitsche & Paulus, 2000; Nitsche et al., 2007, 2008; Pellicciari, Brignani, & Miniussi, 2013), and have been shown to vary in primary visual cortex (Antal, Nitsche, & Paulus, 2001, 2006a; Antal & Paulus, 2008; Chaieb, Antal, & Paulus, 2008; Hansen et al., 2015; Peters, Thompson, Merabet, Wu, & Shams, 2013;

Richard, Johnson, Thompson, & Hansen, *under review*; Spiegel, Byblow, Hess, & Thompson, 2013). Thus, we first verified if tDCS could generate spatial frequency specific effects on the simpler task of contrast perception to serve as an indication of the susceptibility of spatial frequency channel to the modulatory effects of tDCS (**Chapter 3A**; Richard et al., 2015). In **Chapter 3B**, after verifying the effects on tDCS on simpler, sinusoidal gratings, we implemented it in the α discrimination task of **Chapter 2** (with a stimulus size of 1° of visual angle presented at fovea; see Kraft et al., 2010 for a discussion on the eccentricity dependent effects of tDCS).

As a final verification to the contribution of spatial frequency channels to α discrimination, we used a classification image paradigm in **Chapter 4** to measure the relative weights associated with particular spatial frequency bands observers have when asked to discriminate noise images that vary in α. The contrast of 8 discreet spatial frequency bands in noise images was randomly modulated by ± 8dB as observers completed an α identification task, a spatial variant of the α discrimination task, and the temporal α discrimination task identical to that of **Chapters 2** and **3B**. To measure the classification image of our observers, their performance on the identification and discrimination tasks was correlated, over multiple trials, to the particular luminance contrast within each spatial frequency band for that trial. This technique offered a glimpse into the relative contribution of the spatial frequency channels to the discrimination of α.

Chapter 2

SIZE MATTERS: AMPLITUDE SPECTRUM SLOPE DISCRIMINATION THRESHOLDS ARE INFLUENCED MOST BY LOW SPATIAL FREQUENCY LUMINANCE CONTRAST WHEN THE SLOPE IS EQUAL TO OR GREATER THAN THE NATURAL SCENE AVERAGE AMPLITUDE SPECTRUM SLOPE.

Bruno Richard, Bruce C. Hansen, & Aaron P. Johnson

Abstract

Sensitivity to the slope (α) of the amplitude spectrum of natural images has been used to argue that human observers are tuned to process broadband information with properties similar to those of natural scenes. Human observers show higher sensitivity (measured via α discrimination) to α values near 1.0 and decreased sensitivity to shallower or steeper αs. However, little is known as to how human observers may detect, and subsequently discriminate, a change in α. There is evidence that the detection of a change in α is completed according to the responses of spatial frequency channels in the early visual system. The goal of this chapter was to test for psychophysical evidence that α discrimination thresholds are contingent upon the representation of spatial frequency content. The initial approach increased the low spatial frequency content of noise images, generated according to five different reference αs, by increasing their size and monitoring any subsequent change in α discrimination thresholds. We observed that increases in stimulus size had a facilitative effect on α discrimination, and was largest for reference α = 1.0, while facilitation decreased as the reference α deviated from 1.0. The facilitation effect we found is similar to that of the perceived contrast of noise images with varying αs, and thus a mechanism that is similar to that of perceived contrast may be involved in the discrimination of α. However, the facilitation effect observed according to increases in stimulus size might have also stemmed from other psychophysical mechanisms (e.g., summation). To account for these other factors, and isolate the contribution of low spatial frequency luminance contrast to α discrimination thresholds, we replicated the center-surround paradigm of Johnson et al (2011), but increased the gap size between the center stimulus and the surround. The surround facilitated α discrimination thresholds for all gap sizes. This suggests that, while interactions between a range of spatial frequency channels is required to discriminated α, low spatial frequency tuned spatial frequency channels may contribute more heavily, particularly in regards to the facilitative effect of the surround.

One of the most explored statistical properties of natural scenes is the slope of the orientation-averaged amplitude spectrum (for review: Geisler, 2008). The slope of the amplitude spectrum (α) represents the rate of descent of luminance contrast as a function of spatial frequency, and on average falls by a factor of 1.0 ($1/f$) on logarithmic axes (α ranges between 0.6 – 1.6 in natural scenes; Billock, 2000; Burton & Moorhead, 1987; Hansen & Essock, 2005; Oliva & Torralba, 2001; Tolhurst, Tadmor, & Chao, 1992; van der Schaaf & van Hateren, 1996). As humans are most likely to encounter natural environments with amplitude spectrum slopes values near 1.0, it has been argued by multiple studies that the human visual system should be tuned to best process broadband[3] visual information with $1/f$ amplitude spectra (Field, 1987; Geisler, 2008; Knill, Field, & Kersten, 1990; Párraga, Troscianko, & Tolhurst, 2000; Tadmor & Tolhurst, 1994). One of the most utilized techniques to verify if human observers are ideally suited to process images with naturalistic (α = 1.0) amplitude spectra has been to measure their ability to discriminate between images (noise or natural) that vary in their α (Ellemberg, Hansen, & Johnson, 2012; Hansen & Hess, 2006; Johnson, Richard, Hansen, & Ellemberg, 2011; Knill et al., 1990; Párraga & Tolhurst, 2000; Tadmor & Tolhurst, 1994). While the psychophysical techniques used to measure the tuning characteristics of α discrimination thresholds have varied[4], there is a general concensus that human observers show lower thresholds (i.e., highest sensitivity) when α is between 1.2 – 1.4, and elevated threshods when α is less than 1.0 or greater than 1.4. These data further support the notion that the human visual system is best suited to process natural images with $1/f$ amplitude spectra with exponents near the average α of natural scenes. Yet, they offer little information regarding the characteristics of the encoding mechanism responsible for the discrimination of images that vary in α.

The early stages of vision rely on a series of functionally different neurons tuned to a narrow range of orientation and spatial frequency - that behave like non-linear filters (Bergen, Wilson, & Cowan, 1979; Blakemore & Campbell, 1969; Campbell & Robson, 1968; Carandini et al., 2005; De Valois, Albrecht, & Thorell, 1982; De Valois, Morgan, & Snodderly, 1974;

[3] The term broadband here is used to define a stimulus that contains a significant amount of luminance contrast across multiple spatial frequencies and orientations.

[4] Part of the differences in the measured α discrimination thresholds can be attributed to the psychophysical methods employed by experimenters. For example, Hansen and Hess (2006) demonstrated that peak in α discrimination thresholds found for reference α values of 0.8 is only prominent when stimuli are presented in the parafovea (Tolhurst and Tadmor, 1994) and not at fovea (Knill et al., 1990). Other differences can also be explained by the use of natural images as opposed to fractal noise patterns ($1/f^{\alpha}$ noise images) to measure α discrimination thresholds.

Enroth-Cugell & Robson, 1966; Graham & Nachmias, 1971; Graham, 1989; Henning, Hertz, & Broadbent, 1974; Maffei & Fiorentini, 1973; Stromeyer & Julesz, 1972; Wilson & Bergen, 1979; Wilson, McFarlane, & Phillips, 1983). Within the psychophysical literature, groups of neurons with similar spatial frequency and/or orientation selectivity are collectively referred to as channels. These channels were once thought to operate independently (Blakemore & Campbell, 1969; Campbell & Robson, 1968), but are now known to interact with similarly and differently tuned channels (DeAngelis, Robson, Ohzawa, & Freeman, 1992; Henning et al., 1974; Legge & Foley, 1980; Meese & Hess, 2004; Meese & Holmes, 2010; Morrone, Burr, & Maffei, 1982; Olzak & Thomas, 1999; Petrov & Mckee, 2006; Polat & Sagi, 1993; Stromeyer & Julesz, 1972; Wilson & Wilkinson, 1997). The interactive behaviour of channels is of particular relevance to the description of the encoding of a stimulus broadband in spatial frequency and orientation content (i.e., natural scenes; Hansen, Essock, Zheng, & DeFord, 2003; Hansen, Haun, & Essock, 2008; Haun & Essock, 2010). However, initial attempts to define the contribution of spatial frequency channels exposed to stimuli with naturalistic α relied more heavily on the description of single channel behaviour (i.e., grating contrast discrimination), than on their potential interactive properties (Tadmor & Tolhurst, 1994; Tolhurst & Tadmor, 1997). Specifically, these early attempts to define α discrimination according to the responses of channels in early vision attributed the ability to detect a change in α to the activity of a single spatial frequency channel, and thus defined α discrimination as a band-limited contrast operation (Peli, 1990). However, this band-limited contrast approach to the definition of contrast in natural images has since been shown to be a poor predictor of detectability of contrast (Bex & Makous, 2002), and could only somewhat predict the measured α discrimination thresholds (Tadmor & Tolhurst, 1994; Tolhurst & Tadmor, 1997). Furthermore, it is difficult to justify that the behaviour of a single spatial frequency channel is sufficient to describe the detection and the discriminability of broadband images (Bex et al., 2009; DeAngelis et al., 1992; Elliott, Georgeson, & Webster, 2011; Hansen et al., 2003, 2008; Haun & Essock, 2010; Párraga et al., 2005; Párraga & Tolhurst, 2000; Wilson & Wilkinson, 1997). Instead, interactive multi-channel approaches to the definition of channel behaviour under naturalistic stimulation seem a more likely approach to describe natural scene perception (Brady & Field, 1995; Field & Brady, 1997; Párraga & Tolhurst, 2000; Párraga et al., 2005; Tolhurst & Tadmor, 1997).

There is psychophysical evidence that human observers may use contrast within multiple spatial frequency bands in order to discriminate between images that vary in α. By increasing or decreasing the contrast of the entire spatial frequency spectrum of natural images, Párraga and Tolhurst (2000) were able to modulate the contrast of an image while leaving its original α unaltered. They postulated that if observers relied on single spatial frequency band to discriminate α, then discrimination thresholds should be affected by the contrast manipulation they implemented in a manner similar to the band-limited contrast modulations of Tadmor and Tolhurst (1994) and Tolhurst and Tadmor (1997). Similarly, they argued that α discrimination thresholds would not be altered if observers compared contrast between two of more spatial frequency bands, as the relative difference in contrast between two or more bands remains the same. They found that α discrimination thresholds were unaffected by their contrast modulation when the reference α had a value of 1.0 or 1.4, which indicates that observers rely on the relative difference in contrast across multiple spatial frequency bands when discriminating αs. When α was very shallow (α = 0.4), discrimination thresholds were affected by their manipulation, which suggest discrimination of very shallow αs (beyong the natural range) may operate according to a different process (e.g., within a single spatial frequency band).

Although Párraga and Tolhurst (2000) demonstrated that a multi-channel approach to α discrimination was a more likely mechanism than earlier single-channel models, they did not postulate on the underlying interactions between multiple channels that may be involved in α discrimination. That is, subsequent multi-channel approaches to broadband stimulus perception have shown that the introduction of a bias in the weights given to the responses of different spatial frequency channels tends to better predict human performance than when all channels are weighted equally (typically defined as low-pass contrast gain control processes; Bex, Mareschal, & Dakin, 2007; Bex et al., 2009; Cass, Alais, Spehar, & Bex, 2009; Haun & Essock, 2010; Haun & Peli, 2013; Schwartz & Simoncelli, 2001; Tajima & Okada, 2010). For example, human observers adapted to 1/*f* noise patterns (with different αs) showed reduced contrast sensitivity to lower and mid-range spatial frequencies, while contrast sensitivity to higher spatial frequencies remained unaltered (Webster & Miyahara, 1997). As adaptation effects are believed to stem from readjustments in contrast gain control (Wilson & Humanski, 1993) this suggests that the reduced contrast sensitivity to low spatial frequencies can be attributed to the disproportionately large responses of low spatial frequency channels to 1/*f* noise images (Webster & Miyahara, 1997).

There are additional neurophysiological studies that point to a low spatial frequency bias in the processing of broadband stimuli (Hansen et al., 2012, 2011).

Spatial frequency channels tuned to lower spatial frequencies generate disproportionally large responses to noise images with 1/*f* amplitude spectra, and thus, may serve as the dominant coding signal for α (Hansen et al., 2012, 2011; Webster & Miyahara, 1997). Interestingly, the influence of lower spatial frequency channels may be dependent on the value of α. That is, while contrast sensitivity to low spatial frequency was always decreased following adaptation to a noise image, regardless of its α value, the extent of higher spatial frequencies affected by the adaptation protocol did vary according to α. That is, when α was equal to 0 (i.e., white noise), the slight decrease in contrast sensitivity was equal across all spatial frequencies. However, when α was fairly steep (between 2 and 2.5) adaptation effects were concentrated to spatial frequencies equal to or less than 2 cycles/°. Noise images with α = 1.0 had the broadest impact on contrast sensitivity, which decreased contrast sensitivity to spatial frequencies up to 8 cycles/°, and is most likely explained by the response characteristics of channels to broadband images with α of 1.0[5] (Brady & Field, 1995; Field & Brady, 1997; Field, 1987). This correlation between the adaptation effects and the α value indicates that the underlying spatial frequency channel interactions responsible for readjusting the activity of channels are dependent not only on low spatial frequency luminance contrast, but also on the particular distribution of luminance contrast across spatial frequency (i.e., α).

There is evidence that the responses of spatial frequency channels to broadband stimuli with 1/*f* amplitude spectrum may be biased towards lower spatial frequencies, and that this may be regulated by the rate of descent of luminance contrast across spatial frequency (α). However, there is to date no psychophysical evidence that this may influence observer's ability to detect, and discriminate, a change in α. Therefore, the goal of this study was to assess whether luminance contrast at lower spatial frequencies is involved in α discrimination. In **Experiment 2.1**, α discrimination thresholds were measured to progressively larger 1/*f* noise images in, generated according to 5 different reference αs (0.4, 0.7, 1.0, 1.3, and 1.6) in order to measure how the additional low spatial frequency content of larger stimuli may influence α discrimination thresholds. We opted to manipulate the low spatial frequency content of our stimuli via changes

[5] See the results and discussion section of Experiment 1 for further details on the model defined by Field (1987), Brady and Field (1995) and Field and Brady (1997).

in size, as opposed to any form of band-pass or low-pass filters, because the removal of spatial frequency content in 1/*f* noise images rapidly leads to a loss of their spectral quality that alters α discrimination thresholds in a manner too extreme to compare with other studies (Richard, Hansen, Ellemberg, & Johnson, 2013). We found that slope discrimination thresholds decreased as stimulus size increased most when the reference α equalled 1.0, and less so for steeper ($\alpha > 1.0$) and shallower ($\alpha < 1.0$), which suggests that this effect may be attributed to the perceived contrast of 1/*f* noise images (Baker & Graf, 2009; Brady & Field, 1995; Hansen & Hess, 2012; McDonald & Tadmor, 2006).

The nature of our manipulation in **Experiment 2.1** cannot account for other factors than additional low spatial frequency luminance contrast in the facilitation effect we identified in **Experiment 2.1**. Specifically, summation effects of both medium and high spatial frequency luminance contrast may account for the decrease in slope discrimination thresholds that followed increases in stimulus size in **Experiment 2.1**. In **Experiment 2.2** we aimed to address this issue by with a centre-surround α discrimination paradigm (Johnson et al., 2011), and varied the gap size between the centre and surround stimuli in order to isolate the involvement low spatial frequency channel interactions in our slope discrimination task. For all gap sizes, α discrimination thresholds for steep (α equal to or greater than 1), but not shallow α, decreased with the presence of a surround. These findings suggest that, in a manner similar to the perceptual effects described by Webster and Miyahara (1997), α discrimination thresholds are subject to the response, and interactions, of low spatial frequency channels, but that these are somewhat regulated by the reference α of the discrimination task.

Experiment 2.1

Method

Participants

Seven adults (5 females) between the ages of 19 and 23 (Median Age =21 years) participated in the experiment. All participants were experienced psychophysics observers with normal or corrected-to-normal visual acuity, and were all naïve to the aims of the experiment. Informed consent was obtained from all participants and all were treated in accordance the Tri-Council Policy Statement: Ethical Conduct for Research Involving Humans (2014). Participants were all consenting volunteers.

Apparatus

Stimuli were presented on a 22.5" Viewsonic (G225fB) monitor driven by an Apple Mac Pro (2 X 2.66GHz processor) equipped with 8GB of RAM and a 1GB PCIe x16 ATI Radeon HD 5770 Graphics card with 10-bit grayscale resolution. Stimuli were displayed using a linearized look-up table, generated by calibrating with a Color-Vision Spyder3 Pro sensor. Maximum luminance output of the display monitor was 100 cd/m^2 (50 cd/m^2 mean luminance after calibration) the frame rate was set to 100 Hz, and the resolution was set to 1024 X 768 pixels. Single pixels subtended .0381° of visual angle (i.e., 2.23 arc min.) when viewed from 1.0 meter. Head position was maintained using a chin rest, and participant input was recorded via keyboard press.

Stimuli

All stimuli consisted of synthetic visual noise patterns that were constructed in the Fourier domain using MATLAB (ver. 2012b; Mathworks, Natick, MA, ver. 2012b) and corresponding Image Processing (ver 6.4) toolbox. We created the visual noise stimuli by constructing a 512^2 polar matrix for the amplitude spectrum, and assigning all coordinates the same arbitrary amplitude coefficient (except at the location of the DC component, which was assigned a value of 0). The result is a flat isotropic broadband spectrum (i.e., $\alpha = 0.0$), referred to as the template amplitude spectrum (Hansen & Hess, 2006; Tadmor & Tolhurst, 1994). In this form, the α of the template spectrum can be adjusted by multiplying each spatial frequency's amplitude coefficient by f^{α}. The phase spectra were constructed by assigning random values from $-\pi$ to π to the different coordinates of a 512^2 polar matrix, while maintaining an odd symmetric phase relationship. The phase spectrum for all stimuli presented within a trial was identical, but was randomized from trial-to-trial. The noise patterns were rendered into the spatial domain by taking the inverse Fourier transform of an α-altered template amplitude spectrum and a given random phase spectrum.

When the slope of the amplitude spectrum is changed, the total power within the spectrum is also changed. This may introduce a cue to observers during the slope discrimination task, as observers may no longer discriminate the images based on their relative slopes, but instead detect changes in the overall power of images. To avoid this potential artefact, all noise patterns were scaled in the spatial domain to have the same grayscale mean (0.5 on a 0 – 1 scale)

and RMS contrast (RMS = 0.15), defined as $RMS = \frac{1}{NM}\sqrt{\sum_{i=1}^{N}\sum_{j=1}^{M}\left(I_{ij} - \bar{I}_{ij}\right)^2}$, (see Tadmor & Tolhurst, 1994; Hansen & Hess , 2006), to ensure that the total power across all noise images (regardless of assigned α value) was equivalent (i.e., RMS contrast of an image is equal to the square root of the power spectrum; Smith, 2007). This transformation does not, however, equate the amplitude coefficients across all assigned α value (see **Figure 2.1**). It is important to note that with broadband images, RMS contrast has been found to be the most reliable indicator of visibility of the image (as opposed to non-squared metrics, including Michelson Contrast), in line with others that have used compound gratings and noise images (Bex & Makous, 2002; Watson, 2000). Therefore, RMS contrast is the standard metric to use when defining contrast in natural images (Frazor & Geisler, 2006), and equating the power spectrum by adjusting the RMS contrast of our images ensures observers do not use spurious cues other than changes in the slope of the amplitude spectrum (or power spectrum) in our task. The noise patterns were rendered into the spatial domain by taking the inverse Fourier transform of the amplitude spectrum and a given random phase spectrum, with both shifted to Cartesian coordinates prior to the inverse DFT From each 512^2 polar matrix noise image, an image patch was cropped from its centre and windowed with a cosine-tapered envelope, which ramped 5% of the image pixels in the proximity of the circle's edge to mean luminance (50 cd/m^2). Stimuli were generated with respect to five reference slope (α) values (0.4, 0.7, 1.0, 1.3, and 1.6) and cropped with respect to 9 window sizes (0.75, 1, 1.41, 2, 2.83, 4, 5.66, 8, and 11.3 degrees of visual angle). The smallest stimulus, 0.75°, contained slightly over four octaves of spatial frequency content (1.346 – 22.881 cpd), while the largest stimulus contained nearly eight octaves of spatial frequency content (0.088 – 22.881 cpd; see **Figure 2.2C**), with its lowest spatial frequency nearly 4 octaves below that of our smallest stimulus.

Psychophysical Procedures

The experimental conditions consisted of 5 reference slope values and 9 stimulus sizes for a total of 45 stimulus condition blocks. Each block was repeated twice, and the calculated thresholds for both blocks were averaged prior to data analysis. Stimulus size remained constant within each block, and the order of blocks was randomized between repetitions and observers. Thresholds were estimated by a temporal three-interval, two-alternative "Odd-Man-Out" forced choice task similar to that used by Hansen & Hess (2006) and Johnson and colleagues (2011).

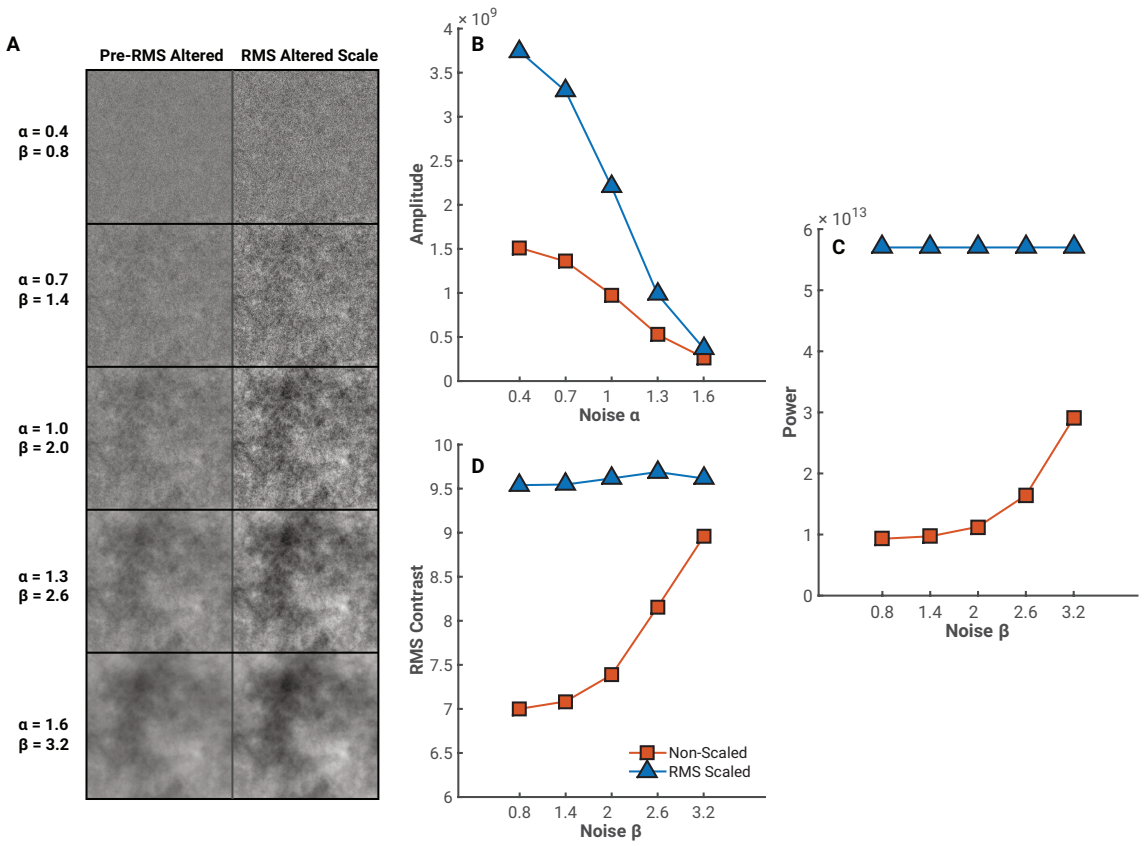

Figure 2.1. A Examples of the 5 reference α presented to observers prior to and following RMS normalization. The slope value measured in the amplitude spectrum (α) and power spectrum (β) are reported here for notation consistency when describing the spectral properties of our stimuli. **B** The sum of the amplitude coefficients of our stimuli for all 5 reference α values prior to and following RMS adjustments. Note that the sum of the amplitude coefficients, both prior to and following RMS adjustments, is greatest for shallow slope values (α = 0.4) and smallest for steeper slopes (α = 1.6). **C** The sum of the power spectrum coefficients for all 5 reference β values presented to observers. While the total power in our stimuli increases as a function of slope (β – red line) it is identical for all reference β values following RMS normalization. **D** The RMS contrast measured for our stimuli both prior to and following RMS normalization. As RMS contrast is directly related to the power spectrum, the effect of RMS normalization on total power in our stimuli is identical to that seen with RMS contrast.

Participants were asked to select the stimulus, either the first or third presented, that contained the odd-amplitude spectrum – different from the reference stimulus, presented in the second interval. For any given trial, the phase spectrum of all three stimuli presented was identical, and stimuli only varied in their slope (α).

At the beginning of each trial, a white (RGB [255, 255, 255]) fixation cross, which subtended 0.3° of visual angle in diameter was presented for one second at the centre of the screen. This was followed by three stimulus presentation intervals that each lasted 250ms. The second interval always contained the reference amplitude spectrum set at one of the five fixed reference α values (0.4, 0.7, 1.0, 1.3, and 1.6). One interval, either the first or the third, contained the same amplitude spectrum as that of the reference interval, while the other contained the test amplitude spectrum with a slope α steeper than the slope α of the reference interval. Each stimulus interval was interlaced by a screen set to the mean luminance of our display (RGB [128, 128, 128]) for 500ms (see **Figure 2.2**). The interval that contained the test amplitude spectrum was randomized on each trial. At the end of each trial, the screen was set to mean luminance, and participants indicated which interval, either the first or the third, they perceived as being the "Odd-Man-Out" in comparison to the second interval (reference) via keyboard press. Viewing was binocular and the duration of the response interval was unlimited.

The trial-to-trial change in the image's slope exponent (α) was controlled by a transformed 1-up, 2-down staircase procedure using the *PAL_AMUD_setupUD* and *PAL_AMUD_updateUD* functions from the Palamedes toolbox for MATLAB (Prins & Kingdom, 2009). The staircase approached the reference α value from above; hence, the α of the test interval was always steeper than that of the reference α. The initial α of the odd stimulus was α+0.5 units above the reference value. The α of the test interval was decreased in linear steps (step size down = 0.02) towards the reference α when the observer made two consecutive correct responses, and was increased in linear steps (step size up = 0.02) back towards the start value when the observer made an incorrect response (1 Up / 2 Down Rule). The procedure targeted the 70.71% performance level on a psychometric function (Kaernbach, 1991; Prins & Kingdom, 2009). In order to prevent extreme α values when estimating thresholds, the minimum possible α of the odd stimulus was set to the reference α value and the maximum was set to an α = 3. The experimental block continued until 12 reversals had occurred, at which point the block was terminated. Thresholds were estimated by averaging the slope α values of the odd stimulus for the last 5 reversals.

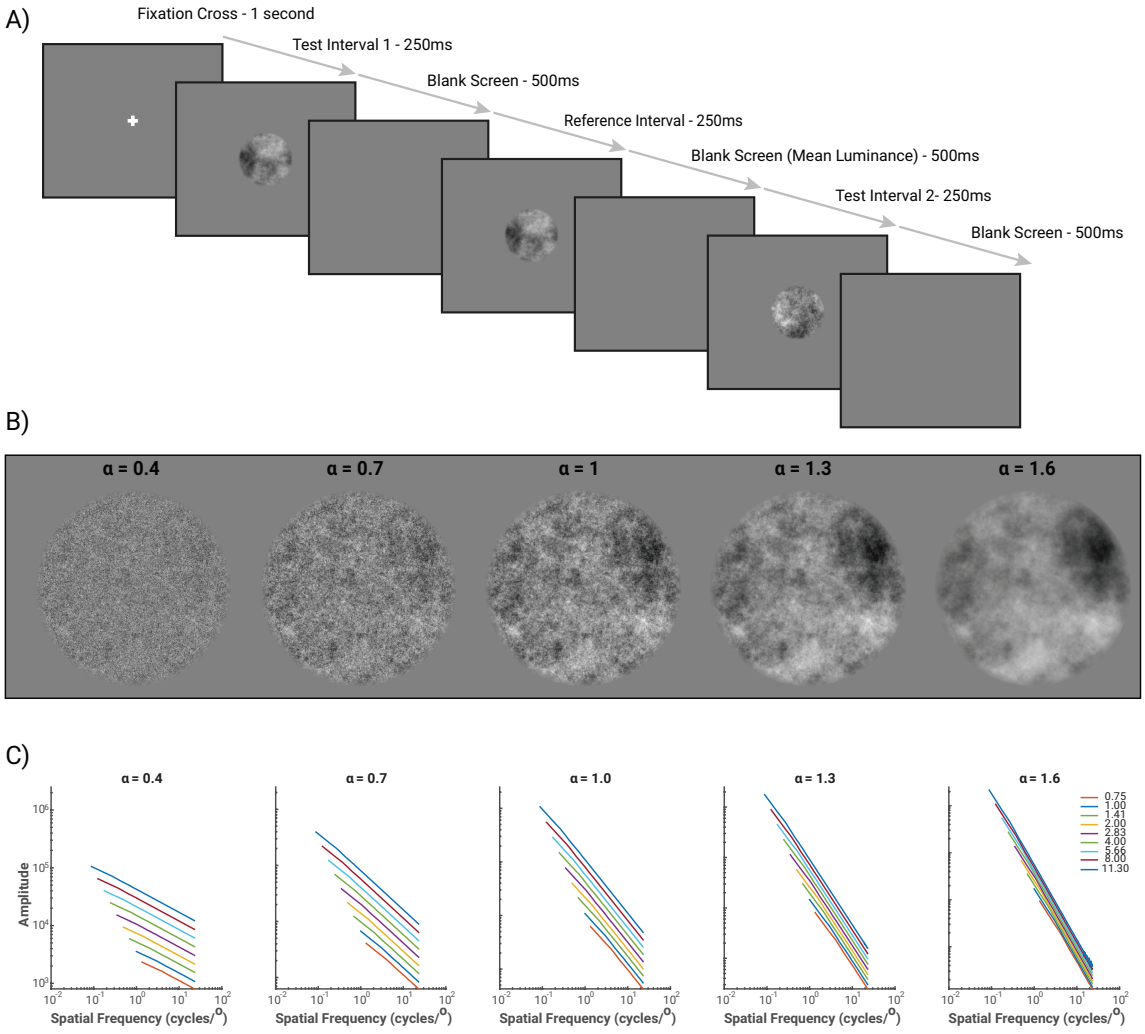

Figure 2.2. A General psychophysical procedure employed in our experiment. To estimate slope discrimination thresholds, all observers completed a 3-IFC, 2-AFC "Odd-Man-Out" psychophysical procedure. Observers had to indicate, which of the 1st or 3rd interval contained the stimulus that was different from the second – reference – interval (here the odd stimulus is the 3rd). **B** Example stimuli of the 5 reference α values used in this experiment. The phase spectrum of all 5 stimuli presented is identical. **C** The amplitude spectrum for all 5 reference α values and 9 stimulus sizes presented to observers in this study. Increases in stimulus size lead to addition low spatial frequencies for all stimuli. The smallest stimulus (0.75 degrees) contained nearly 4 octaves of spatial frequency content (min_{sf} = 1.346 cpd, max_{sf} = 22.881 cpd) while the largest contained nearly 8 octaves of spatial frequency content (min_{sf} = 0.088, max_{sf} = 22.881 cpd), which is an additional 4 octaves of low spatial frequency content in comparison to our smallest stimulus size.

Results and Discussion

The average decrease of α discrimination thresholds (Δαs) as a function of stimulus size for all five reference αs is show in **Figure 2.3A**. We first conducted a 9 (stimulus size) by 5 (reference α) repeated measures ANOVA on slope discrimination thresholds to verify for any interactive effects between stimulus size and reference α (see **Tables 2.1 – 2.3**). The interaction term was not statistically significant, $F(32, 192) = 0.675$, $p = .906$, $\eta_p^2 = .101$. However, both the main effects of stimulus size, $F(8, 48) = 41.85$, $p < .001$, $\eta_p^2 = .875$, and reference α, $F(4, 24) = 4.10$, $p = .011$, $\eta_p^2 = .406$ were statistically significant. The main effect of size on Δαs was well explained by a linear trend with coefficients [4 3 2 1 0 -1 -2 -3 -4], $F(1, 6) = 60.00$, $p < .001$, $\eta_p^2 = .909$. Increases in area, and therefore the additional low spatial frequency content of our stimuli, had a facilitatory effect on slope discrimination thresholds. The main effect of reference α on Δαs was best fit by a cubic trend (coefficients [-1 2 0 -2 1]), $F(1,6) = 31.16$, $p = .001$, $\eta_p^2 = .839$, which follows the typically reported shape of slope discrimination thresholds across different α (Hansen & Hess, 2006; Johnson et al., 2011; Knill et al., 1990; Tadmor & Tolhurst, 1994).

Given that no interactive effects between stimulus size and reference α were statistically significant, we calculated log ratios [$\log(\Delta\alpha_i/\Delta\alpha_{largest})$] in order to compare, for each reference α, the relative influence of increases in stimulus size on Δαs. Specifically, we aimed to identify the size at which Δαs showed no significant improvement from further increases in stimulus size. The average log ratios for all five reference αs are shown in **Figure 2.3B**. It is clear that log ratios followed a quadratic trend across all stimulus sizes (coefficients [-2 -1 1 -1 -2]), $F(1,6) = 15.02$, $p = .008$, $\eta_p^2 = .715$, whereby log ratios for α = 1.0 were greater than all other αs (see **Tables 2.4-2.6**). There is a small asymmetry in our experimental results between αs > 1 and αs < 1, as the latter shows a slightly steeper descent than the former. Specifically, while Δαs for shallow slopes showed little change for stimulus sizes larger than 4° (α = 0.4: log ratio_{4°= -0.06, 95% CI [-0.69 0.56]) or 5.66° (α = 0.7: log $\text{ratio}_{5.66^\circ}$= .23 95% CI [-0.13 0.59]), Δα for reference stimuli with α = 1 still improved when stimulus was increased from 8° to 11.3° stimulus (log ratio_{8°= 0.49, 95% CI [0.03 0.96]). Steep reference slopes (α = 1.3 and 1.6) both showed improvements in Δαs that mirrored the shallower αs (α = 0.4 and 0.7): α = 1.3 showed significant improvement in Δαs at our largest stimulus size (log ratio_{8°= 0.34, 95% CI [0.10 0.58]), while the

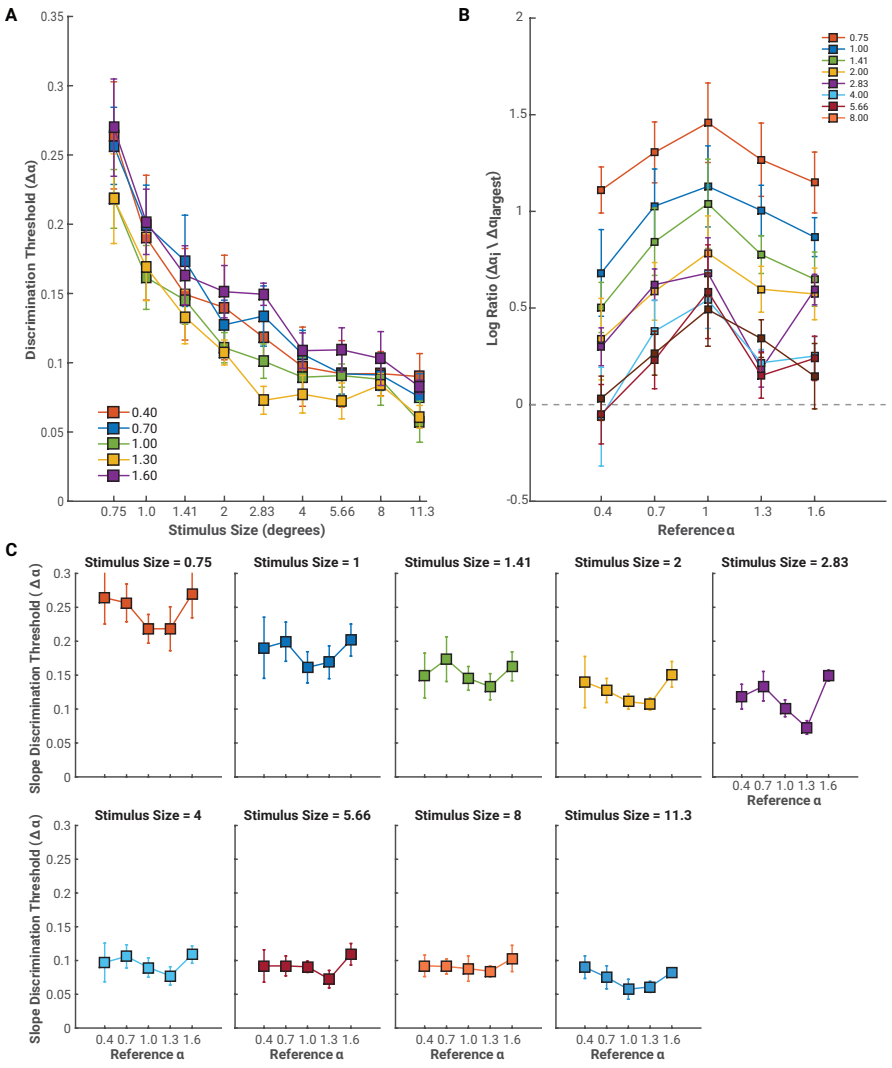

Figure 2.3. A The average slope discrimination threshold plotted as a function of stimulus size (abscissa). Each line represents averages thresholds for a given reference α. We find a statistically significant effect of stimulus size and a statistically significant effect of reference α, but no interaction effect. Therefore, all slope discrimination thresholds decreased as a function of increased stimulus size and this effect was similar for all reference α used in this study. **B** Average log ratios between slope discrimination thresholds (Δαs) against our largest stimulus size (11.3°). Values larger than 0 indicate that Δαs were greater than those of the 11.3° stimulus. Most observers show the largest log ratio for a reference α = 1 and smaller log ratios for steeper and shallower slope. **C** Slope discrimination thresholds for all 5 reference alpha at each stimulus size. Error bars in **A**, **B** and **C** represent ± 1 standard error of the mean.

steepest reference α used here showed no improvement for stimulus sizes beyond 4°(log $ratio_{5.66°}$= .24 95% CI [-0.04 0.52]).

We had hypothesized that steeper αs (α > 1) should be most subject to the effects of increases in stimulus size as the low spatial frequency luminance contrast is significantly greater in steep αs, and may thus be more relevant to discrimination than for shallower αs (e.g., α = 0.4). However, increases in stimulus size had a facilitatory effect on α discrimination thresholds for all reference α: α discrimination thresholds for a reference α of 1.0 benefitted most from increases in stimulus size, while steeper and shallower reference αs showed more moderated decreases in α discrimination thresholds. This suggests that the luminance contrast at low spatial frequencies might be important in a slope discrimination task, particularly when the reference α is close to the natural scene average (α = 1.08; Billock, 2000; Burton & Moorhead, 1987; Field, 1987; Hansen & Essock, 2005; Tolhurst et al., 1992). It is also interesting to find that α discrimination thresholds continued to benefit from increases in stimulus size beyond a stimulus size of 8° in diameter, as it indicates that observer may sample luminance contrast from fairly low spatial frequency bands in an α discrimination task, at least lower than what has previously been described (~ 1 cycle/°; Tadmor & Tolhurst, 1994; Tolhurst & Tadmor, 1997). That is, if observers sampled the luminance contrast within a single spatial frequency band, we should have found no facilitation of α discrimination thresholds when increasing size beyond a certain critical value as the additional luminance contrast added should eventually extend beyond the monitored band. This account may only hold for α values typically encountered within the natural environment as the facilitation observed for α discrimination thresholds for reference α of 0.4 floored at a stimulus size of 4°. This finding is analogous to others that have found images with very shallow α (e.g., 0.4) to be discriminated according to a different mechanism than images with more "naturalistic" αs (Párraga & Tolhurst, 2000).

A potential account for the quadratic trend observed across αs in our log ratio data may lie in how the visual system pools contrast over spatial frequency and space, and its effects on the perceived contrast of broadband images (Baker & Graf, 2009; Field & Brady, 1997; Hansen & Hess, 2012; McDonald & Tadmor, 2006; Tolhurst & Tadmor, 2000). It has been demonstrated that human observers perceive noise stimuli with an α = 1.0 to have greater contrast than steeper or shallower α (Baker & Graf, 2009; Hansen & Hess, 2012). These effects have also been measured in centre-surround paradigms where a surround annulus with an α = 1.0 suppresses the

perceived contrast of a centre stimulus more than a surround with any other α (McDonald & Tadmor, 2006). The benefits of increasing stimulus size on α discrimination thresholds show a similar effect as thresholds for reference α = 1.0 decreased most as stimulus size increased. There exist a multi-channel model of perceived contrast in complex images, including noise images with 1/*f* amplitude spectra proposed by Field, (1987), Brady and Field (1995), and Field and Brady (1997) that predicts larger responses from psychophysical spatial frequency channels to noise images with α = 1.0. In their model, filter bandwidth (1 octave) is held constant in octaves on logarithmic axes, and the peak sensitivity of filters is held constant as well. When given noise images with varying α, the pooled responses of these psychophysical channels to the stimulus are greatest when α = 1.0, and decrease in magnitude for steeper (α > 1.0) and shallower (α < 1.0) αs. While their model generates filter outputs that are correlated with the perceptual experience of observers, there is little evidence to suggest that the channel bandwidth (constant, 1 octave bandwidth) used in this model is neurophysiologically relevant. Indeed, most evidence (both psychophysical and neurophysiological) has demonstrated that the bandwidth of visually responsive neurons within striate cortex (De Valois et al., 1982; Tootell, Switkes, Silverman, & Hamilton, 1988; Yu et al., 2010), and psychophysical spatial frequency channels (Wilson et al., 1983) decreases with increasing preferred spatial frequency. That said, this is of little impact on the model's ability to predict larger pooled filter outputs, as more physiologically plausible channel bandwidths still generate larger responses to noise images with an α = 1.0 (Hansen & Hess, 2012)[6].

The quadratic trend observed across α was maintained across all increments in stimulus size (see **Figure 2.3B**), which is required for supra-threshold stimuli (Cannon & Fullenkamp, 1988), and thus indicates that the responses of spatial frequency channels are adjusted via a contrast gain control mechanism in accordance with stimulus size changed (Brady & Field, 2000; Carandini, Heeger, & Movshon, 1997; Carandini & Heeger, 1994; Foley, 1994; Graham & Sutter, 2000; Heeger, 1992; Watson & Solomon, 1997; Wilson & Humanski, 1993; Yu, Romero,

[6]Hansen and Hess (2012) demonstrated that the exact bandwidth of the spatial frequency filters used, either those defined by Brady and Field (1995) or those of Wilson and colleagues (1983), to generate spatial frequency channel responses to broadband noise images had little impact on the response magnitude to images with an α = 1.0. However, the pooled (summed) filter responses to noise images with different α did change according to the bandwidth of filters. Specifically, the response magnitude of constant 1 octave bandwidth filters to noise images with α = 1.5 were slightly greater than to α = 0.0 (although quasi-identical), while the difference in the response magnitude for both αs increase drastically when the filter bandwidth was made to decrease with increasing spatial frequency (the model outputs to α = 1.5 and α = 1.0 were much more similar).

& Lee, 2005). Given that our stimulus manipulation was intended to increase the representation of low spatial frequency luminance contrast within our stimuli, any form of normalization following the pooling of responses from spatial frequency channels should be low-pass in spatial frequency (Cass, Stuit, et al., 2009; Haun & Peli, 2013; Meese & Holmes, 2007). That said, it is difficult to reconcile how a contrast gain control process that is predominantly low-pass may allow for human observers to sample the low-spatial frequency luminance contrast of 1/*f* noise images when asked to discriminate their α and generate large increases in sensitivity as stimulus size increases. It is possible that the contrast gain control mechanism, which normalizes the activity of channels tuned to various spatial frequencies, is not perfect as has previously been argued by Párraga and Tolhurst (2000). However, it is also likely that observers do not sample the additional luminance contrast at low spatial frequencies, and instead benefit from other psychophysical mechanism that can take advantage of the increases in stimulus size. For example, the summation of higher spatial frequency content may have facilitated α discrimination thresholds (Baker & Meese, 2011; Graham & Sutter, 1998; Graham, 1989; Hutchinson & Ledgeway, 2010; Meese & Baker, 2011, 2013; Meese & Summers, 2007; Taylor, Bennett, & Sekuler, 2009), and other types of interactions between spatial frequency channels (e.g., contextual interactions) than contrast gain control may also have been responsible for the effects found here. We test these assumptions in **Experiment 2.2**.

Experiment 2.2

The changes in stimulus size implemented in **Experiment 2.1**, while a simple and convenient manipulation of low spatial frequency content in our stimuli, cannot account for other factors that can modulate α discrimination thresholds. For example, the increase in stimulus size will also lead to spatial summation effects, which may cloud any contribution of low spatial frequencies to slope discrimination thresholds (Baker & Meese, 2011; Graham & Sutter, 1998; Graham, Robson, & Nachmias, 1978; Meese, Summers, & Baldwin, 2012; Meese & Summers, 2007). Spatial summation of luminance contrast - defined as an increase in sensitivity to a grating when its size or period is increased - is known to occur both at threshold (Graham & Sutter, 1998; Graham & Nachmias, 1971; Robson & Graham, 1981; Stromeyer & Klein, 1975; Watson, 1979), and suprathreshold (Meese & Baker, 2011; Meese & Summers, 2007) and may therefore have been a component of the facilitatory effects witness on α discrimination thresholds in **Experiment 2.1**. Thus, the spatial summation effect of mid- or high spatial

frequencies may also account for any benefits in slope discrimination thresholds we find as a function of increased stimulus size.

Furthermore, it is difficult to assess the particular nature of interactions between spatial frequency channels in α discrimination thresholds from the manipulation we implemented in **Experiment 2.1**. That is, the decrease in α discrimination thresholds as stimulus sized increased may also be attributed to contextual interactions. We have previously shown that α discrimination thresholds are facilitated by the presence of a 1/*f* noise surround annulus with an α similar to that of the centre stimulus (Johnson et al., 2011). As the size of the stimuli we presented to observers in **Experiment 2.1** were fairly large, the facilitatory effects on α discrimination thresholds may stem from centre-surround type interactions, similar to the one we have previously identified. Centre-surround interactions have a longstanding history in psychophysics, and have been the subject of extensive research on how the spatial characteristics of both the centre and surround may inhibit or facilitate psychophysical performance of observers on the centre stimulus, and these are well defined for narrowband stimuli (Cannon & Fullenkamp, 1988; Chubb, Sperling, & Solomon, 1989; Legge & Foley, 1980; Petrov, Carandini, & McKee, 2005; Petrov, Popple, & McKee, 2007; Petrov & Mckee, 2006; Polat & Sagi, 1993; Xing & Heeger, 2000; Xing & Heeger, 2001; Yu, Klein, & Levi, 2001). Typically, the addition of an annulus around the centre stimulus will lead to suppressive interactions, particularly when the centre and surround stimuli have the same, or similar, spatial configurations (e.g., orientation and spatial frequency; Chubb et al., 1989; Petrov et al., 2005; Xing & Heeger, 2000; Xing & Heeger, 2001). Facilitatory effects tend to be slightly more tuned for the dimensions of both the centre and surround stimuli (Xing & Heeger, 2001; Yu et al., 2001; Yu, Klein, & Levi, 2002). Foveally presented stimuli (Xing & Heeger, 2000), surrounds with a greater temporal frequency than that of the centre (Takeuchi & De Valois, 2000), and large gap sizes - up to 12 cycles of the centre spatial frequency - (Polat & Sagi, 1993, 1994) will all generate a net enhancement in the psychophysical performance of observers.

Centre-surround interactions with spatially complex stimuli (i.e., images broadband in spatial frequency and/or orientation) have also been shown to elicit either suppression or facilitation on psychophysical performance both at threshold and above threshold (Goddard, Clifford, & Solomon, 2008; Hansen, Haun, et al., 2008; Hansen et al., 2015, 2003; Haun & Essock, 2010; Johnson et al., 2011; Kim, Haun, & Essock, 2010; McDonald & Tadmor, 2006),

and is known to be regulated by the α of the surround (McDonald & Tadmor, 2006). In their study, McDonald and Tadmor (2006) demonstrated that the perceived contrast of a broadband target (i.e., centre stimulus) decreased most when the surround had an α = 1.0 (identical to that of the target), while the suppressive effects were reduced in magnitude when the difference between the α of the centre stimulus and the surround increased. We have, in addition, show that the ability to discriminate a change in α can be affected by the presence of a surround (Johnson et al., 2011). Observers were asked to discriminate the α of noise images (identical to those presented here) either with or without the presence of a 1/*f* noise surround annulus generated according to an α of 0.7, 1.0, and 1.3, and gap sizes between the center and surround stimuli of 0, 20, 40 and 60 minutes of arc. We found that α discrimination thresholds were facilitated by the presence of a surround, and this effect was greatest when the α of the center and surround stimuli were similar. Most interestingly, we found that changes in the size of the gap between the centre and surround stimuli had little effect on the facilitation of α discrimination thresholds if the surround had an α of 1.0 or 1.3, but the magnitude of the facilitation effect decreased as the gap increased when the surround had an α of 0.7. This decrease in facilitation at larger gap sizes for a surround α of 0.7 was attributed to a loss of high spatial frequency channel interactions that may have contributed to the facilitation effect at smaller gap sizes. Analogously, the perseverance of surround facilitation at large gap sizes when they had steeper αs suggested that any spatial interactions involved in facilitation were based in lower spatial frequency channels. However, facilitation effects in center-surround interactions have been shown to persist up to about 8 – 12 cycles of the center, narrowband target, spatial frequency (Polat & Sagi, 1993, 1994). This means the largest gap size used in our 2011 study of 1° of visual angle (60 arc minutes) was too small to clearly implicate low spatial frequency channel interactions in our surround facilitation findings for steeper surround αs, as interactions between channels with peak frequencies up to 12 cycles/° could have contributed to the facilitation effect. **Experiment 2.2** replicated the Johnson et al. (2011) study, but increased the gap size between the centre stimulus and the surround annulus up to 3.2° of visual angle in order to better isolate the role of lower spatial frequency channel interactions in α discrimination thresholds.

Method

Participants

Six adults (3 females) between the ages of 19 and 27 (Median Age =20.5 years) participated in the experiment. Of the six psychophysical observers, three participated in both experiments. Two of the remaining three observers were also experienced psychophysics observers with normal or corrected-to-normal visual acuity, and all were naïve to the aims of the experiment. The last observer was not naïve to the goals of the study and participated in the original 2011 study. Informed consent was obtained from all participants and all participants were treated in accordance the Tri-Council Policy Statement: Ethical Conduct for Research Involving Humans (Medical Research Council of Canada, 2014). Participants were all consenting volunteers.

Apparatus

Same as **Experiment 2.1**.

Stimuli

The construction of the reference stimuli in **Experiment 2.2** was identical to that of **Experiment 2.1**, with the addition of a second stimulus creation procedure to make the surrounding annuli. The surround annuli were generated from the same 512^2 polar matrix used to generate the centre reference stimuli. This ensured that the phase spectrum of the surround annulus was identical to that of the centre stimulus for each trial. The centre stimuli were cropped to subtend 2°[7] of visual angle on the retina, and their size was fixed for the entire experiment. The surround annulus was windowed with two circular linear edge ramps so to create an annulus, and both its internal and external borders were windowed with a cosine-tapered envelope, which ramped 5% of the image pixels in the proximity of the circle's edge to mean luminance (50 cd/m^2). The visible surround diameter was set to subtend 4° of visual angle on the retina, and its area was constant for all gap sizes. Each stimulus block was generated according to 5 reference α values for the centre stimulus (α = 0.4, 0.7, 1.0, 1.3, and 1.6), 3 α values for the surround annuli (α = 0.7, 1.0, and 1,3) and 5 gap sizes between the centre stimulus and surround annulus (gap = 0, 0.2, 0.4, 0.8, 1.6, and 3.2° of visual angle; see **Figure 2.4**).

[7] We chose a 2° stimulus size as this was the size we used in our original center-surround study (Johnson et al., 2011).

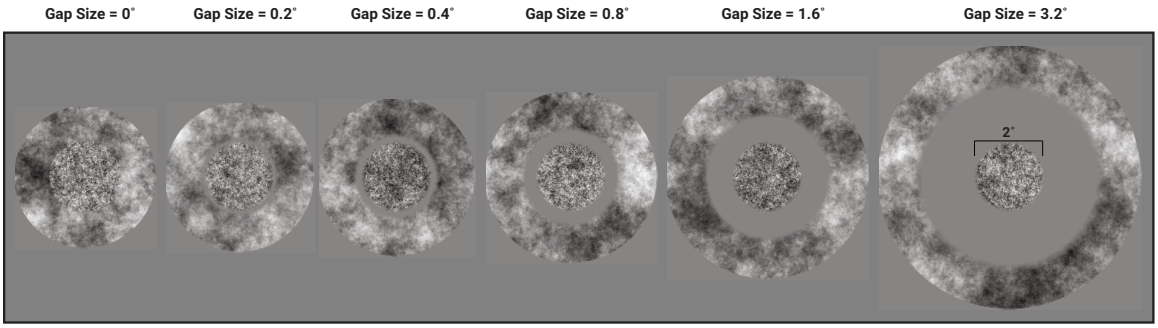

Figure 2.4. All gap sizes used to measure centre-surround interactions in experiment 2. For clarity, the centre α = 0.7, while the surround α = 1.3. The centre stimulus size was kept at 2° of visual angle for all stimulus condition blocks.

Psychophysical Procedures

The experimental conditions consisted of 5 reference slope values, 3 surround slope values, and 6 gap sizes for a total of 90 stimulus condition blocks. As in **Experiment 2.1**, each block was repeated twice, and the calculated thresholds for both blocks were averaged prior to data analysis. Stimulus size remained constant within each block, and the order of blocks was randomized between repetitions and observers. Observers were instructed to ignore the surround for all trials and only base their decision on differences in α for the centre stimulus. All remaining psychophysical procedures were identical to those of **Experiment 2.1** (see **Figure 2.2A**).

Result and Discussion

Average slope discrimination thresholds (Δα) measured both with and without a surround, at each gap size are shown in **Figure 2.5**. The discrimination thresholds measured in this study are lower than those of Johnson et al., (2011). The Johnson et al. (2011) study showed little tuning for α and high discrimination thresholds in the no surround condition (2011: $M_{\Delta\alpha}$ = 0.43, SD = 0.02), however, the centre only thresholds measured here never exceed Δα = 0.15, and show a clear depression in thresholds for α = 1.3 (following typical Δαs; Hansen & Hess 2006). The magnitude of the surround facilitation effect measured here is also smaller than that of the previous study, which is most likely attributable to the lower Δαs (see **Figure 2.5** and **Figure 2** in Johnson et al., 2011).

The effects of a surround on Δα obtained here are similar to those previously reported by Johnson and colleagues (2011). We verified how Δαs varied as a function of gap size for each surround condition separately with a 5 (reference α) X 6 (gap size) repeated measures ANOVA (see Tables **2.7-2.8**). There were no statistically significant interactions, but there was a main effect of gap size on Δαs when the surround α = 0.7, $F(5,25) = 4.61$, $p = .004$, $\eta_p^2 = .480$. The statistically significant main effect was followed by a trend analysis, but none of the typical trends (e.g., linear, quadratic, and cubic) were found to explain a significant portion of the main effect of gap size. In order to define the main effect of gap size, all Δαs were converted into suppression ratios[8] ($SR_{\Delta\alpha}$) by dividing the Δα for a centre with surround conditions by the Δα for

[8] While we only found facilitatory effects of the surround, we use the term suppression ratio as it is a transformation used in the masking literature to define the magnitude of the suppression effect generated by a surround mask.

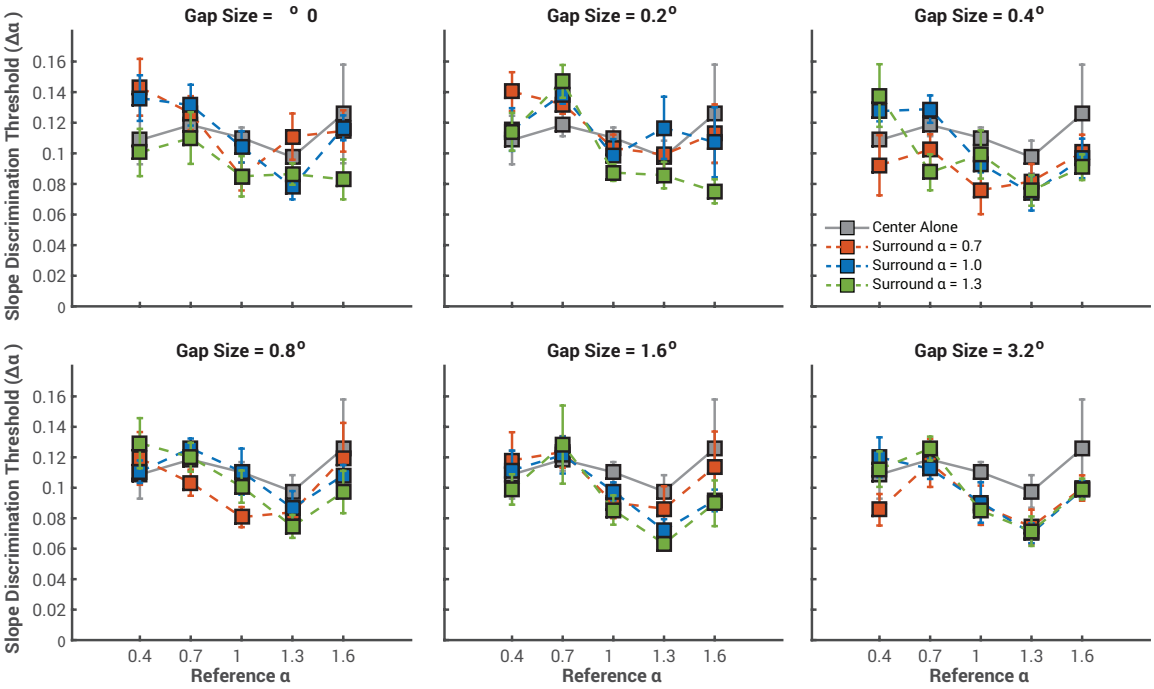

Figure 2.5. Slope discrimination thresholds (Δα) for all stimulus condition blocks. Error bars represent ± 1 standard error of the mean.

the respective centre alone condition, for each participant and gap size configuration (Kim et al., 2010; Petrov et al., 2005; Petrov & Mckee, 2006; Spiegel, Hansen, Byblow, & Thompson, 2012; Xing & Heeger, 2001). $SR_{\Delta\alpha}$ were log transformed prior to all analyses, thus values less than 0 designate net facilitation of Δαs when the surround was present. Cross participant average $SR_{\Delta\alpha}$, for each surround α, gap size and reference α are show in **Figure 2.6A.** Each $SR_{\Delta\alpha}$ was analyzed descriptively by constructing 95% confidence intervals. A $SR_{\Delta\alpha}$ was considered to be "significant" when its confidence interval did not overlap with a value of 0 (no suppression or facilitation from the surround). Two of the six gap sizes, when the surround α was 0.7, showed a significant facilitation effects: the 0.2° gap ($SR_{\Delta\alpha}$ =-0.19, 95% CI [-0.30 -0.09]) and the 1.6° gap ($SR_{\Delta\alpha}$ =-0.24, 95% CI [-0.39 -0.10]). Other than for these two conditions, there was no clear effect of gap size on $SR_{\Delta\alpha}$. The lack of any noticeable effects of gap size on Δα, similar to the findings of the original study (Johnson et al., 2011), suggests that the centre-surround interactions found here operate on a non-local (i.e., global) level, which may be accounted for by the low spatial frequency component of the signal used in higher order stimulus segmentation (Beck, Sutter, & Ivry, 1987; Gurnsey & Fleet, 2001).

The centre-surround effects measured here, while not dependent on gap size were dependent on the α of both the centre and surround stimulus. We found no influence of surround α on Δαs when the centre stimulus reference α was shallow (0.4 and 0.7), but did find that all surround αs decreased slope discrimination thresholds when the reference α = 1.0 (Surround α = 0.7: $SR_{\Delta\alpha}$ = -0.272, 95% CI [-0.421 -0.123], Surround α = 1.0, $SR_{\Delta\alpha}$ = -0.127, 95% CI [-0.214 -0.040], Surround α = 1.3, $SR_{\Delta\alpha}$ = -0.227, 95% CI [-0.323 -0.132]). For centre stimuli with steeper reference αs (1.3 and 1.6) the facilitation observed was slightly smaller than that of the reference α = 1.0 condition. However, this seemed determined by the difference between the centre stimulus α and the surround α, as Δαs for reference α = 1.3 ($SR_{\Delta\alpha}$ = -0.246, 95% CI [-0.377 -0.115]) and 1.6 ($SR_{\Delta\alpha}$ = -0.267, 95% CI [-0.395 -0.138]) showed a significant facilitation effect when the surround α = 1.3. Very similar to the findings of the Johnson et al. (2011) study, center-surround facilitation effects on Δαs are determined by the difference between the centre and surround αs, when both are similar in value and steep (α is equal to or greater than 1), a net facilitation effect is observed, and this effect decreases as the difference between the center and surround αs increases (see **Figure 2.6B**).

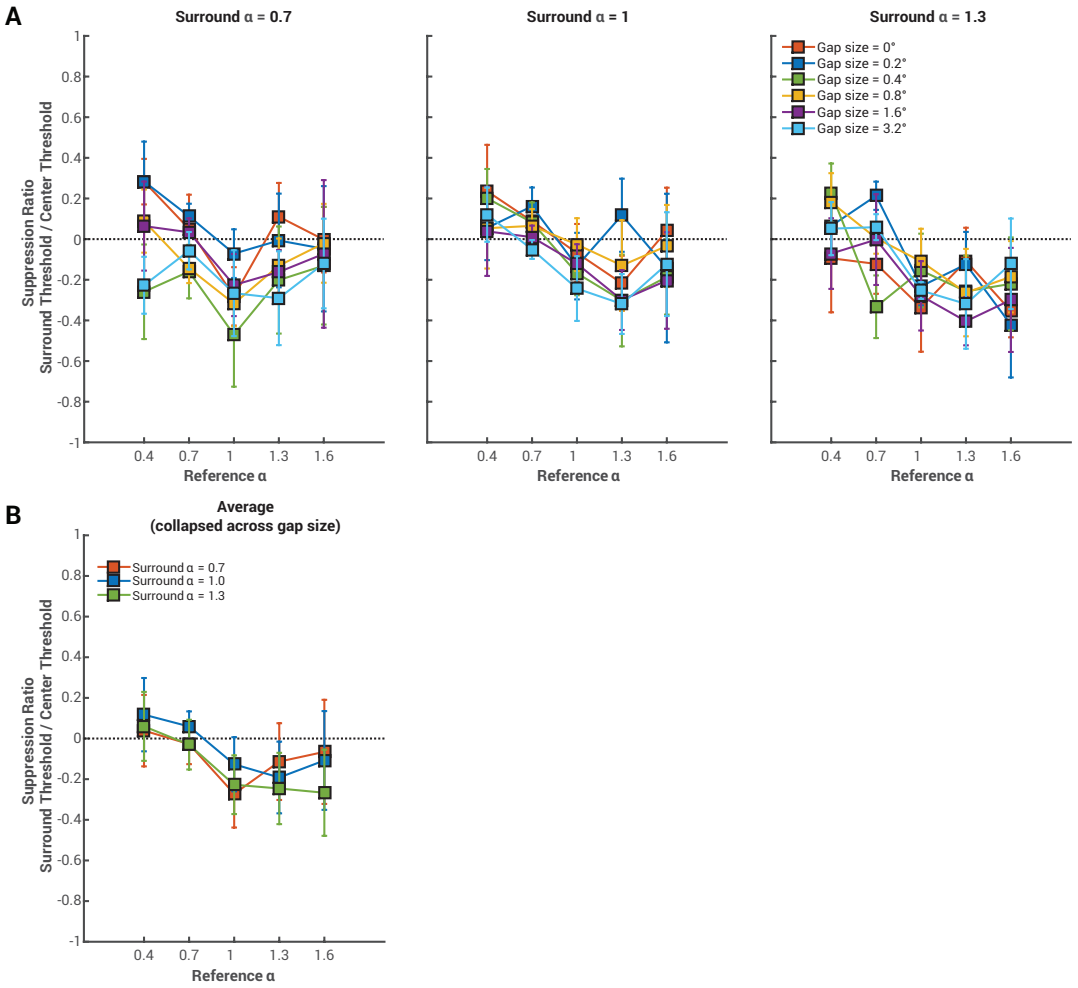

Figure 2.6. A Suppression ratios ($SR_{\Delta\alpha}$ - ordinate) for each reference α for the three surround αs and six gap sizes. Error bars represent the 95% confidence interval of the $SR_{\Delta\alpha}$. Gap size had no specific effect on $SR_{\Delta\alpha}$, and we therefore averaged all suppression ratios across gap size. **B** Average $SR_{\Delta\alpha}$ collapsed across gap size. There is a clear facilitation effect from all three surrounds on Δα for a reference α = 1. Surround α = 1.3 led to net facilitation effects for all reference α > 1, while both the surround α = 0.7 and 1.0 had diminished facilitation effects at steeper reference α. Error bars represent the 95% confidence interval of the gap size averaged $SR_{\Delta\alpha}$.

We found the centre-surround interactions of 1/*f* noise stimuli to be facilitative in nature, and present only when the α of both the centre and the surround are similar, and relatively steep (α equal to or greater than 1.0). Facilitation effects are often found in more tradition center-surround studies that use narrowband gratings to measure the interactive properties of the center and the surround. For example, facilitation from the surround is observed when the spatial frequency of the surround is lower than that of the center (Meese & Hess, 2004; Meese, 2004; Xing & Heeger, 2000, 2001; Yu et al., 2001). Conversely, surrounds with a spatial frequency higher than that of the centre will have a suppressive effect on the perception of the centre stimulus (Cannon & Fullenkamp, 1988; Sutter, Sperling, & Chubb, 1995; Xing & Heeger, 2001). This is interesting, as our shallowest surround (α = 0.7) showed no suppressive effects on slope discrimination thresholds for any reference α, and even showed facilitative effects when the reference α = 1. Evidently, a noise stimulus with an amplitude spectrum slope of 0.7, while perceptually dominated by higher spatial frequency content, contains a significant proportion of luminance contrast at low spatial frequencies, which may have been the dominant spatial frequency content to modulate the centre surround interactions seen here (at least when the reference α = 1).

In **Experiment 2.1**, we found that it was the perceived contrast of our stimuli that seemed to modulate the facilitative effects associated with increases in stimulus size. However, as we found the presence of a surround to have only facilitatory effects on α discrimination thresholds, it is unlikely the perceived contrast of the noise images contributed to facilitation. Perceived contrast effects of the surround on the centre stimulus are always suppressive in nature, both for narrowband (Ellemberg, Wilkinson, Wilson, & Arsenault, 1998; Snowden & Hammett, 1998) and broadband stimuli (McDonald & Tadmor, 2006). Thus, as our effects show consistent facilitation of Δαs when the reference α was steep (in addition to a steeper surround), and the lack of any noticeable effect of gap size for all surround αs, the surround facilitation observed here results from low spatial frequency channels responding to both the centre and surround stimuli.

General Discussion

The findings of the current study offer psychophysical evidence that the ability of observers to detect, and discriminate, a change in the α of 1/*f* noise images occurs via a multi-channel process that is influenced by the representation of low spatial frequency luminance

contrast, when the reference α is relatively steep (α >1). By increasing the area of 1/*f* noise stimuli and consequently adding progressively lower spatial frequency luminance contrast within the stimulus (**Experiment 2.1**), our observer's ability to detect a difference in α increased. Additionally, this effect was tuned to reference α: observers benefitted most from an increase in stimulus size when the reference α = 1.0, while steeper (α > 1.0) and shallower (α < 1.0) reference αs showed smaller benefits. This facilitatory effect is analogous to the perceived contrast of 1/*f* noise stimuli in that stimuli with α = 1.0 are perceived to have higher contrast than steeper or shallower αs (Baker & Graf, 2009; Chubb et al., 1989; Hansen & Hess, 2012; McDonald & Tadmor, 2006). Thus, it is possible that the facilitatory effect generated by increases in stimulus size may be due to changes in the perceived contrast of our stimuli. However, given that perceived contrast has been demonstrated to have little influence on the psychophysical performance of observers in masking studies (Hansen & Hess, 2012; Hansen & Loschky, 2013), it is unlikely the perceived contrast of our images is a likely contributor to the facilitation we obtained here. That said, our findings have interesting implications on the known contrast pooling strategies employed by the early visual system. That is, as that the facilitation effect across α was constant for all stimulus sizes, the pooling of responses across multiple spatial frequency channels to 1/*f* noise stimuli must be normalized according to a contrast gain control mechanism (Carandini & Heeger, 1994; Heeger, 1992; Wilson & Humanski, 1993). Additionally, given that the increases in stimulus size predominantly influence the representation of low spatial frequency luminance contrast, it is likely that any form of normalization must have been weighted towards lower spatial frequency channel activity (Bex et al., 2007; Cass, Stuit, et al., 2009; Haun & Peli, 2013).

In **Experiment 2.2**, we aimed to isolate the nature of low spatial frequency channel interactions by replicating a study originally conducted in 2011 (Johnson et al., 2011), which measured centre-surround effects on slope discrimination thresholds, but increased the gap size between the centre and surround stimulus to better isolate low spatial frequency channel interactions. We found centre-surround interactions to be facilitatory in nature and constrained to reference 1/*f* noise images with steeper αs (α > 1), similar to the findings of the Johnson and colleagues (2011) study. Most interestingly, center-surround effects were somewhat tuned to the α of the surround. That is, while surrounds with α of 0.7 and 1.0 only elicited facilitatory effects for centre stimuli with steeper α (by 0.3), our steepest surround (α = 1.3) facilitated slope

discrimination thresholds for reference αs of 1.0 to 1.6. Center-surround interactions are known to modulate contrast detection and discrimination with narrowband stimuli (Bonneh & Sagi, 1998; Cannon & Fullenkamp, 1988; Chubb et al., 1989; Ellemberg et al., 1998; Petrov et al., 2005; Petrov & Mckee, 2006; Polat & Sagi, 1993; Snowden & Hammett, 1998; Xing & Heeger, 2001) and with broadband stimuli (Johnson et al., 2011; Kim et al., 2010; McDonald & Tadmor, 2006). The effects of a surround on the perception of the centre stimulus are usually inhibitory in nature, but the addition of a surround can also facilitate perception (both detection and discrimination) of the centre stimulus under certain stimulus constraints (i.e., when contrast of the surround is lower than that of the centre, or when the spatial frequency between the centre and the surround are matched; Huang, Jiao, & Jia, 2008; Linares, Motoyoshi, & Nishida, 2012; Meese, Summers, Holmes, & Wallis, 2007; Meese, 2004; Xing & Heeger, 2000; Yu et al., 2002, 2001). Facilitation and inhibition effects in center-surround paradigms are traditionally shown with abutting stimuli (i.e., no gap between the centre and the surround), but the introduction of a gap between the centre and surround has also been shown to generate both inhibitory and facilitatory effects on centre stimulus perception (Mareschal, Sceniak, & Shapley, 2001; Polat & Sagi, 1993, 1994). The addition of the gap has the added benefit of investigating the region of interaction between the two parts of the stimuli. For sinusoidal gratings, the interactive region can extend up to 8-12 cycles of the centre stimulus spatial frequency, and will be facilitative when the gap extends beyond 2 cycles of the centre spatial frequency, well beyond the spatial integration range of a single receptive field (Polat & Sagi, 1993). The consistent facilitatory effects we observed in **Experiment 2.2** on slope discrimination thresholds from the surround at all gap sizes suggest our observers may have been integrating over a fairly large region of the stimulus (i.e., non-local operations), and given the known constraints in the extent of facilitatory effects from the surround, must rely on spatial frequency content no more than 4 cycles/° for a gap size of 3.2° to elicit a facilitation effect (Polat & Sagi, 1993, 1994). It is possible that a similar global operation, whereby luminance contrast is integrated over a large region of space via lower spatial frequency channels, is responsible for the size effect we obtained in **Experiment 2.1**. Thus, when asked to discriminate between to noise images that vary in α, the ability of observers to detect the change may stem from the activity or the interactions between channels tuned to lower spatial frequencies, at least for $1/f$ noise images with steeper α ($\alpha > 1.0$).

Limitations

We tried to account for spatial summation of higher spatial frequency luminance contrast effects in our study by implementing a centre-surround paradigm where the centre and surround stimuli were separated by a gap. That said, it is known that summation over space is extensive, which means that summation of higher spatial frequencies may have still influenced α discrimination thresholds when the gap size was small (Baker & Meese, 2011; Hutchinson & Ledgeway, 2010; Meese & Baker, 2011; Meese & Summers, 2007; Meese, 2004). Summation effects have been well described with narrowband stimuli (Bonneh & Sagi, 1998; Graham & Sutter, 1998; Graham et al., 1978; Graham, 1989; Movshon, Thompson, & Tolhurst, 1978), but they may function under broadband conditions, when many differently tuned channels are active (Meese & Holmes, 2010). Thus, we cannot fully account for the influence of summation at higher spatial frequencies in the facilitatory effects witnessed in both **Experiment 2.1** and **Experiment 2.2**, that said, given that the facilitatory effect was sustained at our largest gap size of 3.2°, it is likely the dominant factor in the decrease of α discrimination thresholds is nested within the responses of channels to luminance contrast at lower spatial frequencies.

Conclusions

Initial attempts to define the mechanism that underlies the perceptual ability of observers under "naturalistic" stimulation (i.e., broadband) relied on the activity of a single spatial frequency channels (Tadmor & Tolhurst, 1994; Tolhurst & Tadmor, 1997). While it has since been shown that multi-channel approaches to broadband stimulation better define the perception of natural scene stimuli (Field & Brady, 1997; Field, 1987; Graham, Chandler, & Field, 2006; Graham, Friedenberg, & Rockmore, 2009; Hansen & Hess, 2012; Olshausen & Lewicki, 2004; Párraga et al., 2005; Simoncelli & Olshausen, 2001; Simoncelli, 2003), there remained to obtain psychophysical evidence that the perception of natural stimuli was contingent upon the representation of spatial frequency content within the stimuli. Thus, in this study, we aimed to demonstrate that the discriminability of the distribution of luminance contrast in a broadband stimulus (α) was contingent upon the representation of spatial frequency content within the image. Additionally, as there is evidence that the natural scenes elicit high activity within lower spatial frequency channels (Hansen et al., 2012, 2011; Haun & Peli, 2013; Webster & Miyahara, 1997) we aimed to investigate how the representation of low spatial frequency luminance contrast may affect α discrimination. We have shown here that α discrimination thresholds are

susceptible to low spatial frequency channel interactions when the reference α is steep. The facilitatory effects witnessed on α discrimination from our manipulations of low spatial frequency content (in particular **Experiment 2.2**) only occurred when the reference α was steeper than or equal to the average value of α in natural images (α = 1.08; Billock, 2000). These findings may be indicative that while 1/*f* noise images are broadband in spatial frequency, in that they contain a significant amount of luminance contrast across multiple spatial frequencies, their discriminability may be dependent on the activity differences between a subset of spatial channels tuned to the perceptually dominant scale within the stimulus to that of other channels. Thus, stimuli with steep α, which are perceptually dominated by lower spatial frequency content, may be discriminated upon according to the disproportionate responses of lower spatial frequency channels in comparisons to higher tuned channels.

Chapter 2 Tables

Table 2.1. Reference α X Stimulus Size Repeated Measures ANOVA source table on Δαs

Source	*SS*	*df*	*MS*	*F*	*p*	η_p^2
A	0.06	4	0.02	4.10	.011	.406
B	0.85	8	0.11	41.85	.000	.875
AxB	0.02	32	0.001	0.68	.906	.101
S	0.36	6	0.06			
AxS	0.09	24	0.004			
BxS	0.12	48	0.003			
AxBxS	0.19	192	0.001			
Total	1.70	314	0.01			

Note. A – Reference α, B – Stimulus Size, S - Subjects

Table 2.2. Main effect analysis of reference α

Source	*SS*	$SS_{adjusted}$	*df*	*MS*	*F*	*p*	η_p^2
A_{cubic}	0.15	0.03	1	0.15	31.16	.001	.839
S	1.39	0.28	6	0.23			
A_{cubic} x S	0.03	0.01	6	0.01			
Total	15.64	0.32	13	1.20			

Note. A – Reference α, S – Subjects, cubic coefficients = [-1 2 0 -2 1]. Sums of Squares (SS) are adjusted by dividing each SS by an adjustment factor defined as: $\sum c_j^2/2$, where *c* is the linear weights vector.

Table 2.3. Main effect analysis of stimulus size

Source	*SS*	$SS_{adjusted}$	*df*	*MS*	*F*	*p*	η_p^2
B_{linear}	22.02	0.73	1	22.02	60.00	<.001	.909
S	9.14	0.31	6	1.52			
B_{linear} x S	2.20	0.07	6	0.37			
Total	166.58	1.11	13	12.81			

Note. B – Stimulus Size, S – Subjects, linear coefficients = [4 3 2 1 0 -1 -2 -3 -4]. Sums of Squares (SS) are adjusted by dividing each SS by an adjustment factor defined as: $\sum c_j^2/2$, where *c* is the linear weights vector.

Table 2.4. Reference α X Stimulus Size Repeated Measures ANOVA source table on log ratios

Source	*SS*	*df*	*MS*	*F*	*p*	η_p^2
A	6.84	4	1.71	2.54	.066	.297
B	33.54	7	4.79	63.28	< .001	.913
AxB	1.47	28	0.05	0.83	.709	.122
S	5.63	6	0.94			
AxS	16.15	24	0.67			
BxS	3.18	42	0.08			
AxBxS	10.63	168	0.06			
Total	77.44	279	0.28			

Note. A – Reference α, B – Stimulus Size, S - Subjects

Table 2.5. Trend analysis of the main effect of stimulus size with log ratio data

Source	*SS*	$SS_{adjusted}$	*df*	*MS*	*F*	*p*	η_p^2
B_{linear}	2532.70	30.15	1	2532.70	178.84	<.001	0.968
S	403.15	4.80	6	67.19			
B_{linear} x S	84.97	1.01	6	14.16			
Total	10437.42	35.96	13	802.88			

Note. B – Stimulus Size, S – Subjects, * p < .001, linear coefficients = [7 5 3 1 -1 -3 -5 -7]. $SS_{adjusted}$ are the adjusted sums of squares according to the adjustment factor: $\sum c_j^2/2$, where *c* is the linear weights vector.

Table 2.6. Trend analysis of the main effect of reference α with log ratio data

Source	*SS*	$SS_{adjusted}$	*df*	*MS*	*F*	*p*	η_p^2
$A_{quadratic}$	58.07	8.30	1.00	58.07	15.02	0.008	0.715
S	38.82	5.55	6.00	6.47			
$A_{quadratic}$ x S	23.20	3.31	6.00	3.87			
Total	664.33	94.90	13.00	51.10			

Note. A – Reference α, S – Subjects, * p < .001, quadratic coefficients = [-2 -1 1 -1 -2] $SS_{adjusted}$ are the adjusted sums of squares according to the adjustment factor: $\sum c_j^2/2$, where *c* is the linear weights vector.

Table 2.7. Reference α X Gap Size Repeated Measures ANOVA on Δαs in our center-surround experiment

Source	*SS*	*df*	*MS*	*F*	*p*	η_p^2
			Surround α = 0.7			
A	1.97	4	0.49	0.70	.600	.123
B	2.11	5	0.42	4.61	.004	.480
AxB	1.15	20	0.06	0.76	.751	.132
S	3.63	5	0.73			
AxS	14.06	20	0.70			
BxS	2.29	25	0.09			
AxBxS	7.56	100	0.08			
Total	32.78	179	0.18			
			Surround α = 1.0			
A	2.50	4	0.62	1.01	.425	.168
B	0.59	5	0.12	2.14	.093	.300
AxB	1.06	20	0.05	0.99	.477	.166
S	3.91	5	0.78			
AxS	12.34	20	0.62			
BxS	1.38	25	0.06			
AxBxS	5.34	100	0.05			
Total	27.11	179	0.15			
			Surround α = 1.3			
A	3.13	4	0.78	1.44	.259	.223
B	0.46	5	0.09	1.62	.191	.245
AxB	2.02	20	0.10	1.46	.112	.226
S	3.62	5	0.72			
AxS	10.90	20.	0.55			
BxS	1.43	25	0.06			
AxBxS	6.91	100	0.07			
Total	28.48	179	0.16			

Note – A – Reference α, B – Gap Size, S – Subject.

Table 2.8. Trend analyses on the main effect of gap size (Surround α = 0.7)

Source	*SS*	*SSadj*	*df*	*MS*	*F*	*p*	η_p^2
B_{linear}	6.27	0.18	1	0.18	0.15	.894	.560
S	7.59	0.22	5	0.04			
B_{linear} X S	4.93	0.14	5	0.03			
Total	193.30	5.52	11	0.50			
$B_{quadratic}$	0.74	0.02	1	0.02	0.00	.954	.035
S	8.49	0.20	5	0.04			
$B_{quadratic}$ X S	20.57	0.49	5	0.10			
Total	188.49	4.49	11	0.41			
B_{cubic}	5.22	0.06	1	0.06	0.03	.928	.177
S	45.01	0.50	5	0.10			
B_{cubic} X S	24.19	0.27	5	0.05			
Total	699.94	7.78	11	0.71			

Note. B – Gap Size, S – Subject. $SS_{adjusted}$ are the adjusted sums of squares according to the adjustment factor: $\sum c_j^2 / 2$, where *c* is the linear weights vector.

Prologue to Chapter 3A

The following experiment strays from the broadband approach we have previously used to measure the functional properties of spatial frequency channels. However, this study (**Chapter 3A**) was used as a preparatory experiment for the experiment of **Chapter 3B**, where we use trans-cranial Direct Current Stimulation (tDCS) to modulate the activity of cells in the primary visual cortex, and verify if this technique has any impact on α discrimination thresholds. In **Chapter 3A** we first characterize the effects of tDCS across both the spatial frequency and orientations that define the Contrast Sensitivity Function (CSF) in order to better assess the spatial frequency channels most subject to the influence of tDCS. There is evidence to suggest that tDCS can only influence spatial frequency channels tuned to higher spatial frequency, but the evidence towards such a selective modulation is sparse, and often conducted with a limited stimulus set and a wide variety of stimulation protocols. Consequently, we opted to measure the effects of tDCS on contrast sensitivity to a wider range of spatial frequencies within the same group of observers, all under the same stimulation protocol, in order to better define the influence of tDCS on the CSF and guide the interpretations of our findings in **Chapter 3B**.

CHAPTER 3A

THE EFFECTS OF TDCS ACROSS THE SPATIAL FREQUENCIES AND ORIENTATIONS THAT COMPRISE THE CONTRAST SENSITIVITY FUNCTION

Bruno Richard, Aaron P. Johnson, Benjamin Thompson, Bruce C. Hansen

An edited version of this experimental chapter has been accepted for publication in the Journal *Frontiers in Psychology: Perception Science*

Citation: Richard, B., Johnson, A. P, Thompson, B., & Hansen, B. C. (2015). The effects of tDCS across the spatial frequencies and orientations that comprise the contrast sensitivity function. *Frontiers in Psychology: Perception Science, 6*, 1784. doi: 10.3389/fpsyg.2015.01784.

Abstract

Trans-cranial Direct Current Stimulation (tDCS) has recently been employed in traditional psychophysical paradigms in an effort to measure direct manipulations on spatial frequency channel operations in the early visual system. However, the effects of tDCS on contrast sensitivity have only been measured at a single spatial frequency and orientation. Since contrast sensitivity is known to depend on spatial frequency and orientation, we ask how the effects of anodal and cathodal tDCS may vary according to these dimensions. We measured contrast sensitivity with sinusoidal gratings at four different spatial frequencies (0.5, 4, 8, and 12 cycles/°), two orientations (45° Oblique and Horizontal), and for two stimulus size conditions [fixed size (3 degrees) and fixed period (1.5 cycles)]. The results showed that only contrast sensitivity measured with a 45° oblique grating with a spatial frequency of 8 cycles/° (period = 1.5 cycles) demonstrated clear polarity specific effects of tDCS, whereby cathodal tDCS increased, and anodal tDCS decreased contrast sensitivity. Overall, effects of tDCS were largest for oblique stimuli presented at high spatial frequencies (i.e., 8 and 12 cycles/°), and were absent at lower spatial frequencies. Further, the modulatory effects of tDCS were dependent on the sensitivity of the observer to the stimulus, and its spatial characteristics. It therefore seems that the effects of tDCS are only found for high spatial frequency stimuli that generally elicit lower contrast sensitivity, while the effects are diminished, or absent to stimuli that elicit higher contrast sensitivity.

The early stages of visual processing rely on a series of psychophysical channels, which are believed to result from the outputs of functionally different neurons. Further, the neurons contributing to those channels are known to operate like non-linear filters that act to extract a narrow range of spatial frequency and orientation content from the retinal image (Graham, 1989; Bergen et al., 1979; Blakemore and Campbell, 1969; Campbell and Robson, 1968; Carandini et al., 2005; De Valois et al., 1982, 1974; Graham and Nachmias, 1971; Maffei and Fiorentini, 1973; Wilson et al., 1983; Enroth-Cugell and Robson, 1966; Henning et al., 1974; Stromeyer and Julesz, 1972). In terms of contrast detection, the psychophysical characterization of the combined relative outputs of those channels is described by the Contrast Sensitivity Function (CSF), which serves as an index for the relative sensitivity of different psychophysical channels to different spatial frequencies (Blakemore & Campbell, 1969; Campbell, Maffei, & Piccolino, 1973; De Valois et al., 1982; De Valois et al., 1974; Robson, 1966; Sachs, Nachmias, & Robson, 1971; Tolhurst & Movshon, 1975). The shape of the CSF, which is bandpass in spatial frequency, peaks at a spatial frequency of about 1 cycle/° when measured with a grating of fixed period over spatial frequency, while its peak shifts towards higher frequencies (~4 cycles/°) when measured with gratings of a larger, fixed size[9] (Peli, Arend, Young, & Goldstein, 1993). The fall-off from the peak as a function of increasing and decreasing spatial frequency can be attributed to several cortical constraints (Snyder and Srinivasan, 1979; Banks et al., 1987; Campbell et al., 1966; Robson, 1966; Kelly, 1975; Hoekstra et al., 1974; Yang et al., 1995), which means that measurements of contrast sensitivity for stimuli that vary in spatial frequency, orientation and size, can be indicative of the functional organization of channels in the early visual system. Psychophysical approaches have long relied on the manipulation of contrast sensitivity with methodologies including selective adaptation (Blakemore & Campbell, 1969; Kohn, 2007), masking (Legge, 1978; Legge & Foley, 1980; Olzak & Thomas, 1999; Petrov, Carandini, & McKee, 2005; Polat & Sagi, 1993; Sagi & Hochstein, 1985; Snowden & Hammett, 1998; Stromeyer & Julesz, 1972; Watson & Solomon, 1997; Xing & Heeger, 2001, 2000), and

[9] When measuring contrast sensitivity with sinusoids, gratings of fixed size vary in spatial frequency by changing the number of grating cycles within a fixed-size aperture. This approach stems from models that viewed visual spatial analysis as a global Fourier analysis, which required a stimulus well localized in the Fourier domain (Campbell & Robson, 1968; Peli et al., 1993). More recent approaches to spatial vision view spatial analyzers as localized both in space and spatial frequency, which has led to the use of two-dimensional patches of gratings. The most common is the Gabor, a sinusoidal grating with a Gaussian envelope. It is the bandwidth of the Gaussian that sets the periodicity of the Gabor pattern, which is fixed across spatial frequency, while the size of the Gabor is scaled according to spatial frequency.

sub-threshold summation (Graham & Sutter, 1998; Graham & Nachmias, 1971; Robson & Graham, 1981; Stromeyer & Klein, 1975; Watson, 1979) to define the independent and interactive properties of spatial frequency and orientation channels in striate cortex. While these methods have been seminal in our current understanding of the early visual system, their approach to channel analysis has predominantly been indirect: altered channel behaviour, which results in a change of performance from the observer, cannot be attributed to anything other than manipulations of the stimulus presented to observers.

Neuro-stimulation techniques have recently been combined with traditional psychophysical paradigms in an effort to obtain a measure of a direct manipulation on channel behaviour in the early visual system (review: Antal, Nitsche, & Paulus, 2006). One technique that is gaining popularity due to its affordability and simplicity is trans-cranial Direct Current Stimulation (tDCS), a non-invasive brain stimulation technique that transiently modulates excitation and inhibition in the human brain via alterations in the membrane potential of neurons (Antal, Nitsche, & Paulus, 2001; Antal et al., 2006; Nitsche et al., 2008; Stagg & Nitsche, 2011; Stagg et al., 2009). The technique involves a stimulating device that delivers a mild direct current (DC) between two electrodes (anode and cathode) placed on the scalp of an observer in order to create a resistive DC circuit that induces a mild intra-cerebral electrical current from the anode electrode where current enters cortex, to the cathode electrode where current exits the cortex. The direction of current flow, whether it enters (anode) or exists (cathode) a particular cortical area has been reported to have differential effects on the behaviour of neurons located directly beneath the electrode (Antal et al., 2012; Bikson & Rahman, 2013; Jacobson, Koslowsky, & Lavidor, 2012; Paulus, 2011; Stagg & Nitsche, 2011). Specifically, when applied over motor cortex (M1), anodal stimulation (a-tDCS) generates a sub-threshold depolarization, while cathodal (c-tDCS) stimulation hyperpolarizes the membrane potential of neurons (Bikson & Rahman, 2013; Jacobson et al., 2012; Nitsche et al., 2008; Paulus, 2011; Pellicciari, Brignani, & Miniussi, 2013; Radman, Ramos, Brumberg, & Bikson, 2009; Rahman et al., 2013; Reato, Rahman, Bikson, & Parra, 2010; Stagg & Nitsche, 2011). The polarity specific effects of tDCS on motor cortex have also been associated with measurable performance changes, with a-tDCS reported to have a facilitative effect and c-tDCS an inhibitive effect on task performance (Antal & Paulus, 2008; Jacobson et al., 2012; Nitsche & Paulus, 2000; Nitsche, Fricke, et al., 2003; Nitsche, Nitsche, et al., 2003; Pellicciari et al., 2013; Stagg & Nitsche, 2011; Stagg et al., 2009).

In motor cortical areas (M1), these effects are robust: a recent meta-analysis found that the a-tDCS facilitatory effect and c-tDCS inhibitory effect over motor cortex both generated average effect sizes of ~0.6 standard deviations (Jacobson et al., 2012). However, in other cortical areas, the polarity specific effects of tDCS readily found in M1 are often absent, and in the primary visual cortex, are rarely found at all. Only effects of either anodal or cathodal tDCS are usually observed in striate cortex, or if there are polarity specific effects, they are opposite to those found in motor cortex (Accornero, Li Voti, La Riccia, & Gregori, 2007; Antal, Kincses, Nitsche, Bartfai, & Paulus, 2004; Antal & Paulus, 2008; Antal et al., 2012; Antal, Ambrus, & Chaieb, 2014; Antal, Kincses, Nitsche, & Paulus, 2003a, 2003b; Antal et al., 2001; Antal, Nitsche, et al., 2004; Jacobson et al., 2012; Kraft et al., 2010; Lang et al., 2007; Olma, Kraft, Roehmel, Irlbacher, & Brandt, 2011; Peters et al., 2013; Spiegel et al., 2013, 2012). Part of the variability in the effectiveness and polarity specific effect of tDCS over various cortical loci can be attributed to structural differences (e.g., cell type and morphology and the direction of current flow in relation to the somatodendritic axis), or the functional complexity difference between stimulated areas (Bikson & Rahman, 2013; Radman et al., 2009; Reato et al., 2010; Rushton, 1927; Shipp, 2005; Ward & Weiskrantz, 1969). It should therefore come as no surprise that effects of tDCS over the visual cortex, which is both structurally and functionally different than motor cortex, are less clear.

There are indications that the resistive DC circuit generated by tDCS can modulate visually responsive areas, and have distinctive effects according to the polarity of the circuit (anodal or cathodal). There have been a multitude of approaches to define the effects of tDCS over striate cortex (Accornero et al., 2007; Antal et al., 2014, 2003a, 2003b; Antal, Kincses, et al., 2004; Antal, Nitsche, et al., 2004), of note to the goals of the current study have been the findings pertaining to contrast detection thresholds modulation by tDCS. These have been shown to be facilitatory (i.e., contrast sensitivity improved) under a-tDCS when contrast sensitivity was measured with a grating of spatial frequency at the peak of the CSF (Peters et al., 2013; Spiegel et al., 2013), while effects at or next to the peak have been both facilitatory under a-tDCS (Kraft et al., 2010) and inhibitory under c-tDCS (Antal et al., 2001; Chaieb et al., 2008). However, it is important to note that these studies have used a varied set of stimulus spatial frequency and orientations to define the effects of tDCS, which clouds any in-depth assessment of how the magnitude of the effects of tDCS may vary according to the particular stimulus dimensions

presented to observer (e.g., a spatial frequency and orientation). This is of particular importance as the shape of the CSF is known to vary according to changes in stimulus dimensions (Campbell et al., 1966; Graham, 1989; Peli, Arend, Young, & Goldstein, 1993). In addition, the trademark anodal-excitatory and cathodal-inhibitory polarity specific effect of tDCS has yet to be reported on contrast sensitivity measurements completed within the same sample of "normal" psychophysical observers (note that a sample of individuals with amblyopia did show facilitatory effects of a-tDCS in their amblyopic eye, and inhibitory effects of c-tDCS in their fellow eye; Spiegel et al., 2013). Nevertheless, these findings are impressive as changes in contrast detection thresholds to simple sinusoidal gratings, particularly facilitatory effects, are traditionally quite difficult to obtain (Adini, Sagi, & Tsodyks, 2002; Adini, Wilkonsky, Haspel, Tsodyks, & Sagi, 2004; Dorais & Sagi, 1997; Li, Polat, Makous, & Bavelier, 2009; Maehara & Goryo, 2007). Typically, extensive training on contrast sensitivity tasks will only show improvement when measured under situations that generally elicit poor contrast sensitivity (e.g., peripheral viewing, or gratings with non-cardinal orientations; Sowden et al., 2002). The current findings on the effects of tDCS on contrast sensitivity suggest similar limitation to the benefits, or detriment, of this stimulation technique. That is, although the neuro-modulatory effects of tDCS may be sufficient to manipulate the response characteristics of visually responsive cells in striate cortex, and generate measurable changes in psychophysical performance, they too may be subject to the stimulus dimensions presented to observers, as has been suggested by other neuro-stimulation studies (Antal et al., 2001; Thompson, Mansouri, Koski, & Hess, 2008). It remains unclear how the dimensions of the stimulus used to measure contrast sensitivity may influence the magnitude of tDCS related effects.

The goal of the current study was to assess how the effects of tDCS vary according to the stimulus dimensions (spatial frequency and orientation) presented to observers when measuring contrast sensitivity. Given the known functional organization of the early visual system, and the properties of the DC circuit generated by tDCS, certain predictions as to the interaction of tDCS and stimulus dimension can be made. The effects of either a-tDCS or c-tDCS on contrast sensitivity should be greatest at high spatial frequencies, and diminish with decreasing spatial frequency. The magnitude of the electrical field generated by tDCS is greatest on the cortical surface, and decreases within the sulci of cortex (Miranda, Lomarev, & Hallett, 2006; Miranda, Mekonnen, Salvador, & Ruffini, 2013; Rahman et al., 2013). In striate cortex, this means that

stimuli presented further than 2° eccentricity from fovea are not affected by tDCS (Kraft et al., 2010; but see Costa et al., 2015). As neurons located deeper into the calcarine sulcus have lower preferred spatial frequencies than cells at the apex of cortex, they should not be modulated by tDCS (De Valois et al., 1982; Engel, Glover, & Wandell, 1997; Foster, Gaska, Nagler, & Pollen, 1985; Henriksson, Nurminen, Hyvärinen, & Vanni, 2008; Horton, 2006; Tootell, Silverman, & De Valois, 1981; Tootell, Switkes, Silverman, & Hamilton, 1988; Yu et al., 2010). In regards to the orientation of the gratings used to measure contrast detection thresholds, as previous work has shown the effects of tDCS to be constrained by the sensitivity of the observer to the stimulus dimensions, greater effects of tDCS to oblique orientations than cardinal orientations may be expected, as humans are less sensitive to oblique (the "Oblique Effect"; Appelle, 1972; Campbell et al., 1966). It is possible we will find polarity specific effects of tDCS on the orientation of gratings that would reduce the magnitude of contrast sensitivity differences between cardinal and non-cardinal orientations; a-tDCS may increase contrast sensitivity measured with oblique gratings, while c-tDCS may decrease contrast sensitivity to horizontal gratings, effectively decreasing the magnitude of the “Oblique Effect”. However, we may also find the higher contrast sensitivity obtained with horizontal gratings to be completely unaffected by tDCS, in a manner similar to experiments that have tried to increase contrast sensitivity with more traditional training techniques (Sowden et al., 2002). We aimed to better define how the effects of tDCS on low-level visual processes might be constrained, or altered, by the stimulus dimensions presented to observers. We measured changes in contrast sensitivity from a non-stimulation baseline under both a-tDCS and c-tDCS to gratings at four different spatial frequencies that span the contrast sensitivity function (0.5, 4, 8, and 12 cycles/°) and two stimulus orientations (45° oblique or Horizontal). Whilst we find effects of tDCS on contrast sensitivity, we also show that these effects are, just as has been previously reported (Antal et al., 2001; Li et al., 2009; Sowden et al., 2002; Thompson et al., 2008), constrained to stimulus dimensions that generally elicit poorer contrast sensitivity.

Experiment 3.1

Method

Participants

A total of 26 undergraduate students participated in the behavioural portion of this study (baseline), out of which 20 continued onto the tDCS portion of this study. All observers but two

were naïve to the goals of the experiment. Observers were prevented from moving onto the tDCS sessions when their contrast detection thresholds measured just prior to the application of tDCS exceeded 2 standard deviations of their average thresholds measured in the behavioural portion of this study. Participants that continued onto the tDCS sessions were separated into two groups; 10 (N_{female} = 7, M_{age} = 20.2) participants were presented with oblique gratings while the other 10 (N_{female} = 5, M_{age} = 20.5) saw horizontal gratings. Two of the participants in the oblique orientation completed the experiment at Concordia University (Montreal, Quebec, Canada), while data for all other participants in this study were collected at Colgate University (Hamilton, New York, USA). All participants had normal, or corrected-to-normal visual acuity (Snellen cut-off = 20/25) and no astigmatism. Written informed consent was obtained from all participants and all participants were treated in accordance to the Tri-Council Policy Statement: Ethical Conduct for Research Involving Humans (Medical Research Council of Canada, 2003), and were compensated financially for their time.

Apparatus

All stimuli were presented on 22.5" Viewsonic (G225fB) monitors driven by a dual core Intel® Xeon® processor (1.60GHz x2) equipped with 4GB RAM and a 256MB PCIe x16 ATI FireGL V7200 dual DVI/VGA graphics card with 8-bit grayscale resolution at Colgate University and an Apple Mac Pro (2 X 2.66GHz processor) equipped with 8GB of RAM and a 1GB PCIe x16 ATI Radeon HD 5770 Graphics card with 8-bit grayscale resolution. The color management settings for the graphics card (i.e., 3D display settings) were adjusted such that the luminance "gain" of the green gun was twice that of the red gun, which was set to twice that of the blue gun. A bit-stealing algorithm (Bex et al., 2007; Tyler, 1997) was employed to yield 10.8 bits of luminance (i.e., grayscale) resolution (i.e., 1785 unique levels) distributed evenly across a 0-255 scale. Stimuli were displayed using a linearized look-up table, generated by calibrating with a Color-Vision Spyder3 Pro sensor. Maximum luminance output of both display monitors was 100 cd/m^2 (50 cd/m^2 mean luminance after calibration). The frame refresh rate was set to 85 Hz (100 Hz at Concordia), and the resolution was set to 1600 x 1200 pixels (1024 X 768 pixels at Concordia). Single pixels subtended .0134° (.0381° at Concordia) of visual angle, i.e., 0.80 arc min. (2.28 arc min. at Concordia) as viewed from 1.0 meter. Head position was maintained with a chin rest. Participants viewed the display monitor from 2 meters in a dark room through an

aperture (16° of visual angle in diameter) of a large black circular mask that was fit to the monitor bezel in order to obscure any monitor or room orientation cues.

Trans-cranial Direct Current was generated with a 9V battery driven direct current stimulator (Chattanooga Ionto, USA) and delivered via a pair of carbon-rubber electrodes (The Magstim Company Ltd., UK). The electrodes were encased in potassium chloride soaked Spontex sponge pockets (The Magstim Company Ltd., UK). The size of the stimulating electrode was 6 × 8 cm, and the size of the reference electrode was 12 × 8 cm. The larger size of the reference electrode renders it inert due to low current density (Nitsche et al., 2007; Spiegel et al., 2012). Both electrodes were held in place with four Magstim rubber headbands (The Magstim Company Ltd., UK), applied in a manner that maximized complete electrode sponge surface contact over the targeted scalp regions.

Stimuli

Stimuli consisted of foveally presented sinusoidal gratings generated at one of either two orientations: oblique (45°) or horizontal (90°). All gratings were windowed by a 2D Gaussian, which ramped down the contrast to mean luminance. Stimulus spatial frequency was 0.5, 4, 8, or 12 cycles/°, with a period of 1.5 cycles (fixed period condition). The electrical field generated by tDCS is prominently focused onto the surface of the visual cortex, which limits the spatial extent of the visual field modulated by tDCS to the central 1-2° of the visual field (Kraft et al., 2010). As the effects of tDCS change as both a function of spatial frequency and stimulus area, we added a second stimulus condition and measured contrast sensitivity with a fixed stimulus size (3°), and adjusted the period of the stimulus with spatial frequency (fixed stimulus size condition). All stimuli were surrounded by a low contrast ring (Michelson Contrast = 10%) 1 pixel in size, 0.78° away from the border of the grating, and paired with a low frequency tone; both served to minimize participant doubt as to the location and/or presence of the stimulus on the screen. Stimulus contrast was expressed as Michelson contrast = $\left[\left(L_{\max} - L_{\min}\right)/\left(L_{\max} + L_{\min}\right)\right]$ scaled to have zero mean and then normalized to 1.0.

Psychophysical Procedure

The within-subject stimulus conditions for this experiment consisted of four spatial frequencies (0.5, 4, 8, and 12 cycles/°), and two period conditions (fixed period and fixed size). Observers were grouped according to the stimulus orientation (45° oblique or horizontal). The psychophysical procedure for both the training and test phases were identical. The stimulus

presentation procedure consisted of a 2-Interval Force Choice (2-IFC) procedure where participants had to indicate the interval, either the first or the second, which contained the target. Target contrast was controlled by a 2-up, 1-down staircase setup and controlled by the *PAL_AMUD_setupUD* and the *PAL_AMUD_updateUD* functions from the Palamedes toolbox for MATLAB (Kingdom & Prins, 2010; Prins & Kingdom, 2009). Threshold was approached from above with a target contrast step size of 0.05% Michelson contrast. Each staircase ran until 12 reversals were observed and the averaged target contrast value of the last 5 reversals was used as an estimate of target contrast threshold (70.71% correct on the psychometric function).

All staircases completed by observers began with an instruction screen that informed them of the spatial frequency and size condition of the stimulus (orientation never changed within observers). Each trial began with a black fixation dot (0.1°) presented at the center of the screen. The fixation dot served both to remind the observer a stimulus will appear shortly and the location of said stimulus. The fixation screen (300ms) was followed by a blank screen (150ms) set to mean luminance, and then the first stimulus interval, with an onset that followed a square-wave function and remained on the screen for 150ms. This sequence was repeated for the second stimulus interval (see **Figure 3A.1**). One interval contained the stimulus, surrounded by a low-contrast ring, while the other interval contained only a low-contrast ring. Participants indicated, via keyboard press, the interval that they believed contained the target. The duration of the response interval was unlimited, and participants received no feedback on their accuracy. Each spatial frequency by stimulus size block was repeated 10 times by observers in the baseline portion of the study, for a total of 80 staircase blocks, which approximately took 5 hours to complete over multiple sessions that lasted no more than an hour. All staircase blocks were randomly interleaved for each observer, and only the final 8 stimulus blocks were kept for data analysis. The contrast sensitivity of observers across each sequential measurement for all spatial frequency and stimulus size conditions is shown in **Figure 3A.A1** (**Supplemental Material A**), separated by orientation group. The 20 observers (10 per orientation group) that continued onto the tDCS portion of this study showed no statistically significant increment or decrement in contrast sensitivity across the final 8 stimulus blocks completed during baseline (the slope of the line of best fit across all 8 stimulus blocks was tested against 0, all ps > .05), which is consistent with others that have shown either small (Li, Polat, Makous, & Bavelier, 2009; Sowden, Rose, & Davies, 2002), or no changes in the CSF over sequential measurements in healthy adults (Adini

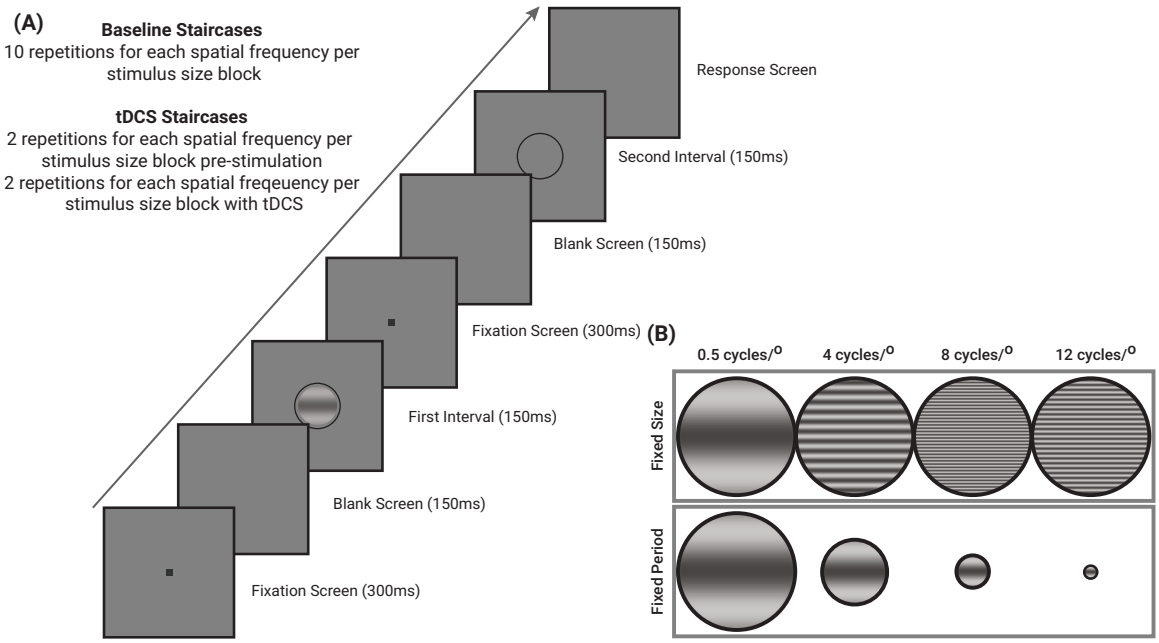

Figure 3A.1. General psychophysical procedures completed by all observers in this study. **A** Stimulus presentation sequence (see text for details). **B** Contrast sensitivity was measured for both stimuli of a fixed size and fixed period, at 4 different spatial frequencies (0.5, 4, 8, and 12 cycles/°). Groups (n = 10 per group) were split according to stimulus orientation (45° oblique, and horizontal). Stimuli in the fixed period condition do not represent the actual change in size of our stimuli during the staircase, and are a graphical representation of the different stimulus dimensions used in this study. Stimuli of a fixed size subtended 3° of visual angle while stimuli of a fixed period had a period of 1.5 cycles.

et al., 2002, 2004; Dorais & Sagi, 1997; Maehara & Goryo, 2007).

tDCS Procedure

Trans-cranial Direct Current Stimulation is known to be a safe neuro-stimulation technique with no long lasting negative side effects, it is nevertheless important to limit the duration of stimulation to no more than 30-35 minutes (Bikson, Datta, & Elwassif, 2009; Nitsche, Liebetanz, et al., 2003; Poreisz, Boros, Antal, & Paulus, 2007). In order to meet this time restriction, the number of repetitions for each spatial frequency by stimulus size block was set to two. The total number of staircases completed by observers while receiving tDCS was 16 (four spatial frequencies by two stimulus size conditions by two repetitions). Prior to receiving either anodal or cathodal stimulation, participants completed two staircases for each spatial frequency by stimulus size blocks, which were combined with the 8 stimulus blocks from the baseline portion of this study and used as a pre-stimulation baseline (see **Supplemental Material A, Figure A2**). If contrast detection thresholds exceed their average baseline thresholds by at least two SDs, participants were asked to repeat the pre-stimulation baseline measurements. If thresholds following the repetition remained two SDs away from average thresholds, participants were excused from the study.

Immediately following baseline measurements, participants repeated the 16 staircases while receiving tDCS (time to complete: M = 21.05 minutes, SD = 2.74). All observers completed two stimulation sessions (anodal and cathodal, counterbalanced across participants) with no less than 48 hours between sessions. As both anodal and cathodal tDCS have been shown to produce differential effects on contrast detection performance (see Antal et al., 2001; Jacobson et al., 2012; Spiegel et al., 2012; Kraft et al., 2010), we used both stimulation conditions to serve as a control of the other. Specifically, we prioritize any relative effects whereby tDCS polarity differentially modulated contrast sensitivity for a particular stimulus dimension within our observers. This allowed us to avoid certain confounds that have been associated with sham stimulation in neurostimulation designs (for review: Duecker & Sack, 2015), specifically, while observers are unable to differentiate between anodal and cathodal tDCS, they have been shown to easily detect when they receive sham stimulation (Minhas, Datta, & Bikson, 2011; Peters et al., 2013; Spiegel et al., 2012), which may alter their response pattern and therefore serve as a poor control for neurostimulation.

Injecting current was set to 2mA, which yielded a stimulation current density of 0.042 mA/cm^2 over striate cortex. The stimulation and reference electrode were positioned over Oz and Cz respectively, in accordance with the 10-20 EEG system (Antal, Kincses, et al., 2004; Chatrian, Lettich, & Nelson, 1985). Under anodal stimulation, current was sent from the smaller, stimulating electrode placed over Oz to the larger reference electrode placed over Cz, while current direction was reversed under cathodal stimulation. The current was initially ramped up, over a period of 30 seconds and participants waited for a minute once the current ramped-up so the experimenter could verify comfort levels. When participants completed the 16 staircases, the current was ramped back down to 0 over a period of 30 seconds. Once the experimental session was completed, participants completed a post-stimulation checklist to verify for any minor side-effects (Nitsche et al., 2008) – none were reported.

Statistical Analyses

Contrast detection thresholds ($c_{threshold}$) were transformed to dB sensitivity units, $CS_{dB} = 20\log_{10}\left(1/c_{threshold}\right)$, prior to analyses. Given that the non-shunted direct current that enters cortex with tDCS is several orders of magnitude less than what is required to elicit action potentials, we expected any influence of tDCS on psychophysical performance to be relatively small and therefore approached our analysis both at the group level (i.e., ANOVAs and appropriate effect sizes reported using both Hedge's g and η_p^2) and at the case level (e.g., Left Tail Ratios). Left-Tail Ratios (LTRs) are a case level analysis designed to assess the relative proportion of contrast sensitivity measurements recorded during stimulation to those of pre-stimulation in the left-tail of the combined distribution (Kline, 2004). When combined, both group and case level analyses offer a thorough descriptive approach of the data by quantifying effects both in central tendency and spread of the distribution of contrast sensitivity values. LTRs are calculated with the largest proportion as the numerator (regardless of time-point affiliation), in the following sections, values marked by an asterisk (*) indicate that the pre-stimulation contrast sensitivity values were over-represented in the left tail of the combined distribution. Interval estimates reported for Hedge's g effect size measures are exact 95% confidence intervals calculate from the non-central t distribution (see **Supplemental Material B**; Cumming & Finch, 2001; Kline, 2004). Interval estimates for η_p^2 variance accounted for effect sizes are not reported,

as their distribution in correlated designs are complex and do not follow a central nor a non-central test distribution (Kline, 2004).

Results

As data collection for two observers in the oblique orientation group was completed at Concordia University, we verified that their contrast sensitivity values from both the baseline and tDCS phases of the study were identical to those of the Colgate University sample by calculating U1 (see **Supplemental Material B;** Cohen, 1988), a measure of overlap with range [0 1]: values of 0 indicate complete overlap between both samples, while values of 1 indicate no overlap whatsoever. The average contrast sensitivity values from baseline, and both the a-tDCS and c-tDCS sessions for both the Colgate and Concordia samples can be seen in **Figure 3A.2**. At baseline, there was significant overlap between contrast sensitivity measures collected at both testing facilities (U1 never exceeded .27). We found similar overlap between the Concordia and Colgate samples for both the a-tDCS and c-tDCS sessions, U1 values were all below .37, except for contrast sensitivity measured under a-tDCS with fixed size stimuli of spatial frequency 4 cycles/° (U1 = .87). However, given that contrast sensitivity values were slightly discrepant for a single stimulus condition block, and that data still overlapped slightly between both samples, we decided to average contrast sensitivity values collected at both testing locations for all subsequent analyses.

Fixed period oblique and horizontal stimuli

The average effects of both a-tDCS and c-tDCS on fixed period oblique gratings can be seen in **Figure 3A.3**. We conducted a 2 (tDCS polarity) × 4 (spatial frequency) repeated measures ANOVA on the difference scores (stimulation – pre-stimulation) to test for any spatial frequency dependent or polarity specific effect of tDCS on contrast sensitivity values. We found a statistically significant interaction between tDCS polarity and spatial frequency, $F(3, 27) = 8.10$, $p < .001$, $\eta_p^2 = .474$. A simple effect analysis, found that the interaction term stemmed from a contrast sensitivity decrease under a-tDCS and increase under c-tDCS at a spatial frequency of 8 cycles/°, $F(1, 9) = 20.79$, $p < .001$, $\eta_p^2 = .698$. At a descriptive level, a-tDCS decreased contrast sensitivity during stimulation to higher spatial frequencies (≥ 4 cycles/°) by a third of a standard deviation (4 cycles/°: g = -0.40, 95% CI [-0.78 -0.03], LTR = 4.34; 8 cycles/°: g = -0.32, 95% CI [-0.60 -0.03], LTR = 12.67; 12 cycles/°: g = -0.36, 95% CI [-0.70 -0.01], LTR = 124.19). Left- Tail Ratios increased as a function of spatial frequency, and observers under a-

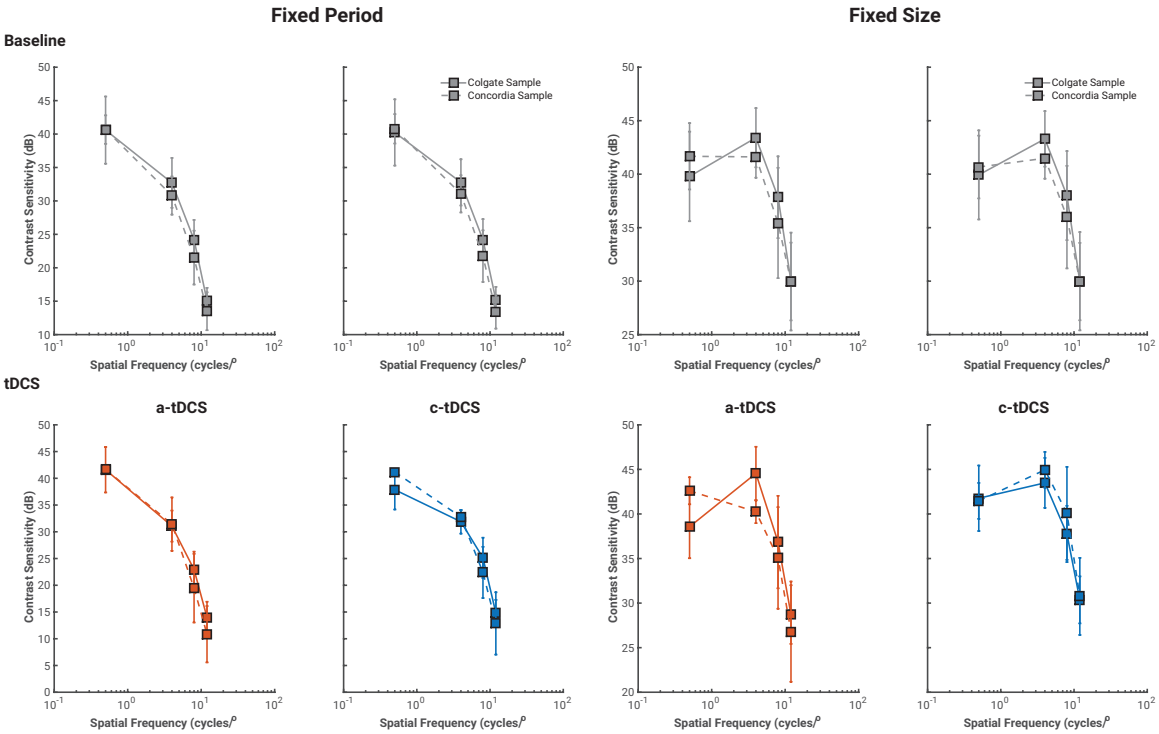

Figure 3A.2. Contrast sensitivity values collected from Colgate University (solid lines) and Concordia University (dashed line) at baseline and during tDCS for all oblique stimulus condition blocks. For all conditions, contrast sensitivity values from both samples overlapped significantly and were therefore averaged for all analyses.

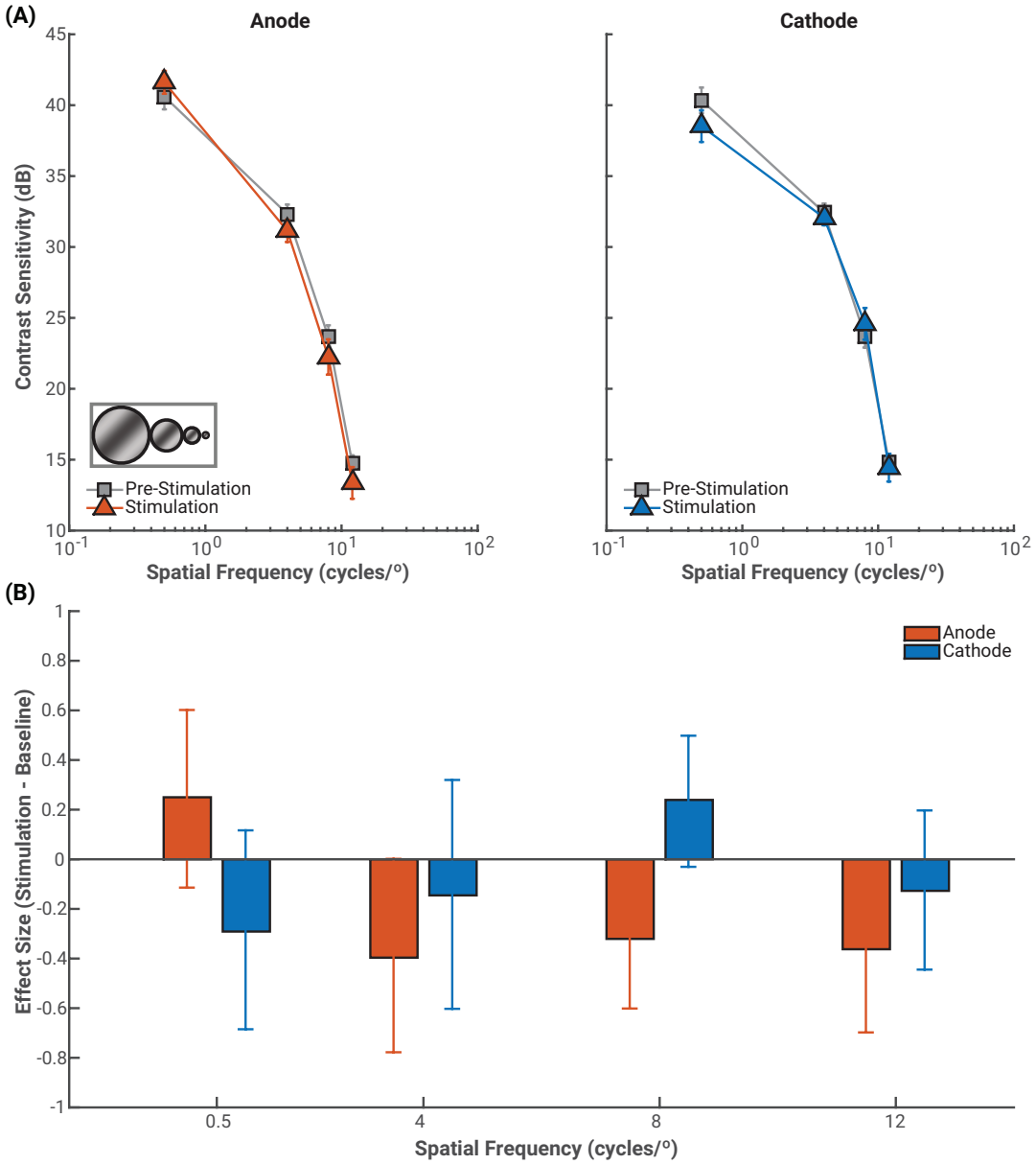

Figure 3A.3. A Average pre-stimulation (gray) and stimulation contrast sensitivity functions for both a-tDCS (red) and c-tDCS (blue) measured with the oblique fixed period gratings (at spatial frequencies of 0.5, 4, 8, and 12 cycles/°). Contrast sensitivity is presented in decibels (dB). Error bars represent the standard error of the mean difference calculated across observers. **B** Effect size measures of the mean difference contrast sensitivity measured at stimulation and at pre-stimulation. Contrast sensitivity measured at 8 cycles/° shows a polarity specific effect of tDCS, whereby a-tDCS decreased contrast sensitivity and c-tDCS increased contrast sensitivity. Error bars represent the exact 95% confidence interval of the effect size.

tDCS were 124 than in the pre-stimulation condition at a spatial frequency of 12 cycles/°. Conversely, c-tDCS had little influence on contrast sensitivity values, other than for the increase in contrast sensitivity to the 8 cycles/° (g = 0.24, 95% CI [-0.03 0.50], LTR = 1.66). The average effects of both a-tDCS and c-tDCS on fixed period horizontal gratings are shown in **Figure 3A.4**. Unlike the oblique fixed period grating, we do not find a statistically significant interaction between tDCS and spatial frequency, $F(3,27) = 1.97$, $p = .585$, $\eta_p^2 = .179$. In fact, the magnitude of the difference scores under a-tDCS decreased as a function of increasing spatial frequency (4 cycles/°: g = 0.22, 95% CI [-0.13 0.57], LTR = 1.34*; 8 cycles/°: g = -0.15, 95% CI [-0.42 0.13], LTR = 1.23; 12 cycles/°: g = -0.02, 95% CI [-0.34 0.31], LTR =3.39). At the case-level, observers receiving a-tDCS were more likely to have a contrast sensitivity value one standard deviation below the mean of the combined distribution at higher spatial frequencies. Cathodal tDCS increased contrast sensitivity for all four spatial frequencies (0.5 cycles/°: g = 0.25, 95% CI [-0.19 0.67], LTR = 2.53*; 4 cycles/°: g = 0.13, 95% CI [-0.17 0.42], LTR = 24.80; 8 cycles/°: g = 0.19, 95% CI [-0.11 0.48], LTR = 7.52) and this effect was most pronounced at a spatial frequency of 12 cycles/° (g = 0.35, 95% CI [-0.02 0.71], LTR = 1.70). Although we found small effects at the group-level, case-level analyses showed that as spatial frequency increased, observers receiving c-tDCS were progressively less likely to have a contrast sensitivity score one standard deviation below the mean of the combined distribution, which suggest some improvement in contrast sensitivity under c-tDCS.

In order to directly compare the effects of tDCS across orientation, we calculated Hedge's g (with 95% confidence intervals – built for an independent sample design – see **Supplementary Materials B**) to standardize the mean difference in contrast sensitivity values between oblique and horizontal gratings for baseline measures (combined across baseline and both pre-stimulation sessions), and for both stimulation conditions (see **Figure 3A.5**). At baseline, we found that the magnitude of the difference between horizontal and oblique grating contrast sensitivity increased as a function of spatial frequency. Horizontal contrast sensitivity exceeded that of oblique by two thirds of a standard deviation at a spatial frequency of 12 cycles/° (g = 0.62, 95% CI [-0.29 1.51]). Under tDCS, we found that a-tDCS increased the difference between contrast sensitivity to horizontal and oblique gratings at a spatial frequency of 4 cycles/° (g = 0.96, 95% CI [.02 1.88]) while c-tDCS had the same effect for a spatial frequency of 12 cycles/° (g = 0.96, 95% CI [0.02 1.88]). The difference in contrast sensitivity

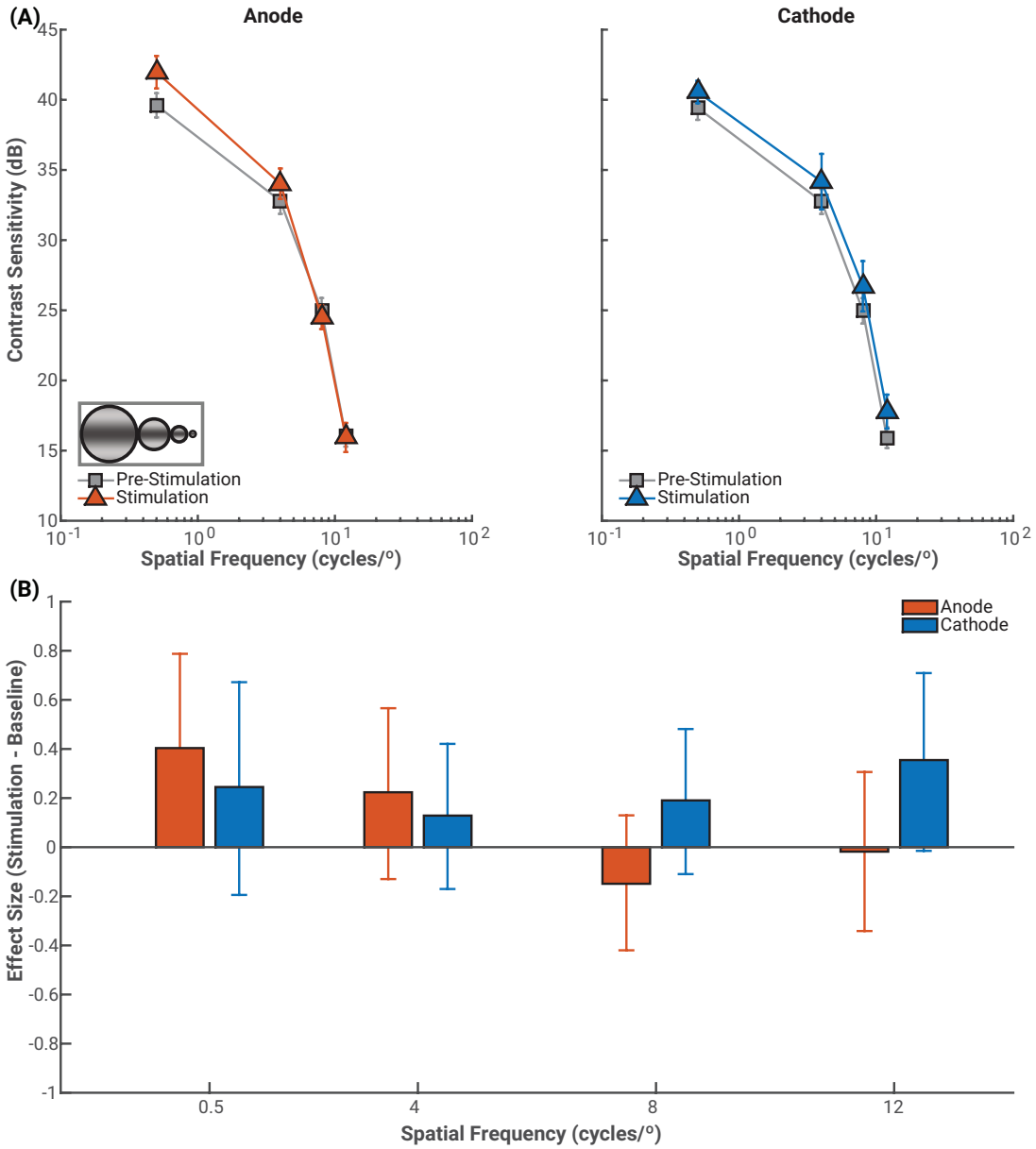

Figure 3A.4. A Average pre-stimulation and stimulation contrast sensitivity functions for both a-tDCS and c-tDCS measured with the horizontal fixed period gratings (at spatial frequencies of 0.5, 4, 8, and 12 cycles/°). Contrast sensitivity is presented in decibels (dB). Error bars represent the standard error of the mean difference calculated across observers. **B** Effect size measures of the mean difference contrast sensitivity measured at stimulation and at pre-stimulation. We found a large increase in contrast sensitivity measured with the 12 cycles/° horizontal, fixed period grating during c-tDCS. Error bars represent the exact 95% confidence interval of the effect size.

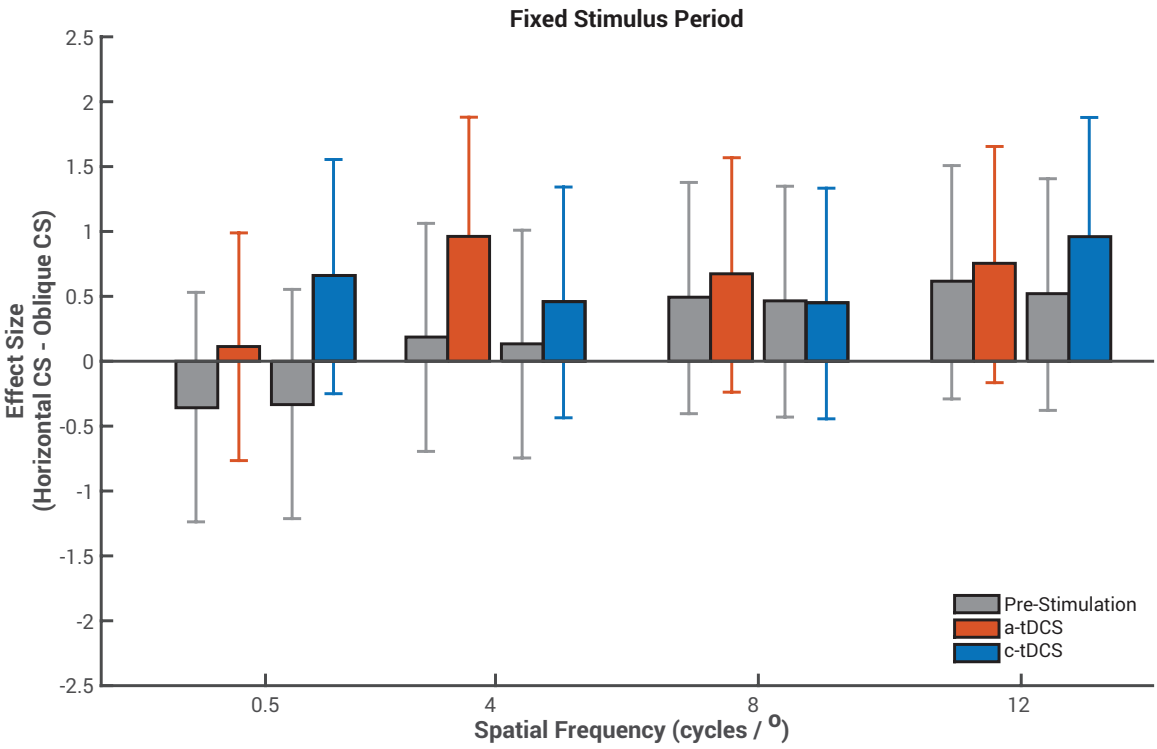

Figure 3A.5. Effect size of the mean difference between contrast sensitivity measured with horizontally orientated gratings and oblique orientated gratings. Gray bars represent the respective pre-stimulation baseline for either a-tDCS (red) or c-tDCS (blue) contrast sensitivity difference between horizontal and oblique gratings. We do find a-tDCS to increase the difference between contrast sensitivity measured to horizontal gratings and that of oblique gratings at a spatial frequency of 4 cycles/° and for c-tDCS to have a similar effect at a spatial frequency of 12 cycles /°. Error bars represent the exact 95% confidence interval for the mean difference effect size (effect sizes here are standardized on the pooled standard deviation).

between horizontal and oblique gratings measured to other spatial frequencies was not affected by a-tDCS or c-tDCS.

Fixed size oblique and horizontal stimuli

The average effects of both a-tDCS and c-tDCS on oblique gratings of a fixed size are shown in **Figure 3A.6**. The repeated measures ANOVA conducted on the difference scores (stimulation – pre-stimulation) of the fixed size oblique stimuli did not return a statistically significant interaction of tDCS by spatial frequency, $F(3, 27) = 0.65$, $p = .585$, $\eta_p^2 = .068$. However, the analysis did return a statistically significant main effect of tDCS polarity $F(1, 9) = 9.23$, $p = .014$, $\eta_p^2 = .506$. Anodal tDCS, on average, decreased contrast sensitivity while c-tDCS increased contrast sensitivity, regardless of spatial frequency. At high spatial frequencies, a-tDCS decreased contrast sensitivity to the 8 cycles/° grating slightly (g = -.14, 95% CI [-0.41 0.68], LTR = 34.84) and the 12 cycles/° grating (g = -.33, 95% CI [-0.65 0.01], LTR = 14.25). Interestingly, the LTRs did not increase as a function of spatial frequency, but instead were greatest at spatial frequencies of 4 and 8 cycles/° and slightly smaller for the 12 cycles/° grating. Cathodal tDCS increased contrast sensitivity for all spatial frequencies, but its largest effects were found for gratings of a spatial frequency of 4 cycles/° (g = 0.31, 95% CI [-0.26 0.86], LTR = 15.65). Unlike the fixed period oblique gratings, we find no clear tDCS polarity specific effect for any of the high spatial frequencies tested here as c-tDCS had little effect on the 8 cycles/° grating contrast sensitivity (g = 0.13, 95% CI [-0.25 0.51], LTR = 1.28*) and the 12 cycles/° grating contrast sensitivity (g = 0.21, 95% CI [-0.10 0.51], LTR = 2.37*). The case-level analyses do, however, suggest there may be a tDCS polarity specific effect. Observers were more likely to have a contrast sensitivity value one standard deviation below the mean of the combined distribution at a spatial frequency of 12 cycles/° when receiving a-tDCS while they were not when receiving c-tDCS. Larger stimuli with varying period may have moderated the effects of tDCS and shifted any noticeable effects to higher spatial frequencies.

The effects of tDCS on contrast sensitivity values measured to a horizontal grating of a fixed size and variable period can be seen in **Figure 3A.7**. We found no interaction effect between tDCS polarity and spatial frequency, $F(3,27) = 2.83$, $p = .057$, $\eta_p^2 = .239$. Similarly, no discernable spatial frequency dependent effects of a-tDCS were observed when directly measuring the magnitude of the difference score in contrast sensitivity: under a-tDCS, effect sizes were small and oscillated between increments 8 cycles/°: g = 0.05, 95% CI [-0.30 0.40],

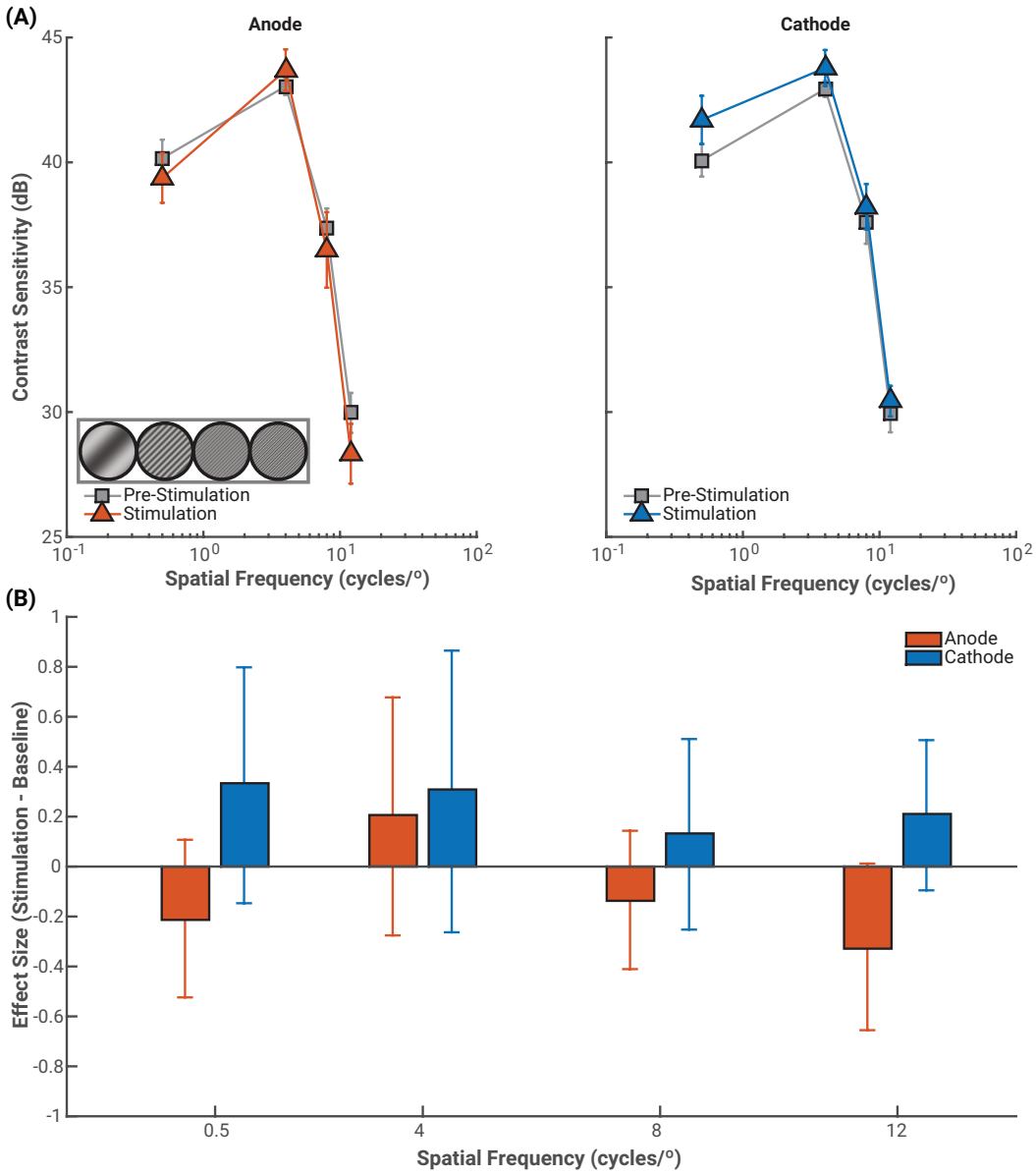

Figure 3A.6. A Average pre-stimulation (gray) and stimulation contrast sensitivity functions for both a-tDCS (red) and c-tDCS (blue) measured with the oblique fixed size gratings (at spatial frequencies of 0.5, 4, 8, and 12 cycles/°). Contrast sensitivity is presented in decibels (dB). Error bars represent the standard error of the mean difference calculated across observers. **B** Effect size measures of the mean difference contrast sensitivity measured at stimulation and at pre-stimulation. We find a-tDCS to decrease contrast sensitivity while c-tDCS increases it. We found no statistically significant polarity specific effect of tDCS on contrast sensitivity measured here. However, at there are indications (both at the group-level and case-level analyses) of a tDCS polarity specific effect on contrast sensitivity measured to our highest spatial frequency (12 cycles/°). Error bars represent the exact 95% confidence interval of the effect size.

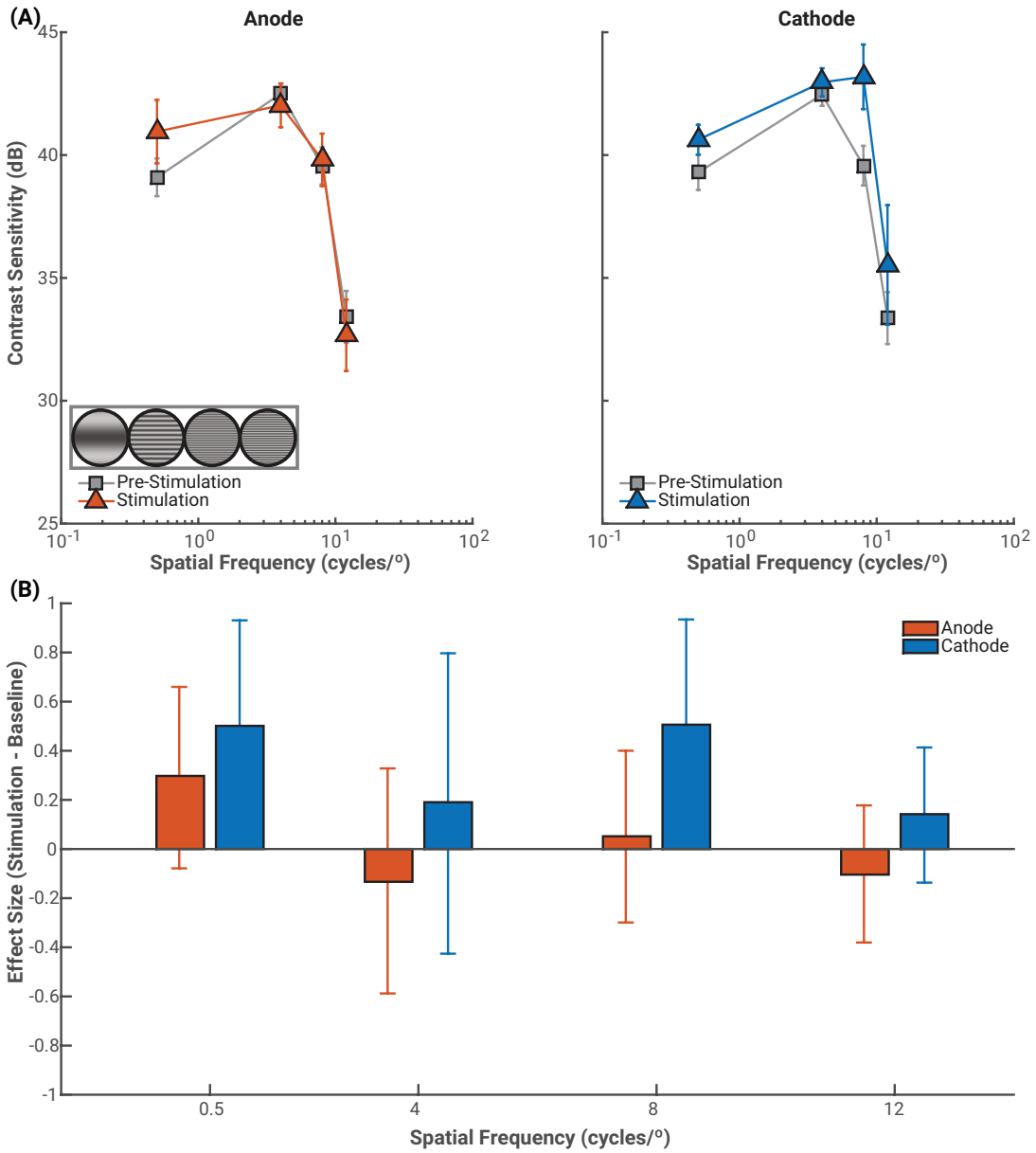

Figure 3A.7. A Average pre-stimulation (gray) and stimulation contrast sensitivity functions for both a-tDCS (red) and c-tDCS (blue) measured with the horizontal fixed size gratings (at spatial frequencies of 0.5, 4, 8, and 12 cycles/°). Contrast sensitivity is presented in decibels. Error bars represent the standard error of the mean difference calculated across observers. **B** Effect size measures of the mean difference contrast sensitivity measured at stimulation and at pre-stimulation. We found no effect of tDCS polarity on contrast sensitivity measured with this particular stimulus, but do find a large increase in contrast sensitivity to our 8 cycle/° grating under c-tDCS. Error bars represent the exact 95% confidence interval of the effect size.

LTR = 2.61) and decrements (4 cycles/°: g = -0.13, 95% CI [-0.59 0.33], LTR = 109.22; 12 cycles/°: g = -0.10, 95% CI [-0.38 0.18], LTR = 4.17) in contrast sensitivity across spatial frequency. Unlike its oblique counterpart, LTRs for horizontal stimuli under a-tDCS were small, which is indicative of little change in the proportion of scores in the left tail of the combined distribution (the large LTR for the 4 cycle/° is most likely due to the high sensitivity and low variability of contrast sensitivity measured prior to stimulation, see **Figure 3A.A4**). There was a large facilitatory effect of c-tDCS on contrast sensitivity measured to the 8 cycles/° (g = 0.51, 95% CI [0.06 0.93], LTR = 1.60*) horizontal gratings. However, at the case-level, the effect is relatively small as observer contrast sensitivity to horizontal 8 cycle/° gratings were only 1.6 times more likely to fall in the left tail of the combined distribution at baseline than when receiving stimulation.

tDCS modulated the magnitude of the oblique effect (see **Figure 3A.8**). We did observe an increase in the magnitude of the oblique effect by half a standard deviation from baseline under c-tDCS for the 8 cycles/° grating (g =1.38, 95% CI [0.39 2.36]), which reflects the large increase in the average contrast sensitivity of observers to the 8 cycles/° horizontal grating that was not observed for the oblique grating. The overlap between baseline and tDCS contrast sensitivity difference scores suggests the application of tDCS had no impact on the magnitude of the oblique effect in our fixed size stimuli.

The effects of tDCS on low spatial frequency contrast sensitivity

It is important to note that while we do find that the contrast sensitivity to a grating with a spatial frequency of 0.5 cycles/° can be affected by tDCS, these effects are unlikely to be indicative of a true modulation in contrast sensitivity under tDCS. The 0.5 cycles/° grating were identical in both the fixed period and fixed size condition, and attributing contrast sensitivity to either condition was arbitrary in our analysis. When both the fixed period and fixed size conditions are combined, we find that both a-tDCS (g = 0.46, 85% CI [0.05 0.85], LTR = 1.61*) and c-tDCS (g = 0.44, 95% CI [0.02 0.85], LTR = 4.44*) increased contrast sensitivity from baseline to stimulation equally. As both a-tDCS and c-tDCS had an identical influence on contrast sensitivity values, neither can serve as a control for the other, which complicates how tDCS effects may be defined at lower spatial frequencies. Given the known physiology of striate cortex, we had not anticipated any modulation of contrast sensitivity under tDCS for our lowest spatial frequency grating. Our 0.5 cycles/° gratings differ from all others used in this study as it

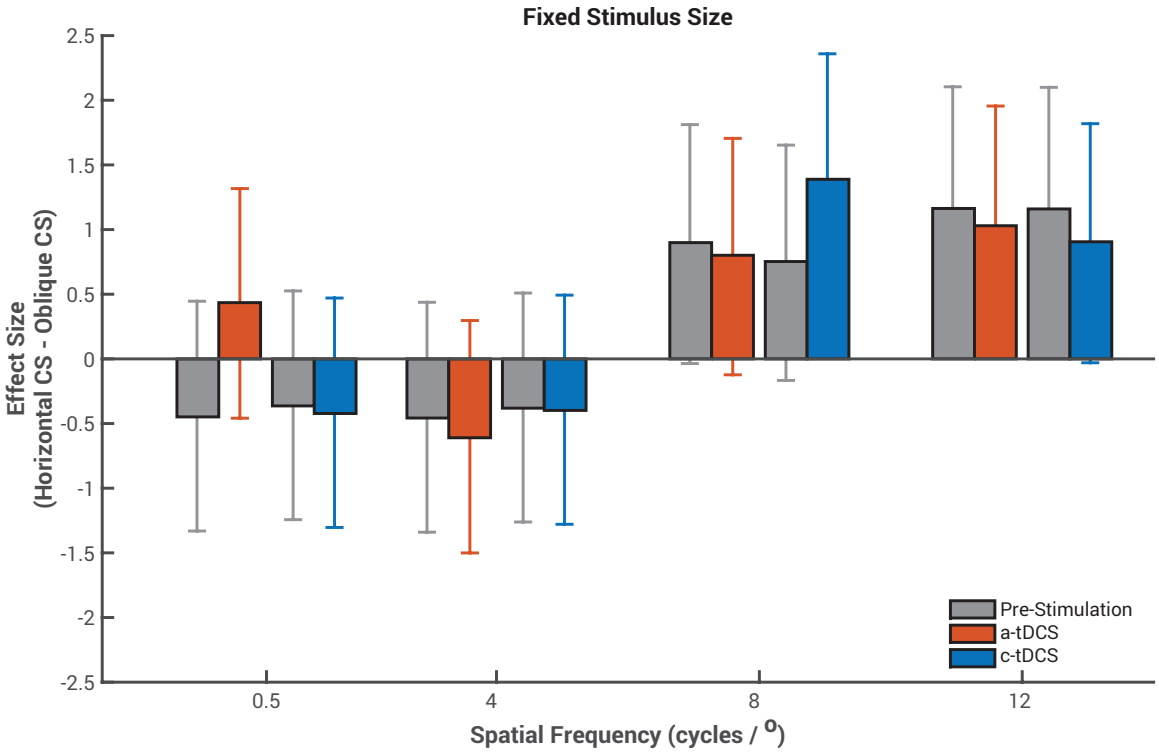

Figure 3A.8. Effect size of the mean difference between contrast sensitivity measured with horizontally orientated gratings and oblique orientated gratings. Gray bars represent the respective pre-stimulation baseline for either a-tDCS (red) or c-tDCS (blue) contrast sensitivity difference between horizontal and oblique gratings. The large difference in contrast sensitivity between horizontal and oblique gratings can easily be seen at the high spatial frequencies used in this study when contrast sensitivity was measured with stimuli of a fixed size. However, tDCS polarity (anode and cathode) had no impact on the oblique effect: the contrast sensitivity difference between both oblique and horizontal gratings remained under both stimulation conditions. Error bars represent the exact 95% confidence interval for the mean difference effect size (effect sizes here are standardized on the pooled standard deviation).

is part of the low spatial frequency rollover in the CSF, and is presumably subject to additional inhibition than the other gratings (Meese & Hess, 2004; Webster & Miyahara, 1997). If the application of tDCS over striate cortex creates an imbalance in the interactive properties of neurons (i.e., excitatory and inhibitory interactions), regardless of polarity, then contrast sensitivity to low spatial frequency gratings may be affected differently by the current generated with tDCS than to high spatial frequencies. Our findings here suggest that the application of a current, regardless of polarity, will increase contrast sensitivity to low spatial frequencies. Thus, tDCS seems to be of not true influence on contrast sensitivity to low spatial frequencies.

Discussion

The goal of the current study was to assess whether the stimulus dimensions of gratings (spatial frequency, size, and orientation) could modulate the effectiveness of tDCS on contrast sensitivity. We measured changes in contrast sensitivity, from a pre-stimulation baseline, to gratings of a fixed period (1.5 cycles) and fixed size (3°) at 4 different spatial frequencies (0.5, 4, 8, and 12 cycles/°) and 2 orientations (oblique and horizontal) while observers received either a-tDCS or c-tDCS over striate cortex. As expected, we found particular stimulus dimensions to be more susceptible to the effects of tDCS. Polarity specific effects of tDCS in visually responsive cortical areas are uncommon (Accornero et al., 2007; Antal, Kincses, et al., 2004; Antal et al., 2001; Jacobson et al., 2012), however, we found that contrast sensitivity measured with an 8 cycles/° fixed period 45° oblique grating showed a large polarity specific effect of tDCS, in that a-tDCS decreased while c-tDCS increased contrast sensitivity. Similar effects were obtained with the horizontal grating of the same spatial frequency, but the magnitude of the effect was smaller than that of the 45° oblique grating, and not statistically significant. The 45° oblique grating of a fixed size also showed indications of a polarity specific effect of tDCS at our highest spatial frequency (12 cycles/°), however, this effect, while large, was not statistically significant. Our results suggest that stimulus dimensions that generally elicit greater contrast sensitivity from observers are less susceptible to the influence of both a-tDCS and c-tDCS than stimulus dimensions that generally elicit poor contrast sensitivity (high spatial frequencies when measured with a fixed period and non-cardinal orientations)[10], as is typical of other experiment findings

[10] Our findings suggest a correlation between the observer internal sensitivity to contrast from a particular set of stimulus dimensions and the magnitude of the tDCS modulation obtained, specifically, the improvements in contrast sensitivity should be negatively correlated with baseline contrast sensitivity, while the inverse holds true for decrements in contrast sensitivity. Under a-tDCS, only the 12 cycles/° fixed period oblique gratings showed a

that have tried to increase contrast sensitivity in human observers (Adini et al., 2002, 2004; Dorais & Sagi, 1997; Li et al., 2009; Maehara & Goryo, 2007; Sowden et al., 2002; Thompson et al., 2008)**.**

The constraints of stimulus dimensions on tDCS as described above highlight the importance of considering both the electrical components of this stimulation technique (e.g., ampere, current density, stimulation duration; Paulus, 2011; Miranda et al., 2006), and the structural organization of the stimulated cortical area. In striate cortex, neurons with receptive fields of higher preferred spatial frequencies are typically found in superficial layers of cortex, near the apex of the calcarine sulcus (De Valois et al., 1982; Engel, Glover, & Wandell, 1997; Foster, Gaska, Nagler, & Pollen, 1985; Henriksson, Nurminen, Hyvärinen, & Vanni, 2008; Horton, 2006; Tootell, Silverman, & De Valois, 1981; Tootell, Switkes, Silverman, & Hamilton, 1988; Yu et al., 2010). These neurons are more likely to be influenced by tDCS, as the magnitude of the electric field is greatest at the cortical surface (Bikson & Rahman, 2013; Miranda et al., 2006; Nitsche et al., 2007). Similarly, tDCS effects are limited to the central visual field, which is retinotopically mapped to the apex of the calcarine sulcus (Engel et al., 1997; Grill-Spector & Malach, 2004; Horton, 2006; Tootell, Switkes, et al., 1988). It has already been shown that stimuli presented at eccentricities greater than 2° are unaffected by tDCS (Kraft et al., 2010), and is therefore unsurprising that detection of large gratings, which cover more than the central 2° of the visual field, was only be mildly modulated by tDCS. This may have been exacerbated for large gratings with a high period due to summation effects, which also increase contrast sensitivity (Graham, Robson, & Nachmias, 1978; Legge, 1978; Meese & Summers, 2007; Peli et al., 1993). We note, however, that other mechanisms may have been involved, as a recent study by Costa and colleagues (2015) has failed to replicate the findings of Kraft and colleagues (2010).

Of note to the goals of the current study, we have shown that the direction and magnitude of the modulation in contrast sensitivity caused by tDCS can vary when other parameters, including stimulus orientation and period, are varied. This can lead to a diminished effect of

---

statistically significant positive correlation between contrast sensitivity and tDCS effect magnitude (Hedge's g), r(9) = .85, p = .002, 95% CI [.47 .96]. Under c-tDCS, only the 4 cycles/° fixed period oblique gratings showed a statistically significant negative correlation, r(9) = -.64, p = .045, 95% CI [-.91 -.02]. We note that the number of observers in our study is small and consequently, we are probably underpowered to properly identify any correlation between stimulus dimension and tDCS modulation magnitude. Nevertheless, the two correlations obtained here suggest a link between internal sensitivity and the magnitude of tDCS effects.

tDCS on contrast sensitivity, change the direction of the effect (from an increment to a decrement), or abolish the effect completely (e.g., we found no effect of a-tDCS for large horizontal gratings). Consequently, our findings emphasize caution when linking effect direction to tDCS polarity in vision paradigms. Many of the confidence intervals calculated here contained both positive and negative values. As 95% of all confidence intervals calculated in this way will contain the true effect size of a-tDCS and c-tDCS on contrast sensitivity measurements, both increments and decrements in contrast sensitivity appear equally valid directions of effects to be obtained under either a-tDCS or c-tDCS, at least when measuring contrast sensitivity under our tDCS protocol. In fact, the expected directionality of tDCS polarity - a-tDCS excites while c-tDCS inhibits - which stems predominantly from findings in motor cortex (Jacobson et al., 2012; M. A. Nitsche et al., 2007; M. A. Nitsche, Fricke, et al., 2003; Pellicciari et al., 2013; Stagg et al., 2009), should be disregarded for cortical areas that are functionally and structurally different (Shipp, 2005, 2007). It is best when implementing tDCS within a vision paradigm to utilize stimulus dimensions that will reliably elicit large effects of tDCS and to infer directionality post hoc.

tDCS Polarity and Psychophysical Performance

Whilst we find facilitatory and inhibitory effects of tDCS on visual function, the direction of these effects is opposite to that of previous tDCS vision studies, which have reported increases in contrast sensitivity during a-tDCS (Kraft et al., 2010; Peters et al., 2013; Spiegel et al., 2013), and decreases during c-tDCS (Antal et al., 2001; Chaieb et al., 2008). However, we are not the first to report polarity specific effects of tDCS over striate cortex inverted to those generally found in motor cortex (Accornero et al., 2007; Hansen et al., 2015; Antal et al., 2004a; Pirulli et al., 2014). The association between the effects induced by neuro-stimulation protocols on neuronal behaviour, whether it is “excitatory” or “inhibitory” in nature, and the behavioural outcome remains unclear. This holds true for other neuro-stimulation protocols (e.g., rTMS), that have shown both inhibitory and excitatory stimulation can generate increases in contrast sensitivity (Thompson et al., 2008; Waterston & Pack, 2010). Granted, there are many factors that contribute to the net influence of the current on cell activity, including but not limited to the stimulation onset relative to stimulus onset, stimulation duration, and the direction of current in relation to the somatodendritic axis of cells beneath the electrode (Bikson & Rahman, 2013; Peterchev et al., 2012; Pirulli et al., 2014; Radman et al., 2009). Nevertheless, the net effects of

tDCS polarity on the behaviour of cells has been shown to follow the expected directionality (a-tDCS excites while c-tDCS inhibits) both at the single cell and network level, at least in motor cortex (Medeiros et al., 2012; M. A. Nitsche, Fricke, et al., 2003; Radman et al., 2009; Rahman et al., 2013; Reato et al., 2010). If the influence of current polarity on cells in the primary visual cortex is similar to that of motor cortex, then our finding that inhibitory stimulation (c-tDCS) benefits contrast sensitivity may be explained by a reduction the overall cortical excitability below a certain threshold noise level, thus minimizing stimulus uncertainty in observers (Pelli, 1985), and increasing contrast sensitivity. Conversely, a-tDCS, which increases the overall excitability of cells beneath the electrode, may lower the signal-to-noise ratio, and lead to a reduction in contrast sensitivity attributed to increased uncertainty in observers. This noise-reduction hypothesis has previously been used to account for the facilitatory effect of c-tDCS in a noise limited motion discrimination task (Antal, Nitsche, et al., 2004). However no direct evidence for tDCS effects on neural noise currently exist.

The few neuro-imaging studies that have measured striate cortex activity following c-tDCS suggest that the impact on the behaviour of cells, at least at a network level, from a mild direct current may be counter to that of motor cortex. Cathodal tDCS is known to decrease both neuronal and cortical activity of cells in motor cortex (Jacobson et al., 2012; M. A. Nitsche et al., 2007, 2008; M. A. Nitsche, Fricke, et al., 2003; Rahman et al., 2013; Reato et al., 2010), however, over striate cortex, both inhibitory (Antal, Kincses, et al., 2004) and excitatory effects of c-tDCS on behaviour have been reported (Accornero et al., 2007; Antal, Kincses, et al., 2004; Antal et al., 2012; Pirulli et al., 2014). Given the variability in the net effects of tDCS in primary visual cortex, a noise reduction explanation to the benefits c-tDCS seems an unlikely explanation. The injection of a mild electrical current in striate cortex changes the balance of excitation and inhibition between neurons, which is a known neuro-mechanism responsible for the tuning characteristics of visually responsive neurons (tuning curve bandwidth orientation and spatial frequency), and in particular their response to contrast (Blin et al., 1993; Edden et al., 2009; Ferster and Miller, 2000; Rose and Blakemore, 1974; Li et al., 2008; Katzner et al., 2011). If tDCS affects this balance, then its effects may lie in low-level gain mechanisms that adjust the responses of a cell to a given level of contrast.

Limitations

Trans-cranial Direct Current Stimulation is a popular neuro-stimulation technique that is affordable and relatively simple to implement. However, there are certain caveats that accompany the implementation of tDCS in vision experiments. Of interest to the current study is the underlying cortical structure being influenced by tDCS. It is well known that the polarizing effects of tDCS are dictated by the alignment of the cells in relation to the direction of current (Radman et al., 2009; Rahman et al., 2013; Rushton, 1927). Pyramidal cells with apical or basal dendrites oriented towards the cortical surface (i.e., neurons perpendicular to the cortical surface), will be correctly aligned with an electrode placed on a gyral surface, and therefore subject to the polarizing effects of the electric field generated by tDCS (with the net polarization dependent on the direction of current; Radman et al., 2009; Rushton, 1927). However, for cells located within cortical layers buried in a sulcus would be oriented parallel to the electrode, and likely not altered by tDCS. Cortical folding of the stimulated area is therefore a crucial component in the net results of tDCS, as it will dictate which neurons are innervated by tDCS. This is of particular relevance here, as we used fairly large electrodes (48 cm^2 over Oz and 96 cm^2 over Cz) in our stimulation protocol, and most likely covered both striate and extrastriate cortical areas, which differ in their cortical folding properties (Horton, 2006; Rosa, Casagrande, Preuss, & Kaas, 1997; Rosa, Fritsches, & Elston, 1997). It is unclear how the stimulation of both striate and extrastriate cortex may have impacted our findings here, however, more focal approaches that use smaller electrodes (HD-tDCS; Miranda et al., 2013; Rahman et al., 2013), may help prevent the simultaneous stimulation of multiple visually responsive cortical sites in future studies.

Conclusions

The effects of tDCS on contrast sensitivity were most noticeable when measured at high spatial frequencies with 45° oblique oriented gratings with a fixed period of 1.5 cycles, which suggests that the magnitude of tDCS effects in vision are dependent upon the baseline sensitivity of observers to the presented stimuli: stimulus dimensions that will generally elicit high contrast sensitivity from observers (large, cardinally orientation gratings with a spatial frequency near the peak of the CSF) are not as suceptible to be modulated by tDCS. In addition, we found that under certain conditions, tDCS effects may be facilitatory or inhibitory within a particular group of observers, regardless of stimulation polarity, and that careful use of stimuli that reliably elicit tDCS polarity specific effects should favoured when implementing tDCS in vision studies.

Chapter 3A Tables

Table 3A.1 – Repeated Measures ANOVA – Fixed Period Oblique Stimuli

Factors	SS	*df*	MS	F	*p*	η_p^2
tDCS	1.98	1	1.98	0.52	0.489	0.055
SF	5.19	3	1.73	0.29	0.830	0.032
tDCS x SF	72.30	3	24.10	8.10	0.001	0.474
Subjects	57.57	9	6.40			
tDCS x Subjects	34.17	9	3.80			
SF x Subjects	159.36	27	5.90			
tDCS x SF x Subjects	80.29	27	2.97			
Total	410.85	79	5.20			

Table 3A.2 – Simple Effect Comparison - Fixed Period Oblique Stimuli

Factors	SS	*df*	MS	F	*p*	η_p^2
tDCS $_{\text{at SF = 8 cpd}}$	26.35	1	26.35	20.79	0.001	0.698
Subjects	34.83	9	3.87			
tDCS X Subjects	11.41	9	1.27			
Total	72.58	19	3.82			

Table 3A.3 – Repeated Measures ANOVA – Fixed Size Oblique Stimuli

Factors	SS	*df*	MS	F	*p*	η_p^2
tDCS	48.45	1	48.45	9.23	0.014	0.506
SF	20.46	3	6.82	1.35	0.278	0.131
tDCS x SF	14.41	3	4.80	0.66	0.585	0.068
Subjects	64.89	9	7.21			
tDCS x Subjects	47.25	9	5.25			
SF x Subjects	135.93	27	5.03			
tDCS x SF x Subjects	197.21	27	7.30			
Total	528.60	79	6.69			

Table 3A.4 – Repeated Measures ANOVA – Fixed Period Horizontal Stimuli

Factors	SS	*df*	MS	F	*p*	η_p^2
tDCS	12.27	1	12.27	1.08	0.325	0.107
SF	14.26	3	4.75	0.58	0.631	0.061
tDCS x SF	39.13	3	13.04	1.97	0.142	0.179
Subject	284.48	9	31.61			
tDCS x Subject	101.86	9	11.32			
SF x Subject	219.68	27	8.14			
tDCS x SF x Subject	178.88	27	6.63			
Total	850.56	79	10.77			

Table 3A.5 - Repeated Measures ANOVA – Fixed Size Horizontal Stimuli

Factors	SS	*df*	MS	F	*p*	η_p^2
tDCS	56.38	1	56.38	4.80	0.056	0.348
SF	45.33	3	15.11	0.97	0.423	0.097
tDCS x SF	48.72	3	16.24	2.83	0.057	0.239
Subject	278.77	9	30.97			
tDCS x Subject	105.70	9	11.74			
SF x Subject	421.96	27	15.63			
tDCS x SF x Subject	154.98	27	5.74			
Total	1111.84	79	14.07			

Chapter 3B

DOES TRANS-CRANIAL DIRECT CURRENT STIMULATION (TDCS) MODIFY DISCRIMINATION THRESHOLDS OF THE SLOPE OF THE AMPLITUDE SPECTRUM?

Bruno Richard, Bruce C. Hansen, Aaron P. Johnson

Abstract

The discrimination of α is dependent on the representation of low spatial frequency content within an image when the reference α is steep (see **Chapter 2**). Thus, the discriminability of steep αs seems subject to the activity of low spatial frequency tuned channels within the early visual system. We aimed to explore this effect further by directly manipulating the activity of spatial frequency channels in an α discrimination task with trans-cranial Direct Current Stimulation (tDCS). tDCS is a neuro-stimulator that modulates the membrane potential of cortical neurons and alters their responses to visually presented stimuli. The effects of tDCS are spatial frequency dependent, and as we have previously shown, only modulate contrast detection of higher spatial frequencies. The findings of **Chapter 2** indicated that the spatial frequency tuning of the contributing channels might be correlated with the α of the reference stimulus. Thus, if the discrimination of shallower reference αs is subject to the activity of higher spatial frequency channels, it is possible that tDCS will only influence discrimination thresholds of shallow αs. Discrimination thresholds to steeper slopes should remain unaffected by tDCS. Participants completed two stimulation sessions, and began with either a-tDCS or c-tDCS, while a third group received sham in both sessions. The effects of tDCS on α discrimination were small and unspecific. The current applied by tDCS is much smaller than that required to illicit action potentials in neurons directly beneath the electrode. As tDCS only raises or decreases the likelihood of the release of an action potential, its neuro-modulatory effects may be too weak to influence the behaviour of cells exposed to 1/*f* noise stimuli. Given that previous research has shown that tDCS effects are constrained to high spatial frequencies and are orientation specific, the use of tDCS on stimuli that are broadband in both spatial frequency and orientation may be an ill-suited approach to investigate the behaviour of V1 cells when exposed to naturalistic stimuli.

Early visual processes (e.g., contrast detection) can be altered in humans by the application of trans-cranial Direct Current Stimulation (tDCS) over the primary visual cortex (Antal, Nitsche, & Paulus, 2001, 2006a, 2006b; Kraft et al., 2010; Peters, Thompson, Merabet, Wu, & Shams, 2013; Spiegel, Byblow, Hess, & Thompson, 2013). The change in perception induced by tDCS is both polarity and stimulus specific, and we have shown in the preceding chapter (**Chapter 3A**) that for contrast detection, the effects of tDCS can be best observed at higher spatial frequencies (i.e., 8 cycles/°) and non-cardinal orientations (i.e., 45°; Richard, Johnson, Thompson, & Hansen, *under review*). Specifically, cathodal tDCS (c-tDCS) increased contrast sensitivity to high frequency oblique gratings, while anodal tDCS (a-tDCS) generated a net decrease in contrast sensitivity. The magnitude of the change induced by tDCS was somewhat correlated with the baseline contrast sensitivity of observers, and larger when contrast sensitivity to a particular stimulus dimension is low, similar to more traditional psychophysical training techniques on contrast sensitivity (Adini, Sagi, & Tsodyks, 2002; Adini, Wilkonsky, Haspel, Tsodyks, & Sagi, 2004; Li, Polat, Makous, & Bavelier, 2009; Sowden, Rose, & Davies, 2002). Trans-cranial Direct Current Stimulation may, therefore, temporarily modify mechanisms that relate to observer learning and task performance (i.e., consolidation of visual information; Peters et al., 2013), with the added benefit of control over the directionality of observer performance, as it can either improve or diminish it according to the stimulation polarity. Most of the literature on the perceptual effects of tDCS has centred on modulating the performance of observers to simple, narrowband stimuli; however, there are indications that tDCS can modify the complex visual processes of broadband stimulation as well. These findings propose that the modulation induced by tDCS on vision may be sufficient to alter the behaviour of multiple neurons – differently tuned in spatial frequency and/or orientation (Antal, Kincses, Nitsche, Bartfai, & Paulus, 2004; Antal, Nitsche, et al., 2004; Spiegel et al., 2013). Consequently, tDCS could be a useful tool to explore the neuronal mechanisms that underlie naturalistic vision. Here, we asked if tDCS could alter the perception of a stimulus broadband in both spatial frequency and orientation. Specifically, we tested whether the application of either a-tDCS or c-tDCS could modulate α discrimination thresholds of the noise stimuli (1/*f* noise) used in **Experiment 2.1** and **2.2**. Additionally, we investigated if the effects of tDCS on α discrimination thresholds were reference α specific. Given that the effects of tDCS on spatial vision seem constrained to higher spatial frequencies (Richard, et al., *under review*), and stimulus conditions that observers are

generally less sensitive to, we may expect tDCS to have larger effects on α discrimination of shallower reference αs (i.e., $\alpha < 1.0$, which are perceptually dominated by higher spatial frequency content).

The exact processes that lead to the modulatory effects of tDCS on the activity of cells in striate cortex remain unclear (as described in **Chapter 3A**). But, it is known that the effects of tDCS are largest on visually responsive neurons with receptive fields at or near fovea (i.e., cells located on the cortical surface; Kraft et al., 2010; but see Costa et al., 2015 for contrasting findings), and that there is a negative correlation between the effects of neuro-stimulation and the baseline performance of observers (Antal et al., 2001; Thompson et al., 2008). Most recently, it has been demonstrated that neuro-stimulation (rTMS) may modify the neuronal interactions responsible for adjusting the tuning width (both spatial frequency and orientation) of cells in striate cortex (Kim, Allen, Pasley, & Freeman, 2015). The perceptual effects of tDCS, therefore, may lie in the interactive properties of neurons within the visual cortex, which renders it an interesting tool to assess the role of early neuronal interactions in perception. That said, the studies mentioned above were all conducted with simple, narrowband stimuli, which are purposefully designed to activate only a small subset of neurons in striate cortex. Under naturalistic stimulation, however, the image on the retina will stimulate a large number of visually responsive cells with varied tuning properties. Furthermore, the output of these cells will be weighted according to the activity of other, similarly and differently tuned cells. Thus, the activity of cells in striate cortex exposed to naturalistic (i.e., broadband) stimuli is poorly approximated by findings obtained with narrowband stimuli (Dan, Atick, & Reid, 1996; David, Vinje, & Gallant, 2004; Kayser, Salazar, & Konig, 2003; Maldonado & Babul, 2007; Olshausen & Field, 1996; Zetzsche & Röhrbein, 2001). Thus, it is unclear how tDCS may alter visual processes in tasks that employ broadband, or naturalistic, stimuli.

There is evidence that tDCS is able to modulate the performance of observers on psychophysical tasks that incorporate spatially more complex stimuli than single narrowband gratings. Two studies, to date, have explicitly measured the modulatory effects of tDCS on the perception of spatially complex patterns (Hansen et al., 2015; Spiegel, Hansen, Byblow, & Thompson, 2012). Both used masking paradigms (overlay suppression and surround suppression, respectively) to assess if tDCS could enhance or diminish the strength of the masking effect on

the perception of a target stimulus[11]. Surround-suppression occurs when neural responses to a target are diminished by a stimulus presented outside of, or surrounding, their classical receptive field (Akasaki, Sato, Yoshimura, Ozeki, & Shimegi, 2002; Cavanaugh, Bair, & Movshon, 2002; DeAngelis et al., 1992; Fitzpatrick, 2000; Osaki, Naito, Sadakane, Okamoto, & Sato, 2011; Walker, Ohzawa, & Freeman, 2000), which stems from suppressive lateral interactions between cells in primary visual cortex (Cavanaugh et al., 2002). In humans, surround suppression is narrowly tuned for both orientation [Half-Width Half-Height (HWHH) = 30°] and spatial frequency (~ 1.4 octaves), which indicates that the suppression originates within striate cortex (Petrov et al., 2005). In their study, Spiegel and colleagues (2012) measured the contrast detection threshold of a narrowband Gabor target both with and without the presence of a surround annulus, matched in frequency, but free to vary in orientation. They found that a-tDCS applied over the primary visual cortex negated the suppressive effects of the surround mask, and returned contrast detection thresholds to baseline values, while c-tDCS had no effect. Thus a-tDCS may be capable of changing the lateral interactions that underlie surround suppression (Cavanaugh et al., 2002; Huang et al., 2008; Petrov et al., 2005; Petrov & Mckee, 2006; Spiegel et al., 2012; Xing & Heeger, 2000, 2001). But, it is unclear which of the neuronal responses, either to the mask or to the target (Baker & Vilidaite, 2014) are altered by tDCS. That is, tDCS may alter the suppressive effects of a surround mask directly, or may somehow increase neural responses to the target stimulus to exceed the suppressive effects of the mask.

There is evidence that the spatial characteristics of the mask, whether it is narrowband or broadband in spatial frequency content, will change the strength of the tDCS effect on the suppression induced by the mask, which suggest tDCS is modulating neural responses to the mask. Overlay suppression (i.e., simultaneous masking) occurs when a mask is placed over a target and alters perception (Foley, 1994; Kim, Haun, & Essock, 2010; Meese & Holmes, 2010; Petrov et al., 2005). Unlike surround suppression, overlay suppression is broadly tuned both in spatial frequency (approximate bandwidth is 3 octaves) and orientation (HWHH = 90°), and for this reason was thought to occur in stages of processing prior to striate cortex (Petrov et al., 2005). Yet, we have recently shown that the magnitude of overlay masking can be altered by the

[11] In both studies, the target stimulus was always a narrowband Gabor. Spiegel and colleagues (2012) presented an oblique (45°) oriented Gabor with a spatial frequency of 3.5 cycles/°, while Hansen and colleagues (*in press*) used a Gabor oriented either at vertical, 45° oblique or horizontal, with a spatial frequency of 8 cycles/°. The complexity within these studies stem from tDCS modulating the strength of the masking effect (i.e., suppression factors), and not the effects of tDCS on the perception of the narrowband Gabor.

orientation of the mask when it is broadband in spatial frequency (Hansen et al., 2015). That is, when the mask contains a large amount of luminance contrast energy across spatial frequency (the masks had a 1/*f* amplitude spectrum over ~ 2 octaves of spatial frequencies centred on 8 cycles/°), but is narrowband in orientation (HWHH = 10°), overlay masking shows orientation tuning characteristics that could not originate from a pre-cortical process. Additionally, when c-tDCS was applied over the primary visual cortex of observers, it reduced the suppression of the broadband overlay mask on a Gabor target much more than that of the identically oriented narrowband mask (spatial frequency HWHH = 1 octave). As the spatial characteristics of the mask altered the tDCS induced effects in the overlay masking paradigm, it would suggest that tDCS does modify cortical signals to a mask, and furthermore, does so most when the mask is broadband in spatial frequency.

The application of tDCS over striate cortex has a noticeable impact on observer psychophysical performance both with narrowband stimuli, and more complex, broadband stimuli that have naturalistic αs (α = 1.0; Billock, 2000). In **Chapter 2**, we demonstrated that α discrimination thresholds were subject to the representation of contrast energy at low spatial frequencies within our noise images. These effects were only found when α was relatively steep (α equal to or greater than 1), which suggest that there is a negative correlation between the tuning of the contributing spatial frequency channel and the perceptually dominant spatial frequency content within 1/*f* noise images (Boynton et al., 1999; Britten, Shadlen, Newsome, & Movshon, 1992; Campbell & Kulikowski, 1972; Haynes et al., 2003; Kwon, Nelson, Toth, & Sur, 1992; Ross & Speed, 1991; Shadlen & Newsome, 1998; Zenger-Landolt & Heeger, 2003). Thus, the spatial frequency bands used by observers to discriminate α of noise images may change in accordance with the reference α (Hansen, Ellemberg, & Johnson, 2012; Hansen, Jacques, Johnson, & Ellemberg, 2011; Párraga & Tolhurst, 2000; Tolhurst & Tadmor, 1997). As the effects of tDCS appear to be constrained to higher spatial frequencies (Richard et al., 2015), we ask here if α discrimination thresholds can be altered by tDCS, and if this effect may be most prominent when the reference α is shallow (as they are perceptually dominated by higher spatial frequency content). We measured α discrimination thresholds according to the same psychophysical procedure defined in **Experiment 2.1** in a group of inexperienced psychophysical observers and tested for changes in thresholds between tDCS and a non-stimulation baseline. Furthermore, we added a sham group in this study to verify for any effects

of stimulation that may be attributed to confounding variables (e.g., the presence of the electrodes), which was not implemented in **Chapter 3A**.

Experiment 3.2

Method

Participants

Fifteen undergraduate students in psychology (14 females), with a median age of 22 years (range: 19 – 39 years) took part in this study. All participants had normal or corrected to normal visual acuity (cut-off = 20/25). Informed consent was obtained from all participants and all were treated in accordance the Tri-Council Policy Statement: Ethical Conduct for Research Involving Humans (2014). Participants were financially compensated for their time. None of our participants in this study had any prior psychophysical testing experience.

Apparatus

Stimuli were presented on a 22.5" Viewsonic (G225fB) monitor driven by an Apple Mac Pro (2 X 2.66GHz processor) equipped with 8GB of RAM and a 1GB PCIe x16 ATI Radeon HD 5770 Graphics card with 10-bit grayscale resolution. Stimuli were displayed using a linearized look-up table, generated by calibrating with a Color-Vision Spyder3 Pro sensor. Maximum luminance output of the display monitor was 100 cd/m^2 (50 cd/m^2 mean luminance after calibration) the frame rate was set to 100 Hz, and the resolution was set to 1024 X 768 pixels. Single pixels subtended .0381° of visual angle (i.e., 2.23 arc min.) when viewed from 1.0 meter. Head position was maintained using a chin rest, and participant input was recorded via keyboard press.

Stimuli

All stimuli in this experiment were constructed in an identical fashion to those of **Experiment 2.1** and **Experiment 2.2** (center stimulus) and generated according to the same 5 reference α values (0.4, 0.7, 1.0, 1.3, and 1.6). All stimuli consisted of synthetic amplitude spectrum noise and were constructed in the Fourier domain using MATLAB (ver. 2014b; Mathworks, Natick, MA), and corresponding Image Processing (ver. 6.4) toolbox. The noise patterns were rendered into the spatial domain by taking the inverse Fourier Transform of amplitude spectrum and a given random phase spectrum, which was randomized each trial. All stimuli were normalized to have an RMS contrast of 0.15. An image patch, with diameter of 1° of visual angle, was cropped from its center and windowed with a cosine-tapered envelope,

which ramped 5% of the image pixels in the proximity of the circle's edge to mean luminance (50 cd/m^2).

Psychophysical Procedures

The psychophysical procedures used to estimate threshold in this experiment were similar to those of **Experiment 2.1** and **Experiment 2.2**, and only an abridged version is presented here. The experimental condition consisted of five reference amplitude spectrum slope values. All observers completed four repetitions of each experimental condition as training prior to the tDCS component of this study, which took approximately two hours to complete. Thresholds were estimated by a temporal three-interval, two-alternative "Odd-Man-Out" forced choice. Participants were asked to select the stimulus, either the first or third presented, that contained the odd-amplitude spectrum – different from the reference stimulus, presented in the second interval in their α (see **Figure 3B.1**). Threshold estimation was identical in both the training and experimental phases of this study.

At the beginning of each trial, a white (RGB [255, 255, 255]) fixation cross, which subtended 0.3° of visual angle in diameter was presented for one second at the center of the screen. This was followed by three stimulus presentation intervals that each lasted 250ms, which were each interlaced by a screen set to mean luminance for 500ms. The second interval always contained the reference amplitude spectrum set at one of the five fixed reference α values. One interval, either the first of the third, contained the same amplitude spectrum as that of the reference interval, while the other contained the test amplitude spectrum with a slope α steeper than the slope α of the reference interval. The interval that contained the test amplitude spectrum was randomized on each trial. At the end of each trial, the screen was set to mean luminance, and participants indicated which interval, either the first or the third, they perceived as being the "Odd-Man-Out" in comparison to the second interval (reference) via keyboard press. The duration of the response interval was unlimited. The trial-to-trial change in the image's slope exponent (α) was controlled in an identical fashion to **Experiment 2.1** and **2.2**.

tDCS Procedures

Our tDCS procedures were similar to those used by Peters, Thompson, and Merabet (2013). After completing the four baseline staircases, observers were separated into three groups, based on the first tDCS session polarity: Anodal tDCS first (a-tDCS First), Cathodal tDCS First

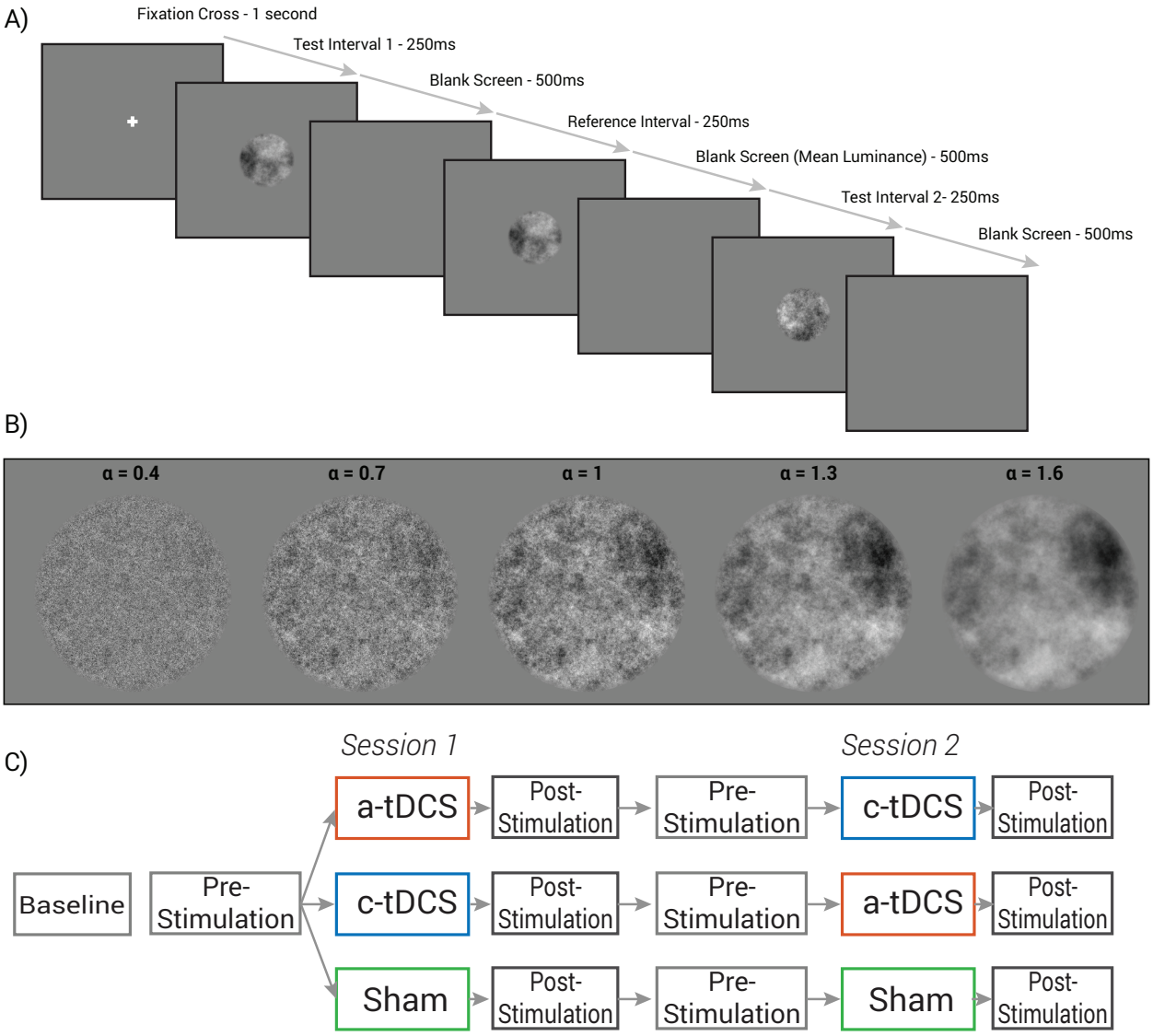

Figure 3B.1. A General psychophysical procedure employed in our experiment, and graphical representation of the "Odd-Man-Out" psychophysical procedure. Observers had to indicate, which of the 1st or 3rd interval contained the stimulus that was different from the second – reference – interval (here the odd stimulus is the 3rd). **B** Example stimuli of the 5 reference α values used in this experiment. The phase spectrum of our stimuli was identical within a trial, and randomized between trials. **C** Experiment sequence completed by observers in this study. All observers completed a baseline session. At the first stimulation session, observers were placed into one of three possible experimental paths (a-tDCS First, c-tDCS First, Sham). They continued on the same path in their second experimental session.

(c-tDCS First), or Sham. Observers completed two experimental sessions, and tDCS polarity was reversed on the second session for both experimental groups, while the sham group received sham stimulation once more (see **Figure 3B.1 - C**). This experimental stimulation design allowed us to minimize any confounds from observers awareness of their current stimulation condition as observers can reliably differentiate between real and sham stimulation, but not anodal and cathodal tDCS (Duecker & Sack, 2015; Minhas et al., 2011; Peters et al., 2013; Spiegel et al., 2012). The total number of staircases completed by observers in the tDCS phase of the study was 25. They completed 2 staircases per reference α prior to and following tDCS, and a single staircase per reference α during tDCS to prevent the duration of stimulation to exceeded 30 minutes (Bikson, Datta, & Elwassif, 2009; Nitsche, Liebetanz, et al., 2003; Poreisz, Boros, Antal, & Paulus, 2007). In total, each tDCS session took about one and a half hours to complete. All observers completed two stimulation sessions, with no less than 48 hours and no more that 7 days between sessions. All stimulation parameters used here were identical to those reported in **Chapter 3A**.

Results

Baseline

The average α discrimination thresholds (Δα) and the change in Δαs as a function of sequential measurement in time during the training session are shown in **Figure 3B.2**. The average Δαs from our 15 inexperienced observers show little tuning to steeper reference α (α = 1.0 and 1.3), as opposed to typical quadratic trend seen with Δαs (see **Results** of **Experiment 1.1** and **2.1**; Hansen & Hess, 2006; Knill, Field, & Kersten, 1990; Tadmor & Tolhurst, 1994). We verified if observer Δαs remained constant across all four baseline measurements of each experimental condition by fitting the Δαs with a linear regression (see **Table 3B.1**). None of the lines of best fit deviated statistically significantly from 0. That said, given that Δαs were fairly high in the baseline portion of the study (see **Figure 3B.2)**, we opted to only compare Δαs while observers received tDCS to their same day (pre-stimulation) Δαs, and did not use the baseline data in subsequent analyses. In addition, we did not analyze all Δαs collected following tDCS (post-stimulation), as regardless of stimulation condition, all observers showed an increase in thresholds.

tDCS

We began our analyses by collapsing over our two tDCS groups (Anode First and

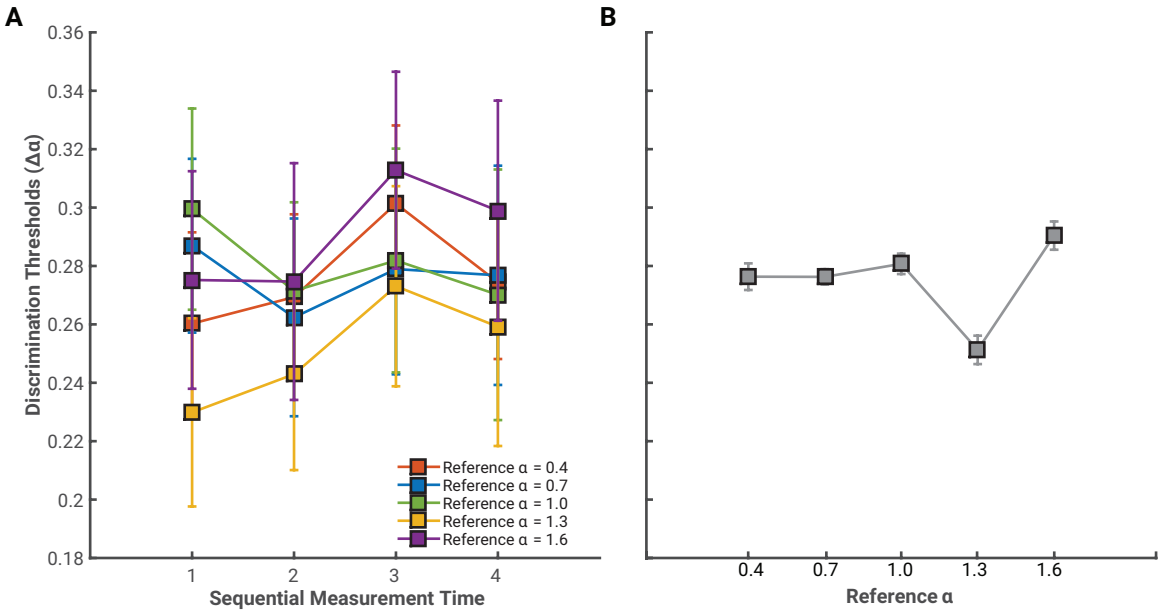

Figure 3B.2. Baseline slope discrimination thresholds averaged across all 15 observers in this study. **A** Average α discrimination threshold across each sequential measurement in the baseline session of the study. Thresholds for all reference α were stable across all 4 repetitions, except for α = 1, which was found to have a statistically significant decrease over all four measurements. **B** The average slope discrimination function, averaged across all 15 observers and the final four measurements for each reference α in the baseline portion of the study. Error bars represent 1 standard error of the mean.

Cathode First) to measure the overall effects of tDCS polarity on Δαs. Effect sizes, which show the magnitude of the change in Δα under tDCS from pre-stimulation, and were calculated in a manner identical to those of **Chapter 3A**, are shown **Figure 3B.3**. It is clear from the collapsed data that neither a-tDCS nor c-tDCS elicited any measurable effect on Δαs (all confidence intervals contained 0).

The second step in our analysis was to verify if the sequence of stimulation for each individual group (receiving a-tDCS first, c-tDCS first or sham) might have altered Δα in a way we could not see in the collapsed data. We conducted a repeated-measures ANOVA with within-subject factors: reference α (5 levels: α = 0.4, 0.7, 1.0, 1.3, 1.6), time (2 levels: pre-stimulation and stimulation), and stimulation session (2 levels: session 1 and session 2) according to the order of stimulation polarity received by observers, and between-subject factor of group (a-tDCS First, c-tDCS First, and Sham). Only the interaction term for Stimulation Group X Stimulation Session X Time was statistically significant, $F(2, 12) = 5.098$, $p = .025$, $\eta_p^2 = .459$ (see **Table 3B.2**). Observers in both the a-tDCS First group (g = -0.54, 95% CI [-1.14 0.11]) and c-tDCS First group (g = -0.91, 95% CI [-1.78 0.01]) showed a decrease in Δαs at the first experimental session from pre-stimulation to stimulation, while observers under sham did not (g = 0.004, 95% CI [-0.52 0.52]). This effect was only observed at the first experimental session (see **Figure 3B.4**), and was not polarity specific, as both the a-tDCS First group and the c-tDCS First group showed a decrease in Δαs of similar magnitude.

Finally, we decided to conduct a descriptive analysis, similar to that of **Chapter 3A** and calculated the effect size for the mean difference in Δαs for each stimulation group and reference αs (see **Figure 3B.4**). Statistical significance was assed by constructing 95% confidence intervals around each effect size measure, and evaluating whether the interval contained an effect size value of 0. The effect sizes we calculated here are relatively large for tDCS induced effects (g ~ 0.6 SD; Jacobson, Koslowsky, & Lavidor, 2012), particularly in the cathode First group. Most had interval estimates that encompassed 0, and are therefore not considered to be statistically significant. We did find a large decrease in Δαs in the first stimulation session of the cathode First group for a reference α of 1.6 (g = -1.01, 95% CI [-1.89 -0.09]). However, the sham stimulation group also showed an equally large decrease in Δαs for the same reference in their second session (g = -0.89, 95% CI [-1.57 -0.20]). Given the null effects of the grand averaged Δαs, the Δαs analyzed by stimulation session and the descriptive analysis of Δαs for each

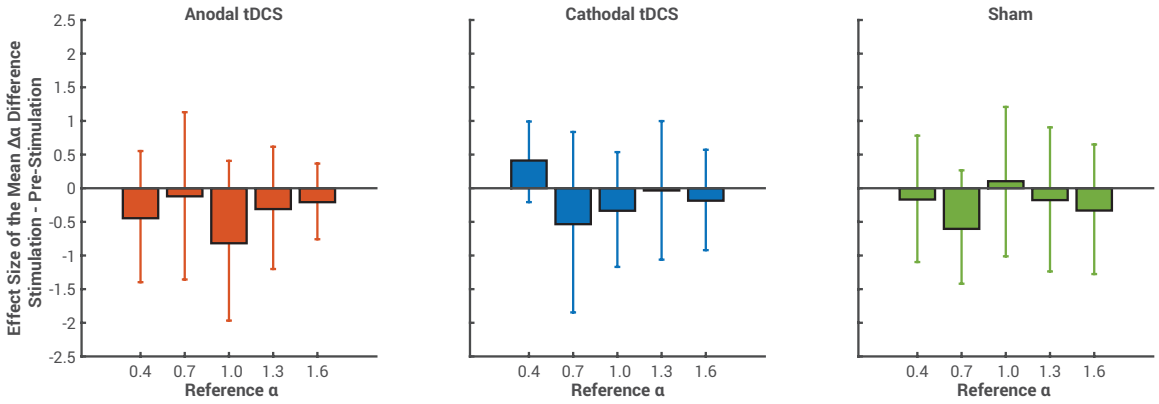

Figure 3B.3. The magnitude (Hedge's g) of the difference between slope discrimination thresholds measured while observers received a-tDCS, c-tDCS or sham and pre-stimulation thresholds, collapsed across stimulation sessions. We find a fairly large effect of a-tDCS on slope discrimination thresholds to a reference $\alpha = 1$, however, the interval estimate of this effect is too large to infer any statistical significance. Error bars represent the exact 95% confidence interval.

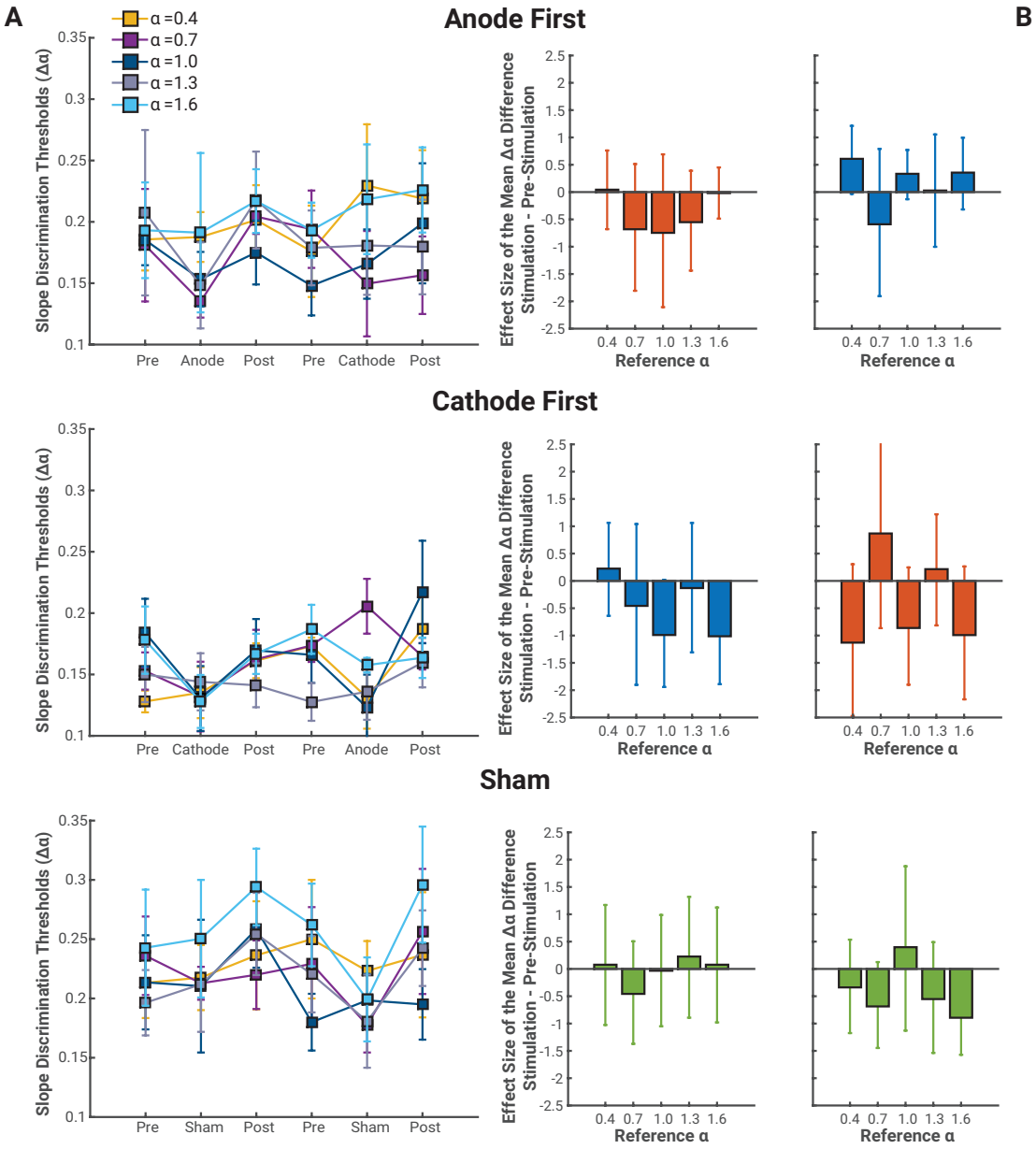

Figure 3B.4. A Slope discrimination thresholds across all measurements in time for both stimulation sessions. Both the Anode First group and the Cathode first group showed a statistically significant decrease in slope discrimination thresholds from pre-stimulation to stimulation at the first stimulation session, while the sham group did not. No other changes in slope discrimination thresholds were observed at any other time points. Error bars are +/- 1 Standard Error of the Mean. **B** Effect size of the mean difference between slope discrimination thresholds measured prior to and during stimulation. Negative effect sizes represent a decrease in thresholds (increase in sensitivity). We found no meaningful change in thresholds at any reference α across all three groups. Error bars are exact 95% confidence intervals.

reference α, we cannot attribute any measureable effect of tDCS on Δαs.

Discussion

We had aimed to alter α discrimination thresholds with the application of tDCS over primary visual cortex, but found no measurable impact of either anodal or cathodal tDCS on the discriminability of α. The effects of tDCS on contrast perception are constrained to higher spatial frequency gratings presented foveally (Antal et al., 2001; Chaieb, Antal, & Paulus, 2008; Kraft et al., 2010; Peters et al., 2013; Richard et al., 2015; Spiegel et al., 2013), and recent evidence suggests its effects are sufficiently large to alter neural responses to complex images broadband in spatial frequency, but narrowband in orientation (Hansen et al., 2015), and thus had expected tDCS would modulate the perception of a stimulus broadband in spatial frequency and orientation, but found no sign of this in this dataset.

The addition of tDCS to psychophysical paradigms offers a novel approach to manipulate channel behaviour in the early visual system directly (Antal et al., 2006a, 2006b). To date, most studies that have implemented tDCS in visual paradigms have constrained their stimulus set to be narrowband both in spatial frequency and orientation, (e.g., sinusoidal gratings, random dot kinematograms). Stimuli restricted in dimensionality, like sinusoidal gratings, offer a high level of control to the experimenter, but given they only stimulate a limited number of channels (or potentially, a limited number of cells), they can, at best, serve as an incomplete approximation of visual function within natural environments. Using natural stimuli, or noise images with naturalistic α can be argued as a more suitable approach to investigate visual function, particularly given that the visual system is ideally suited to encode said images (Brady & Field, 1995; Carandini et al., 2005; Dan et al., 1996; Field, 1987, 1994). However, the use of natural stimuli may add a level of complexity to the experimental design that may surpass any mild influence from a neuro-stimulator like tDCS. Our experimental findings are a sign that the mechanisms changed by tDCS used in more traditional psychophysical paradigms may function differently under natural stimulation. The interactive properties of cells in striate cortex under natural stimulation may alter the known influence of tDCS on perception (Baddeley et al., 1997; Baker & Vilidaite, 2014; Bieniek, Pernet, & Rousselet, 2012; Brady & Field, 1995; Dan et al., 1996; David et al., 2004; Field, 1994; Hansen et al., 2012, 2011; Prenger, Wu, David, & Gallant, 2004; Rieger et al., 2013; Vinje & Gallant, 2000). The following describes what we consider to be most likely reasons for the null effect we obtained in this study.

The magnitude of the influence of tDCS (and other neuro-stimulation techniques) on psychophysical performance seems tied to the underlying sensitivity of observers to the stimulus dimensions (Antal et al., 2003a, 2001; Pirulli et al., 2014; Thompson et al., 2008). As we showed in **Chapter 3A**, both a-tDCS and c-tDCS showed larger modulatory effects to stimuli that elicit low contrast sensitivity, while contrast sensitivity to spatial frequencies near the peak of the CSF (1 – 4 cycles/°) and gratings cardinally orientated (e.g., horizontal) mildly altered by tDCS. Sensitivity to a particular stimulus property is correlated with the magnitude of neural responses to the property (Boynton et al., 1999; Britten et al., 1992; Campbell & Kulikowski, 1972; Haynes et al., 2003; Kwon et al., 1992; Ross & Speed, 1991; Shadlen & Newsome, 1998; Zenger-Landolt & Heeger, 2003), and thus, tDCS will influence perception by modulating the activity of cells responding to the stimulus. Trans-cranial Direct Current Stimulation will influence signal-to-noise ratios, which dictate the early perceptual responses of the observer to the stimulus, by either increasing the responses of cells beyond the noise threshold (a-tDCS) or by lowering the noise threshold (c-tDCS; Antal et al., 2003a; Baker & Vilidaite, 2014; Klein & Levi, 2009; Levi, Klein, & Chen, 2005; Pirulli et al., 2014; Thompson et al., 2008; Tyler & Chen, 2000). Noise images with $1/f$ spectra contain a significant amount of luminance contrast across spatial frequency and orientation, and will therefore elicit activity from a wide set of cells with varied tuning properties. It is likely, therefore, that the activity of cells attributed to the spectral characteristics of $1/f$ noise images, coupled with any non-linear adjustments that follow broadband stimulation (Bex et al., 2007; Brady & Field, 2000; Carandini & Heeger, 1994; David et al., 2004; Heeger, 1992; Prenger et al., 2004), may have been too great to allow for any influence of a mild neuro-stimulator (tDCS; Bikson & Rahman, 2013; Miranda, Lomarev, & Hallett, 2006; Miranda, Mekonnen, Salvador, & Ruffini, 2013; Peterchev et al., 2012; Sadleir, Vannorsdall, Schretlen, & Gordon, 2010).

Psychophysical performance under broadband conditions can often differ greatly from performance on an identical task but with narrowband stimuli, and thus it may not be surprising that tDCS will have different effects on both types of stimuli. For example, contrast sensitivity to a narrowband grating is highest for horizontally oriented gratings and worse for oblique (Campbell et al., 1966), but under broadband conditions, contrast sensitivity to cardinal orientations (e.g., horizontal) is worse than that of oblique contrast sensitivity (i.e., the horizontal effect; Hansen, Essock, Zheng, & DeFord, 2003; Hansen, Haun, & Essock, 2008; Haun &

Essock, 2010; Kim et al., 2010). Briefly, the horizontal effect has been argued to stem from an anisotropic contrast gain control mechanism that pools the activity of cells, numerically biased in preferred orientation, into multiple local gain pools, which reapplies inhibition accordingly (Hansen et al., 2015; Kim et al., 2010). Lower contrast sensitivity to horizontally orientated content in natural scenes, according to this model, stems from the activation of the contrast gain control mechanism that reapplies inhibition accordingly to the most active cells (Hansen et al., 2015). In a numerically biased population of cells, whereby there are more cells tuned to horizontal than any other orientation (Li, Peterson, & Freeman, 2003), the responses pooled by a normalization mechanisms would be greatest for horizontally orientated cells, which would lead to a decreased response, and decreased sensitivity of the observer to horizontal content (Hansen et al., 2003).

Interestingly, the horizontal effect was recently shown to be susceptible to the effects of tDCS (Hansen et al., 2015). When a horizontal mask broadband in spatial frequency and narrowband in orientation, is overlaid onto a Gabor target (of the same orientation), the large suppression due to the mask can be reduced by c-tDCS. This may be odd, given our null effect of tDCS on α discrimination thresholds, but there are methodological differences between our study and that of Hansen and colleagues (2015) that may account for the discrepancy in tDCS effects. Both studies that have implemented tDCS to modulate the perception of spatially complex stimuli, and found measureable effects, have done so by measuring the influence of tDCS on perceptibility of a masked target (Hansen et al., 2015; Spiegel et al., 2012). In masking paradigms, the perceptual outcome is dictated by the interactions between the spatial properties of the mask and target stimuli (Hansen & Loschky, 2013; Meese, 2004; Petrov et al., 2005; Polat & Sagi, 1993; Snowden & Hammett, 1998; Stromeyer & Julesz, 1972). It is possible that the interactions between the mask and target (i.e., suppressive influence of masks), particularly when the mask is broadband in spatial frequency content, differ considerably in function from the neural interactions that occur when observers are asked to detect a change in, or discriminate between, natural images (e.g., Bex, Mareschal, & Dakin, 2007; Brady & Field, 2000; Cass, Alais, Spehar, & Bex, 2009). Hence, the facilitative effect of c-tDCS on the suppressive effects of a mask broadband in spatial frequency may lie in the interaction of the narrowband target and mask signals (or the net combination of both), and less on the individual processing of each stimulus. It might be worth verifying if tDCS can alter the suppressive influence of a mask

broadband in both spatial frequency and orientation (e.g., 1/*f* noise images) on the perception of a Gabor stimulus. As Hansen and colleagues (2015) used masks broadband in spatial frequency only, the effects they got may have in part been due to the restricted orientation content of their masks, which may have restricted neural activity sufficiently to adduce any effect of tDCS.

Conclusions

Trans-cranial Direct Current Stimulation has been shown to modulate early visual processes (Antal, Kincses, et al., 2004; Antal et al., 2003b, 2001, 2006a, 2006b; Kraft et al., 2010; Olma et al., 2011; Spiegel et al., 2013). The directionality of these effects (either facilitatory or inhibitory) have varied (Jacobson et al., 2012) as both tDCS polarities have to been shown to have facilitatory and inhibitory effects on early visual processes, which vary according to a variety of methodological factors (see **Chapter 3A**; Accornero, Li Voti, La Riccia, & Gregori, 2007; Antal, Kincses, et al., 2004; Antal et al., 2003a, 2001; Bikson & Rahman, 2013; Chaieb et al., 2008; Kraft et al., 2010; Nitsche et al., 2008; Olma et al., 2011; Peterchev et al., 2012; Peters et al., 2013; Pirulli et al., 2014; Richard et al., 2015; Spiegel et al., 2013, 2012). Nevertheless, the application of tDCS can have measureable impact on visual perception, and we have recently shown that contrast sensitivity measured at higher spatial frequencies and non-cardinal orientations will be most susceptible to the influence of tDCS. We had hypothesized that α discrimination threshold, particularly those of shallower reference α ($\alpha < 1.0$), would be affected by the application of tDCS. However, we found no measureable impact of tDCS on α discrimination thresholds regardless of the reference α.

In **Chapter 2**, we found that α discrimination thresholds to noise images with steeper reference α (α between 1.0 and 1.6), while a broadband process that involves both low and high spatial frequency channel interactions, were most susceptible to the responses of low spatial frequency channel. We thus proposed that the dominant coding spatial frequency may be correlated with the perceptually salient spatial frequency content in our noise images (as steeper α are perceptually dominated by lower spatial frequencies). We had expected that observers' ability to discriminate between 1/*f* noise images perceptually dominated by higher spatial frequency content ($\alpha < 1.0$) would be most affected by tDCS as its effects are largest at higher spatial frequencies (for contrast detection thresholds). While found no evidence that tDCS could influence α discrimination thresholds, this is most likely due to the overall neural responses to 1/*f* noise images, and not necessarily the actual encoding mechanism. The null effects are not

evidence that the contributing spatial frequency channel to α discrimination does not scale according to the reference α. Instead, our findings here suggest that tDCS may be an ill-suited approach to measure spatial frequency coding mechanisms of broadband stimuli.

Chapter 3B Tables

Table 3B.1. Linear regression conducted on baseline α discrimination thresholds

	b	β	*t*(2)	*p*	95% CI		r^2
Reference α					LL	UL	
0.4	0.007	0.000	0.136	.905	-0.229	0.244	.296
0.7	-0.001	0.000	-0.014	.990	-0.424	0.421	.031
1.0	-0.008	0.000	-0.056	.960	-0.601	0.586	.547
1.3	0.012	0.000	0.090	.936	-0.553	0.577	.655
1.6	0.011	0.000	0.079	.944	-0.585	0.607	.568

Table 3B.2. Repeated Measures ANOVA source table

Source	*SS*	*df*	*MS*	*F*	*p*	η_p^2
		Within Subjects Effects				
A	0.032	4	0.008	2.119	.093	.150
Error	0.182	48	0.004			
B	0.016	1	0.016	5.996	.031	.333
Error	0.032	12	0.003			
C	0.002	1	0.002	0.395	.541	.032
Error	0.047	12	0.004			
A x B	0.005	4	0.001	0.519	.722	.041
Error	0.120	48	0.003			
A x C	0.006	4	0.001	0.553	.698	.044
Error	0.126	48	0.003			
B x C	0.001	1	0.001	0.025	.876	.002
Error	0.019	12	0.002			
A x B x C	0.008	4	0.002	0.879	.484	.068
Error	0.108	48	0.002			
		Between Subjects Effects				
Group	0.207	2	0.103	3.070	.084	.338
Error	0.404	12	0.034			
A x Group	0.022	8	0.003	0.724	.670	.108
B x Group	0.002	2	0.001	0.313	.737	.050
C x Group	0.005	2	0.002	0.613	.558	.093
A x B x Group	0.030	8	0.004	1.472	.192	.197
A x C x Group	0.017	8	0.002	0.825	.585	.121
B x C x Group	0.016	2	0.008	5.098	.025	.459
A x B x C x Group	0.008	8	0.001	0.444	.888	.069

Note. A – Reference α, B – Session Time (Pre-Stimulation and Stimulation), C – Stimulation Session (a-tDCS c-tDCS)

Chapter 4

THE TASK DEPENDENT CONTRIBUTION OF SPATIAL FREQUENCY CHANNELS TO THE PERCEPTION OF THE SLOPE OF THE AMPLITUDE SPECTRUM OF NOISE IMAGES

Bruno Richard, Bruce C. Hansen, Aaron P. Johnson

Abstract

Human observers are thought to be most sensitive to deviations in the slope of the amplitude spectrum near the average slope value of natural scenes (α = 1.0), and slightly less so at values that exceed the range typically found within the natural environment (Billock, 2000; Hansen & Essock, 2005; Hansen & Hess, 2006; Johnson et al., 2011; Knill et al., 1990; Párraga & Tolhurst, 2000). While the sensitivity characteristics of human observers to α are now well defined, the underlying mechanism that underlies α discriminability remains unclear. We have previously demonstrated that α discrimination is subject to the representation of luminance contrast across spatial frequency in a noise image, but were unable to show how spatial frequency content is used to discriminate α. Here, we implemented an image classification paradigm, whereby contrast was randomly increased or decreased (by ± 8dB) within 8 discrete spatial frequency bands, to assess how the contrast of each spatial frequency band is weighted by observers to identify a change in α. Observers to complete two tasks: an α identification, and an α discrimination task. We began with a slope identification task in order to define how observers may view, or weight, the spatial frequency content of $1/f^{\alpha}$ noise images when no discrimination task is assigned. We found that observers rely on progressively lower spatial frequency bands when viewing stimuli with steeper amplitude spectra. This correlated with the perceptually salient scale within our noise images (e.g., lower spatial frequencies for steep αs and higher spatial frequencies for shallow αs), which may reflect the activity of particular spatial frequency channels in the early visual system exposed to different αs (Boynton et al., 1999; Campbell & Kulikowski, 1972; Hansen et al., 2012, 2011; Haynes et al., 2003; Ress et al., 2000; Ross & Speed, 1991; Zenger-Landolt & Heeger, 2003). Yet, when asked to discriminate between stimuli that vary in their amplitude spectra, we found observers to forgo the spatial frequency dependent process identified in **Experiment 4.1**. In **Experiments 4.2** and **4.3**, we combined the "Odd-Man-Out" psychophysical procedure (a spatial and temporal variant) with the classification image paradigm, and found that observers no longer adjusted the peak of the critical spatial frequency band according to the α of the reference stimulus. While the decision weights between all three observers varied, on average, they identified the stimulus with the odd α according to the difference in contrast between low and high spatial frequency bands. The loss of the spatial frequency dependent process in our α discrimination paradigm has interesting implications towards the definition of a coding mechanism involved in α discrimination.

Over the past 20 years, researchers have investigated, and demonstrated that human observers are sensitive to the autocorrelation function of natural images, a second-order statistic of natural scenes that reflects the variance of luminance contrast within an image (Hansen & Hess, 2006; Johnson, Richard, Hansen, & Ellemberg, 2011; Knill, Field, & Kersten, 1990; Párraga & Tolhurst, 2000; Tadmor & Tolhurst, 1994; Thomson & Foster, 1997; Tolhurst & Tadmor, 1997, 2000). Second-order statistics are typically defined according to the slope of the Fourier amplitude spectrum of natural scenes, which represents a linear decrease in log amplitude as a function of log spatial frequency by a factor of $1/f^{\alpha}$. Across multiple scenes, the slope (α) has been shown to range from 0.6 – 1.6, and has a mean value of about 1.0 (Billock, 2000; Burton & Moorhead, 1987; Hansen & Essock, 2005; Tolhurst et al., 1992; van der Schaaf & van Hateren, 1996). Generally, human observers show greater sensitivity to images with an α near that of the average α (i.e., α = 1.0; Billock, 2000), and lower sensitivity to steeper and shallower αs (Hansen & Hess, 2006; Knill et al., 1990). The sensitivity of human observers to α suggest this statistical property may be relevant to the early processing stages of the visual system, and additionally, be necessary to encode the broadband information of natural scenes in some optimal fashion (Barlow, 1961, 2001; Graham & Field, 2007; Knill et al., 1990; Olshausen & Field, 2000; Olshausen & Field, 1996; Párraga et al., 2005; Párraga et al., 2000; Simoncelli & Olshausen, 2001; Simoncelli, 2003; Tolhurst & Tadmor, 2000). However, the description of the psychophysical mechanism involved in α discrimination remains to be defined. That is, while it is now well understood that human observers are able to detect and discriminate a change in α, how they discriminate between distributions of luminance contrast across spatial frequency remains to be defined.

There is evidence that human observers may rely on diagnostic[12] spatial frequency bands to discriminate α (Tadmor & Tolhurst, 1994; Tolhurst & Tadmor, 1997). When a change in α occurred only within the diagnostic spatial frequency bands, thresholds were unaltered as if the change had occurred across the entire spectrum. However, when the change in α occurred outside of the diagnostic band, thresholds no longer resembled those of a normal α discrimination task, as observers were now forced to use spatial frequency bands they do not

[12] A diagnostic spatial frequency band refers to a band of spatial frequency content that contains the necessary information for observers to complete a particular task. In an α discrimination task, this means that the comparison between αs is completed according to differences in contrast within that single spatial frequency band, which changes according to the reference α.

typically use to discriminate an α value. These findings suggest that observers may not rely on contrast across the entire spatial frequency spectrum to discriminate α, and may instead weight certain bands more heavily than others. That said, the diagnostic bands defined by Tolhurst and Tadmor (1997) were larger (at least 2 octaves) than the typical bandwidth given to psychophysical spatial frequency channels (Field, 1987; Párraga et al., 2005; Wilson & Humanski, 1993; Wilson et al., 1983) and the known spatial frequency bandwidth of cells in striate cortex (De Valois et al., 1982; Tootell, Silverman, et al., 1988; Yu et al., 2010). Thus, it is difficult to assess which particular band, or bands, were used by observers to complete the α discrimination task of Tolhurst and Tadmor (1997).

We have also demonstrated that humans rely on luminance contrast within particular spatial frequency bands to discriminate α, which may be indicative of a diagnostic process. Specifically, in **Chapter 2,** we found that increases in the size of 1/*f* noise stimuli, which increases the representation of low spatial frequency content in the image, caused a decrease in α discrimination thresholds. Interestingly, this effect was most pronounced for a reference α of 1.0 and decreased as the reference α was made steeper or shallower. We proposed our findings could be well described according to the summed responses of multiple one-octave bandwidth spatial frequency channels to noise images 1/*f* amplitude spectra (Brady & Field, 1995; Field & Brady, 1997; Field, 1987; Hansen & Hess, 2012). The combined response of these channels has been demonstrated to be greatest for images with an α of 1.0, and decreased as α deviates from 1.0 (an inverted U-shape function). However, the size manipulation of **Experiment 2.1** did not reveal any biases in the sampling characteristics of spatial frequency content across α. We had anticipated that α discrimination thresholds to noise images perceptually dominated by lower spatial frequency content (α > 1.0) would be most influenced by the increase in stimulus size, but found no indication of this effect[13]. In order to isolate the contribution of low spatial frequency content to α discrimination thresholds, we replicated the centre-surround study conducted by Johnson et al. (2011) and increased the gap sizes between the centre stimulus and surround annulus (**Experiment 2.2**). Similar to the findings of Johnson et al. (2011), the presence of a surround lowered α discrimination thresholds when the reference α equalled or was greater than 1.0, and generated the largest facilitation when the surround α was steep (α = 1.3). Most

[13] The facilitation of discrimination thresholds with shallower reference αs was argued to stem from the spatial summation of higher spatial frequency luminance contrast.

interestingly, we found the distance between the centre stimulus and surround annulus to have no impact on the facilitation of α discrimination thresholds, which suggests the spatial interactions involved in our surround facilitation effect are low spatial frequency based. Thus, the responses of channels tuned to low spatial frequency luminance contrast play a key role in regulating α discrimination thresholds, at least when the reference α is equal to or greater than 1.0. The contribution of low spatial frequency channels to α discrimination thresholds corroborates neurophysiological evidence that the perception of noise stimuli with steep αs is dominated by the responses of lower spatial frequency channels (Hansen et al., 2012; Hansen, Jacques, Johnson, & Ellemberg, 2011), and psychophysical findings that adaptation to natural scenes primarily reduces contrast sensitivity to low spatial frequencies (Webster & Miyahara, 1997). As the contribution of low spatial frequency tuned channels was only evident when the reference α was relatively steep, we proposed that the contributing spatial frequency channel might scale in spatial frequency tuning according to the reference α, in a manner similar to that proposed by Tolhurst and Tadmor (1997).

Noise images with steep α are perceptually dominated by low spatial frequency content (i.e., a significantly large proportion of the contrast energy is in the lower spatial frequencies), while noise images with shallow α tend to be perceptually dominated by higher spatial frequency content. If the perceptually salient spatial frequency content of our noise images reflect the dominant activity of particular spatial frequency channels, as has been proposed elsewhere (Boynton et al., 1999; Britten et al., 1992; Campbell & Kulikowski, 1972; Haynes et al., 2003; Kwon et al., 1992; Ross & Speed, 1991; Shadlen & Newsome, 1998; Zenger-Landolt & Heeger, 2003) then they might indicate the tuning of the diagnostic spatial frequency band used by observers to discriminate α. It followed that modulating the activity of channels tuned to higher spatial frequencies should have modulated α discrimination thresholds to shallower αs (e.g., α = 0.4, 0.7). In **Chapter 3B**, we attempted to modulate the activity of cells in striate cortex with trans-cranial Direct Current Stimulation (tDCS) to affect slope discrimination thresholds for shallow reference α. However, tDCS seems an ill-suited tool to the modulate suprathreshold perception of broadband stimuli as it had no measureable effect on slope discrimination thresholds.

A difficulty we have encountered with our previous experiments when identifying the function of differently tuned spatial frequency channels exposed to broadband noise stimuli may

lie in the appearance of noise images. Broadband images, which contain a significant amount of luminance contrast across a wide range of spatial frequencies, do not appear to human observers as a set of identifiable, or separate, spatial frequency bands, but instead appear unified across scale (i.e., the perception of contrast is unified across spatial frequency). Indeed, nearly all models of broadband feature perception will pool the transduced contrast across spatial frequency prior to the decision stage (Azzopardi & Petkov, 2012; Brady & Field, 1995; Hansen & Hess, 2012; Haun & Peli, 2013; Johnson, Prins, Kingdom, & Baker, 2007; Kim, Haun, & Essock, 2010; Morgan & Watt, 1997; Párraga et al., 2005). While the contribution of individual spatial frequency channels can be studied in isolation with filtering methods, removing spatial frequency content from broadband noise images can transform the task observers complete from an α discrimination task to one of contrast discrimination (i.e., narrowband discrimination). Additionally, segregating the high or low spatial frequency content from broadband noise images (i.e., high-pass or low-pass filters, respectively), and asking observers to discriminate the α of these altered images, generates α discrimination threshold that show little tuning to α (i.e., α discrimination thresholds are identical for all reference αs; Richard, Hansen, Ellemberg, & Johnson, 2013), and can therefore not be interpreted according to the findings of more typical α discrimination tasks (see **Figure 4.1** for an example of the appearance of filtered 1/*f* noise images). Indeed, there are indications that observers may require the entire spatial frequency spectrum to complete an α discrimination task (at least for reference α values greater than 0.4; Párraga & Tolhurst, 2000) and thus, the study of the function of spatial frequency channels in α discrimination should aim to use 1/*f* noise images that contain a complete representation of their spatial frequency content.

The image classification paradigm (Ahumada, Jr. & Ahumada, 2002; Ahumada, Jr., 1971, 1975; Beard & Ahumada, Jr., 1998) may be better suited to identify the function or contribution of individual spatial frequency channels as it does not remove any spatial frequency content from the noise images. In an image classification paradigm, observers are asked to make perceptual judgements on the entirety of a signal while the individual components of the stimulus are modulated over multiple trials. The observer responses are then correlated with the stimulus variation, which identifies the average weight an observer attributes to the individual components of the signal. The benefit of this technique is that it allows observers to judge the entire image, as they would within a traditional α discrimination paradigm, without the

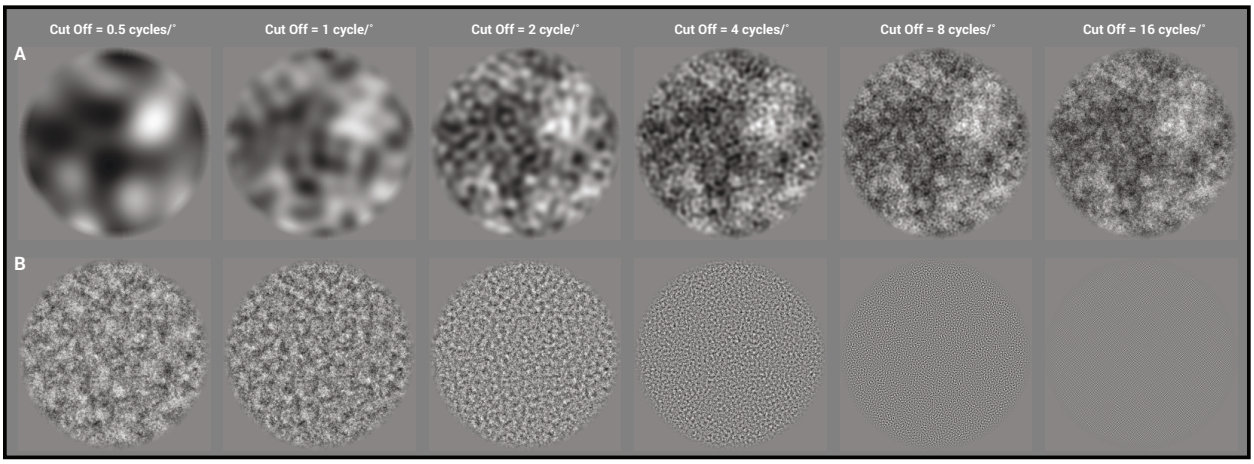

Figure 4.1. Filtered 1/*f* noise images with α = 1.0. Each image is filtered with an ideal low-pass (**A**) or high-pass (**B**) filter of varying spatial frequency cut off.

requirement that a particular spatial frequency band be removed, or attention be paid to a particular spatial frequency band. Image classification paradigms have previously been used to identify spatial frequency tuning functions in white noise (Levi et al., 2005), of targets within noise (Klein & Levi, 2009; Kontsevich & Tyler, 2004; Levi, Klein, & Chen, 2008; Murray, Bennett, & Sekuler, 2005; Taylor, Bennett, & Sekuler, 2009), and most recently, identify the role of individual spatial frequency components in the perceived contrast of natural images (Haun & Peli, 2013).

Haun and Peli (2013) used an image classification paradigm in order to derive the spatial frequency weighting functions for subjective estimates of broadband image contrast. They randomly modulated contrast of natural images within eight discrete spatial frequency bands, and in a 2-AFC task, asked observers to identify the image that had the greater contrast. According to their findings, the overall contrast of a natural image is determined by the amount of contrast in the spatial frequency bands between 1 and 6 cycles/°, which corresponds to the peak of the contrast sensitivity function (Peli, Arend, Young, & Goldstein, 1993; Robson, 1966). Most relevant to the current study, they demonstrated that the peak spatial frequency band used by observers to determine contrast changed according to the α of the original, un-modulated image. Observers weighted lower spatial frequency bands more heavily when the image α was steep, and higher spatial frequency bands when the image α was shallow. The change in weights of spatial frequency bands used by observers suggest that the mechanism involved in the perception of low level characteristics in broadband images (e.g., perceived contrast) may rely on diagnostic spatial frequency bands. The image classification paradigm, therefore, seems an appropriate approach to verify if observers rely on more "diagnostic" spatial frequency bands in an α discrimination task.

Experiment 4.1

In an image classification paradigm, observers are asked to make a simple perceptual judgement of an image while the individual components of the images are varied over multiple trials. As we were uncertain of how this method would translate to our α discrimination task, we opted to first measure the classification images of our observers to different αs. Specifically, we asked observers to identify the α of a noise image while the magnitude of contrast within eight discrete spatial frequency bands was changed across multiple trials. This technique simplified the task, and additionally, allowed us to generate a representation of how observers may use the

distribution of contrast across spatial frequency to judge the particular α of an image. The identification of α is not a representation of observer sensitivity to α as is the resulting threshold of an α discrimination task (for review on the measurement of sensitivity to α see Hansen & Essock, 2005), but does allow us to assess the internal representation observers may have built of noise images with different α.

Method

Participants

Three experienced psychophysical observers (2 females), who were all 21 years of age at the start of the study, participated in all three experiments of this study. All were experienced psychophysical observers, and participated in **Experiments 2.1** and **2.2** (P1 was P1 in Chapter 1, P2 was P3, and P3 was P4). All participants had normal or corrected to normal visual acuity (cut-off = 20/25). Informed consent was obtained from all participants and all were treated in accordance the Tri-Council Policy Statement: Ethical Conduct for Research Involving Humans (2014). Participants were consenting volunteers.

Apparatus

The apparatus was identical in all three experiments of this study, and are therefore only described here. Stimuli were presented on a 22.5" Viewsonic (G225fB) monitor driven by an Apple Mac Pro (2 X 2.66GHz processor) equipped with 8GB of RAM and a 1GB PCIe x16 ATI Radeon HD 5770 Graphics card with 10-bit grayscale resolution. Stimuli were displayed using a linearized look-up table, generated by calibrating with a Color-Vision Spyder3 Pro sensor. Maximum luminance output of the display monitor was 100 cd/m^2 (50 cd/m^2 mean luminance after calibration) the frame rate was set to 100 Hz, and the resolution was set to 1024 X 768 pixels. Single pixels subtended .0381° of visual angle (i.e., 2.23 arc min.) when viewed from 1.0 meter. Head position was maintained using a chin rest, and participant input was recorded via keyboard press.

Stimuli

All stimuli were constructed in an identical fashion to those of **Experiment 2.1, Experiment 2.2,** and **Experiment 3.2**, and subsequently modified according to a re-weighting vector defined below. The image classification paradigm requires a large number of trials, and therefore we only generated stimuli according to 3 reference α values, equidistant (± 0.2) around an α = 1.0 (α = [0.8, 1.0, 1.2]). This ensured the difference in αs was large enough for observers

to differentiate between all three αs. All stimuli consisted of synthetic amplitude spectrum noise, were constructed in the Fourier domain using MATLAB (ver. 2012b; Mathworks, Natick, MA, ver. 2012b) and corresponding Image Processing (ver 6.4) toolbox, and were presented using the Psychophysics Toolbox extensions (Brainard, 1997; Kleiner et al., 2007; Pelli, 1997). The noise patterns were rendered into the spatial domain by taking the inverse Fourier Transform of amplitude spectrum and a given random phase spectrum, which was randomized on each trial. All stimuli were normalized to have an RMS contrast of 0.15. Each $1/f^{\alpha}$ noise image was then divided into eight spatial frequency bands, including seven bands of one-octave bandwidth centred on 1, 2, 4, 8, 16, 32, and 64 cycles per picture (cpp), and an eighth that plateaued at 128 cpp. We define the centre spatial frequencies of our filters in cycles per picture for the general description of our stimulus creation procedure as the size of our stimuli differed between **Experiment 4.1** and **Experiment 4.2** and **4.3**. As the appropriate metric to define the spatial frequency bands is in cycles per degree of visual angle (see Haun & Peli, 2013), the centre spatial frequency of each filter is stated in cycles per degree within the results section of each experiment. The seven one-octave bands were defined by a raised-cosine of log frequency envelope *h* (see **Figure 4.2**) defined as

$$h(s)=\begin{cases}\frac{1}{2}\left[1+\cos\left(\pi\log_2(f)-\pi\log_2(s)\right)\right], \text{ if } \left\{\frac{1}{2}s<f<2s\right\}\\ 0, \text{ otherwise}\end{cases}\Bigg\} \textbf{ Equation 4.1}$$

where *s* is the centre frequency (in cycles per picture) of the raised-cosine filter, and *f* is spatial frequency (Haun & Peli, 2013; Peli, 1990). The remaining high spatial frequency content was assigned to the eighth, residual, spatial frequency band (i.e., for $f \geq 128$, $h(s) = 1$). We defined the contrast modulation of each spatial frequency band by creating a vector (ω) of random reweighting coefficients ranging from -8 dB to +8 dB [$dB = 20\log_{10}(\text{contrast amplitude})$], and applied to the series of spatial frequency bands to generate a new set of reweighted series, which were then summed to obtain an altered version of the original image (see **Figure 4.2**). The image was then normalized to fit within the 0 – 1 pixel value display range. We chose the range of ± 8dB as this change was large enough to generate noticeable changes in the appearance of the stimulus, but small enough to not alter the α of the original image, and completely disrupt the appearance of the 1/*f* noise stimuli. Following the alteration of our stimuli, an image patch with diameter of 8° of visual angle was cropped from its centre and windowed with a cosine-tapered

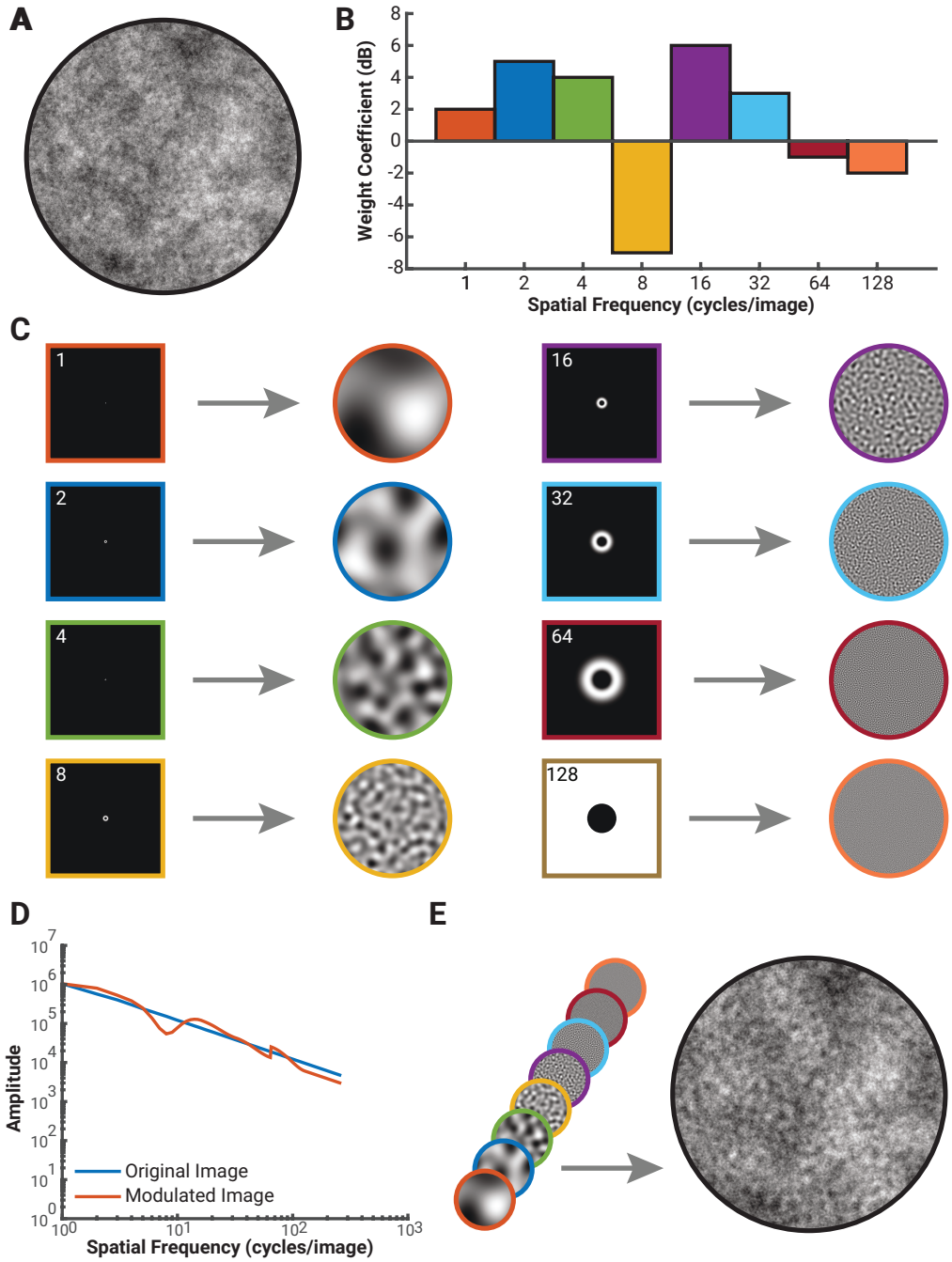

Figure 4.2. Stimulus generation procedure. **A** Original $1/f^{\alpha}$ noise image with $\alpha = 1$. **B** The weight coefficients applied to the 8 pre-defined spatial frequency bands. **C** The 8 raised-cosine filters used to separate the image into 8 spatial frequency bands. Once each band is extracted, its contrast is modulated by their respective weight coefficients – defined in **B**, shown in the circles to the right of each filter. **D** The original and modulated image orientation-averaged amplitude spectrum. **E** The 8 modulated images are summed together to generate the final contrast band modulated image.

envelope, which ramped 5% of the image pixels in the proximity of the circle's edge to mean luminance (50 cd/m^2). Examples of the original and altered stimuli for all three reference α, in addition to a schematic illustration of the weighting coefficients for each image can be seen in **Figure 4.3**.

Psychophysical Procedures

Viewing was binocular in all experiments of this study. Observers completed a α identification task, whereby they were asked to indicate if the presented stimulus had an α of 0.8, 1.0, or 1.2. Observers first completed a practice block that consisted of 250 trials per α (750 total trials) of unaltered stimuli, where the particular α of the stimulus was randomly interleaved between trials. The baseline component of **Experiment 1** took on average an hour to complete for each observer. Average accuracy for our baseline measure was quite high (P1 = 94.7%; P2 = 88.8%, P3 = 89.8%), which demonstrates our participants could reliably differentiate between the three α used in this study (see **Figure 4.4**).

The experimental condition of this study consisted of the same αs presented in the practice blocks, but stimuli were now altered according to the stimulus generation procedures defined above. Participants completed 1000 trials per α (3000 total), and the presentation of any of the three αs was randomized on every trial. All stimuli were generated on a trial-by-trial basis, and therefore, both their phase spectrum and the vector of weighted coefficients were randomized on every trial. Each trial began with a white fixation cross (RGB = [255, 255, 255]), which subtended 0.3° of visual angle in diameter was presented for 250ms at the centre of the screen. This was followed by the presentation of the stimulus, which remained on screen until the observer indicated the α of the presented stimulus. Participants knew the three possible α values presented, and every 200 trials, were presented with an unaltered stimulus that had an α = 1.0 to serve as a reference for their decision. Once observers indicated the α of the image, they were asked to indicate their confidence level in their decision, they used a keyboard press to indicate whether they were confident or not confident with their selection[14]. These confidence levels were then transformed into scalars used to scale the decision weights (see **Results**). Observers took, on average, 4 hours to complete the α identification task.

[14] We chose to implement a binary confidence rating approach as observers preferred this rating method, compare to one with four confidence levels in pilot studies.

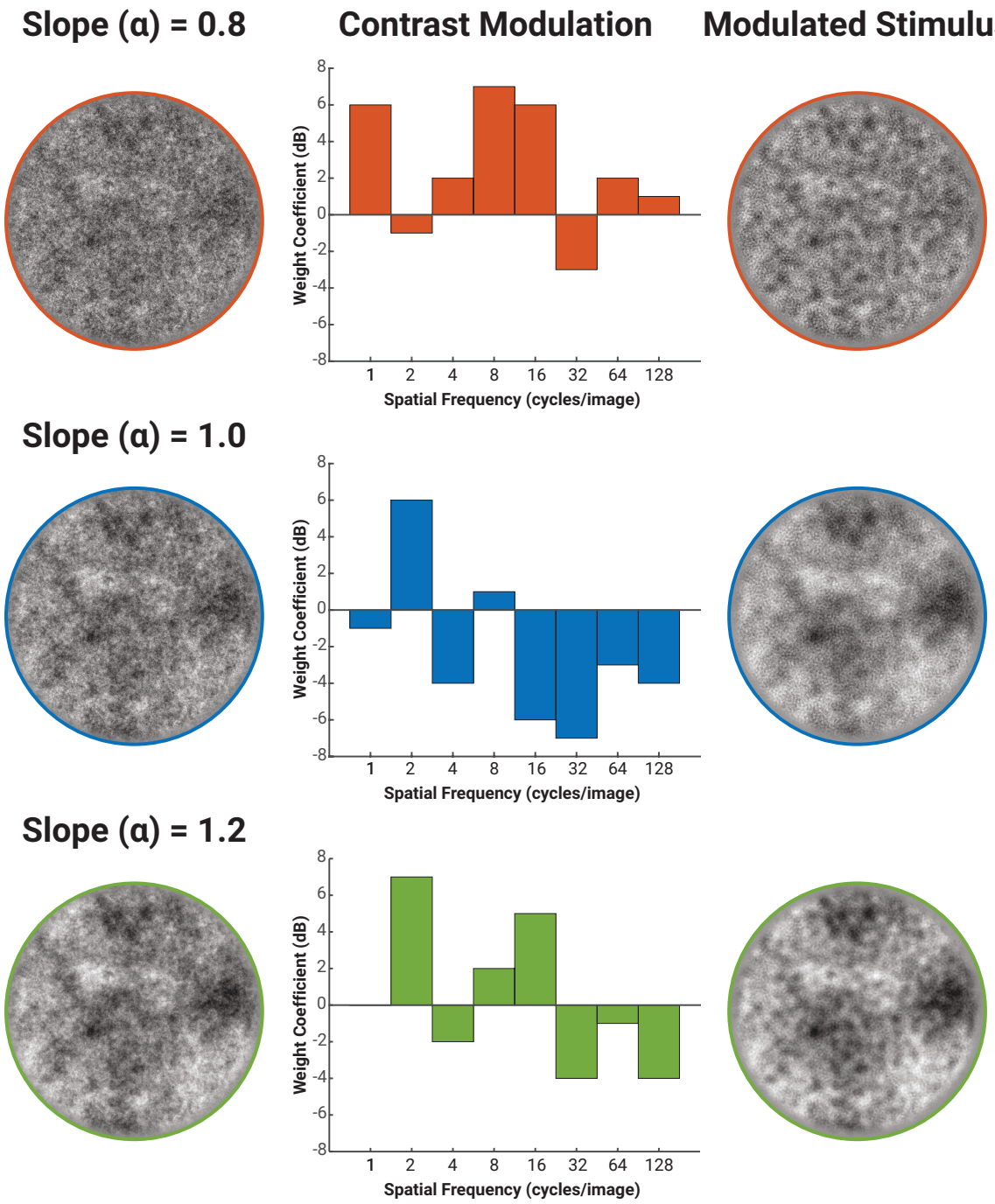

Figure 4.3. Example of the 3 αs (right column) used in **Experiment 1**, their schematic vector of re-weighting coefficients (centre column), and the altered stimulus (left column).

Results and Discussion

The goal of **Experiment 4.1** was to understand how observers might use contrast within particular spatial frequency bands to identify the α of noise images. We report decision weights (β_f) as a function of spatial frequency defined in cycles per degree of visual angle (cycles/°). Noise images, in **Experiment 4.1**, subtended 8° of visual angle in diameter, and therefore, the centre spatial frequencies of our cosine filters were 0.25, 0.5, 1, 2, 4, 8, 16, and 32 cycles/°). In order to calculate the average contrast value of stimuli defined as having a particular α (0.8. 1.0, or 1.2), we calculated the average band-limited contrast modulation (ω_f) for a given spatial frequency, weighted by the confidence rating (γ_i) of the observer, for a correct trial (i) define in symbols as:

$$\beta_f = \frac{1}{T}\sum_{i=1}^{T}\gamma\left(\omega_{f,i}\right) \qquad \textbf{Equation 4.2}$$

Each observer's confidence rating (γ_i) was given a weight of 2 when they reported being confident in their decision, and a weight of 1 when they reported not being confident in their decision. Note that this technique is not a model of contrast perception. Instead it is used to quantify subject performance according to the altered contrast within each spatial frequency band of our stimuli. This technique is a measure of how contrast within a particular spatial frequency band may influence the perceived α of an image, not how it is encoded.

The decision weights (β_f) for each observer, and chosen image α are shown in **Figure 4.4**. Observers P1 and P2 both showed distinct peaks in their decision weights, which shift towards lower spatial frequencies as the α of the stimulus steepen. Images with positive contrast weights in lower spatial frequency bands (2 cycles/°) were typically judged as having a steeper α (α = 1.2) than images with positive contrast weights in higher spatial frequency bands (8 – 16 cycles/°), which were described as having shallower α values (0.8). Observer P1 had slightly higher peak spatial frequencies than observer P2.

In comparison to observers P1 and P2, observer P3 had relatively flat decision weights, with little preference for any particular spatial frequency. The peak in decision weights for observer P3 was similar to those of observers P1 and P2 for α = 1.0 at a spatial frequency of 4 cycles/°. However, observer P3 showed no positive peak for α = 0.8 (other than the 32 cycles/° band), but did show a similar negative contrast weight at a spatial frequency of 16 cycles/°. Oddly, observer P3 had two moderate positive deflections in the decision weights for an α of 1.2

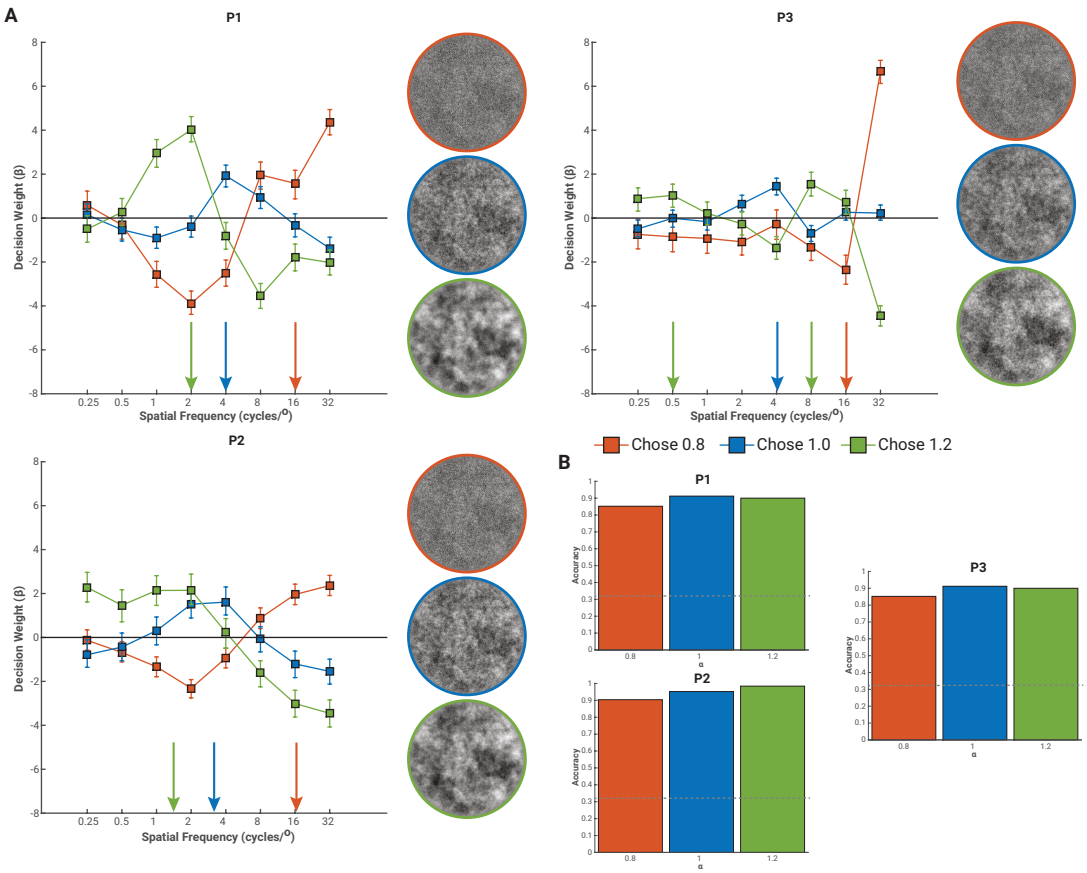

Figure 4.4. A Decision weights for all centre spatial frequency of our cosine filters for observers P1, P2, and P3. As described in text, all observers showed a progression in the peak spatial frequency band used according to the chosen α value. To the right of each decision weight plots are the schematic illustrations of the decision weights for each observer. Each classification image was generated by modulating a noise stimulus according to the decision weights of each observer. Error bars represent 95% confidence intervals calculated via bootstrapping the average decision weight with replacement and 2000 repetitions. **B** Accuracy for each α. All observers performed well above chance (dashed gray line). Both observer P1 and P3 show greatest identification accuracy for α = 1.0 (91.2% and 94.4% respectively), and lowest identification accuracy when α = 0.8 (85.2% and 90.4% respectively). Observer P2 was most accurate at identifying stimuli with α = 1.2 (98.4%) and least for stimuli with α = 0.8 (90.4%).

(0.5 and 8 cycles/°). We generated schematic representations of the decision weight vector for all three observers by modulating noise images by the weight vector of each observer (see **Figure 4.4**). In all three observers, there is a clear progression in the dominant scale observed within each image (which follows the decision weight vector of each observer). The schematic representations we generated are particularly useful to understand the weight vector of observer P3. While the absolute value of the contrast weight vector remained relatively shallow, there is still somewhat of a progression in the perceptually dominant scale in the schematic representation of the decision weights (β_f) for observer P3. Just as the other two observers, observer P3 viewed noise images perceptually dominated by low spatial frequency content to have a steeper α than images with dominated by higher spatial frequency content.

The approach taken by our observers to identify the α of a noise image corroborates our assumption that contrast increments within a particular spatial frequency band should correlated with the perceptually dominant spatial frequency content of noise images. Similarly, spatial frequency content that is not perceptually salient in these images (e.g., high spatial frequency information in images with shallow α) should be attenuated. We found that observers identified the slope of the amplitude spectrum of $1/f^{\alpha}$ noise images as shallow or steep according to the magnitude of luminance contrast in higher (~16 cycles/°) or lower (~2 cycles/°) spatial frequency bands respectively, and increments in contrast near the peak of the CSF (~ 4 cycles/°) when the stimulus has an α of 1.0, while other spatial frequency bands showing decrements in decision weights. This suggests that the internal template of α, in noise images, is adaptive similar to other classification image paradigms (Kersten, 1987; Levi et al., 2005; Taylor et al., 2009). Specifically, the shape of the decision function we found in **Experiment 4.1** suggests that the identification of α in noise images is more than a passive filtering of contrast across spatial frequency. It is unlikely that the shape of the decision weights we have obtained stem solely from spatial frequency channel interactions (Levi et al., 2005), and given the nature of the task, most probably falls within the realm of higher-order mechanisms similar to those defined in categorization paradigms (Gosselin & Schyns, 2001; Hansen, Farivar, Thompson, & Hess, 2008; Morrison & Schyns, 2001; Oliva & Schyns, 1997; Schyns & Gosselin, 2003; Schyns & Oliva, 1994, 1999).

Particular spatial frequency bands (i.e., low or high spatial frequencies) are known to carry different information of relevance for a particular task. It is well established in natural

scene categorization, that observers will rely more heavily on information within lower spatial frequency bands to complete the task (Brand & Johnson, 2014; Oliva & Schyns, 1997; Schyns & Oliva, 1994). However, this is subject to the particular demands of the categorization task. When observers are asked to identify the presence of an expression in hybrid images, which contain different content within their high and low spatial frequency bands (e.g., the presence of an expression), observers relied heavily on high spatial frequency content to make their decision (Schyns & Oliva, 1999). Conversely, when asked to identify the particular emotion expressed on the face, observers relied more heavily on low spatial frequency content within the image. Our findings for the identification of α for a noise image highlight a similar process to the diagnostic spatial frequency bands defined within the scene categorization literature, but interestingly, with much simpler stimuli that are not designed to be recognizable other than by their α. Additionally, these diagnostic bands scale according to α, in that observers rely on the amount of luminance contrast at low spatial frequencies to identify steep αs, and high spatial frequencies for shallow αs, in accordance with the dominant spatial scale of $1/f^{\alpha}$ noise images. We ask now if observers may use a similar process in an α discrimination task.

Experiment 4.2

Identification and discrimination differ considerably. In an identification task, observers are required to match the properties of an image to some form of internal template, which may be as simple as the distribution of responses of spatial frequency channels to luminance contrast or more complex features that require the integration of contrast across multiple spatial frequencies (e.g., an edge or border; Hansen et al., 2008). Conversely, image discrimination can be completed without any prior knowledge of the stimulus properties. In an α discrimination task like the one we have implemented in previous studies, observers need only compare the relative differences of luminance contrast between noise images, a process that is irrespective of α. Thus, while we find that observers rely of diagnostic bands to identify the α of an image in **Experiment 4.1**, it is unclear if such a mechanism may carry over to α discrimination. In **Experiments 4.2** and **4.3** implemented the classification image paradigm defined in **Experiment 4.1** in the α discrimination task we have used throughout this dissertation. Given that the contrast modulated noise images required for the image classification task are relatively complex, observers first completed a spatial variant of the "Odd-Man-Out" procedure in order to minimize any added difficulty from having to integrate and hold, over time, three complex images

presented sequentially (Blackwell, 1952; Jäkel & Wichmann, 2006). The spatial "Odd-Man-Out" procedure presented all noise images simultaneously, and observers were free to fixate all three stimuli.

Method

Stimuli

The stimuli of **Experiment 4.2** were constructed in an identical fashion to those of **Experiment 4.1**. All stimuli subtended 6 degrees of visual angle when viewed from one meter (stimuli were smaller in **Experiments 4.2** and **4.3** in order to fit on the screen). The centre spatial frequency of our cosine filters remained identical to those of **Experiment 1**, in cycles per picture (in cycles/°: 0.27, 0.53, 1.07, 2.14, 4.28, 8.56, 17.12, and 34.23). The following algorithm was used to produce two re-weighting coefficient vectors: **(1)** create a vector (**ω1**) of uniformly distributed random coefficients within the range of ±8dB. **(2)** Create a second vector (**ω2**) by randomly rearranging the values in vector. **(3)** If the positive or negative coefficients in **ω1** have the same position in **ω2**, repeat step **(2)**. This meant the two stimuli presented on screen had the same relative amount of contrast change, but these changes did not occur in the same spatial frequency bands for both stimuli.

Psychophysical Procedures

The spatial variant of the "Odd-Man-Out" procedure asked observers to identify the stimulus, either on the left or right of the screen, which contained the odd amplitude spectrum slope compared to that of the centre reference stimulus. Observers first completed a practice block of 1500 trials with unaltered $1/f^{\alpha}$ noise images generated according to an α of 0.8, 1.0, or 1.2 (i.e., 500 trials per reference α). The psychophysical procedure implemented here is similar to that of the preceding chapters, but have a few key differences that are described here. In **Experiment 4.2**, slope discrimination thresholds were estimated using a spatial 2-Alternative Forced Choice (2-AFC) "Odd-Man-Out" psychophysical procedure, whereby observers had to select either the leftmost or rightmost stimuli that had an odd amplitude spectrum slope (steeper α) different from that of the unaltered reference α (centre stimulus; see **Figure 4.5**). At the beginning of each trial, a white fixation cross, 0.3° degrees of visual angle in diameter, appeared at the centre of the screen for 1000ms, which was followed by the presentation of all three stimuli. Reference α were randomly interleaved across trials. Observers indicated, via keyboard

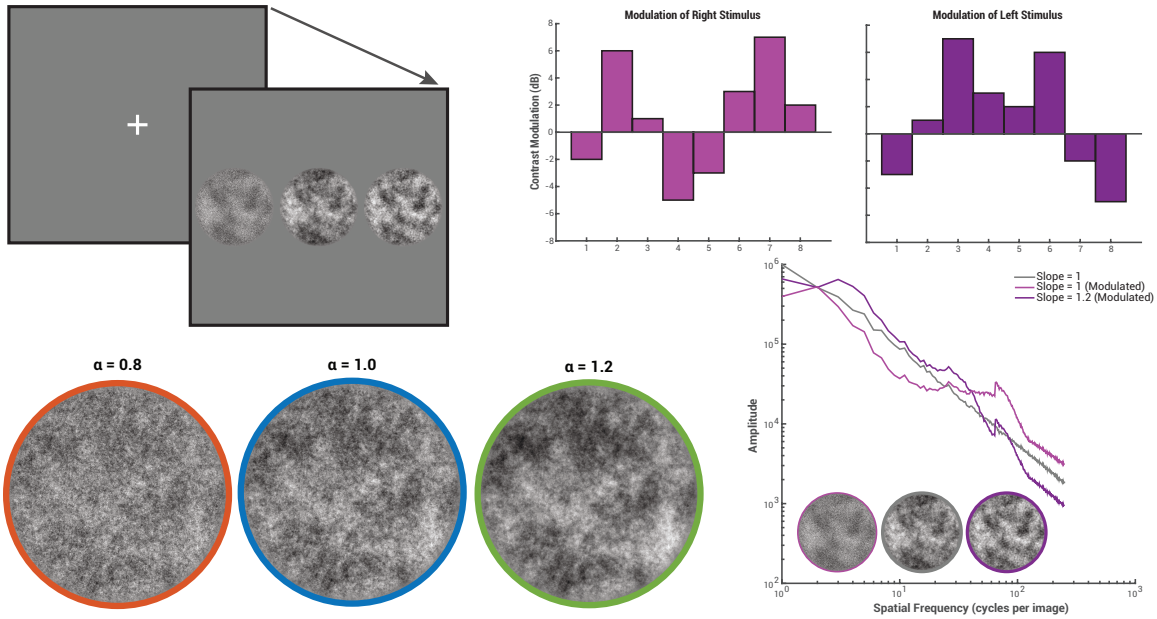

Figure 4.5. A Procedures of **Experiment 4.2**. Observers completed a spatial "Odd-Man-Out" task whereby either the left or right stimulus had an odd amplitude spectrum slope in comparison to that of the centre, reference stimulus. This task was completed both with the original noise stimuli **B** examples three reference α used in the task, and with noise stimuli that varied in contrast within 8 predefined spatial frequency bands. **C** Example weight vectors used to modulate the right and left stimulus. Weight vectors contained the same 8 contrast weight values, but their position on the spatial frequency axis was randomized for both stimuli so that neither would have the same modulation (either positive or negative) within the same spatial frequency band. **D** The resulting orientation-averaged amplitude spectrum slope of our noise stimuli for a given trial.

press, which stimulus (the left or right stimulus) had an amplitude spectrum slope that was odd from the reference. The reference stimulus remained unaltered (did not undergo the band-limited contrast modulation) for all trials in this study. A blank screen, set to mean luminance for 500ms, interlaced each trial and the response interval was unlimited. Viewing was binocular.

The trial-to-trial change in the images slope exponent (α) was defined by a constant stimulus approach. The amplitude spectrum slope of the odd stimulus was pre—defined by generating a vector of random Δα values that ranged from reference α + [0.01 - 0.30] (50 trials per Δα), with the upper limit of Δαs according to that used in previous studies (see **Experiment 2.1**). Given that Δαs were constrained to be greater than 0.01, α discrimination thresholds were estimated by fitting a cumulative Weibull psychometric function defined, in symbols as:

$$P = 1 - e^{-\left(\frac{x}{\Delta\alpha}\right)^b} \qquad \textbf{Equation 4.3}$$

with *x* the random vector of Δα values, and the threshold (Δα), which corresponds to the 63.21% accuracy rate. The slope parameter (*b*), which was not of interest to this study, is not reported. When participants completed all trials from the practice block, they repeated the experiment, however, both odd stimuli were modulated according to the procedure defined in above (see **Stimuli, Experiment 4.2)**. Participants completed 1500 trials per reference α, for a total of 4500 trials, which took approximately 6 hours to complete.

Results and Discussion

The data from the practice block of **Experiment 4.2** is plotted for all three observers in the form of psychometric functions, in addition to their α discrimination thresholds for each reference α, in **Figure 4.6**. The quality of the fits of the psychometric function varied significantly between observers and reference αs, and thus, the α discrimination thresholds should be interpreted with this caveat in mind. Note that the Weibull function used estimate thresholds targets the 63.21% accuracy rate, which estimates a lower accuracy threshold than the staircase procedure used in **Experiments 2.1** and **2.2** that targets 70.71% accuracy. α discrimination thresholds for both observers P2 and P3 followed the typical sensitivity profile to $1/f^{\alpha}$ noise stimuli, whereby thresholds for reference within the range of α = [1.0 1.2] are lower than for shallower reference αs. Conversely, observer P1 showed a high threshold for a reference α of 1.0, while their thresholds for reference αs of 0.8 and 1.2 were approximately equal.

We report decision weights (β_f) as a function of spatial frequency defined in cycles per degree of visual angle, which vary slightly from those of **Experiment 4.1** (stimulus size changed

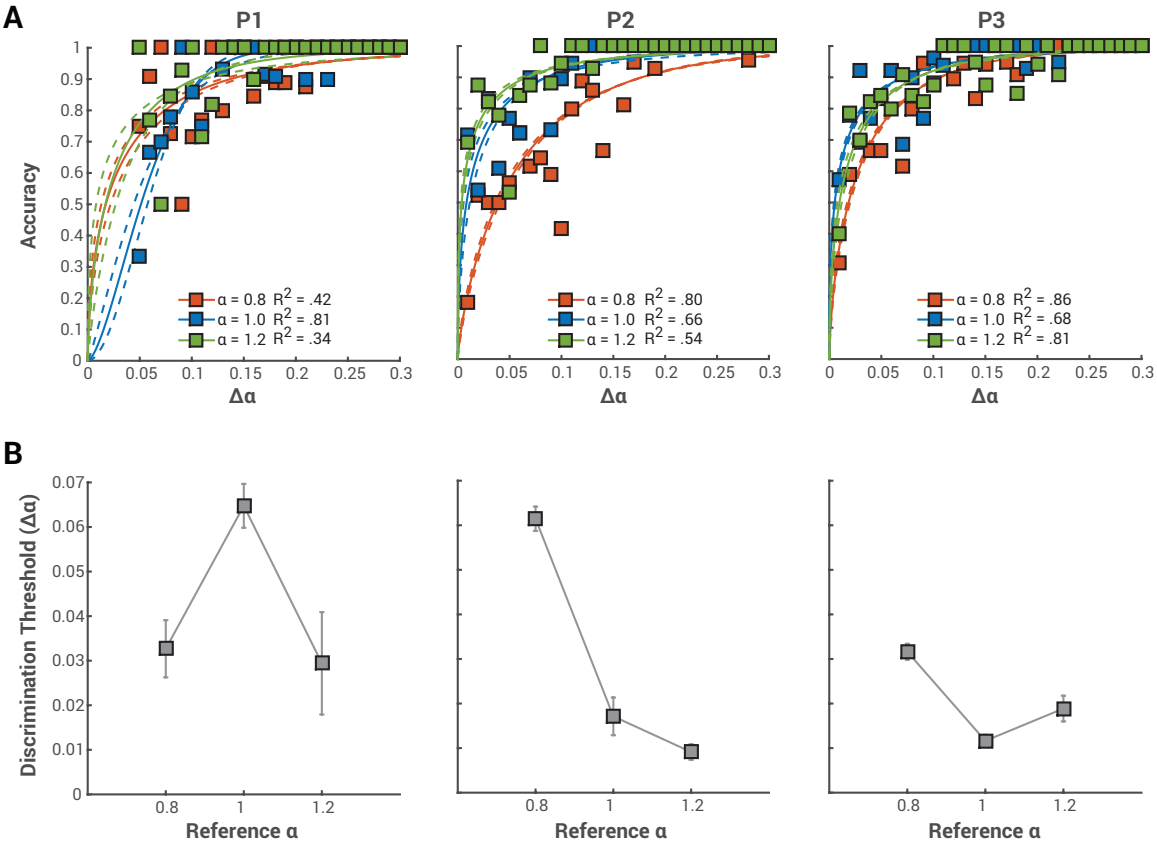

Figure 4.6. A Psychometric functions that relate the accuracy of observers (ordinate) to identify the odd amplitude spectrum stimulus for a particular Δα (abscissa). The dashed lines represent the upper and lower bounds of the 95% confidence interval of the line of best fit, calculated via bootstrapping procedures, with replacement and 2000 repetitions. **B** Each observer's α discrimination threshold (63.21% accuracy) for all three reference αs. Observers P2 and P3 showed normal α discrimination thresholds (lower for steeper α) while observer P1 had low threshold for α = 0.8 and α = 1.2.

from 8° to 6°). The centre spatial frequency of our octave bandwidth filters, in cycles per degree, were: 0.27, 0.53, 1.07, 2.14, 4.28, 8.56, and 17.12 cycles/°, while the remaining high spatial frequency content was assigned to the eight band that plateaued at 34.23 cycles/°. As the two test stimuli presented to observers in the spatial α discrimination task had different native spectra (α and α+Δα), we normalized all decision weights in accordance to the α of a particular image for a given trial. For correct trials, the weight vector of the chosen stimulus ($\omega_{f,i}^{chose}$) was divided by the α of the odd stimulus (reference $\alpha_i+\Delta\alpha_i$)**,** according to **Equation 4.4:**

$$\beta_f = \frac{1}{T}\sum_{i=1}^{T}\gamma\left(\frac{\omega_{f,i}^{choose}}{\alpha_i+\Delta\alpha_i} - \frac{\omega_{f,i}^{reject}}{\alpha_i}\right) \qquad \textbf{Equation 4.4}$$

For incorrect trials, where the stimulus with the odd α was rejected, its weight vector ($\omega_{f,i}^{reject}$) that was divided by α+Δα. Given that we were predominantly interested in the attributes given by observers to the odd stimulus in the α discrimination task, decision weights (β_f) were calculated for all trials, regardless of observer accuracy. We only labelled trials as correct or incorrect in order to adjust the decision weights of observers according to the α of each image. Observers rated their confidence (γ; confident or not) in the chosen / rejected stimulus on all trials, which was used to adjust the magnitude of the weight vector difference score for a particular trial (see **Equation 4.4**). Trials rated as confident by observers were given a scalar weight of 3 (the chosen image received a score of 4 while the rejected image received a score of 1), while trials rated low in confidence received a scalar weight of 1. The decision weights (β_f), which reflect the difference in the weight vectors of the chosen ($\omega_{f,i}^{chose}$) and rejected ($\omega_{f,i}^{reject}$) images of the α discrimination task, are shown in **Figure 4.7.**

Unlike in **Experiment 4.1**, we found no discernable shift in the peak spatial frequency band with reference α in the α discrimination task. There is individual observer variability in the pattern of decision weights across spatial frequency. However, observers showed identical peaks in their respective decisions weights for all reference αs. Observer P1 shows a clear segregation in the weights given to low and high spatial frequencies between the chosen and the rejected stimulus. That is, the stimulus chosen as odd by observer P1 had a contrast increment within the low spatial frequency bands (peak = 1 cycle/°) and a contrast decrement at higher spatial frequencies (peak = 8 cycles/°). Observer P2, on the other hand, had negative decision weights (representative of a contrast decrement) at low spatial frequencies (peak = 1.07 cycles/°) and

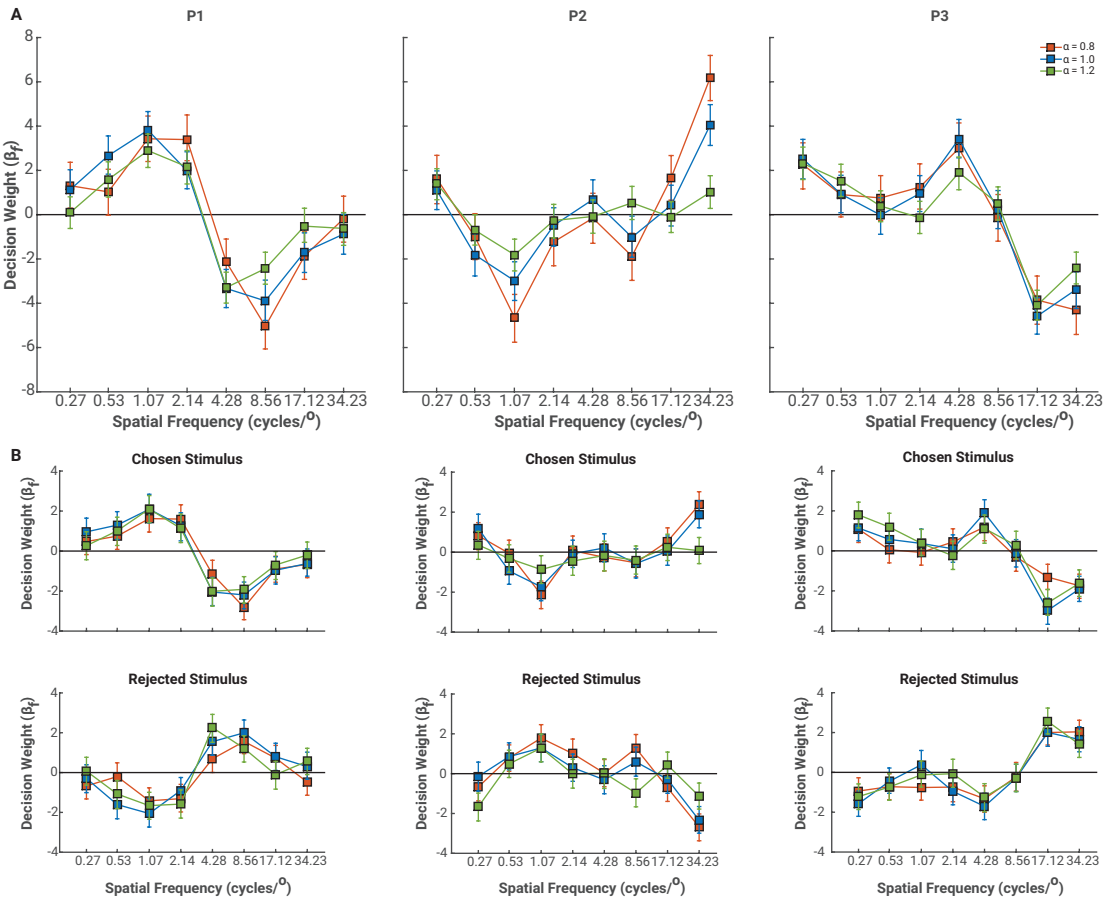

Figure 4.7. A Spatial AFC - Decision weights of all three observers for the difference in the weight vectors between the stimulus chosen as having the odd amplitude spectrum slope and the rejected stimulus. These decision weights, unlike those reported in Experiment 1 represent the difference in contrast weights between the chosen and rejected stimulus. Observer P1 had a clear separation between the contrast weights of low and high spatial frequencies they used to identify the odd stimulus, while observers P2 and P3 showed much flatter decision weights. **B** The decision weights for both the chosen and rejected stimuli. These are used to verify that non-linear operations (e.g., uncertainty) were not part of the process observers used to complete the task. Given that their decision weights only differed in signs, observers used similar processes to select the chosen and rejected stimulus. Error bars represent 95% confidence intervals calculated via bootstrapping the average decision weight (or difference in decision weights) with replacement and 2000 repetitions.

positive decision weights for higher spatial frequencies (peak near 17 cycles/°). Observer P3 had two positive deflections in their decision weights (0.27 and 4.28 cycles/°) and a large negative deflection at a spatial frequency of 17.12 cycles/°. In a manner similar to observer P1, it seems observer P3 identified stimuli with positive contrast weights near the peak of the CSF (1-4 cycles/°) and negative contrast weights at higher spatial frequencies to have an odd α. While each observer may have used luminance contrast across spatial frequency differently to identify the odd α (there is no consensus in positive or negative decision weights for all three observers), it is evident that none relied on a diagnostic spatial frequency band that scaled in accordance with α to complete the discrimination task as they did in the α identification task.

Given the large variability in the decision weights between all three observers in this study, we wondered if the modified stimulus might have lead to certain non-linear operations in the discrimination of α, which are not typically observed with unaltered stimuli. Under a linear observer model, the shape of the decision weights function under the chosen and rejected stimuli should be the same, except for a change in sign (if positive weights are given to a particular band in the chosen stimulus, then the rejected stimulus should have negative weights for the same band; Beard & Ahumada, 1999). If non-linear operations are involved in this α discrimination task (e.g., uncertainty), then the shape of the decision weight functions for the chosen and rejected stimuli should vary beyond a simple change in sign. We compared the decision weights for the chosen ($\omega_{f,i}^{chose}$) and rejected noise images ($\omega_{f,i}^{reject}$; see **Figure 4.7B**) for all three observers and references α by correlating their absolute values. The correlations between $\omega_{f,i}^{chose}$ and $\omega_{f,i}^{reject}$ were fairly high for all three observers, except for a single condition in the data of observer P2 (see **Table 4.1**). The correlation between the chosen and rejected noise image decision weights of observer P2, for a reference α = 1.2, was not statistically significant (r = .292, p = .484). This seems to be accounted for by variability in the decision weights of higher spatial frequency bands (> 8 cycles/°). Given that high spatial frequency bands carry little luminance contrast energy in comparison to lower spatial frequency bands when the α of an image is steep, they may be more susceptible to non-linear operations (e.g., uncertainty) from the observer. Nevertheless, all other conditions showed decision weights between the noise image chosen as the odd α and that rejected only differed in sign (i.e., their absolute value was strongly correlated), which suggests that non-linear operations in the discrimination task, if present, only played a minor role in the responses of our observers.

In **Experiment 4.1**, observers relied on critical, and potentially diagnostic bands of spatial frequency to identify the α of a noise image. That is, the location of the peak in decision weights scaled according to reference α, whereby increments in low spatial frequency contrast led observers to identify the image as having a steep α (α = 1.2), while images with increments in high spatial frequencies were identified as containing a shallow α (α = 0.8). However, when asked to discriminate between stimuli that vary in α, observers forgo the use of any diagnostic spatial frequency band, and instead seem to use general changes in contrast between low and high spatial frequencies, regardless of the reference α. This is compelling evidence that the spatial frequency dependent processes involved in the identification of α are different from those of α discrimination (Hansen, et al., 2008). We return to this point in the general discussion.

Experiment 4.3

The findings of **Experiment 4.2** suggest that for α discrimination, observers do not rely on some form of internal template (e.g., diagnostic spatial frequency bands) and instead rely solely on the luminance contrast differences between low and high spatial frequencies. That said, we simplified the task for observers in **Experiment 4.2** and allowed them to freely fixate all three stimuli on screen during a particular trial. While this minimized a potential difficulty in having to integrate, and hold over time, three relatively complex images (Blackwell, 1952; Jäkel & Wichmann, 2006), we may have simultaneously avoided measuring the traditional discrimination mechanism used by observers in temporal version of the discrimination task. That is, we may find that observers rely on diagnostic spatial frequency bands when they must hold the distribution of luminance contrast in memory in order to discriminate between different αs. Therefore, to rule out the possibility that the change in psychophysical procedure is causing the difference in findings, in **Experiment 4.3**, we asked observers to complete a slope discrimination task identical to that of **Experiments 2.1, 2.2, and 3.2**, the temporal version of the "Odd-Man-Out" psychophysical procedure, to gauge for any differences between the findings of its spatial counterpart.

Method

Psychophysical procedures

The stimuli were generated in an identical fashion to those of **Experiment 4.2**. **Experiment 4.3** was a replication of **Experiment 4.2** in all respects, other than the stimulus presentation sequence. Here, observers completed a temporal, 3-IFC, 2-AFC "Odd-Man-Out"

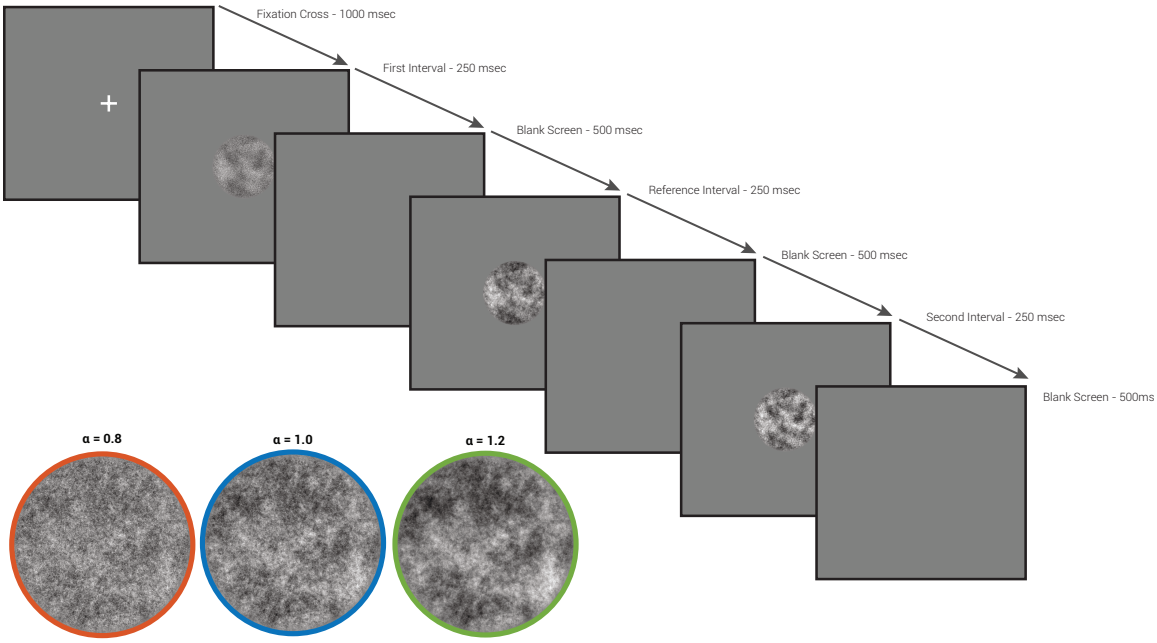

Figure 4.8. The 3-AFC, 2-IFC "Odd-Man-Out" psychophysical procedure of **Experiment 4.3**, identical to that of Experiment 1 and 2 in Chapter 1 and that of Chapter 2B. All stimulus intervals were presented for 250ms, while the inter-stimulus interval (a screen set to mean luminance) was presented for 500ms. The three stimuli in the lower left corner are examples of the three reference alpha presented to observers. Just as in Experiment 2, the reference stimulus (here, the second interval) was never modulated, while both test stimuli (the first and the third interval) had random contrast variations in the 8 spatial frequency bands (see Stimuli – Experiment 2). The weight vectors used to modulate both stimuli were generated in an identical fashion to those of Experiment 2.

slope discrimination task (see **Figure 4.8**) similar to that of **Experiment 2.1, 2.2 and 3.2**. Each trial began with a white fixation cross at the centre of the screen for 1000ms. This was followed by the presentation of the three stimulus intervals, which remained on screen for 250ms, interlaced by a blank screen set to mean luminance for 500ms. The response interval, at the end of the trial, was unlimited.

Results and Discussion

All data in **Experiment 4.3** were analyzed in an identical fashion to those of **Experiment 4.2**. The data from the practice block of **Experiment 4.3** is plotted for all three observers in the form of psychometric functions, in addition to their α discrimination thresholds for each reference α, in **Figure 4.9**. As expected, discrimination accuracy for all three observers, did not reach ceiling performance as rapidly as it did in the spatial counterpart of the "Odd-Man-Out" task. Nevertheless, thresholds for all three reference α were relatively low (never exceeding $\Delta\alpha = .075$), however, these should be interpreted under the consideration that goodness of fit values were mediocre for most psychometric functions. Once more, we find typical α discrimination thresholds, whereby thresholds are lowest for an α of 1.0 with observer P1 and P3. Observer P3, however, showed an inverted function, as they had higher thresholds for a reference α of 1.0 than to steeper and shallower αs. The psychophysical paradigm used here is identical to that of previous chapters, but nevertheless differs in regards to the blocking of reference α. While it is unclear if classification image paradigms are subject to block designs (i.e., multiple trials are conducted, in sequence with an identical reference stimulus), we opted to interleaved the reference α across trials in order to minimize hysteresis, and prevent any alterations in the classification image of our observers attributable to blocking (Levi et al., 2005). Thus, it may be that α discrimination thresholds here will differ slightly from those previously reported in **Experiments 2.1** and **2.2**.

The decision weights for each spatial frequency in our temporal version of the amplitude spectrum slope discrimination task can be seen in **Figure 4.10A**. Interestingly, the decision weights for all observers in **Experiment 4.3** are nearly identical to those of **Experiment** 4.2. Observer P1 shows a clear separation in the decision weights between low and high spatial frequencies, while observers P2 and P3 have decision weights that oscillate near 0, with small peaks or troughs at high and low spatial frequency bands. Importantly, and the same as we found in **Experiment 4.2**, there is no difference in the spatial frequency bands of peak decision weights

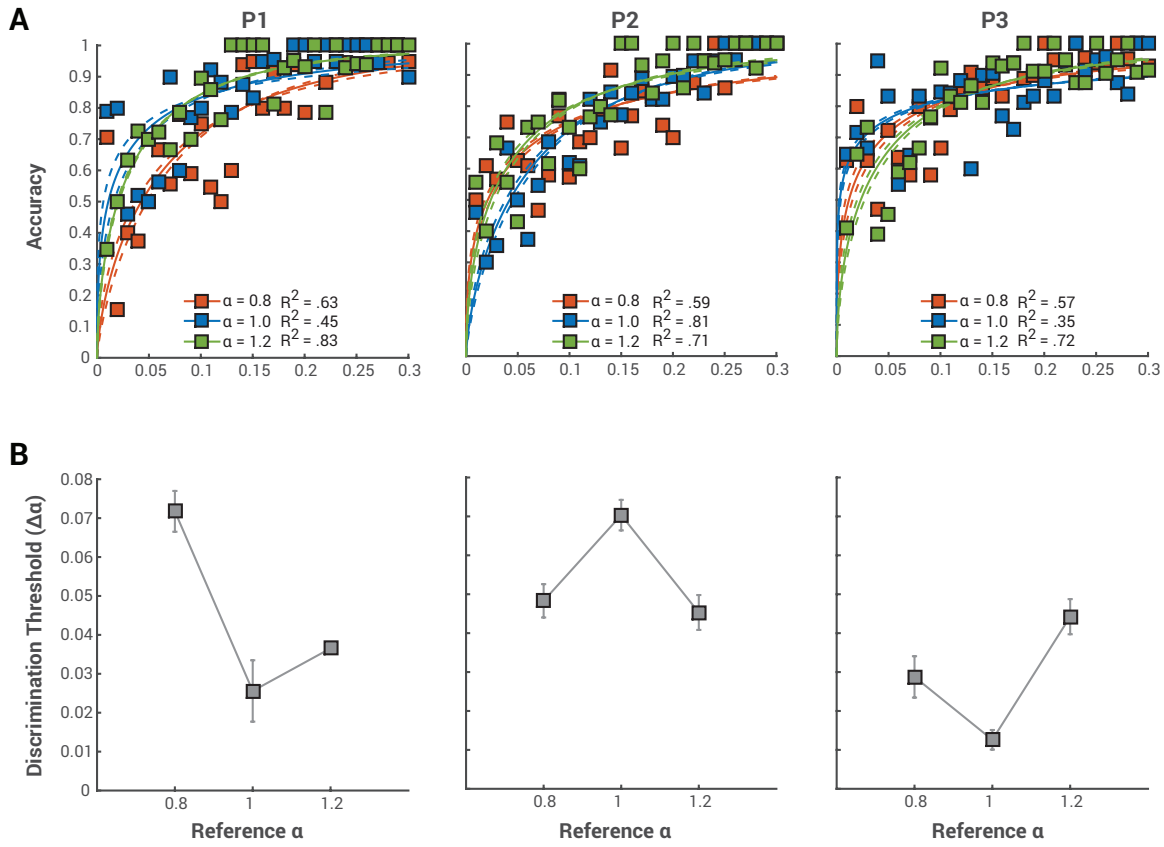

Figure 4.9. A Psychometric functions that relate the accuracy of observers (ordinate) to identify the odd amplitude spectrum stimulus for a particular Δα (abscissa). The dashed lines represent the upper and lower bounds of the 95% confidence interval of the line of best fit, calculated via bootstrapping procedures, with replacement and 2000 repetitions. **B** Each observer's α discrimination threshold (63.21% accuracy) for all three reference αs. Observers P2 and P3 showed normal α discrimination thresholds (lower for steeper α) while observer P1 had low threshold for α = 0.8 and α = 1.2.

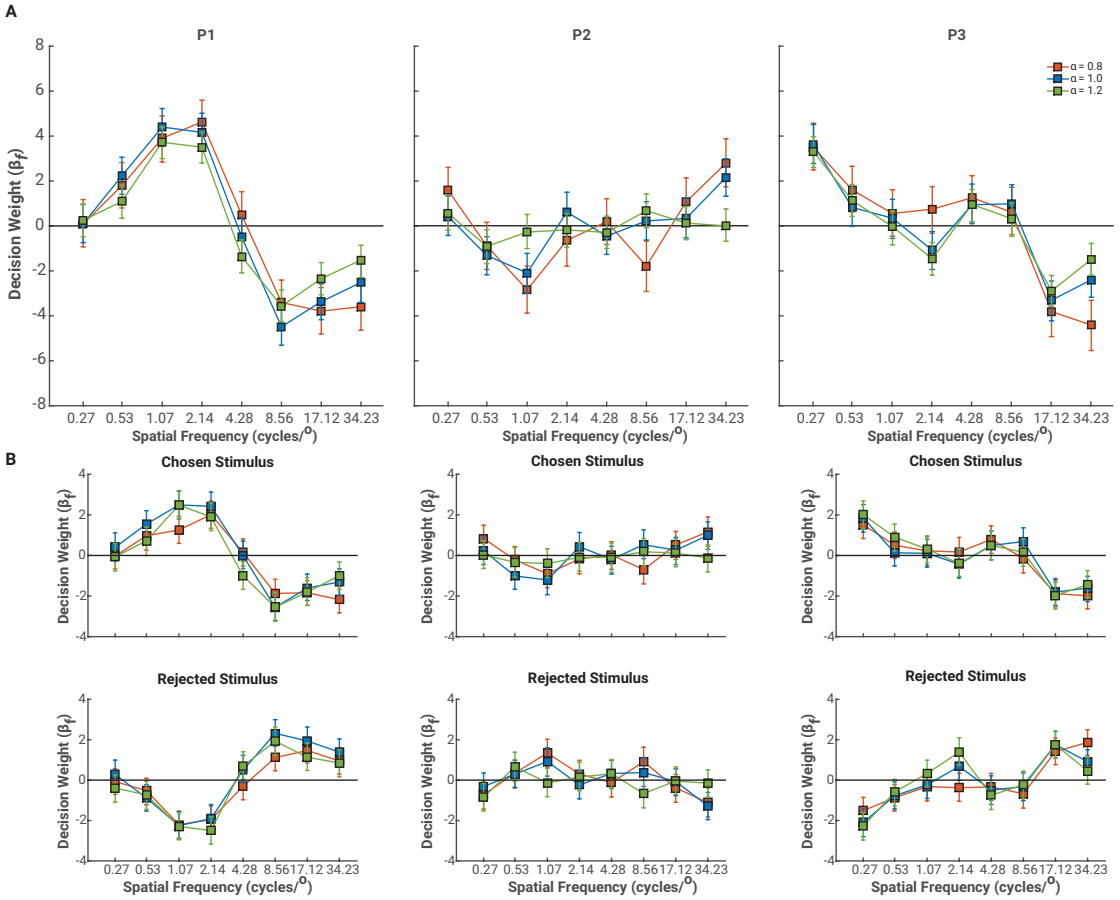

Figure 4.10. A Decision weights of all three observers for the difference in the weight vectors between the stimulus chosen as having the odd amplitude spectrum slope and the rejected stimulus for the temporal force-choice psychophysical procedure. The decision weights of our three observers are identical to those of Experiment 2. **B** The decision weights for both the chosen and rejected stimuli. These are used to verify that non-linear operations (e.g., uncertainty) were not part of the process observers used to complete the task. Given that their decision weights only differed in signs, observers used similar processes to select the chosen and rejected stimulus. Error bars represent 95% confidence intervals calculated via bootstrapping the average decision with replacement with 2000 repetitions.

between the three reference α presented to observers. The pattern of results we have obtained in **Experiment 4.2** seems, therefore, to not be attributable to the psychophysical paradigm itself, but instead highlight the true spatial frequency mechanism used by observers when asked to discriminate images that vary in α.

We, again, verified that the processes used by observers to discriminate α were linear, and did not include any non-linear operations, like uncertainty, by correlating the absolute value of the decision weights for the chosen and rejected noise images (see **Figure 4.10B**). Once more, decision weights mostly differed in sign alone (see **Table 4.3**), although observer P2 still showed a poor correlation between decision weights for the chosen and rejected stimuli for a reference α = 1.2 (r = -.091, p = .830, 95% CI [-.748 .656]). Additionally, the correlation coefficient of observer P1 for a reference α of 0.8 did not reach statistical significance (r = .672, p = .068, 95% CI [-.063 .934]), which suggest that both observer P1 and P2 had certain non-linear operations involved when selecting the odd stimulus in the temporal version of the "Odd-Man-Out" psychophysical paradigm. While the weak correlation of Observer P1 seems attributable to variability in their decision weights for higher spatial frequency bands, observer P2 showed fairly large differences in their decision weights towards the lower spatial frequency bands defined in this study. The decision weights of observer P2, particularly for a reference α = 1.2 should be interpreted with caution as they showed poor correlations in both the spatial and temporal version of the task. For all other conditions, the correlation between the decision weights of the chosen and rejected stimuli were high, which suggest that non-linear operations were not involved in the temporal forced-choice version of our psychophysical procedure (Beard & Ahumada, 1999).

General Discussion

In the current chapter, we implemented an image classification paradigm in order to better define the use of luminance contrast across spatial frequency in an α discrimination task. We found that the spatial frequency based mechanism varies according to the task observers must complete. When asked to identify the α of a noise image, observers rely on diagnostic spatial frequency bands that correlate with the dominant perceptual scale within the noise image. Thus, noise images with increased contrast in lower spatial frequency bands and decreased contrast in higher spatial frequency bands will be identified as having steeper αs. Conversely, those with contrast increments in higher spatial frequency bands, and contrast decrements in low

spatial frequency bands will be identified as having shallower αs. Most interestingly, when asked to discriminate between noise images that vary in α (i.e., α discrimination task), observers no longer rely on diagnostic spatial frequency bands. Instead, they use the general differences between low and high spatial frequency luminance contrast to detect the noise image with the odd α. Their decision weights do not vary according to the reference α, nor do they vary when the images are presented simultaneously (spatial 2-AFC) or in sequence (temporal 2-AFC). Thus, there seem to be strong task dependencies (identification versus discrimination) on the contribution and use of spatial frequency channels to the perception of α.

α Identification

In order to identify or categorize an image, observers are known to rely on critical spatial frequency bands (Gosselin & Schyns, 2001; Hansen, et al., 2008; Kwon & Legge, 2011; Morrison & Schyns, 2001; Oliva & Schyns, 1997; Schyns & Gosselin, 2003; Schyns & Oliva, 1994, 1999). It is interesting to find that observers rely on a similar mechanism to identify the αs of noise images. Granted, all participants in this study were all experienced psychophysical observers that have been exposed to 1/*f* noise stimuli multiple times. Still, observers showed clear diagnostic spatial frequency bands to identify α, which suggests that they have some form of internal representation of the appearance of noise images with different αs. Thus, our observers identified the α of a noise image in a manner similar to how observers categorize, or identify more complex natural scenes.

There is neurophysiological evidence of a spatial frequency tuned process used to encode natural scenes that relates to the spatial frequency shifts in the decision weights of the α identification task. Early visual processes are know to rely on a progression of spatial frequency tuned mechanisms (i.e., from low spatial frequencies to high spatial frequencies) to encode naturalistic images, which are adjusted according to image complexity (i.e., these processes are dependent on the amount of edge density, or structural complexity within the image; Hansen et al., 2012, 2011). Hansen and colleagues (2011) demonstrated that the magnitude of the P1 component, a Visually Evoked Potential (VEP) waveform marked as the first positive deflection from baseline within an EEG signal, serves as the dominant perceptual code for relatively sparse images, including 1/*f* noise. That is, the magnitude of the P1 scaled according to the α of the noise image presented to observers. Conversely, the first negative deflection from baseline (N1) showed no such scaling. While the N1 magnitude did not scale with α, its magnitude was greater

than that of the P1 for noise images with shallow α (α < 1.0). This suggests that the dominant component (in terms of absolute magnitude) within the EEG signal shifted from the N1 to the P1 as the α of the noise image increased (i.e., steepened). The P1 deflection is thought to reflect activity within the magnocellular pathway of the early visual processing streams, and the N1 the parvocellular pathway (Ellemberg, Hammarrenger, Lepore, Roy, & Guillemot, 2001; Tobimatsu, Tomoda, & Kato, 1995). Thus, these findings may indicate that the progression we observed in the decision weights in the α identification task reflect the transition in the magnitude of responses of higher or lower tuned spatial frequency channels to progressively shallower or steeper αs, respectively. However, we note that observers in the Hansen and colleagues (2011) study were not given any particular task other than to look at the images presented on screen, and it is unclear if observers tried to identify the α of the 1/*f* noise images in a manner similar to the requirements of **Experiment 4.1**.

How the shift in the activity of differently tuned spatial frequency channels may be used to label α remains to be defined. One possibility, at least for steep αs, is that observers compare response increments of low spatial frequency channels to the decrement of high spatial frequency channels to an internal template for blur. Indeed, the perception of blur has often been considered as analogous to that of the α of a noise images (e.g., a noise image with a steep α is considered to be blurred), and α discrimination has often been defined in terms of blur discrimination (Elliott et al., 2011; Tadmor & Tolhurst, 1994; Watson & Ahumada, 2011; Webster, Georgeson, & Webster, 2002). However, scenes only appear blurred when their natural α is artificially steepened (scenes with naturally steep αs are in focus and do not appear blurred), and it has recently been demonstrated that this change in α does not actually simulate the perception of blur (Murray & Bex, 2010). That is, steepening α affects the relative amount of contrast energy between low and high spatial frequencies within an image, but this is not equal to blurring in the conventional definition (i.e., low-pass filtering). Instead, observers may rely directly on increments in activity within a single spatial frequency band (and conversely the decrement in activity of other bands) as a diagnostic indication of α. This mechanism would mirror those of diagnostic spatial frequency bands identified in the scene categorization or face identification literature (Gosselin & Schyns, 2001; Hansen et al., 2008; Morrison & Schyns, 2001; Oliva & Schyns, 1997; Schyns & Gosselin, 2003; Schyns & Oliva, 1994, 1999).

α Discrimination

The initial description of a mechanism responsible for α discrimination was defined in a similar fashion to models of contrast discrimination. Specifically, observers monitor a change in luminance contrast energy within a single spatial frequency band (a critical band) and adjusted the bands' center spatial frequency in accordance to the reference α (Tadmor & Tolhurst, 1994; Tolhurst & Tadmor, 1997). While we have also found that the discrimination of α may rely on increments and decrements of luminance contrast within select spatial frequency bands, these bands do not shift according to the value of the reference α, unlike previous reports on the contribution of spatial frequency channels to α discrimination (Tadmor & Tolhurst, 1994; Tolhurst & Tadmor, 1997). Thus, while observers may rely on the activity of certain spatial frequency bands to discriminate α, these bands do not appear to be diagnostic of the reference α. Additionally, this comparison (and potential mechanism) seems to be unaffected by stimulus presentation paradigm, as the decision weights were identical in both the spatial and temporal variants of the α discrimination task. Observers seem to make general comparisons between the luminance contrast of low and high spatial frequency bands in order to discriminate α, and do so even if multiple noise images must be held in memory (via the temporal AFC), or if all are simultaneously (via the spatial AFC) available to observers.

These findings are concordant with other psychophysical evidence for the contribution of multiple spatial frequency channels to α discrimination (Párraga & Tolhurst, 2000), at least when the reference α falls within the range of αs in the natural environment (α [0.6 - 1.6]; Billock, 2000; Burton & Moorhead, 1987; Hansen et al., 2003; Párraga & Tolhurst, 2000; Tolhurst et al., 1992). Párraga and Tolhurst (2000) demonstrated that changes in the global contrast of an image, which leaves the original α of the image unaltered, had no impact on α discrimination thresholds (for reference $\alpha > 0.4$). They argued that if observers relied on a single spatial frequency band to discriminate natural images with different amplitude spectra, then their manipulation should have affected α discrimination thresholds. Conversely, thresholds should be unaffected if observers compute the actual slope (by comparing the luminance contrast energy across two or more bands) to complete the discrimination task. Here, we show direct evidence for a multi-channel mechanism involved in slope discrimination. However, we also show that the use of multiple spatial frequency channels in an α discrimination task may only serve to segragate luminance contrast energy between high and low spatial frequencies, and not directly estimate the α of the

noise image (i.e., the spatial frequency mechanism involved in discrimination is not tuned to nor selective for reference α). The decision weights of Observer P1 are most representative of this process: they chose the odd amplitude spectrum slope as the stimulus that contained a contrast increment in lower spatial frequencies, and a contrast decrement in higher spatial frequencies, regardless of reference α. The decision weights of observer P3 were not as clear as those of P1, but still showed a similar low versus high spatial frequency approach to the discrimination of α. Observer P2, on the other hand, may have completed the task in a manner quite dissimilar to the other observers, and may therefore not be representative of the true spatial frequency dependent mechanism involved in α discrimination.

Identification VS Discrimination

The differences observed in the classification images of the α identification and α discrimination tasks speak to the potential internal representation of the α of noise images and how they may serve early visual processes. The shift in the peak spatial frequency bands observed under identification suggests observers rely on diagnostic channel activity, as it scales in spatial frequency across α, to identify the α of a noise image. Consequently, observers must have some internal representation of the perceptually dominant scale in noise images, which may potentially extend to natural scenes. Most studies that have assess the mechanistic properties of recognition, which are traditionally done with face identification paradigms, have shown that the mechanism of face recognition is discrete in spatial frequency and relies on a match between an internal representation and the visual input within the critical,spatial frequency band (typically located above the peak of the CSF; Hansen, et al., 2008; Schyns & Oliva, 1999). This suggests that a close match between the internal representation and the visual input must be met in order for the recognition process to be accurate. However, this seems unnecessary in the α discrimination task implemented here as the classification images showed no scaling or change in the spatial frequency representation of α across different α values. Thus, the discrimination of α seems to be completed based solely on the differences of spatial frequency channel activity: that is, increments in contrast at low spatial frequencies, and decrements in contrast at high spatial frequencies were indicative of the odd stimulus, regardless of reference α.

Limitations

There are certain differences between the psychophysical methodology we implemented here, and those that are typically used in an α discrimination task. Of note is the interleaved

designed we used to measure slope discrimination thresholds in **Experiments 4.2** and **4.3**. In previous studies (Hansen & Hess, 2006; Johnson et al., 2011), we have always measured slope discrimination thresholds in a blocked designed, where observers completed a staircase for each reference α separately. However, the methodological requirements (e.g., the large number of trials) of the classification image paradigm prevented the use of our typical staircase method, and instead required a constant stimulus psychophysical method, where the presentation of the three reference αs was interleaved. Observers could not predict the reference α they were asked to discriminate from trial to trial, which may have generated a bias in their decision weights. For example, in a blocked design, observers are consistently discriminating according to a fixed reference α. This may have allowed them to better adjust the monitored spatial frequency bands according to the reference α. Given that observers responded in a fairly consistent manner and did not show signs of uncertainty in their decision weights, in both the spatial and temporal variants of this task, it is unlikely that the use of an interleaved design, as opposed to a blocked design, had any significant impact on the decision weights of our observers.

Second, the stimulus with the odd amplitude spectrum always had a steeper α than the reference α. While this most likely did not affect the slope discrimination thresholds of our observers, it may have contributed to the pattern of decision weights we observers in **Experiments 4.2 and 4.3**. That is, the low spatial frequency contrast increment observed in the decision weights of Observers P1 and P3 may stem from the odd stimulus always containing a steeper amplitude spectrum slope (as it has for all previous α discrimination experiments they have participated in). It is possible that the pattern of their decision weights would have inverted in sign if the odd stimulus always contained a shallower amplitude spectrum slope. While not crucial to the interpretations of this study, a change in sign of the decision weights, in according with how α discrimination threshold is approach (from above or from below the reference α) could indicate some form of prior knowledge, and strategizing from participants completing an α discrimination task.

Conclusion

Natural images contain statistical regularities that the early visual system is believed to be ideally suited to encode (Field, 1987). One such regularity is the slope of the amplitude spectrum, a second-order statistic that defines the variance of luminance contrast in natural images. It is thought that the encoding of α is completed via a spatial frequency based process in

early vision (Brady & Field, 1995; Field & Brady, 1997; Field, 1987; Hansen et al., 2012, 2011; Hansen & Hess, 2012; Knill et al., 1990; Párraga & Tolhurst, 2000; Tadmor & Tolhurst, 1994; Tolhurst & Tadmor, 1997). While there are certain models that suggest α can be discriminated according to the responses of spatial frequency channels, there lacks psychophysical evidence that may define the underlying properties of such a mechanism. Here, we implemented a modified classification image paradigm in order to assess how human observers may use luminance contrast energy across multiple spatial frequency bands to discriminate the α of noise images. We first measured how observers used luminance contrast in an α identification task and found, congruent with neurophysiological findings of natural scene perception (Hansen et al., 2012, 2011), that observers rely on diagnostic spatial frequency bands, whereby the spatial frequencies used by observers scales according to the α of the image, to identify its α. However, in a discrimination task, observers forgo the use of any diagnostic spatial frequency bands instead compare the general luminance contrast between high and low spatial frequencies, regardless of reference α. There are task dependent contributions of spatial frequency channels to the encoding of the α of noise images, and measurements of α discrimination thresholds may not be fully representative of the spatial frequency dependent processes completed by the early visual system to encode the α natural stimuli.

Chapter 4 Tables

Table 4.1. Correlation between the absolute decision weight vectors for the chosen and rejected stimulus, Experiment 4.2

			95% CI	
	r	p	LL	UL
P1				
α = 0.8	.859	.006	.392	.974
α = 1.0	.910	.002	.573	.984
α = 1.2	.833	.010	.313	.969
P2				
α = 0.8	.841	.009	.334	.970
α = 1.0	.789	.020	.191	.960
α = 1.2	.292	.484	-0.512	.826
P3				
α = 0.8	.861	.006	.398	.975
α = 1.0	.886	.003	.482	.979
α = 1.2	.959	<.001	.786	.993

Table 4.2. Correlation between the absolute decision weight vectors for the chosen and rejected stimulus, Experiment 4.3

			95% CI	
	r	p	LL	UL
P1				
α = 0.8	.672	.068	-.063	.934
α = 1.0	.914	.002	.588	.985
α = 1.2	.870	.005	.427	.976
P2				
α = 0.8	.904	.002	.549	.983
α = 1.0	.712	.048	.015	.943
α = 1.2	-.091	.830	-.748	.656
P3				
α = 0.8	.896	.003	.517	.981
α = 1.0	.839	.009	.328	.970
α = 1.2	.717	.045	.026	.945

Chapter 5

General Discussion

GENERAL DISCUSSION

The early processing stages of vision are composed of a series of channels, which act like filters to extract a narrow range of spatial frequency and orientation content from the retinal image (Bergen, Wilson, & Cowan, 1979; Blakemore & Campbell, 1969; Campbell & Robson, 1968; Campbell & Kulikowski, 1972; Carandini et al., 2005; De Valois, Albrecht, & Thorell, 1982; De Valois, Morgan, & Snodderly, 1974; Enroth-Cugell & Robson, 1966; Graham & Nachmias, 1971; Graham, 1989; Henning, Hertz, & Broadbent, 1974; Maffei & Fiorentini, 1973; Movshon, Thompson, & Tolhurst, 1978; Stromeyer & Julesz, 1972; Stromeyer & Klein, 1974; Wilson & Bergen, 1979; Wilson, McFarlane, & Phillips, 1983; Wörgötter & Koch, 1991). It has been posited that the functional attributes of these channels are strongly tied to the properties of the environment they have developed in (Carandini et al., 2005; Field, 1987; Geisler, 2008; Hyvärinen, Hoyer, Hurri, & Gutmann, 2005; Hyvärinen, Hurri, & Hoyer, 2009; Olshausen & Field, 1996b, 1997, 2005; Olshausen & Lewicki, 2004; Simoncelli, 2003). Hence, these channels may be optimally tuned to extract, and process, visual inputs regularly encountered by the visual system (on either an evolutionary or developmental time scale). However, most investigations on the function of channels have measured their contribution to the early stages of visual processing with simple stimuli, which are narrowband in both spatial frequency and orientation (e.g., sine-wave gratings). While a useful approach to assess the contribution of a subset of channels tuned to the dimensions of the stimulus, this method serves as a poor representation of how these channels function under more naturalistic conditions. That is, narrowband stimuli fail to generate sufficient channel activity to simulate the interactive properties of channels under naturalistic stimulation (Bex et al., 2009; DeAngelis et al., 1992; Elliott, Georgeson, & Webster, 2011; Hansen et al., 2003, 2008; Haun & Essock, 2010; Párraga et al., 2005; Párraga & Tolhurst, 2000; Wilson & Wilkinson, 1997). It may, therefore, be beneficial to approach the study of psychophysical channels in the early visual system with more naturalistic, broadband stimuli.

Natural scenes can be represented by their characteristic Fourier amplitude spectrum slope (α), which represents the autocorrelation property of natural images (Ellemberg et al., 2012; Field, 1987, 1989; Gaspar & Rousselet, 2009; Hansen & Hess, 2006; Hansen & Loschky, 2013; Hyvärinen et al., 2009; Johnson et al., 2011; Olshausen & Field, 2000; Párraga et al., 2005; Schwartz & Simoncelli, 2001; Simoncelli, 2005; Tadmor & Tolhurst, 1993; Tolhurst et al., 1992; Wainwright & Simoncelli, 2000). The value of α can have a noticeable impact on visual

perception, including the detection and discrimination of contrast (Webster & Miyahara, 1997), the strength of masking effects on both simple (Hansen & Hess, 2012) and complex images (Hansen & Loschky, 2013; Loschky et al., 2010). Additionally, human observers tend to show better performance on visual tasks when images have α values at or near their natural α (Párraga et al., 2000; Párraga et al., 2005). Finally, observers have also shown differing sensitivity to αs, as they are most sensitive to a change in α when it occurs near to or above the average α of natural scenes (α = or > 1.0; Hansen & Hess, 2006; Johnson et al., 2011; Knill et al., 1990). Taken together, these findings suggest that α is relevant to the early processing stages of the visual system (Knill, Field, & Kersten, 1990; Párraga, Troscianko, & Tolhurst, 2000; Párraga et al., 2005; Tolhurst & Tadmor, 2000). That said, the contribution of early visual processes to the encoding of α remain to be properly defined. Specifically, the detection, and subsequent discrimination, of a change in α is believed to be a spatial frequency dependent process,(Hansen et al., 2012, 2011; Párraga & Tolhurst, 2000; Tadmor & Tolhurst, 1994; Tajima et al., 2010; Tolhurst & Tadmor, 1997). Yet, which channels may be most involved in the discrimination of α, and whether this mechanism is specific to α is unclear. The overarching goals of this dissertation were to build upon the findings described above and establish the contribution of spatial frequency channels to the discrimination of α.

The main questions of this dissertation revolved around the behaviourally relevant attributes of a spatial frequency based mechanism responsible for detecting and discriminating a change in α. All experiments in this dissertation, therefore, used a well-established α discrimination procedure (3-IFC, 2-AFC "Odd-Man-Out" task) to estimate the discriminability of α as either the spatial frequency content of stimuli or the activity of spatial frequency channels were manipulated. The following reviews the goals and significant findings of each experimental chapter.

Review and Significance of Main Findings

Chapter 2. The goal of **Chapter 2** was to obtain psychophysical evidence for the influence of spatial frequency channels on α discrimination. In particular, we were interested in measuring the contribution of low spatial frequency channels, as they seem to dominate neural responses to α (Hansen et al., 2011; Webster & Miyahara, 1997). Discrimination thresholds to five different reference αs were measured according to different representation of low spatial frequency content in our 1/*f* noise stimuli (i.e., a change in stimulus size). The findings of

Experiment 2.1 demonstrated that α discrimination thresholds are facilitated by the addition of low spatial frequencies, as all thresholds decreased as the stimulus size increased. This facilitation, measured with log ratios normalized by the α discrimination thresholds to our largest stimulus size, followed an inverted-U function across α. We found that discrimination thresholds for a reference $\alpha = 1.0$ benefitted most from the increases in stimulus size, while steeper ($\alpha > 1.0$) and shallower ($\alpha < 1.0$) αs showed weaker facilitation. There is a multi-channel model that can account for the perceived contrast of broadband images that vary in α. This model, initially developed by Field, (1987), Brady and Field (1995), and Field and Brady (1997), generates filter outputs that correlate well with the effects of stimulus size we obtain in **Experiment 2.1**. The responses of multiple narrowly tuned 1-octave bandwidth spatial frequency filters are greatest for images with $\alpha = 1.0$, and decrease as α steepens ($\alpha > 1.0$) or shallows ($\alpha < 1.0$). It is plausible, therefore, that the discriminability of α is determined by the pooled responses of multiple, narrowly tuned spatial frequency channels (with either constant or decreasing octave bandwidth; Hansen & Hess, 2012; Wilson et al., 1983; Wilson & Wilkinson, 1997).

The change in stimulus size, while a simple manipulation of spatial frequency content, could not account for the influence of other psychophysical mechanisms in the observed facilitation effect. For example, summation effects of higher spatial frequency content within our stimuli may have been responsible for the decrease of α discrimination thresholds may have contributed to the facilitation effect (Baker & Meese, 2011; Graham & Sutter, 1998; Graham, 1989; Hutchinson & Ledgeway, 2010; Meese & Baker, 2011, 2013; Meese & Summers, 2007; Taylor, Bennett, & Sekuler, 2009). In **Experiment 2.2**, we aimed to better isolate the contribution of low spatial frequency channels to the discrimination of α by replicating the center-surround paradigm used by Johnson and colleagues (2011), but increased the width of the gap between the centre and surround annulus to 3.2° of visual angle. The results of our study were similar to those of Johnson and colleagues (2011). We found a facilitative effect of the surround annulus on the discriminability to the centre's α, when the centre α was relatively steep. Furthermore, the gap size had little impact on the magnitude of this facilitation effect in that a surround annulus 3.2° away from the centre stimulus still had a facilitatory effect on α discrimination thresholds. These findings indicate that α discrimination is completed globally (Johnson et al., 2011; Mareschal et al., 2001), and may thus be mediated predominantly by the responses of lower tuned spatial frequency channels. These findings, additionally, suggest the

facilitation effect observed in **Experiment 2.1** may be attributed to the manipulation of low spatial frequency luminance contrast within our stimuli, at least when α is steep. As only relatively steep centre αs were influenced by the presence of a surround annulus, we argued that the spatial frequency channels that contribute most to the discrimination of α have peak spatial frequency tuning that correlates with the perceptually dominant scale in noise stimuli. Thus, as we only found steeper reference αs (αs = 1.0, 1.3, and 1.6) to be influenced by the presence of a surround annulus, α discrimination thresholds for steep αs seem regulated by the activity of low spatial frequency tuned channels. That said, this is not indicative that higher tuned spatial frequency channels are not involved in the discrimination of α, but may not dominate neural responses when α is steep. As the shallower reference αs (α = 0.4 and 0.7) showed no real influence of the surround annulus (when the suppression factors were collapsed across gap size), we proposed α discrimination thresholds for shallower reference αs to be regulated by higher spatial frequency tuned channels. We verified if higher tuned spatial frequency channels may contribute most to the discrimination of shallower αs in **Chapter 3.**

Chapter 3. We aimed, in **Chapter 3** to directly measure the contribution of spatial frequency channels to the discrimination of α with the application of tDCS over the primary visual cortex. The implementation of tDCS to visual paradigms is relatively novel, but has been demonstrated to measurably alter early visual processes (e.g., contrast detection; Antal et al., 2001, 2006a, 2006b; Hansen et al., 2015; Jacobson et al., 2012; Peters et al., 2013; Spiegel et al., 2013, 2012). However, these effects have only been measured to a limited set of stimulus dimensions. Therefore, prior to implementing tDCS in our α discrimination task, we verified how varying sensitivity to contrast according to stimulus spatial frequency and orientation may influenced the effectiveness of tDCS to modulate early visual function. That is, we asked how the effects of tDCS (both anodal and cathodal) change according to the different contrast sensitivity of the sine-wave gratings spatial frequencies that comprise the contrast sensitivity function (CSF). We found, in **Chapter 3A**, that the modulatory effects of tDCS are largest on contrast sensitivity to high spatial frequencies and non-cardinal orientations – stimulus dimensions that generally elicit lower contrast sensitivity (Robson, 1966). The tDCS polarity effects we observed differed slightly from those typically reported within the vision and tDCS literature. Anodal tDCS, which typically has a facilitative effects on behaviour (Antal et al., 2001; Spiegel et al., 2013, 2012), caused a decrease in contrast sensitivity at higher spatial

frequencies (8 cycles/° and 12 cycles/°), while cathodal tDCS, which is normally reported to have a deleterious effects on behavioural performance (Antal et al., 2001; Olma et al., 2011; Spiegel et al., 2013) increased contrast sensitivty to higher spatial frequencies (for a good discussion on the behavioral impact of cathodal tDCS in vision studies, see Pirulli et al., 2014). The spatial frequency dependence of tDCS found on contrast detection is congruent with the findings that the current generated by tDCS influences cells at or near the cortical surface most (Bikson & Rahman, 2013; Datta et al., 2009; Peterchev et al., 2012; Radman et al., 2009; Rahman et al., 2013). Given the selectivity of tDCS we identified in **Chapter 3A**, we thought it an interesting tool to directly assess the contribution of spatial frequency channels in an α discrimination task.

In **Chapter 3B** observers completed an α discrimination task, while they received either anodal or cathodal tDCS (a third group received only sham stimulation). Given the findings of **Chapter 2** and **Chapter 3A**, we had hypothesized that the effects of tDCS would be largest on the discrimination thresholds of shallow α (i.e., perceptually dominated by higher spatial frequency content, and thus regulated by higher spatial frequency channels). We found that neither tDCS polarity had any measurable impact on α discrimination thresholds. That said, the null-effects of tDCS obtained in **Chapter 3B** are mostly likely attributed to the limitations of the stimulation technique, and not an indication that a spatial frequency dependent mechanism is not involved in α discrimination. The ability of tDCS to modulate perception seems constrained to changes in the detectability of a stimulus, and may be unsuited to modulate any discrimination, or other suprathreshold processes completed by the early visual system.

Chapter 4. In **Chapter 4**, we used an image classification paradigm as a final effort to define the contribution of spatial frequency channels to the discrimination of α. To measure the classification image, observers were asked to make a perceptual judgement on the whole stimulus (e.g., determine or discriminate α) while its physical attributes, or components, were randomly changed from trial to trial. The perceptual judgement was then correlated with the change in the stimulus over a large number of trials, and averaged to generate a representation of the weight attributed by observers to the components of a stimulus. The contrast of eight discrete spatial frequency bands of 1/*f* noise stimuli was randomly modulated by ± 8dB over multiple trials, and the generated classification images (i.e., decision weights) were used to assess the weights attributed to contrast within individual spatial frequency bands by observers in either an

identification or discrimination task. Thus, the classification image paradigm allowed us to experimentally verify which spatial frequency bands are behaviourally relevant to the identification and discrimination of α. While we found task dependent contributions of spatial frequency channels to the perception of broadband contrast, in general, we found observers to make a perceptual decision by comparing contrast between low and high spatial frequency channels (Boynton et al., 1999; Britten et al., 1992; Campbell & Kulikowski, 1972; Haynes et al., 2003; Kwon et al., 1992; Ress et al., 2000; Ross & Speed, 1991; Shadlen & Newsome, 1998; Zenger-Landolt & Heeger, 2003). For all three experiments, observers relied on increments in contrast in low spatial frequency bands, and decrements in contrast at higher spatial frequency bands to complete the task. In **Experiment 4.1** we found that when asked to identify the α of a noise image, observers relied on contrast within diagnostic spatial frequency bands. That is, the increment and decrement in contrast used by to identify the α of the image scaled with perceptually dominant scale of the image. When the α of the image was steep (1.2), observers relied on increments in contrast at low spatial frequency and decrements in contrast at higher spatial frequencies to identify α, while the inverse held true for shallower α (0.8). This result suggests that the spatial frequency mechanism used to identify the α of an image (which was done with high accuracy) is adjustable, and may rely on diagnostic spatial frequency bands. That is, the particular ratio of high and low luminance contrast across spatial frequency may be indicative of α. Diagnostic spatial frequency bands are commonly reported in identification paradigms. Observers are known to rely heavily on low spatial frequency content to identify the category of a scene, and similarly, face recognition studies have demonstrated that diagnostic spatial frequency bands carry information about the face identify and the presence or type of an emotion (Gosselin & Schyns, 2001; Hansen, et al., 2008; Kwon & Legge, 2011; Morrison & Schyns, 2001; Oliva & Schyns, 1997; Schyns & Gosselin, 2003; Schyns & Oliva, 1994, 1999). Other features than spatial frequency content, including colour, have also been reported to hold diagnostic properties in the categorization of scenes (Goffaux et al., 2005; Oliva & Schyns, 2000). Thus, when asked to identify or recognize the property of a particular image, observers will rely on the information transmitted by only a few spatial frequency channels, and will adjust the monitored band according to its relevance to the task.

It is interesting to find a similar process used by observers to identify the α of noise images, which are specifically designed to carry no semantically meaningful information. The

recognition process requires a comparison between neural responses to the stimulus and some internal representation of that stimulus. Thus, our findings suggest that experienced psychophysical observers may have an internal representation of α, which is related to the perceptually salient scales of 1/*f* stimuli with different αs (e.g., the perceptually salient low spatial frequency content of noise images with steep αs versus the high spatial frequency content of noise images with shallow αs). These results corroborate neurophysiological findings on the encoding of α in noise images. The Visually Evoked Potentials (VEPs) of human observers to noise images that vary in α have been shown to scale in magnitude according to the α of a noise image (Hansen et al., 2012, 2011). When the α of an image was steep, the dominant neural signal to the noise image was likely carried by cells tuned to lower spatial frequencies (the P1 VEP component; Ellemberg et al., 2001), while cells tuned to higher spatial frequencies likely dominated the neural response to noise images with shallower α (the N1 VEP component). Thus, our findings and those of Hansen and colleagues (2011, 2012) suggest that the peak spatial frequency of the channel that responds most, in comparison to other channels, will signal for the α of an image. Whether the comparison is made solely between low and high spatial frequency tuned channels, or whether this is a fairly discreet process remains to be determined.

Most interestingly, we found that the process of discrimination, unlike identification, showed no spatial frequency selectivity to α. While we found each observer to vary widely in their results, the key observation here for each observer was that decision weights in **Experiments 4.2** and **4.3** were identical for all three reference αs. Similar to the identification task, the odd stimulus was identified according to a comparison between contrast at lower and higher spatial frequency bands, but interestingly, the decision weights did not scale with α. As the reference α had no impact on the decision weights, it seems that observers did not rely on any prior knowledge, or any internal representation of α to complete the discrimination task, which agrees with other findings that discrimination is not specific to the attributes of the stimulus (Hansen et al., 2008). Task dependent effects aside, our findings also suggest that the discrimination model proposed by Tolhurst and Tadmor (1997) is incorrect. Their model defined α discrimination as a process of contrast discrimination within a single and wide spatial frequency band (2-octave bandwidths), with center spatial frequencies that adjusted according to the reference α. Thus, in their model, the discrimination process is dependent on observers collecting information in regards to the reference α in order to adjust the monitored band

accordingly. Our results, however, suggest observers may not need this process to discriminate α, and can complete an α discrimination task without any regards to the value of the reference α (for α values of 0.8, 1.0, and 1.2 – more extreme α values may show significantly different effects; Párraga & Tolhurst, 2000). These findings also suggest that the low spatial frequency interactions we identified in **Experiment 2.2** may not be constrained to steeper αs, but instead a result of the general discrimination mechanism identified in **Experiments 4.2** and **4.3**. We note, however, that decision weights offer a representation of the stimulus attributes observers use or rely on to complete a particular task (Ahumada, Jr. & Ahumada, 2002; Beard & Ahumada, Jr., 1998; Haun & Peli, 2013), and while potentially correlated with the response patterns of spatial frequency channels within the early visual system, are not a model of their behaviour in broadband conditions (Boynton et al., 1999; Klein & Levi, 2009; Levi et al., 2005; Ress et al., 2000; Zenger-Landolt & Heeger, 2003).

Future Directions

The experimental reports mentioned above offer insight on the contribution of spatial frequency channels to α discrimination. We demonstrated that α discrimination is regulated by low spatial frequency channel interactions, and it seems that this process is not specific to the reference α. These findings raise further questions in regards to human sensitivity to the α of natural scenes, which are discussed below.

Tuning to α. The distribution of αs across natural images peaks at a value of 1.08 (Billock, 2000; Ruderman & Bialek, 1994; Tolhurst et al., 1992; van der Schaaf & van Hateren, 1996). Additionally, the range of αs typically encountered is fairly narrow (when careful consideration is taken for the environment) and extends between [0.8 – 1.0] (Hansen & Essock, 2005). Thus, the probability of encountering an environment with an α near 1.0 is high, and this has been used to argue that human observers should show either high sensitivity (Hansen & Hess, 2006; Knill et al., 1990) or high resilience (Tadmor & Tolhurst, 1994; Tolhurst & Tadmor, 1997) to changes in α near 1.0. While both theories on sensitivity to α propose different sensitivity profiles, they both argue that the visual system should be tuned, or show selectivity, in how it responds to αs near those of the average α versus steeper or shallower αs. That is, when asked to discriminate between different αs, human observers show better performance (greater sensitivity) to αs near that or above the average α value of natural images (α = 1.08; Billock, 2000), and worse performance for αs outside of that range. However, we have shown here that

the process involved in the discrimination α is not specific to the reference α, in that the spatial frequency bands used by observers to identify the odd stimulus do not change according to the reference α. Thus, while human observers show tuning to particular α values (typically near 1.0), the discrimination process is not tuned to α. Future research should verify how a general discrimination mechanism generates the sensitivity profile to α previously reported in discrimination studies (Hansen & Hess, 2006; Knill et al., 1990; Tadmor & Tolhurst, 1994; Tolhurst & Tadmor, 1997). Specifically, it could be interesting to generate a model of α discrimination that could incorporate a general discrimination mechanism as the one identified in **Chapter 4**, and verify what other processes are required to generate tuning similar to that typically found. This may lie in the form of interactions between spatial frequency channels prior to pooling between channels and the decision stages. It would be interesting to verify if these interactions are facilitative (Meese, 2004; Xing & Heeger, 2000) or inhibitive (Bex et al., 2007; Carandini & Heeger, 1994; Heeger, 1992; Hugh R. Wilson & Humanski, 1993) in nature, or if any bias in the strength of interactions between channels tuned to particular ranges of spatial frequency content (Cass, Alais, Spehar, & Bex, 2009; Haun & Essock, 2010; Haun & Peli, 2013; Taylor et al., 2009), are required to generate the typical tuning for α with our general discrimination process.

Neurostimulation. In **Chapter 3**, we had aimed to directly measure the contribution of spatial frequency channels to the discrimination α with the application of tDCS over primary visual cortex, but found no effect and proposed tDCS may be inadequate to modulate suprathreshold vision. There are other neurostimulation techniques that may be better suited to investigate, more directly, the contribution of spatial frequency channels to α discrimination. For example, neurostimulation techniques with greater stimulation precision and/or magnitude (e.g., HD-tDCS or TMS; Antal et al., 2006b; Edwards et al., 2013; Kuo et al., 2013; Miranda et al., 2013; Rahman et al., 2013; Thompson et al., 2008; Waterston & Pack, 2010), may be better suited to influence the activity of cells in primary visual cortex, and thus, modulate α discrimination thresholds.

Diagnostic spatial frequency bands. Both the identification of α and the discrimination of α were shown, in **Chapter 4,** to be completed by different processes. For identification, observers completed the task in a manner similar to that of scene categorization and face recognition (Schyns & Gosselin, 2003; Schyns & Oliva, 1999). That is, they relied increments

and decrements in contrast in diagnostic spatial frequency bands to judge the α of an image, which indicates observers may have a an internal representation of α. It is intriguing to find observers approach the identification of noise stimuli in a similar manner to the categorization of meaningful images (e.g., scenes and faces). Future studies should investigate how the diagnostic scale use we have identified for α identification may factor into more complex processes of natural scene perception. That is, the α of an image has been shown to influence lower level perceptual cues like the perceived contrast of an image (Baker & Graf, 2009; Hansen & Hess, 2012; McDonald & Tadmor, 2006), and the peak spatial frequency used by observers to determine perceived contrast (Haun & Peli, 2013). While α, in-of-itself, may be insufficient to contribute to scene identification (Oliva & Torralba, 2001; Torralba & Oliva, 2003) it may serve to regulate the spatial frequency of the diagnostic band used by observers to categorize the scene. The categorization of natural scenes is known to follow a hierarchical structure, whereby coarse scale processing of the scene occurs prior to fine scale processing (Brand & Johnson, 2014; Oliva & Schyns, 1997; Schyns & Oliva, 1994). It is plausible that the α of an image will regulate the peak spatial frequency of the diagnostic band used by observers to categorize the natural image. Thus, α may not be a diagnostic property of a scene, but may aid in the selection of diagnostic information.

Models of α discrimination. Many models of α discrimination have previously been proposed (Brady & Field, 1995; Field & Brady, 1997; Párraga et al., 2005; Tadmor & Tolhurst, 1994; Tajima et al., 2010; Tolhurst & Tadmor, 1997), but given recent evidence from the data presented here, certain modifications to the perception and discrimination of broadband contrast should be brought forth. Specifically, previous models on the discrimination of α, however, relied on the use of diagnostic spatial frequency bands to account for the detectability of a change in α (Tadmor & Tolhurst 1994; Tolhurst & Tadmor 1997). However, the psychophysical data obtained here suggest the discrimination of α to be a passive process, un-tuned to the particular value of the reference α. The psychophysical mechanism defined here compares the luminance contrast across low and high spatial frequencies to detect a change in α, but does not adjust the particular spatial frequency bands used in accordance with α. Thus, a new model, which can accurately define the detectability of a change in α without adaptable or diagnostic spatial frequency bands, should be developed. There have been modern attempts to define human sensitivity to broadband contrast that may aid in developing such a model (Baker & Graf, 2009;

Elliott et al., 2011; Haun & Peli, 2013). These models have aimed to define human sensitivity to broadband contrast by including two important components to the model. The first was to define a spatial frequency dependent pattern of contrast sensitivity for spatial frequency channels, similar to the Contrast Sensitivity Function of human observers, and the second, a weighted contrast gain control mechanism that adjusts the responses of channels differently according to the preferred spatial frequency. Indeed, given spatial frequency channels a response magnitude that mirrors human sensitivity to contrast across scale alone can predict, relatively well, the peak in the detectability of a change in α for reference α values of 1.0 (Baker & Graf, 2009). Suppressive interactions between channels must also be included within novel models of α discrimination, and is most likely low-pass in structure (Elliott et al., 2011; Haun & Peli, 2013). There is evidence that the human visual system is adapted to the distribution of luminance contrast in natural scenes, and may thus adjust neural responses accordingly, in that it will suppress low spatial frequency channel activity more heavily than higher spatial frequency channels (Clifford et al., 2007; Elliott et al., 2011; Webster et al., 2002). Indeed, models that have included a weighted contrast gain control mechanism tend to better predict human observer performance than models that have a flat, or white, contrast gain control mechanism (Hansen et a., 2015; Haun & Peli, 2013). Such a mechanism would effectively lower the dominant responses to lower spatial frequency channels and potentially allow the early visual system to use both low and high spatial frequency channel outputs (now weighted equally) to detect a change in the α of an image. That said, the exact structure of contrast gain control, and any other non-linear interactions, under broadband stimulation remain to be properly defined, and a model of 1/*f* noise discrimination may aid this process.

Concluding Remarks

We have shown that the discrimination of α is dependent on the representation of spatial frequency content within image. Additionally, observers rely predominantly on low spatial frequency luminance contrast changes to detect and discriminate a change in α. We have also shown that this process is not subject to the value of the reference α, which suggests that observers complete the discrimination task in a stimulus unspecific manner. This is not to say that human observers have no representation of α. Indeed, most observers likely do have some form of internal representation of the distribution of luminance contrast across spatial frequency in natural scenes. Perhaps of most importance, given the task dependence of the contribution of

spatial frequency channels to the identification and discrimination of α, are questions surrounding the relevance of discrimination paradigms in the study of human sensitivity to natural scene statistics. Specifically, given that observers undergo α discrimination in a manner that disregards the exact α of the image, this leads to question how the value of α in a natural scene may affect visual processing. Specifically, while the study of human sensitivity to α may be beneficial to develop a better understanding of the function of spatial frequency channels in broadband environments, it remains a poor model of natural scenes and natural scene processing. The amplitude spectrum of natural images is but one aspect of the Fourier representation of natural scenes, and the proper study of naturalistic vision should, additionally, include the structural components of an image (i.e., their phase spectra). Both the amplitude and phase component of natural images carry distinct information but these components are also known to interact in vision and should not be studied in isolation (Tadmor & Tolhurst, 1993). Thus, while we find that the discriminability of α may be a passive process, it may influence the perception of structure, or textural cues in natural scenes, in a way that can only be identified when both the amplitude and phase components of natural images are presented to observers simultaneously. The study of human sensitivity to broadband contrast, in particular when said contrast is distributed in a way similar to that of natural scenes has been crucial in determining how the early visual system functions under naturalistic stimulation. It now follows that more complex representations of natural scenes, which account for the interactive properties of luminance contrast and structure in natural scenes should be studied to generate a more cohesive understanding of natural scene perception.

REFERENCES

Abbonizio, G., Langley, K., & Clifford, C. W. G. (2002). Contrast adaptation may enhance contrast discrimination. *Spatial Vision*, *16*(1), 45–58. http://doi.org/10.1163/15685680260433904

Accornero, N., Li Voti, P., La Riccia, M., & Gregori, B. (2007). Visual evoked potentials modulation during direct current cortical polarization. *Experimental Brain Research*, *178*(2), 261–6. http://doi.org/10.1007/s00221-006-0733-y

Adini, Y., Sagi, D., & Tsodyks, M. (2002). Context-enabled learning in the human visual system. *Nature*, *415*(February), 790–793. http://doi.org/10.1038/415790a

Adini, Y., Wilkonsky, A., Haspel, R., Tsodyks, M., & Sagi, D. (2004). Perceptual learning in contrast discrimination: the effect of contrast uncertainty. *Journal of Vision*, *4*(12), 993–1005. http://doi.org/10.1167/4.12.2

Ahumada, Jr., A. J. (1971). Stimulus Features in Signal Detection. *The Journal of the Acoustical Society of America*, *49*(6B), 1751–1756. http://doi.org/10.1121/1.1912577

Ahumada, Jr., A. J. (1975). Time and frequency analyses of auditory signal detection. *The Journal of the Acoustical Society of America*, *57*(2), 385–390. http://doi.org/10.1121/1.380453

Ahumada, Jr., A. J., & Ahumada, A. J. (2002). Classification image weights and internal noise level estimation. *Journal of Vision*, *2*(1), 121–131. http://doi.org/10.1167/2.1.8

Akasaki, T., Sato, H., Yoshimura, Y., Ozeki, H., & Shimegi, S. (2002). Suppressive effects of receptive field surround on neuronal activity in the cat primary visual cortex. *Neuroscience Research*, *43*(3), 207–220. http://doi.org/10.1016/S0168-0102(02)00038-X

Antal, A., Ambrus, G. G., & Chaieb, L. (2014). Toward unraveling reading-related modulations of tDCS-induced neuroplasticity in the human visual cortex. *Frontiers in Psychology*, *5*(June), 1–4. http://doi.org/10.3389/fpsyg.2014.00642

Antal, A., Kincses, T. Z., Nitsche, M. A., Bartfai, O., & Paulus, W. (2004). Excitability Changes Induced in the Human Primary Visual Cortex by Transcranial Direct Current Stimulation: Direct Electrophysiological Evidence. *Investigative Ophthalmology & Visual Science*, *45*(2), 702–707. http://doi.org/10.1167/iovs.03-0688

Antal, A., Kincses, T. Z., Nitsche, M. A., & Paulus, W. (2003a). Manipulation of phosphene thresholds by transcranial direct current stimulation in man. *Neuropsychologia*, *150*(3),

1802–1807. http://doi.org/10.1007/s00221-003-1459-8

Antal, A., Kincses, T. Z., Nitsche, M. A., & Paulus, W. (2003b). Modulation of moving phosphene thresholds by transcranial direct current stimulation of V1 in human. *Neuropsychologia*, *41*(13), 1802–1807. http://doi.org/10.1016/S0028-3932(03)00181-7

Antal, A., Kovács, G., Chaieb, L., Cziraki, C., Paulus, W., & Greenlee, M. W. (2012). Cathodal stimulation of human MT+ leads to elevated fMRI signal: A tDCS-fMRI study. *Restorative Neurology and Neuroscience*, *30*(3), 255–263. http://doi.org/10.3233/RNN-2012-110208

Antal, A., Nitsche, M. A., Kruse, W., Kincses, T. Z., Hoffmann, K.-P., & Paulus, W. (2004). Direct current stimulation over V5 enhances visuomotor coordination by improving motion perception in humans. *Journal of Cognitive Neuroscience*, *16*(4), 521–527. http://doi.org/10.1162/089892904323057263

Antal, A., Nitsche, M. A., & Paulus, W. (2001). External modulation of visual perception in humans. *Neuroreport*, *12*(16), 3553–3555. http://doi.org/10.1097/00001756-200111160-00036

Antal, A., Nitsche, M. A., & Paulus, W. (2006a). Transcranial direct current stimulation and the visual cortex. *Brain Research Bulletin*, *68*(6), 459–463. http://doi.org/10.1016/j.brainresbull.2005.10.006

Antal, A., Nitsche, M. A., & Paulus, W. (2006b). Transcranial direct current stimulation and visual perception. *Perception*, *68*(3), 459–463. http://doi.org/10.1016/j.brainresbull.2005.10.006

Antal, A., & Paulus, W. (2008). Transcranial direct current stimulation and visual perception. *Perception*, *37*(3), 367–374. http://doi.org/10.1068/p5872

Appelle, S. (1972). Perception and discrimination as a function of stimulus orientation: the "oblique effect" in man and animals. *Psychological Bulletin*, *78*(4), 266–278. http://doi.org/10.1037/h0033117

Arsenault, E., Yoonessi, A., & Baker, C. J. (2011). Higher order texture statistics impair contrast boundary segmentation. *Journal of Vision*, *11*(10), 1–15. http://doi.org/10.1167/11.10.14

Atick, J. J. (1992). Could information theory provide an ecological theory of sensory processing? *Network: Computation in Neural Systems*, *3*(2), 213–251. http://doi.org/10.1088/0954-898X/3/2/009

Atick, J. J., & Redlich, A. N. (1992). What Does the Retina Know about Natural Scenes? *Neural*

Computation, *4*(2), 196–210. http://doi.org/10.1162/neco.1992.4.2.196

Azzopardi, G., & Petkov, N. (2012). A CORF computational model of a simple cell that relies on LGN input outperforms the Gabor function model. *Biological Cybernetics*, *106*(3), 177–189. http://doi.org/10.1007/s00422-012-0486-6

Baddeley, R., Abbott, L. F., Booth, M. C. A., Sengpiel, F., Freeman, T., Wakeman, E. A., & Rolls, E. T. (1997). Responses of neurons in primary and inferior temporal visual cortices to natural scenes. *Proceedings of the Royal Society B: Biological Sciences*, *264*(1389), 1775–1783. http://doi.org/10.1098/rspb.1997.0246

Baker, D. H. (2013). What is the primary cause of individual differences in contrast sensitivity? *PloS One*, *8*(7), e69536. http://doi.org/10.1371/journal.pone.0069536

Baker, D. H., & Graf, E. W. (2009). Natural images dominate in binocular rivalry. *Proceedings of the National Academy of Sciences*, *106*(13), 5436–5441. http://doi.org/10.1073/pnas.0812860106

Baker, D. H., & Meese, T. S. (2011). Contrast integration over area is extensive : A three-stage model of spatial summation. *Journal of Vision*, *11*(14), 1–16. http://doi.org/10.1167/11.14.14

Baker, D. H., & Vilidaite, G. (2014). Broadband noise masks suppress neural responses to narrowband stimuli. *Frontiers in Psychology*, *5*(JUL), 1–9. http://doi.org/10.3389/fpsyg.2014.00763

Banks, M. S., Geisler, W. S., & Bennett, P. J. (1987). The physical limits of grating visibility. *Vision Research*, *27*(11), 1915–1924. http://doi.org/10.1016/0042-6989(87)90057-5

Barlow, H. B. (1961). Possible principles underlying the transformations of sensory messages. In W. A. Rosenblith (Ed.), *Sensory Communication* (pp. 217–234). Cambridge, MA: MIT Press.

Barlow, H. B. (2001). Redundancy reduction revisited. *Network*, *12*(3), 241–253. http://doi.org/10.1088/0954-898X/12/3/301

Barth, E., Beard, B. L., Ahumada, Jr., A. J., Ahumada, A. J., Barth, E., Beard, B. L., & Ahumada, Jr., A. J. (1999). Nonlinear features in vernier acuity. *Proceedings of SPIE*, *3644*(8), 88–96. http://doi.org/10.1117/12.348485

Beard, B. L., & Ahumada, Jr., A. J. (1998). A technique to extract relevant image features for visual tasks. In B. E. Rogowitz & T. N. Pappas (Eds.), *Human Vision and Electronic*

Imaging III (pp. 79–85). San Jose, CA: SPIE. http://doi.org/10.1117/12.320099

Beck, J., Sutter, A., & Ivry, R. (1987). Spatial frequency channels and perceptual grouping in texture segregation. *Computer Vision, Graphics, and Image Processing*, *37*(2), 299–325. http://doi.org/10.1016/S0734-189X(87)80006-3

Bell, A. J., & Sejnowski, T. J. (1997). The "independent components" of natural scenes are edge filters. *Vision Research*, *37*(23), 3327–3338. http://doi.org/10.1016/S0042-6989(97)00121-1

Benson, P. J. (1994). Morph transformation of the facial image. *Image and Vision Computing*, *12*(10), 691–696. http://doi.org/10.1016/0262-8856(94)90044-2

Bergen, J. R., Wilson, H. R., & Cowan, J. D. (1979). Further evidence for four mechanisms mediating vision at threshold: sensitivities to complex gratings and aperiodic stimuli. *Journal of the Optical Society of America*, *69*(11), 1580–1587. http://doi.org/10.1364/JOSA.69.001580

Bex, P. J., & Makous, W. (2002). Spatial frequency, phase, and the contrast of nautral images. *Journal of the Optical Society America, A*, *19*(6), 1096–1106. http://doi.org/10.1364/JOSAA.19.001096

Bex, P. J., Mareschal, I., & Dakin, S. C. (2007). Contrast gain control in natural scenes. *Journal of Vision*, *7*(11), 1–12. http://doi.org/10.1167/7.11.12

Bex, P. J., Solomon, S. G., & Dakin, S. C. (2009). Contrast sensitivity in natural scenes depends on edge as well as spatial frequency structure. *Journal of Vision*, *9*(10), 1–19. http://doi.org/10.1167/9.10.1

Bieniek, M. M., Pernet, C. R., & Rousselet, G. a. (2012). Early ERPs to faces and objects are driven by phase, not amplitude spectrum information: Evidence from parametric, test-retest , single-subject analyses. *Journal of Vision*, *12*(13), 1–24. http://doi.org/10.1167/12.13.12

Bikson, M., Datta, A., & Elwassif, M. (2009). Establishing safety limits for transcranial direct current stimulation. *Clinical Neurophysiology: Official Journal of the International Federation of Clinical Neurophysiology*, *120*(6), 1033–1034. http://doi.org/10.1016/j.clinph.2009.03.018

Bikson, M., Name, A., & Rahman, A. (2013). Origins of specificity during tDCS: anatomical, activity-selective, and input-bias mechanisms. *Frontiers in Numan Neuroscience*, *7*(October), 688. http://doi.org/10.3389/fnhum.2013.00688

Billock, V. (2000). Neural acclimation to 1/f spatial frequency spectra in natural images

transduced by the human visual system. *Physica D: Nonlinear Phenomena*, *137*(3-4), 379–391. http://doi.org/10.1016/S0167-2789(99)00197-9

Blackwell, H. R. (1952). Studies of Psychophysical Methods for Measuring Visual Thresholds. *Journal of the Optical Society of America*, *42*(9), 606–616. http://doi.org/10.1364/JOSA.42.000606

Blakemore, C., & Campbell, F. W. (1969). On the existence of neurones in the human visual system selectively sensitive to the orientation and size of retinal images. *The Journal of Physiology*, *203*(1), 237–260. http://doi.org/10.1113/jphysiol.1969.sp008862

Blin, O., Mestre, D., Paut, O., Vercher, J. L., & Audebert, C. (1993). GABA-ergic control of visual perception in healthy vonlunteers: Effects of midazolam, a benzodiazepine, on spatio-temporal contrast sensitivity. *British Journal of Clinical Pharmacology*, *36*(2), 117–124. http://doi.org/10.1111/j.1365-2125.1993.tb04206.x

Bonneh, Y., & Sagi, D. (1998). Effects of spatial configuration on contrast detection. *Vision Research*, *38*(22), 3541–3553. http://doi.org/10.1016/S0042-6989(98)00045-5

Boynton, G. M., Demb, J. B., Glover, G. H., & Heeger, D. J. (1999). Neuronal basis of contrast discrimination. *Vision Research*, *39*, 257–269. http://doi.org/10.1016/S0042-6989(98)00113-8

Braddick, O., Campbell, F. W., & Atkinson, J. (1978). Channels in vision: Basic Aspects. In *Perception* (pp. 3–38). Heidelberg: Springer.

Brady, N., & Field, D. J. (1995). What's constant in contrast constancy? The effects of scaling on the perceived contrast of bandpass patterns. *Vision Research*, *35*(6), 739–756. http://doi.org/10.1016/0042-6989(94)00172-I

Brady, N., & Field, D. J. (2000). Local contrast in natural images: Normalization and coding efficiency. *Perception*, *29*(9), 1041–1055. http://doi.org/10.1068/p2996

Brainard, D. H. (1997). The psychophysics toolbox. *Spatial Vision*, *10*(4), 433–436. http://doi.org/10.1163/156856897X00357

Brand, J., & Johnson, A. P. (2014). Attention to local and global levels of hierarchical Navon figures affects rapid scene categorization. *Frontiers in Psychology*, *5*(December), 1–19. http://doi.org/10.3389/fpsyg.2014.01274

Britten, K. H., Shadlen, M. N., Newsome, W. T., & Movshon, J. A. (1992). The analysis of visual motion: A comparison of neuronal and psychophysical performance. *The Journal of*

Neuroscience, *12*(12), 4745–4765.

Burton, G. J., & Moorhead, I. R. (1987). Color and spatial structure in natural scenes. *Applied Optics*, *26*(1), 157–170. http://doi.org/10.1364/AO.26.000157

Campbell, F. W., & Kulikowski, J. J. (1972). The visual evoked potential as a function of contrast of a grating pattern. *The Journal of Physiology*, *222*(2), 345–356. http://doi.org/10.1113/jphysiol.1972.sp009801

Campbell, F. W., Kulikowski, J. J., & Levinson, J. (1966). The effect of orientation on the visual resolution of gratings. *The Journal of Physiology*, *187*(2), 427–436. http://doi.org/10.1113/jphysiol.1966.sp008100

Campbell, F. W., Maffei, L., & Piccolino, M. (1973). The contrast sensitivity of the cat. *The Journal of Physiology*, *229*(3), 719–731. http://doi.org/10.1113/jphysiol.1973.sp010163

Campbell, F. W., & Robson, J. G. (1968). Application of fourier analysis to the visibility of gratings. *The Journal of Physiology*, *197*(3), 551–566. http://doi.org/10.1113/jphysiol.1968.sp008574

Cannon, M. W., & Fullenkamp, S. C. (1988). Perceived contrast and stimulus size: Experiment and simulation. *Vision Research*, *28*(6), 695–709.

Carandini, M., Demb, J. B., Mante, V., Tolhurst, D. J., Dan, Y., Olshausen, B. A., … Rust, N. C. (2005). Do we know what the early visual system does? *The Journal of Neuroscience : The Official Journal of the Society for Neuroscience*, *25*(46), 10577–10597. http://doi.org/10.1523/JNEUROSCI.3726-05.2005

Carandini, M., & Heeger, D. J. (1994). Summation and division by neurons in primate visual cortex. *Science*, *264*(5163), 1333–1336. http://doi.org/10.1126/science.8191289

Carandini, M., Heeger, D. J., & Movshon, J. A. (1997). Linearity and normalization in simple cells of the macaque primary visual cortex. *The Journal of Neuroscience : The Official Journal of the Society for Neuroscience*, *17*(21), 8621–8644.

Cass, J., Alais, D., Spehar, B., & Bex, P. J. (2009). Temporal whitening: Transient noise perceptually equalizes the 1/f temporal amplitude spectrum. *Journal of Vision*, *9*(10), 12.1–19. http://doi.org/10.1167/9.10.12

Cass, J., Stuit, S., Bex, P., & Alais, D. (2009). Orientation bandwidths are invariant across spatiotemporal frequency after isotropic components are removed. *Journal of Vision*, *9*(12), 1–14. http://doi.org/10.1167/9.12.17

Cavanaugh, J. R., Bair, W., & Movshon, J. A. (2002). Nature and Interaction of Signals From the Receptive Field Center and Surround in Macaque V1 Neurons. *Journal of Neurophysiology*, *88*(5), 2530–2546. http://doi.org/10.1152/jn.00692.2001

Caywood, M. S., Willmore, B., & Tolhurst, D. J. (2004). Independent components of color natural scenes resemble V1 neurons in their spatial and color tuning. *Journal of Neurophysiology*, *91*(6), 2859–2873. http://doi.org/10.1152/jn.00775.2003

Chaieb, L., Antal, A., & Paulus, W. (2008). Gender-specific modulation of short-term neuroplasticity in the visual cortex induced by transcranial direct current stimulation. *Visual Neuroscience*, *25*(1), 77–81. http://doi.org/10.1017/S0952523808080097

Chatrian, G. E., Lettich, E., & Nelson, P. L. (1985). Ten Percent Electrode System for Topographic Studies of Spontaneous and Evoked EEG Activities. *American Journal of EEG Technology*, *25*(2), 83–92. http://doi.org/10.1080/00029238.1985.11080163

Chubb, C., Sperling, G., & Solomon, J. A. a. (1989). Texture interactions determine perceived contrast. *Proceedings of the National Academy of Sciences*, *86*(23), 9631–9635. http://doi.org/10.1073/pnas.87.3.1257b

Clifford, C. W. G., Webster, M. a., Stanley, G. B., Stocker, A. a., Kohn, A., Sharpee, T. O., & Schwartz, O. (2007). Visual adaptation: Neural, psychological and computational aspects. *Vision Research*, *47*(25), 3125–3131. http://doi.org/10.1016/j.visres.2007.08.023

Coen-Cagli, R., & Schwartz, O. (2013). The impact on midlevel vision of statistically optimal divisive normalization in V1. *Journal of Vision*, *13*(8), 1–20. http://doi.org/10.1167/13.8.13

Cohen, J. (1988). *Statistical power analysis for the behavioral sciences* (2nd ed.). New Jersey: Lawrence Erlbaum Associates.

Costa, T. L., Gualtieri, M., Barboni, M. T. S., Katayama, R. K., Boggio, P. S., & Ventura, D. F. (2015). Contrasting effects of transcranial direct current stimulation on central and peripheral visual fields. *Experimental Brain Research*, 1391–1397. http://doi.org/10.1007/s00221-015-4213-0

Creutzfeldt, O. D., Fromm, G. H., & Kapp, H. (1962). Influence of transcortical d-c currents on cortical neuronal activity. *Experimental Neurology*, *5*, 436–452. http://doi.org/10.1016/0014-4886(62)90056-0

Cumming, G., & Finch, S. (2001). A primer on the understanding, use, and calculation of confidence intervals that are based on central and noncentral distributions. *Educational and*

Psychological Measurement, *61*(4), 532–574. http://doi.org/10.1177/0013164401614002

Dan, Y., Atick, J. J., & Reid, R. C. (1996). Efficient coding of natural scenes in the lateral geniculate nucleus: experimental test of a computational theory. *The Journal of Neuroscience : The Official Journal of the Society for Neuroscience*, *16*(10), 3351–62.

Datta, A., Bansal, V., Diaz, J., Patel, J., Reato, D., & Bikson, M. (2009). Gyri-precise head model of transcranial direct current stimulation: improved spatial focality using a ring electrode versus conventional rectangular pad. *Brain Stimulation*, *2*(4), 201–7, 207.e1. http://doi.org/10.1016/j.brs.2009.03.005

David, S. V, Vinje, W. E., & Gallant, J. L. (2004). Natural stimulus statistics alter the receptive field structure of v1 neurons. *The Journal of Neuroscience : The Official Journal of the Society for Neuroscience*, *24*(31), 6991–7006. http://doi.org/10.1523/JNEUROSCI.1422-04.2004

De Polavieja, G. G. (2002). Errors Drive the Evolution of Biological Signalling to Costly Codes. *Journal of Theoretical Biology*, *214*(4), 657–664. http://doi.org/10.1006/jtbi.2001.2498

De Valois, R. L., Albrecht, D. G., & Thorell, L. G. (1982). Spatial frequency selectivity of cells in macaque visual cortex. *Vision Research*, *22*(5), 545–559. http://doi.org/10.1016/0042-6989(82)90113-4

De Valois, R. L., Morgan, H., & Snodderly, D. M. (1974). Psychophysical studies of monkey vision - III. Spatial luminance contrast sensitivity tests of macaque and human observers. *VIsion Research*, *14*(1), 75–81. http://doi.org/10.1016/0042-6989(74)90118-7

DeAngelis, G. C., Robson, J. G., Ohzawa, I., & Freeman, R. D. (1992). Organization of suppression in receptive fields of neurons in cat visual cortex. *Journal of Neurophysiology*, *68*(1), 144–163. http://doi.org/1517820

Doi, E., Inui, T., Lee, T.-W., Wachtler, T., & Sejnowski, T. J. (2003). Spatiochromatic receptive field properties derived from information-theoretic analyses of cone mosaic responses to natural scenes. *Neural Computation*, *15*(2), 397–417. http://doi.org/10.1162/089976603762552960

Doi, E., & Lewicki, M. M. S. (2005). Relations between the statistical regularities of natural images and the response properties of the early visual system. *Japanese Cognitive Science Society, SIG P&P*, (1), 1–8.

Dorais, A., & Sagi, D. (1997). Contrast masking effects change with practice. *Vision Research*,

37(13), 1725–1733. http://doi.org/10.1016/S0042-6989(96)00329-X

Duecker, F., & Sack, A. T. (2015). Rethinking the role of sham TMS. *Frontiers in Psychology*, *6*(February), 1–5. http://doi.org/10.3389/fpsyg.2015.00210

Edden, R. A. E., Muthukumaraswamy, S. D., Freeman, T. C. a, & Singh, K. D. (2009). Orientation discrimination performance is predicted by GABA concentration and gamma oscillation frequency in human primary visual cortex. *The Journal of Neuroscience*, *29*(50), 15721–15726. http://doi.org/10.1523/JNEUROSCI.4426-09.2009

Edwards, D., Cortes, M., Datta, A., Minhas, P., Wassermann, E. M., & Bikson, M. (2013). Physiological and modeling evidence for focal transcranial electrical brain stimulation in humans: a basis for high-definition tDCS. *NeuroImage*, *74*, 266–275. http://doi.org/10.1016/j.neuroimage.2013.01.042

Ellemberg, D., Allen, H. a., & Hess, R. F. (2006). Second-order spatial frequency and orientation channels in human vision. *Vision Research*, *46*(17), 2798–2803. http://doi.org/10.1016/j.visres.2006.01.028

Ellemberg, D., Hammarrenger, B., Lepore, F., Roy, M.-S., & Guillemot, J.-P. (2001). Contrast dependency of VEPs as a function of spatial frequency: the parvocellular and magnocellular contributions to human VEPs. *Spatial Vision*, *15*(1), 99–111. http://doi.org/10.1163/15685680152692042

Ellemberg, D., Hansen, B. C., & Johnson, A. (2012). The developing visual system is not optimally sensitive to the spatial statistics of natural images. *Vision Research*, *67*, 1–7. http://doi.org/10.1016/j.visres.2012.06.018

Ellemberg, D., Wilkinson, F., Wilson, H. R., & Arsenault, A. S. (1998). Apparent contrast and spatial frequency of local texture elements. *Journal of the Optical Society of America A*, *15*(7), 1733–1739. http://doi.org/10.1364/JOSAA.15.001733

Elliott, S. L., Georgeson, M. A., & Webster, M. A. (2011). Response normalization and blur adaptation: Data and multi-scale model. *Journal of Vision*, *11*(2), 1–18. http://doi.org/10.1167/11.2.7.

Engel, S. A., Glover, G. H., & Wandell, B. A. (1997). Retinotopic organization in human visual cortex and the spatial precision of functional MRI. *Cerebral Cortex*, *7*(2), 181–192. http://doi.org/10.1093/cercor/7.2.181

Enroth-Cugell, C., & Robson, J. G. (1966). The contrast sensitivity of retinal ganglion cells of

the cat. *The Journal of Physiology*, *187*, 517–552. http://doi.org/10.1113/jphysiol.1966.sp008107

Ferster, D., & Miller, K. D. K. (2000). Neuron mechanisms of orientation selectivity in the visual cortex. *Annual Review of Neuroscience*, *23*, 441–471. http://doi.org/10.1146/annurev.neuro.23.1.441

Field, D. J. (1987). Relations between the statistics of natural images and the response properties of cortical cells. *Journal of the Optical Society of America A*, *4*(12), 2379–2394. http://doi.org/10.1364/JOSAA.4.002379

Field, D. J. (1989). What the statistics of natural images tell us about visual coding, *1*, 269–276. http://doi.org/10.1117/12.952724

Field, D. J. (1994). What Is the Goal of Sensory Coding? *Neural Computation*, *6*(4), 559–601. http://doi.org/10.1162/neco.1994.6.4.559

Field, D. J., & Brady, N. (1997). Visual sensitivity, blur and the sources of variability in the amplitude spectra of natural scenes. *Vision Research*, *37*(23), 3367–3383. http://doi.org/10.1016/S0042-6989(97)00181-8

Fitzpatrick, D. (2000). Seeing beyond the receptive field in primary visual cortex. *Current Opinion in Neurobiology*, *10*(4), 438–443. http://doi.org/10.1016/S0959-4388(00)00113-6

Foley, J. M. (1994). Human luminance pattern-vision mechanisms: masking experiments require a new model. *Journal of the Optical Society of America A*, *11*(6), 1710–1719. http://doi.org/10.1364/JOSAA.11.001710

Foley, J. M., & Legge, G. E. (1981). Contrast detection and near-threshold discrimination in human vision. *Vision Research*, *21*(7), 1041–1053. http://doi.org/10.1016/0042-6989(81)90009-2

Foster, K. H., Gaska, J. P., Nagler, M., & Pollen, D. A. (1985). Spatial and temporal frequency selectivity of neurones in visual cortical areas V1 and V2 of the macaque monkey. *The Journal of Physiology*, *365*(1), 331–363. http://doi.org/10.1113/jphysiol.1985.sp015776

Frazor, R. A., & Geisler, W. S. (2006). Local luminance and contrast in natural images. *Vision Research*, *46*(10), 1585–1598. http://doi.org/10.1016/j.visres.2005.06.038

Gaspar, C. M., & Rousselet, G. a. (2009). How do amplitude spectra influence rapid animal detection? *Vision Research*, *49*(24), 3001–12. http://doi.org/10.1016/j.visres.2009.09.021

Geisler, W. S. (2008). Visual perception and the statistical properties of natural scenes. *Annual*

Review of Psychology, *59*, 167–192. http://doi.org/10.1146/annurev.psych.58.110405.085632

Geisler, W. S., Najemnik, J., & Ing, A. D. (2009). Optimal stimulus encoders for natural tasks. *Journal of Vision*, *9*(13), 1–16. http://doi.org/10.1167/9.13.17

Goddard, E., Clifford, C. W. G., & Solomon, S. G. (2008). Centre-surround effects on perceived orientation in complex images. *Vision Research*, *48*(12), 1374–82. http://doi.org/10.1016/j.visres.2008.02.023

Goffaux, V., Jacques, C., Mouraux, A., Oliva, A., Schyns, P. G. P., Rossion, B., … Rossion, B. (2005). Diagnostic colours contribute to the early stages of scene categorization : Behavioural and neurophysiological evidence. *Visual Cognition*, *12*(6), 878–892. http://doi.org/10.1080/13506280444000562

Goris, R. L. T., Wichmann, F. A., & Henning, G. B. (2009). A neurophysiologically plausible population code model for human contrast discrimination. *Journal of Vision*, *9*(7), 1–22. http://doi.org/10.1167/9.8.1004

Goris, R., Wichmann, F., & Henning, B. (2010). A neurophysiologically plausible population-code model for human contrast discrimination. *Journal of Vision*, *9*(8), 1004–1004. http://doi.org/10.1167/9.8.1004

Gosselin, F., & Schyns, P. G. (2001). Bubbles: A technique to reveal the use of information in recognition tasks. *Vision Research*, *41*(17), 2261–2271. http://doi.org/10.1016/S0042-6989(01)00097-9

Graham, D. J., Chandler, D. M., & Field, D. J. (2006). Can the theory of "whitening" explain the center-surround properties of retinal ganglion cell receptive fields? *Vision Research*, *46*(18), 2901–2913. http://doi.org/10.1016/j.visres.2006.03.008

Graham, D. J., & Field, D. J. (2007). Efficient coding of natural images. *New Encyclopedia of Neuroscience*, 1.

Graham, D. J., Friedenberg, J. D., & Rockmore, D. N. (2009). Efficient visual system processing of spatial and luminance statistics in representational and non-representational art. *Proceedings of SPIE*, *7240*, 72401N–72401N–12. http://doi.org/10.1117/12.817185

Graham, N., & Nachmias, J. (1971). Detection of grating patterns containing two spatial frequencies: A comparison of single-channel and multiple-channels models. *Vision Research*, *11*(3), 251–259. http://doi.org/10.1016/0042-6989(71)90189-1

Graham, N., & Sutter, A. (1998). Spatial summation in simple (fourier) and complex (non-fourier) texture channels. *Vision Research*, *38*(2), 231–257. http://doi.org/10.1016/S0042-6989(97)00154-5

Graham, N. V. (1989). *Visual Pattern Analyzers*. New York, NY: Oxford University Press.

Graham, N. V. (2011). Beyond multiple pattern analyzers modeled as linear filters (as classical V1 simple cells): useful additions of the last 25 years. *Vision Research*, *51*(13), 1397–430. http://doi.org/10.1016/j.visres.2011.02.007

Graham, N. V., Robson, J. G., & Nachmias, J. (1978). Grating summation in fovea and periphery. *Vision Research*, *18*(7), 815–25. http://doi.org/10.1016/0042-6989(78)90122-0

Graham, N. V., & Sutter, A. (2000). Normalization: contrast-gain control in simple (Fourier) and complex (non-Fourier) pathways of pattern vision. *Vision Research*, *40*(20), 2737–61. http://doi.org/10.1016/S0042-6989(00)00123-1

Grill-Spector, K., & Malach, R. (2004). The human visual cortex. *Annual Review of Neuroscience*, *27*, 649–677. http://doi.org/10.1146/annurev.neuro.27.070203.144220

Gurnsey, R., & Fleet, D. J. (2001). Texture space. *Vision Research*, *41*(6), 745–757. http://doi.org/10.1016/S0042-6989(00)00307-2

Guyader, N., Chauvin, A., Peyrin, C., Hérault, J., & Marendaz, C. (2004). Image phase or amplitude? Rapid scene categorization is an amplitude-based process. *Comptes Rendus Biologies*, *327*(4), 313–318. http://doi.org/10.1016/j.crvi.2004.02.006

Hancock, P., Baddeley, R., & Smith, L. (1992). The principal components of natural images. *Network: Computation in Neural Systems*, *3*, 61–70. http://doi.org/10.1088/0954-898X/3/1/008

Hansen, B. C., Ellemberg, D., & Johnson, A. P. (2012). Different spatial frequency bands selectively signal for natural image statistics in the early visual system. *Journal of Neurophysiology*, *108*(8), 2160–2172. http://doi.org/10.1152/jn.00288.2012

Hansen, B. C., & Essock, E. A. (2005). Influence of scale and orientation on the visual perception of natural scenes. *Visual Cognition*, *12*(6), 1199–1234. http://doi.org/10.1080/13506280444000715

Hansen, B. C., Essock, E. A., Zheng, Y., & DeFord, J. K. (2003). Perceptual anisotropies in visual processing and their relation to natural image statistics. *Network: Computation in Neural Systems*, *14*(3), 501–526. http://doi.org/10.1088/0954-898X_14_3_307

Hansen, B. C., Farivar, R., Thompson, B., & Hess, R. F. (2008). A critical band of phase alignment for discrimination but not recognition of human faces. *Vision Research*, *48*(25), 2523–2536. http://doi.org/10.1016/j.visres.2008.08.016

Hansen, B. C., Haun, A. M., & Essock, E. A. (2008). The horizontal effect: A perceptual anisotropy in visual processing of naturalistic broadband stimuli. In *Visual Cortex: New Research* (pp. 1–34).

Hansen, B. C., & Hess, R. F. (2006). Discrimination of amplitude spectrum slope in the fovea and parafovea and the local amplitude distributions of natural scene imagery. *Journal of Vision*, *6*(7), 696–711. http://doi.org/10.1167/6.7.3

Hansen, B. C., & Hess, R. F. (2007). Structural sparseness and spatial phase alignment in natural scenes. *Journal of the Optical Society of America A*, *24*(7), 1873–1885. http://doi.org/10.1364/JOSAA.24.001873

Hansen, B. C., & Hess, R. F. (2012). On the Effectiveness of Noise Masks: Naturalistic vs. Un-naturalistic Image Statistics. *Vision Research*, *60*, 101–113. http://doi.org/10.1016/j.visres.2012.03.017

Hansen, B. C., Jacques, T., Johnson, A. P., & Ellemberg, D. (2011). From spatial frequency contrast to edge preponderance: the differential modulation of early visual evoked potentials by natural scene stimuli. *Visual Neuroscience*, *28*(3), 221–37. http://doi.org/10.1017/S095252381100006X

Hansen, B. C., & Loschky, L. C. (2013). The contribution of amplitude and phase spectra-defined scene statistics to the masking of rapid scene categorization. *Journal of Vision*, *13*(13), 1–21. http://doi.org/10.1167/13.13.21

Hansen, B. C., Richard, B., Andres, K., Johnson, A. P., Thompson, B., & Essock, E. A. (2015). A cortical locus for anisotropic overlay suppression of stimuli presented at fixation. *Visual Neuroscience*, *32*, E023. http://doi.org/10.1017/S0952523815000255

Haun, A. M., & Essock, E. A. (2010). Contrast sensitivity for oriented patterns in 1/f noise: contrast response and the horizontal effect. *Journal of Vision*, *10*, 1–21. http://doi.org/10.1167/10.10.1

Haun, A. M., & Peli, E. (2013). Perceived contrast in complex images. *Journal of Vision*, *13*(3), 1–21. http://doi.org/10.1167/13.13.3

Haynes, J. D., Roth, G., Stadler, M., & Heinze, H. J. (2003). Neuromagnetic correlates of

perceived contrast in primary visual cortex. *Journal of Neurophysiology*, *89*(5), 2655–2666. http://doi.org/10.1152/jn.00820.2002

Heeger, D. J. D. (1992). Normalization of cell responses in cat striate cortex. *Visual Neuroscience*, *9*(02), 181. http://doi.org/10.1017/S0952523800009640

Henning, G. B., Hertz, B. G., & Broadbent, D. E. (1974). Some experiments bearing on the hypothesis that the visual system analyses spatial patterns in independent bands of spatial frequency. *Vision Research*, *15*, 887–897. http://doi.org/10.1016/0042-6989(75)90228-X

Henriksson, L., Nurminen, L., Hyvärinen, A., & Vanni, S. (2008). Spatial frequency tuning in human retinotopic visual areas. *Journal of Vision*, *8*(10), 1–13. http://doi.org/10.1167/8.10.5

Hoekstra, J., van der Goot, D. P. J., van den Brink, G., & Bilsen, F. A. (1974). The influence of the number of cycles upon the visual contrast threshold for sptial sine wave patterns. *Vision Research*, *14*(6), 365–368. http://doi.org/10.1016/0042-6989(74)90234-X

Horton, J. C. (2006). Ocular integration in the human visual cortex. *Canadian Journal of Ophthalmology. Journal Canadien D'ophtalmologie*, *41*(415), 584–593. http://doi.org/10.1016/S0008-4182(06)80027-X

Huang, W., Jiao, L., & Jia, J. (2008). Modeling contextual modulation in the primary visual cortex. *Neural Networks : The Official Journal of the International Neural Network Society*, *21*(8), 1182–1196. http://doi.org/10.1016/j.neunet.2008.06.001

Hutchinson, C. V., & Ledgeway, T. (2010). Spatial summation of first-order and second-order motion in human vision. *Vision Research*, *50*(17), 1766–1774. http://doi.org/10.1016/j.visres.2010.05.032

Hyvärinen, A., Hoyer, P. O., Hurri, J., & Gutmann, M. (2005). Statistical models of images and early vision. In *Proceedings of the Int. Symposium on Adaptive Knowledge Representation and Reasoning (AKRR2005)* (pp. 1–14). Citeseer.

Hyvärinen, A., Hurri, J., & Hoyer, P. O. (2009). *Natural Image Statistics: A Probabilistic Approach to Early Computational Vision.* London: Springer.

Issa, N. P., Trepel, C., & Stryker, M. P. (2000). Spatial frequency maps in cat visual cortex. *The Journal of Neuroscience : The Official Journal of the Society for Neuroscience*, *20*(22), 8504–14.

Jacobson, L., Koslowsky, M., & Lavidor, M. (2012). TDCS polarity effects in motor and cognitive domains: A meta-analytical review. *Experimental Brain Research*, *216*(1), 1–10.

http://doi.org/10.1007/s00221-011-2891-9

Jäkel, F., & Wichmann, F. A. (2006). Spatial four-alternative forced-choice method is the preferred psychophysical method for naïve observers. *Journal of Vision*, *6*(11), 1307–1322. http://doi.org/10.1167/6.11.13

Johnson, A. P., & Baker, C. L. (2004). First- and second-order information in natural images: a filter-based approach to image statistics. *Journal of the Optical Society of America. A, Optics, Image Science, and Vision*, *21*(6), 913–25. http://doi.org/10.1364/JOSAA.21.000913

Johnson, A. P., Kingdom, F. A. A., & Baker, C. L. (2005). Spatiochromatic statistics of natural scenes: first- and second-order information and their correlational structure. *Journal of the Optical Society of America. A, Optics, Image Science, and Vision*, *22*(10), 2050–2059. http://doi.org/10.1364/JOSAA.22.002050

Johnson, A. P., Prins, N., Kingdom, F. A. A., & Baker, C. L. (2007). Ecologically valid combinations of first- and second-order surface markings facilitate texture discrimination. *Vision Research*, *47*(17), 2281–2290. http://doi.org/10.1016/j.visres.2007.05.003

Johnson, A. P., Richard, B., Hansen, B. C., & Ellemberg, D. (2011). The magnitude of center – surround facilitation in the discrimination of amplitude spectrum is dependent on the amplitude of the surround. *Journal of Vision*, *11*((7):14), 1–10. http://doi.org/10.1167/11.7.14

Kaernbach, C. (1991). Simple adaptive testing with the weighted up-down method. *Perception & Psychophysics*, *49*(3), 227–229. http://doi.org/10.3758/BF03214307

Katzner, S., Busse, L., & Carandini, M. (2011). GABAA inhibition controls response gain in visual cortex. *The Journal of Neuroscience : The Official Journal of the Society for Neuroscience*, *31*(16), 5931–5941. http://doi.org/10.1523/JNEUROSCI.5753-10.2011

Kayser, C., Salazar, R. F., & Konig, P. (2003). Responses to natural scenes in cat V1. *Journal of Neurophysiology*, *90*(3), 1910–1920. http://doi.org/10.1152/jn.00195.2003

Kelly, D. H. (1975). Spatial frequency selectivity in the retina. *Vision Research*, *15*(6), 665–672. http://doi.org/10.1016/0042-6989(75)90282-5

Kersten, D. (1987). Statistical efficiency for the detection of visual noise. *Vision Reseach*, *27*(6), 1029–1040. http://doi.org/10.1016/0042-6989(87)90016-2

Kim, T., Allen, E. A., Pasley, B. N., & Freeman, R. D. (2015). Transcranial Magnetic

Stimulation Changes Response Selectivity of Neurons in the Visual Cortex. *Brain Stimulation*, (March), 1–11. http://doi.org/10.1016/j.brs.2015.01.407

Kim, Y. J., Haun, A. M., & Essock, E. A. (2010). The horizontal effect in suppression: Anisotropic overlay and surround suppression at high and low speeds. *Vision Research*, *50*(9), 838–849. http://doi.org/10.1016/j.visres.2010.01.020

Kingdom, F. A. A., & Prins, N. (2010). *Psychophysics: a practical introduction* (1st ed.). London: Elsevier.

Klein, S. A., & Levi, D. M. (2009). Stochastic model for detection of signals in noise. *Journal of the Optical Society America, A*, *26*(11), 110–126. http://doi.org/10.1364/JOSAA.26.00B110

Kleiner, M., Brainard, D. H., Pelli, D. G., Ingling, A., Murray, R., & Broussard, C. (2007). What's new in Psychtoolbox-3? In *Perception* (Vol. 36).

Kline, R. B. (2004). *Beyond Significance Testing: Reforming Data Analysis Methods in Behavioral Research*. Washington, DC: American Psychological Association.

Knill, D. C., Field, D. J., & Kersten, D. (1990). Human discrimination of fractal images. *Journal of the Optical Society of America. A, Optics and Image Science*, *7*(6), 1113–1123. http://doi.org/10.1364/JOSAA.7.001113

Kohn, A. (2007). Visual adaptation: physiology, mechanisms, and functional benefits. *Journal of Neurophysiology*, *97*(5), 3155–3164. http://doi.org/10.1152/jn.00086.2007

Kontsevich, L. L., & Tyler, C. W. (2004). What makes Mona Lisa smile? *Vision Research*, *44*(13), 1493–1498. http://doi.org/10.1016/j.visres.2003.11.027

Kraft, A., Roehmel, J., Olma, M. C., Schmidt, S., Irlbacher, K., & Brandt, S. A. (2010). Transcranial direct current stimulation affects visual perception measured by threshold perimetry. *Experimental Brain Research. Experimentelle Hirnforschung. Expérimentation Cérébrale*, *207*(3-4), 283–290. http://doi.org/10.1007/s00221-010-2453-6

Kretzmer, E. R. (1952). Statistics of Television Signals. *Bell System Technical Journal*, *31*(4), 751–763. http://doi.org/10.1002/j.1538-7305.1952.tb01404.x

Kuo, H.-I., Bikson, M., Datta, A., Minhas, P., Paulus, W., Kuo, M.-F., & Nitsche, M. A. (2013). Comparing cortical plasticity induced by conventional and high-definition 4 × 1 ring tDCS: a neurophysiological study. *Brain Stimulation*, *6*(4), 644–648. http://doi.org/10.1016/j.brs.2012.09.010

Kwon, M., & Legge, G. E. (2011). Spatial-frequency cutoff requirements for pattern recognition

in central and peripheral vision. *Vision Research*, *51*(18), 1995–2007. http://doi.org/10.1016/j.visres.2011.06.020

Kwon, Y. H., Nelson, S. B., Toth, L. J., & Sur, M. (1992). Effect of stimulus contrast and size on NMDA receptor activity in cat lateral geniculate nucleus. *Journal of Neurophysiology*, *68*(1), 182–196.

Lang, N., Siebner, H. R., Chadaide, Z., Boros, K., Nitsche, M. A., Rothwell, J. C., … Antal, A. (2007). Bidirectional modulation of primary visual cortex excitability: A combined tDCS and rTMS study. *Investigative Ophthalmology and Visual Science*, *48*(12), 5782–5787. http://doi.org/10.1167/iovs.07-0706

Laughlin, S. B. (1987). Form and function in retinal processing. *Trends in Neurosciences*, *10*(11), 478–483. http://doi.org/10.1016/0166-2236(87)90104-4

Lee, A. B., Mumford, D., & Huang, J. (2012). Occlusion Models for Natural Images : A Statistical Study of a Scale-Invariant Dead Leaves Model. *International Journal of Computer Vision*, *41*(1-2), 35–39. http://doi.org/10.1023/A:1011109015675

Legge, G. E. (1978). Space domain properties of a spatial frequency channel in human vision. *Vision Research*, *18*(8), 959–969. http://doi.org/10.1016/0042-6989(78)90024-X

Legge, G. E., & Foley, J. M. (1980). Contrast masking in human vision. *JOSA*, *70*(12), 1458. http://doi.org/10.1364/JOSA.70.001458

Levi, D. M., Klein, S. a., & Chen, I. (2005). What is the signal in noise? *Vision Research*, *45*(14), 1835–1846. http://doi.org/10.1016/j.visres.2005.01.020

Levi, D. M., Klein, S. A., & Chen, I. (2008). What limits performance in the amblyopic visual system: seeing signals in noise with an amblyopic brain. *Journal of Vision*, *8*(4), 1–23. http://doi.org/10.1167/8.4.1

Li, B., Peterson, M. R., & Freeman, R. D. (2003). Oblique effect: a neural basis in the visual cortex. *Journal of Neurophysiology*, *90*(1), 204–217. http://doi.org/10.1152/jn.00954.2002

Li, G., Yang, Y., Liang, Z., Xia, J., Yang, Y., & Zhou, Y. (2008). GABA-mediated inhibition correlates with orientation selectivity in primary visual cortex of cat. *Neuroscience*, *155*(3), 914–922. http://doi.org/10.1016/j.neuroscience.2008.06.032

Li, R., Polat, U., Makous, W., & Bavelier, D. (2009). Enhancing the contrast sensitivity function through video game training. *Nature Neuroscience*, *12*(5), 549–551. http://doi.org/10.1038/nn.2296

Linares, D., Motoyoshi, I., & Nishida, S. (2012). Surround facilitation for rapid motion perception. *Journal of Vision*, *12*(10), 1–10. http://doi.org/10.1167/12.10.3

Lörincz, A., Palotai, Z., & Szirtes, G. (2012). Efficient sparse coding in early sensory processing: lessons from signal recovery. *PLoS Computational Biology*, *8*(3), e1002372. http://doi.org/10.1371/journal.pcbi.1002372

Loschky, L. C., Hansen, B. C., Sethi, A., & Pydimarri, T. N. (2010). The role of higher order image statistics in masking scene gist recognition. *Attention, Perception, & Psychophysics*, *72*(2), 427–444. http://doi.org/10.3758/APP.72.2.427

Maehara, G., & Goryo, K. (2007). Perceptual learning in monocular pattern masking: experiments and explanations by the twin summation gain control model of contrast processing. *Perception & Psychophysics*, *69*(6), 1009–1021. http://doi.org/10.3758/BF03193939

Maffei, L., & Fiorentini, A. (1973). The visual cortex as a spatial frequency analyser. *Vision Research*, *13*(7), 1255–1267. http://doi.org/10.1016/0042-6989(73)90201-0

Maldonado, P. E., & Babul, C. M. (2007). Neuronal activity in the primary visual cortex of the cat freely viewing natural images. *Neuroscience*, *144*(4), 1536–1543. http://doi.org/10.1016/j.neuroscience.2006.11.021

Mareschal, I., Sceniak, M. P., & Shapley, R. M. (2001). Contextual influences on orientation discrimination: Binding local and global cues. *Vision Research*, *41*(15), 1915–1930. http://doi.org/10.1016/S0042-6989(01)00082-7

McDonald, J. S., & Tadmor, Y. (2006). The perceived contrast of texture patches embedded in natural images. *Vision Research*, *46*(19), 3098–3104. http://doi.org/10.1016/j.visres.2006.04.014

Medeiros, L. F., de Souza, I. C. C., Vidor, L. P., de Souza, A., Deitos, A., Volz, M. S., … Torres, I. L. S. (2012). Neurobiological effects of transcranial direct current stimulation: A review. *Frontiers in Psychiatry*, *3*(DEC), 1–11. http://doi.org/10.3389/fpsyt.2012.00110

Meese, T. S. (2004). Area summation and masking. *Journal of Vision*, *4*(10), 930–943. http://doi.org/10.1167/4.10.8

Meese, T. S., & Baker, D. H. (2011). Contrast summation across eyes and space is revealed along the entire dipper function by a " Swiss cheese " stimulus. *Journal of Vision*, *11*(1), 1–23. http://doi.org/10.1167/11.1.23

Meese, T. S., & Baker, D. H. (2013). A common rule for integration and suppression of luminance contrast across eyes, space, time, and pattern. *I-Perception*, *4*(1), 1–16. http://doi.org/10.1068/i0556

Meese, T. S., & Hess, R. F. (2004). Low spatial frequencies are suppressively masked across spatial scale, orientation, field position, and eye of origin. *Journal of Vision*, *4*, 843–859. http://doi.org/10.1167/4.10.2

Meese, T. S., & Holmes, D. J. (2007). Spatial and temporal dependencies of cross-orientation suppression in human vision. *Proceedings. Biological Sciences / The Royal Society*, *274*(1606), 127–136. http://doi.org/10.1098/rspb.2006.3697

Meese, T. S., & Holmes, D. J. (2010). Orientation masking and cross-orientation suppression (XOS): implications for estimates of filter bandwidth. *Journal of Vision*, *10*(12), 1–20. http://doi.org/10.1167/10.12.9

Meese, T. S., & Summers, R. J. (2007). Area summation in human vision at and above detection threshold. *Proceedings. Biological Sciences / The Royal Society*, *274*(1653), 2891–900. http://doi.org/10.1098/rspb.2008.3002

Meese, T. S., Summers, R. J., & Baldwin, a. (2012). Theory and data for area summation of contrast with and without uncertainty : Evidence for a noisy energy model. *Journal of Vision*, *12*(11), 1–28. http://doi.org/10.1167/12.11.9

Meese, T. S., Summers, R. J., Holmes, D. J., & Wallis, S. A. (2007). Contextual modulation involves suppression and facilitation from the center and the surround. *Journal of Vision*, *7*(4), 1–21. http://doi.org/10.1167/7.4.7

Minhas, P., Datta, A., & Bikson, M. (2011). Cutaneous perception during tDCS: Role of electrode shape and sponge salinity. *Clinical Neurophysiology*, *122*(4), 637–638. http://doi.org/10.1016/j.clinph.2010.09.023

Miranda, P. C., Lomarev, M., & Hallett, M. (2006). Modeling the current distribution during transcranial direct current stimulation. *Clinical Neurophysiology*, *117*(7), 1623–1629. http://doi.org/10.1016/j.clinph.2006.04.009

Miranda, P. C., Mekonnen, A., Salvador, R., & Ruffini, G. (2013). The electric field in the cortex during transcranial current stimulation. *NeuroImage*, *70*, 48–58. http://doi.org/10.1016/j.neuroimage.2012.12.034

Morgan, M. J., & Watt, R. J. (1997). The combination of filters in early spatial vision: a

retrospective analysis of the MIRAGE model. *Perception*, *26*(9), 1073–1088. http://doi.org/10.1068/p261073

Morrison, D. J., & Schyns, P. G. (2001). Usage of spatial scales for the categorization of faces, objects, and scenes. *Psychonomic Bulletin & Review*, *8*(3), 454–469. http://doi.org/10.3758/BF03196180

Morrone, M. C., Burr, D. C., & Maffei, L. (1982). Functional implications of cross-orientation inhibition of cortical visual cells. I. Neurophysiological evidence. *Proceedings of the Royal Society of London. Series B, Containing Papers of a Biological Character. Royal Society (Great Britain)*, *216*(1204), 335–354. http://doi.org/10.1098/rspb.1982.0078

Movshon, J. a, Thompson, I. D., & Tolhurst, D. J. (1978). Spatial and temporal contrast sensitivity of neurones in areas 17 and 18 of the cat's visual cortex. *The Journal of Physiology*, *283*(1), 101–120. http://doi.org/10.1113/jphysiol.1978.sp012490

Movshon, J. A. J. a, Thompson, I. D., & Tolhurst, D. J. (1978). Spatial summation in the receptive fields of simple cells in the cat's striate cortex. *The Journal of Physiology*, *283*(1), 53–77. http://doi.org/10.1113/jphysiol.1978.sp012488

Murray, R. F., Bennett, P. J., & Sekuler, A. B. (2005). Classification images predict absolute efficiency. *Journal of Vision*, *5*(2), 139–149. http://doi.org/10.1167/5.2.5

Murray, S., & Bex, P. J. (2010). Perceived blur in naturally contoured images depends on phase. *Frontiers in Psychology*, *1*(December), 185. http://doi.org/10.3389/fpsyg.2010.00185

Nestares, O., & Heeger, D. J. (1997). Modeling the Apparent Frequency-specific Suppression in Simple Cell Responses. *Vision Research*, *37*(11), 1535–1543. http://doi.org/10.1016/S0042-6989(96)00268-4

Nitsche, M. A., Cohen, L. G., Wassermann, E. M., Priori, A., Lang, N., Antal, A., … Pascual-Leone, A. (2008). Transcranial direct current stimulation: State of the art 2008. *Brain Stimulation*, *1*(3), 206–223. http://doi.org/10.1016/j.brs.2008.06.004

Nitsche, M. A., Doemkes, S., Karaköse, T., Antal, A., Liebetanz, D., Lang, N., … Paulus, W. (2007). Shaping the effects of transcranial direct current stimulation of the human motor cortex. *Journal of Neurophysiology*, *97*(January 2007), 3109–3117. http://doi.org/10.1152/jn.01312.2006

Nitsche, M. A., Fricke, K., Henschke, U., Schlitterlau, A., Liebetanz, D., Lang, N., … Paulus, W. (2003). Pharmacological modulation of cortical excitability shifts induced by transcranial

direct current stimulation in humans. *The Journal of Physiology*, *553*(Pt 1), 293–301. http://doi.org/10.1113/jphysiol.2003.049916

Nitsche, M. A., Liebetanz, D., Lang, N., Antal, A., Tergau, F., Paulus, W., & Priori, A. (2003). Safety criteria for transcranial direct current stimulation (tDCS) in humans [1] (multiple letters). *Clinical Neurophysiology*, *114*(11), 2220–2222. http://doi.org/10.1016/S1388-2457(03)00235-9

Nitsche, M. A., Nitsche, M. S., Klein, C. C., Tergau, F., Rothwell, J. C., & Paulus, W. (2003). Level of action of cathodal DC polarisation induced inhibition of the human motor cortex. *Clinical Neurophysiology : Official Journal of the International Federation of Clinical Neurophysiology*, *114*(4), 600–604. http://doi.org/10.1016/S1388-2457(02)00412-1

Nitsche, M. A., & Paulus, W. (2000). Excitability changes induced in the human motor cortex by weak transcranial direct current stimulation. *The Journal of Physiology*, *527*(3), 633–639. http://doi.org/10.1111/j.1469-7793.2000.t01-1-00633.x

Oliva, A., & Schyns, P. G. (1997). Coarse blobs or fine edges? Evidence that information diagnosticity changes the perception of complex visual stimuli. *Cognitive Psychology*, *107*(1), 72–107. http://doi.org/10.1006/cogp.1997.0667

Oliva, A., & Schyns, P. G. (2000). Diagnostic colors mediate scene recognition. *Cognitive Psychology*, *41*(2), 176–210. http://doi.org/10.1006/cogp.1999.0728

Oliva, A., & Torralba, A. (2001). Modelling the shape of the scene: A holistic representation of the spatial envelope. *International Journal of Computer Vision*, *42*(3), 145–175. http://doi.org/10.1023/A:1011139631724

Olma, M. C., Kraft, A., Roehmel, J., Irlbacher, K., & Brandt, S. A. (2011). Excitability changes in the visual cortex quantified with signal detection analysis. *Restorative Neurology and Neuroscience*, *29*, 453–461. http://doi.org/10.3233/RNN-2011-0607

Olman, C. A., Ugurbil, K., Schrater, P., & Kersten, D. (2004). BOLD fMRI and psychophysical measurements of contrast response to broadband images. *Vision Research*, *44*(7), 669–683. http://doi.org/10.1016/j.visres.2003.10.022

Olshausen, B. A., & Field, D. J. (1996). Emergence of simple-cell receptive field properties by learning a sparse code for natural images. *Nature*, *381*(6583), 607–609. http://doi.org/10.1038/381607a0

Olshausen, B. A., & Field, D. J. (1997). Sparse coding with an overcomplete basis set: A strategy

employed by V1? *Vision Research*, *37*(23), 3311–3325. http://doi.org/10.1016/S0042-6989(97)00169-7

Olshausen, B. a., & Field, D. J. (2000). Vision and the coding of natural images. *American Scientist*, *88*(3), 238–245. http://doi.org/10.1511/2000.3.238

Olshausen, B. A., & Field, D. J. (2005). How close are we to understanding V1? *Neural Computation*, *17*(8), 1665–1699. http://doi.org/10.1162/0899766054026639

Olshausen, B. A., & Lewicki, M. (2013). What Natural Scene Statistics Can Tell Us about Cortical Representation. In L. M. Chalupa & J. S. Werner (Eds.), *The New Visual Neurosciences* (pp. 1247–1262). Boston: The MIT Press.

Olshausen, B., & Field, D. J. (1996). Natural image statistics and efficient coding. *Network: Computation in Neural Systems*, *7*(2), 333–339. http://doi.org/10.1088/0954-898X/7/2/014

Olzak, L. A., & Thomas, J. P. (1999). Neural recoding in human pattern vision: Model and mechanisms. *Vision Research*, *39*(June 1996), 231–256. http://doi.org/10.1016/S0042-6989(98)00122-9

Osaki, H., Naito, T., Sadakane, O., Okamoto, M., & Sato, H. (2011). Surround suppression by high spatial frequency stimuli in the cat primary visual cortex. *The European Journal of Neuroscience*, *33*(5), 923–932. http://doi.org/10.1111/j.1460-9568.2010.07572.x

Párraga, C. A., Troscianko, T., Tolhurst, D. J. (2005). The effects of amplitude-spectrum statistics on foveal and peripheral discrimination of changes in natural images, and a multi-resolution model. *Vision Research*, *45*(25-26), 3145–68. http://doi.org/10.1016/j.visres.2005.08.006

Párraga, C. A., & Tolhurst, D. J. (2000). The effect of contrast randomisation on the discrimination of changes in the slopes of the amplitude spectra of natural scenes. *Perception*, *29*(9), 1101–1116. http://doi.org/10.1068/p2904

Párraga, C. A., Troscianko, T., & Tolhurst, D. J. (2000). The human visual system is optimised for processing the spatial information in natural visual images. *Current Biology*, *10*(c), 35–38. http://doi.org/10.1016/S0960-9822(99)00262-6

Paulus, W. (2011). Transcranial electrical stimulation (tES – tDCS; tRNS, tACS) methods. *Neuropsychological Rehabilitation*, *21*(5), 602–617. http://doi.org/10.1080/09602011.2011.557292

Peli, E. (1990). Contrast in complex images. *Journal of the Optical Society of America. A, Optics*

and Image Science, *7*(10), 2032–2040. http://doi.org/10.1364/JOSAA.7.002032

Peli, E., Arend, L. E., Young, G. M., & Goldstein, R. B. (1993). Contrast sensitivity to patch stimuli: effects of spatial bandwidth and temporal presentation. *Spatial Vision*, *7*(1), 1–14. http://doi.org/10.1163/156856893X00018

Pelli, D. G. (1985). Uncertainty explains many aspects of visual contrast detection and discrimination. *Journal of the Optical Society of America A*, *2*(9), 1508. http://doi.org/10.1364/JOSAA.2.001508

Pelli, D. G. (1997). The VideoToolbox software for visual psychophysics: Transforming numbers into movies. *Spatial Vision*, *10*(4), 437–442. http://doi.org/10.1163/156856897X00366

Pellicciari, M. C. M., Brignani, D., & Miniussi, C. (2013). Excitability modulation of the motor system induced by transcranial direct current stimulation: A multimodal approach. *Neuroimage*, *83*, 569–580. http://doi.org/10.1016/j.neuroimage.2013.06.076

Perna, A., & Morrone, M. C. (2007). The lowest spatial frequency channel determines brightness perception. *Vision Research*, *47*(10), 1282–1291. http://doi.org/10.1016/j.visres.2007.01.011

Peterchev, A. V., Wagner, T. A., Miranda, P. C., Nitsche, M. A., Paulus, W., Lisanby, S. H., … Bikson, M. (2012). Fundamentals of transcranial electric and magnetic stimulation dose: definition, selection, and reporting practices. *Brain Stimulation*, *5*(4), 435–453. http://doi.org/10.1016/j.brs.2011.10.001

Peters, M. A. K., Thompson, B., Merabet, L. B., Wu, A. D., & Shams, L. (2013). Anodal tDCS to V1 blocks visual perceptual learning consolidation. *Neuropsychologia*, *51*(7), 1234–1239. http://doi.org/10.1016/j.neuropsychologia.2013.03.013

Petrov, Y., Carandini, M., & McKee, S. (2005). Two distinct mechanisms of suppression in human vision. *The Journal of Neuroscience : The Official Journal of the Society for Neuroscience*, *25*(38), 8704–8707. http://doi.org/10.1523/JNEUROSCI.2871-05.2005

Petrov, Y., & Mckee, S. P. (2006). The effect of spatial configuration on surround suppression of contrast sensitivity. *Journal of Vision*, *6*, 224–238. http://doi.org/10.1167/6.3.4

Petrov, Y., Popple, A. V, & McKee, S. P. (2007). Crowding and surround suppression: not to be confused. *Journal of Vision*, *7*(2), 1–9. http://doi.org/10.1167/7.2.12

Phillips, G. C., & Wilson, H. R. (1984). Orientation bandwidths of spatial mechanisms measured

by masking. *Journal of the Optical Society of America. A, Optics and Image Science*, *1*(2), 226–232. http://doi.org/10.1364/JOSAA.1.000226

Pirulli, C., Fertonani, A., & Miniussi, C. (2014). Is neural hyperpolarization by cathodal stimulation always detrimental at the behavioral level? *Frontiers in Behavioral Neuroscience*, *8*(June), 226. http://doi.org/10.3389/fnbeh.2014.00226

Polat, U., & Sagi, D. (1993). Lateral interactions between spatial channels: suppression and facilitation revealed by lateral masking experiments. *Vision Research*, *33*(7), 993–999. http://doi.org/10.1016/0042-6989(93)90081-7

Polat, U., & Sagi, D. (1994). The architecture of perceptual spatial interactions. *Vision Research*, *34*(1), 73–78. http://doi.org/10.1016/0042-6989(94)90258-5

Poreisz, C., Boros, K., Antal, A., & Paulus, W. (2007). Safety aspects of transcranial direct current stimulation concerning healthy subjects and patients. *Brain Research Bulletin*, *72*(4-6), 208–214. http://doi.org/10.1016/j.brainresbull.2007.01.004

Prenger, R., Wu, M. C.-K., David, S. V, & Gallant, J. L. (2004). Nonlinear V1 responses to natural scenes revealed by neural network analysis. *Neural Networks : The Official Journal of the International Neural Network Society*, *17*(5-6), 663–679. http://doi.org/10.1016/j.neunet.2004.03.008

Prins, N., & Kingdom, F. A. A. (2009). Palamedes: Matlab routines for analyzing psychophysical data. Retrieved from http://www.palamedestoolbox.org/

Radman, T., Ramos, R. L., Brumberg, J. C., & Bikson, M. (2009). Role of cortical cell type and morphology in sub-and suprathreshold uniform electric field stimulation. *Brain Stimulation*, *2*(4), 215–228. http://doi.org/10.1016/j.brs.2009.03.007

Rahman, A., Reato, D., Arlotti, M., Gasca, F., Datta, A., Parra, L. C., & Bikson, M. (2013). Cellular effects of acute direct current stimulation: somatic and synaptic terminal effects. *The Journal of Physiology*, *591*(Pt 10), 2563–2578. http://doi.org/10.1113/jphysiol.2012.247171

Reato, D., Rahman, A., Bikson, M., & Parra, L. C. (2010). Low-intensity electrical stimulation affects network dynamics by modulating population rate and spike timing. *Journal of Neuroscience*, *30*(45), 15067–15079. http://doi.org/10.1523/JNEUROSCI.2059-10.2010

Ress, D., Backus, B. T., & Heeger, D. J. (2000). Activity in primary visual cortex predicts performance in a visual detection task. *Nature Neuroscience*, *3*(9), 940–945.

http://doi.org/10.1038/78856

Richard, B., Hansen, B. C., Ellemberg, D., & Johnson, A. P. (2013). Size dependent increase in sensitivity to the slope of the amplitude spectrum is not solely dependent on the increased low spatial frequency representation of larger stimuli [Abstract]. *Journal of Vision*, *13*, 1238. http://doi.org/10.1167/13.9.1238

Richard, B., Johnson, A. P., Thompson, B., & Hansen, B. C. (2015). The effects of tDCS across the spatial frequencies and orientations that comprise the Contrast Sensitivity Function. *Frontiers in Psychology: Perception Science*, *6*, 1784. http://doi.org/10.3389/fpsyg.2015.01784

Rieger, J. W., Gegenfurtner, K. R., Schalk, F., Koechy, N., Heinze, H., & Grueschow, M. (2013). BOLD responses in human V1 to local structure in natural scenes: Implications for theories of visual coding. *Journal of Vision*, *13*(2), 1–15. http://doi.org/10.1167/13.2.19

Robson, J. G. (1966). Spatial and Temporal Contrast-Sensitivity Functions of the Visual System. *Journal of the Optical Society of America*, *56*(8), 1141. http://doi.org/10.1364/JOSA.56.001141

Robson, J. G. J. G. J., & Graham, N. (1981). Probability summation and regional variation in contrast sensitivity across the visual field. *Vision Research*, *21*(3), 409–418. http://doi.org/10.1016/0042-6989(81)90169-3

Rohaly, A. M., Ahumada Jr., A. J., Watson, A., B. (1997). Object detection in natural backgrounds predicted by discrimination performance and models. *Vision Research*, *37*(23), 3225–3235. http://doi.org/10.1016/S0042-6989(97)00156-9

Rosa, M. G. P., Casagrande, V. A., Preuss, T., & Kaas, J. H. (1997). Visual field representation in striate and prestriate cortices of a prosimian primate (Galago garnetti). *Journal of Neurophysiology*, *77*(6), 3193–3217.

Rosa, M. G. P., Fritsches, K. A., & Elston, G. N. (1997). The second visual area in the marmoset monkey: Visuotopic organisation, magnification factors, architectonical boundaries, and modularity. *The Journal of Comparative Neurology*, *387*(4), 547–567. http://doi.org/10.1002/(SICI)1096-9861(19971103)387:4<547::AID-CNE6>3.0.CO;2-2

Rose, D., & Blakemore, C. (1974). Effects of bicuculline on functions of inhibition in visual cortex. *Nature*, *249*(5455), 375–377. http://doi.org/10.1038/249375a0

Ross, J., & Speed, H. D. (1991). Contrast adaptation and contrast masking in human vision.

Proceedings. Biological Sciences / The Royal Society, *246*(1315), 61–69. http://doi.org/10.1098/rspb.1991.0125

Ruderman, D. L. (1994). The statistics of natural images. *Network Computation in Neural Systems*, *5*(4), 517–548. http://doi.org/10.1088/0954-898X/5/4/006

Ruderman, D. L., Cronin, T. W., & Chiao, C.-C. (1998). Statistics of cone responses to natural images: implications for visual coding. *Journal of the Optical Society of America A*, *15*(8), 2036–2045. http://doi.org/10.1364/JOSAA.15.002036

Ruderman, D. L., & Bialek, W. (1994). Statistics of natural images: Scaling in the woods. *Physical Review Letters*, *73*(6), 814–817. http://doi.org/10.1103/PhysRevLett.73.814

Rushton, W. A. H. (1927). THe effect upon the threshold for nervous excitation of the length of nerve exposed, and the angle between current and nerve. *The Journal of Physiology*, *63*(4), 357–377. http://doi.org/10.1113/jphysiol.1927.sp002409

Sachs, M. B., Nachmias, J., & Robson, J. G. (1971). Spatial-frequency channels in human vision. *Journal of the Optical Society of America*, *61*(9), 1176–1186. http://doi.org/10.1364/JOSA.61.001176

Sadleir, R. J., Vannorsdall, T. D., Schretlen, D. J., & Gordon, B. (2010). Transcranial direct current stimulation (tDCS) in a realistic head model. *NeuroImage*, *51*(4), 1310–1318. http://doi.org/10.1016/j.neuroimage.2010.03.052

Sagi, D., & Hochstein, S. (1985). Lateral inhibition between spatially adjacent spatial-frequency channels? *Perception & Psychophysics*, *37*(4), 315–22. http://doi.org/10.3758/BF03211354

Schofield, A. J., & Georgeson, M. A. (2003). Sensitivity to contrast modulation: the spatial frequency dependence of second-order vision. *Vision Research*, *43*(3), 243–259. http://doi.org/10.1016/S0042-6989(02)00542-4

Schofield, A. J., Rock, P. B., Sun, P., Jiang, X., & Georgeson, M. A. (2010). What is second-order vision for? Discriminating illumination versus material changes. *Journal of Vision*, *10*(9), 1–18. http://doi.org/10.1167/10.9.2

Schwartz, O., & Simoncelli, E. P. (2001). Natural signal statistics and sensory gain control. *Nature Neuroscience*, *4*(8), 819–25. http://doi.org/10.1038/90526

Schyns, P. G., & Gosselin, F. (2003). Diagnostic use of scale information for componential and holistic recognition. *Perception of Faces, Objects, and Scenes: Analytic and Holistic Processes*, (514), 120–148. http://doi.org/10.1093/acprof:oso/9780195313659.003.0006

Schyns, P. G., & Oliva, A. (1994). From blobs to boundary edges: Evidence for time- and spatial-scale-dependent scene recognition. *Psychological Science*, *5*(4), 195–200. http://doi.org/10.1111/j.1467-9280.1994.tb00500.x

Schyns, P. G., & Oliva, A. (1999). Dr. Angry and Mr. Smile: when categorization flexibly modifies the perception of faces in rapid visual presentations. *Cognition*, *69*(3), 243–265. http://doi.org/10.1016/S0010-0277(98)00069-9

Shadlen, M. N., & Newsome, W. T. (1998). The variable discharge of cortical neurons: implications for connectivity, computation, and information coding. *The Journal of Neuroscience*, *18*(10), 3870–3896.

Shipp, S. (2005). The importance of being agranular: a comparative account of visual and motor cortex. *Philosophical Transactions of the Royal Society B: Biological Sciences*, *360*(1456), 797–814. http://doi.org/10.1098/rstb.2005.1630

Shipp, S. (2007). Structure and function of the cerebral cortex. *Current Biology*, *17*(12), 443–449. http://doi.org/10.1016/j.cub.2007.03.044

Simoncelli, E. P. (2003). Vision and the statistics of the visual environment. *Current Opinion in Neurobiology*, *13*(2), 144–149. http://doi.org/10.1016/S0959-4388(03)00047-3

Simoncelli, E. P. (2005). Statistical Modeling of Photographic Images. In A. Bovik (Ed.), *Handbook of Video and Image Processing* (2nd ed.). Academic Press.

Simoncelli, E. P., & Olshausen, B. A. (2001). Natural image statistics and neural representation. *Annual Review of Neuroscience*, *24*(1), 1193–1216. http://doi.org/10.1146/annurev.neuro.24.1.1193

Smith, J. O. I. (2007). *Mathematics of the Discrete Fourier Transform (DFT)*.

Smyth, D., Willmore, B., Baker, G. E., Thompson, I. D., & Tolhurst, D. J. (2003). The receptive-field organization of simple cells in primary visual cortex of ferrets under natural scene stimulation. *The Journal of Neuroscience*, *23*(11), 4746–4759.

Snowden, R. J., & Hammett, S. T. (1998). The effects of surround contrast on contrast thresholds, perceived contrast and contrast discrimination. *Vision Research*, *38*(13), 1935–1945. http://doi.org/10.1016/S0042-6989(97)00379-9

Snyder, A. W., & Srinivasan, M. V. (1979). Human psychophysics: functional interpretation for contrast sensitivity versus spatial frequency curve. *Biological Cybernetics*, *32*(1), 9–17. http://doi.org/10.1007/BF00337446

Sowden, P. T., Rose, D., & Davies, I. R. L. (2002). Perceptual learning of luminance contrast detection: Specific for spatial frequency and retinal location but not orientation. *Vision Research*, *42*, 1249–1258. http://doi.org/10.1016/S0042-6989(02)00019-6

Spiegel, D. P., Byblow, W. D., Hess, R. F., & Thompson, B. (2013). Anodal transcranial direct current stimulation transiently improves contrast sensitivity and normalizes visual cortex activation in individuals with amblyopia. *Neurorehabilitation and Neural Repair*, *27*(8), 760–9. http://doi.org/10.1177/1545968313491006

Spiegel, D. P., Hansen, B. C., Byblow, W. D., & Thompson, B. (2012). Anodal transcranial direct current stimulation reduces psychophysically measured surround suppression in the human visual cortex. *PloS One*, *7*(5), e36220. http://doi.org/10.1371/journal.pone.0036220

Stagg, C. J., Best, J. G., Stephenson, M. C., O'Shea, J., Wylezinska, M., Kincses, Z. T., … Johansen-Berg, H. (2009). Polarity-Sensitive Modulation of Cortical Neurotransmitters by Transcranial Stimulation. *Journal of Neuroscience*, *29*(16), 5202–5206. http://doi.org/10.1523/JNEUROSCI.4432-08.2009

Stagg, C. J., & Nitsche, M. A. (2011). Physiological Basis of Transcranial Direct Current Stimulation. *The Neuroscientist*, *17*(1), 37–53. http://doi.org/10.1177/1073858410386614

Stromeyer, C. F., & Julesz, B. (1972). Spatial-Frequency Masking in Vision: Critical Bands and Spread of Masking. *Journal of the Optical Society of America*, *62*(10), 1221–1232. http://doi.org/10.1364/JOSA.62.001221

Stromeyer, C. F., & Klein, S. A. (1974). Spatial frequency channels in human vision as asymmetric (edge) mechanisms. *Vision Research*, *14*(12), 1409–20. http://doi.org/10.1016/0042-6989(74)90016-9

Stromeyer, C. F., & Klein, S. A. (1975). Evidence against narrow-band spatial frequency channels in human vision: the detectability of frequency modulated gratings. *Vision Research*, *15*(8-9), 899–910. http://doi.org/10.1016/0042-6989(75)90229-1

Sutter, A., Sperling, G., & Chubb, C. (1995). Measuring the spatial frequency selectivity of second-order texture mechanisms. *Vision Research*, *35*(7), 915–924. http://doi.org/10.1016/0042-6989(94)00196-S

Tadmor, Y., & Tolhurst, D. J. (1993). Both the phase and the amplitude spectrum may determine the appearance of natural images. *Vision Research*, *33*(1), 141–145. http://doi.org/10.1016/0042-6989(93)90067-7

Tadmor, Y., & Tolhurst, D. J. (1994). Discrimination of changes in the second-order statistics of natural and synthetic images. *Vision Research*, *34*(4), 541–554. http://doi.org/10.1016/0042-6989(94)90167-8

Tajima, S., Okada, M., & Gribble, P. L. (2010). Discriminating Natural Image Statistics from Neuronal Population Codes. *PLoS ONE*, *5*(3), e9704. http://doi.org/10.1371/journal.pone.0009704

Takeuchi, T., & De Valois, K. K. (2000). Modulation of perceived contrast by a moving surround. *Vision Research*, *40*(20), 2697–2709. http://doi.org/10.1016/S0042-6989(00)00129-2

Taylor, C. P., Bennett, P. J., & Sekuler, A. B. (2009). Spatial frequency summation in visual noise. *Journal of the Optical Society of America A*, *26*(11), B84–B93. http://doi.org/10.1364/JOSAA.26.000B84

Thompson, B., Mansouri, B., Koski, L., & Hess, R. F. (2008). Brain Plasticity in the Adult: Modulation of Function in Amblyopia with rTMS. *Current Biology*, *18*(14), 1067–1071. http://doi.org/10.1016/j.cub.2008.06.052

Thomson, M. G. A., & Foster, D. H. (1997). Role of second- and third-order statistics in the discriminability of natural images. *Journal of the Optical Society of America A*, *14*(9), 2081–2092. http://doi.org/10.1364/JOSAA.14.002081

Tobimatsu, S., Tomoda, H., & Kato, M. (1995). Parvocellular and magnocellular contributions to visual evoked potentials in humans: stimulation with chromatic and achromatic gratings and apparent motion. *Journal of the Neurological Sciences*, *134*(1-2), 73–82. http://doi.org/10.1016/0022-510X(95)00222-X

Tolhurst, D. J., & Barfield, L. P. (1978). Interactions between spatial frequency channels. *Vision Research*, *18*(8), 951–958. http://doi.org/10.1016/0042-6989(78)90023-8

Tolhurst, D. J., & Movshon, J. A. (1975). Spatial and temporal contrast sensitivity of striate cortical neurones. *Nature*, *257*(5528), 674–675. http://doi.org/10.1038/257674a0

Tolhurst, D. J., Smyth, D., & Thompson, I. D. (2009). The Sparseness of Neuronal Responses in Ferret Primary Visual Cortex. *Journal of Neuroscience*, *29*(8), 2355–2370. http://doi.org/10.1523/JNEUROSCI.3869-08.2009

Tolhurst, D. J., & Tadmor, Y. (1997a). Band-limited contrast in natural images explains the detectability of changes in the amplitude spectra. *Vision Research*, *37*(23), 3203–15.

http://doi.org/10.1016/S0042-6989(97)00119-3

Tolhurst, D. J., & Tadmor, Y. (2000). Discrimination of spectrally blended natural images: Optimisation of the human visual system for encoding natural images. *Perception*, *29*(9), 1087–1100. http://doi.org/10.1068/p3015

Tolhurst, D. J., Tadmor, Y., & Chao, T. (1992). Amplitude spectra of natural images. *Ophthalmic and Physiological Optics*, *12*(2), 229–232. http://doi.org/10.1111/j.1475-1313.1992.tb00296.x

Tootell, R. B., Silverman, M. S., & De Valois, R. L. (1981). Spatial frequency columns in primary visual cortex. *Science (New York, N.Y.)*, *214*(4522), 813–815. http://doi.org/10.1126/science.7292014

Tootell, R. B., Silverman, M. S., Hamilton, S. L., Switkes, E., & De Valois, R. L. (1988). Functional anatomy of macaque striate cortex. V. Spatial frequency. *The Journal of Neuroscience*, *8*(5), 1610–1624.

Tootell, R. B., Switkes, E., Silverman, M. S., & Hamilton, S. L. (1988). Functional anatomy of macaque striate cortex. II. Retinotopic organization. *The Journal of Neuroscience : The Official Journal of the Society for Neuroscience*, *8*(5), 1531–1568.

Torralba, A., & Oliva, A. (2003). Statistics of natural image categories. *Network (Bristol, England)*, *14*(3), 391–412. http://doi.org/10.1088/0954-898X/14/3/302

Tyler, C. W. (1997). Colour bit-stealing to enhance the luminance resolution of digital displays on a single pixel basis. *Spatial Vision*, *10*(4), 369–377. http://doi.org/10.1163/156856897X00294

Tyler, C. W., & Chen, C. C. (2000). Signal detection theory in the 2AFC paradigm: attention, channel uncertainty and probability summation. *Vision Research*, *40*(22), 3121–44. http://doi.org/10.1016/S0042-6989(00)00157-7

van der Schaaf, A., & van Hateren, J. H. (1996). Modelling the Power Spectra of Natural Images: Statistics and Information. *Vision Research*, *36*(17), 2759–2770. http://doi.org/10.1016/0042-6989(96)00002-8

van Hateren, J. H., & van der Schaaf, A. (1998). Independent component filters of natural images compared with simple cells in primary visual cortex. *Proceedings. Biological Sciences / The Royal Society*, *265*(1394), 359–66. http://doi.org/10.1098/rspb.1998.0303

Vinje, W. E., & Gallant, J. L. (2000). Sparse Coding and Decorrelation in Primary Visual Cortex

During Natural Vision. *Science*, *287*(5456), 1273–1276. http://doi.org/10.1126/science.287.5456.1273

Wainwright, M. J., & Simoncelli, E. P. (2000). Scale mixtures of Gaussians and the statistics of natural images. In S. A. Solla, T. K. Leen, & K.-R. Muller (Eds.), *Advances in Neural Information Processing Systems* (Vol. 12, pp. 855–861). MIT Press.

Walker, G. A., Ohzawa, I., & Freeman, R. D. (2000). Suppression outside the classical cortical receptive field. *Visual Neuroscience*, *17*(03), 369–379.

Ward, R., & Weiskrantz, L. (1969). Impaired Discrimination Following Polarisation of the Striate Cortex. *Experimental Brain Research*, *356*, 346–356. http://doi.org/10.1007/BF00235243

Waterston, M. L., & Pack, C. C. (2010). Improved discrimination of visual stimuli following repetitive transcranial magnetic stimulation. *PLoS ONE*, *5*(4). http://doi.org/10.1371/journal.pone.0010354

Watson, A. B. (1979). Probability summation over time. *Vision Research*, *19*(5), 515–522. http://doi.org/10.1016/0042-6989(79)90136-6

Watson, A. B. (2000). Visual detection of spatial contrast patterns: evaluation of five simple models. *Optics Express*, *6*(1), 12–33. http://doi.org/10.1364/OE.6.000012

Watson, A. B., & Ahumada, A. J. (2011). Blur clarified : A review and synthesis of blur discrimination. *Journal of Vision*, *11*(15), 1–23. http://doi.org/10.1167/11.5.10.

Watson, A. B., & Solomon, J. A. (1997). Model of visual contrast gain control and pattern masking. *Journal of the Optical Society of America. A, Optics, Image Science, and Vision*, *14*(9), 2379–2391. http://doi.org/10.1364/JOSAA.14.002379

Webster, M. A., Georgeson, M. A., & Webster, S. M. (2002). Neural adjustments to image blur. *Nature Neuroscience*, *5*(9), 839–840. http://doi.org/10.1038/nn906

Webster, M. A., & Miyahara, E. (1997). Contrast adaptation and the spatial structure of natural images. *Journal of the Optical Society of America A*, *14*(9), 2355–2366. http://doi.org/10.1364/JOSAA.14.002355

Wichmann, F. A., Braun, D. I., & Gegenfurtner, K. R. (2006). Phase noise and the classification of natural images. *Vision Research*, *46*(8-9), 1520–1529. http://doi.org/10.1016/j.visres.2005.11.008

Wilson, H. R., & Wilkinson, F. (1997). Evolving concepts of spatial channels in vision: From

independence to nonlinear interactions. *Perception*, *26*(8), 939–960. http://doi.org/10.1068/p260939

Wilson, H. R., & Bergen, J. R. (1979). A four mechanism model for threshold spatial vision. *Vision Research*, *19*(1), 19–32. http://doi.org/10.1016/0042-6989(79)90117-2

Wilson, H. R., & Humanski, R. (1993). Spatial frequency adaptation and contrast gain control. *Vision Research*, *33*(8), 1133–1149. http://doi.org/10.1016/0042-6989(93)90248-U

Wilson, H. R., McFarlane, D. K., & Phillips, G. C. (1983). Spatial frequency tuning of orientation selective units estimated by oblique masking. *Vision Research*, *23*(9), 873–882. http://doi.org/10.1016/0042-6989(83)90055-X

Wilson, H. R., & Regan, D. (1984). Spatial-frequency adaptation and grating discrimination: predictions of a line-element model. *Journal of the Optical Society of America A*, *1*(11), 1091–1096. http://doi.org/10.1364/JOSAA.1.001091

Wörgötter, F., & Koch, C. (1991). A detailed model of the primary visual pathway in the cat: comparison of afferent excitatory and intracortical inhibitory connection schemes for orientation selectivity. *The Journal of Neuroscience*, *11*(7), 1959–1979.

Xing, J., & Heeger, D. J. (2000). Center-surround interactions in foveal and peripheral vision. *Vision Research*, *40*(22), 3065–3072. http://doi.org/10.1016/S0042-6989(00)00152-8

Xing, J., & Heeger, D. J. (2001). Measurement and modeling of center-surround suppression and enhancement. *Vision Research*, *41*(5), 571–583. http://doi.org/10.1016/S0042-6989(00)00270-4

Yang, J., Qi, X., & Makous, W. (1995). Zero frequency masking and a model of contrast sensitivity. *Vision Research*, *35*(14), 1965–1978. http://doi.org/10.1016/0042-6989(94)00285-T

Yang, Z. (2012). Vision as a Fundamentally Statistical Machine. In S. Molotchnikoff & J. Rouat (Eds.), *Visual Cortex - Current Status and Perspectives* (p. 410). InTech. http://doi.org/10.5772/50165

Yu, C., Klein, S. A., & Levi, D. M. (2001). Surround modulation of perceived contrast and the role of brightness induction. *Journal of Vision*, *1*, 18–31. http://doi.org/10.1167/1.1.3

Yu, C., Klein, S. A., & Levi, D. M. (2002). Facilitation of contrast detection by cross-oriented surround stimuli and its psychophysical mechanisms. *Journal of Vision*, *2*(3), 243–255. http://doi.org/10.1167/2.3.4

Yu, H.-H. H., Verma, R., Yang, Y., Tibballs, H. a., Lui, L. L., Reser, D. H., & Rosa, M. G. P. (2010). Spatial and temporal frequency tuning in striate cortex: functional uniformity and specializations related to receptive field eccentricity. *European Journal of Neuroscience*, *31*(6), 1043–1062. http://doi.org/10.1111/j.1460-9568.2010.07118.x

Yu, Y., Romero, R., & Lee, T. S. (2005). Preference of sensory neural coding for 1/f signals. *Physical Review Letters*, *94*(10), 108103. http://doi.org/10.1103/PhysRevLett.94.108103

Zenger-Landolt, B., & Heeger, D. J. (2003). Response suppression in v1 agrees with psychophysics of surround masking. *The Journal of Neuroscience : The Official Journal of the Society for Neuroscience*, *23*(17), 6884–6893. http://doi.org/23/17/6884 [pii]

Zetzsche, C., & Rhrbein, F. (2001). Nonlinear and extra-classical receptive field properties and the statistics of natural scenes. *Network: Computation in Neural Systems*, *12*(3), 331–350. http://doi.org/10.1080/net.12.3.331.350

Supplementary Materials of Chapter 3A

Supplementary Material A

Baseline Sequential Measurement in Time Data

The baseline portion of this study, completed by all observers, measured their contrast sensitivity to each spatial frequency by size stimulus blocks 10 times. The first two repetitions were practice staircases and removed prior to data analysis. Contrast sensitivity values for all observers in this study (both 45° oblique and horizontal orientation groups) for the final 8 staircases completed during baseline are shown in **Figure 3A.A1**. As described in text, we calculated the linear regression line of best fit for all observers across the 8 sequential measurements in time for all stimulus dimensions (solid lines in **Figure 3A.A1**) and found that no slope deviated from 0. Therefore, contrast sensitivity value for all 20 observers remained relatively stable across the final 8 repetitions of baseline measurements.

We opted to combine both the contrast sensitivity measured during baseline and the pre-stimulation contrast sensitivity measures to use as a pre-stimulation baseline in our data analyses reported in text. There is evidence that same-day and different-day baseline measures may alter the relative effects of tDCS (Peters et al., 2013), however, as observers were constrained to perform similarly to their baseline contrast sensitivity measurements prior to undergoing stimulation, we found no differences in our effects when using either different-day baseline measures or same-day baseline measures alone or combined (see **Figure 3A.A2**).

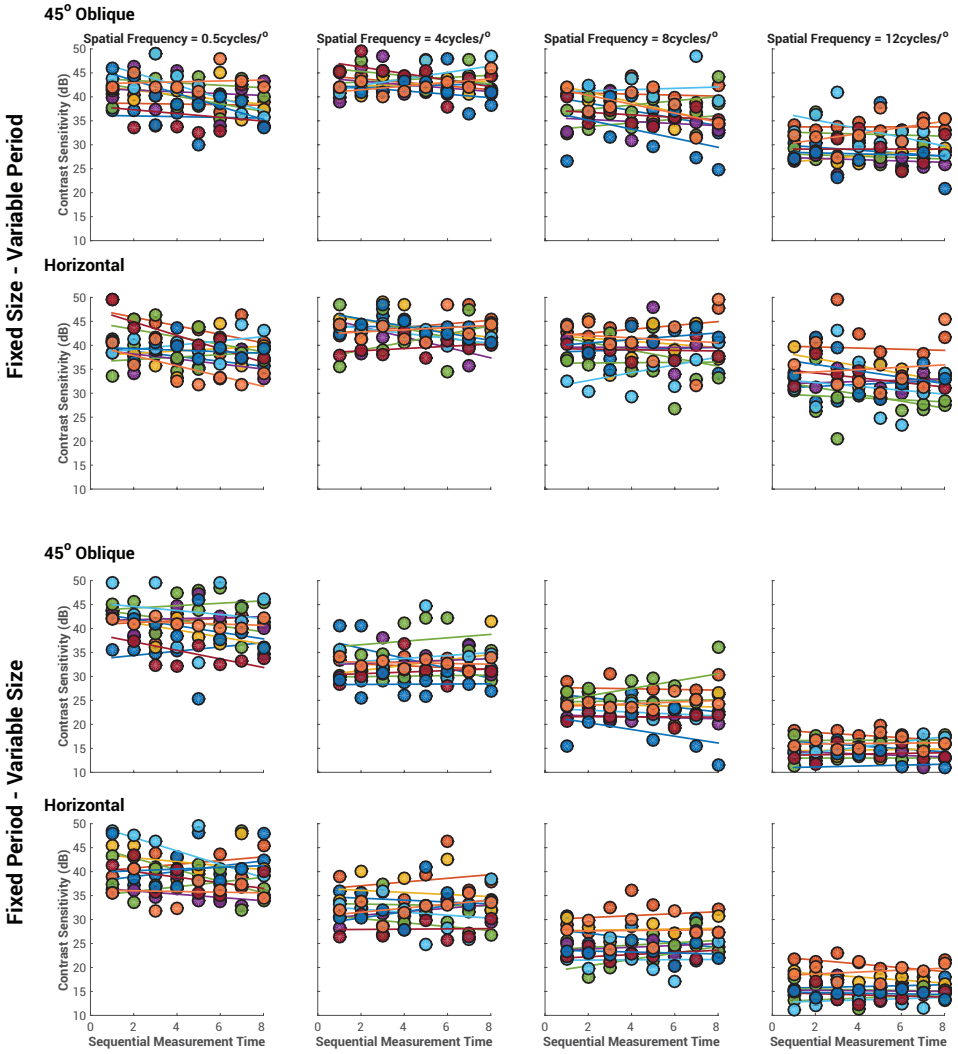

Figure 3A.A1. Observers in the 45° oblique grating group and horizontal grating group showed no statistically significant difference across the sequential measurements in time for all stimulus dimensions used in this study (all *p*s > 0.05). Each color in the figure represents the contrast sensitivity value for an individual observer for the final 8 measurements of contrast sensitivity (in decibels) completed in the baseline portion of the study.

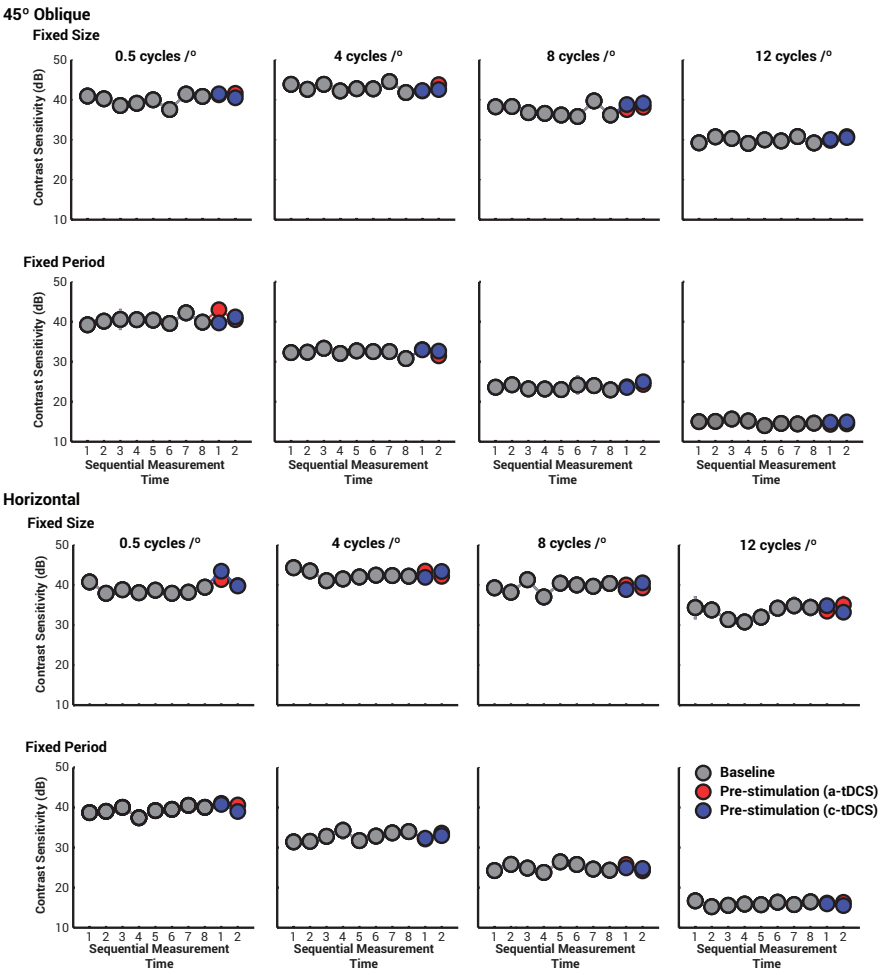

Figure 3A.A2. Average contrast sensitivity values (n = 10 observers per data point) for the last 8 spatial frequency by stimulus size blocks (fixed period and fixed size) of the baseline session, and the pre-stimulation contrast sensitivity values for both for a-tDCS (red) and c-tDCS (blue) sessions. The figure is split by stimulus orientations. Average contrast sensitivity values did not change significantly between baseline measurements sessions or pre-stimulations. Error bars represent 1 standard error of the mean (note that many data points have error bars smaller than the marker).

Supplementary Material B

This appendix offers a brief description of analyses used in this study to estimate the magnitude of both a-tDCS and c-tDCS effects on contrast sensitivity. We begin with a complete table of U1 statistics used to assess overlap between the Colgate University and Concordia Samples, and subsequently offer an overview of building exact [(1-α)*100] confidence intervals around the Hedge's g effect size, and finally define the computation of Left Tail Ratios (LTRs). Further details can be found in Kline (2004) and Cumming and Finch (2001).

Measures of Overlap

Given the large discrepancy in sample size between the Colgate (n = 8) and Concordia (n = 2) samples, we opted to assess overlap between the two prior to averaging their data with a simple measure of overlap, U1, which defines the proportion of scores between two sampling distribution that do not overlap (Cohen, 1988). If the mean contrast between both groups is 0, then U1 is also 0, while it is 1 if both samples do not overlap whatsoever. U1 is calculated by counting the number of scores from one group that lie outside the range of the other group, and divide that number by total sample size (N), reported below in **Table 3A.B1**.

Group-Level Analyses

Traditionally, confidence intervals are constructed in order to estimate the mean of the sampling distribution of the parameter of interest (μ), as the mean of the sampling distribution will be within the confidence interval [(1-α)*100] percent of the time. There are, other approaches to build confidence intervals, which are more intuitive when building a confidence interval around an effect size measure. Instead of defining the confidence intervals as capturing μ [(1-α)*100] percent of the time, the confidence interval is built by defining plausible values of μ. Therefore, the lower limit of the confidence interval is defined as all plausible values of μ having a [(1- α/2)*100]probability below a certain value of x, while the upper limit is defined as all plausible values of μ having a [(α/2)*100] probability below x. In this form, the confidence intervals can be calculated by finding the mean of the distribution for which [(1-α/2)*100] of its proportion lies below our effect size measure to define the lower limit and the mean of a distribution for which [(α/2)*100] of its proportion falls below our effect measure to define the upper limit (see **Figure 3A.B1**).

The sampling distribution of effect sizes (g) is a non-central *t* distribution, a probability density function defined by two parameters, the degrees of freedom (*df*) and a non-centrality

Table 3A.B1. Measures of overlap between the Colgate and Concordia samples (U1) for all stimulus block and time points (Baseline / tDCS) of the study.

	Baseline		tDCS	
	a-tDCS Session	c-tDCS Session	a-tDCS Session	c-tDCS Session
Spatial Frequency		Fixed Stimulus Period		
0.5	0.15	0.15	0.38	0.13
4	0.28	0.20	0.06	0.06
8	0.15	0.16	0.31	0.19
12	0.05	0.05	0.25	0.00
		Fixed Stimulus Size		
0.5	0.05	0.05	0.06	0.19
4	0.16	0.13	0.88	0.19
8	0.11	0.13	0.25	0.00
12	0.03	0.03	0.13	0.13

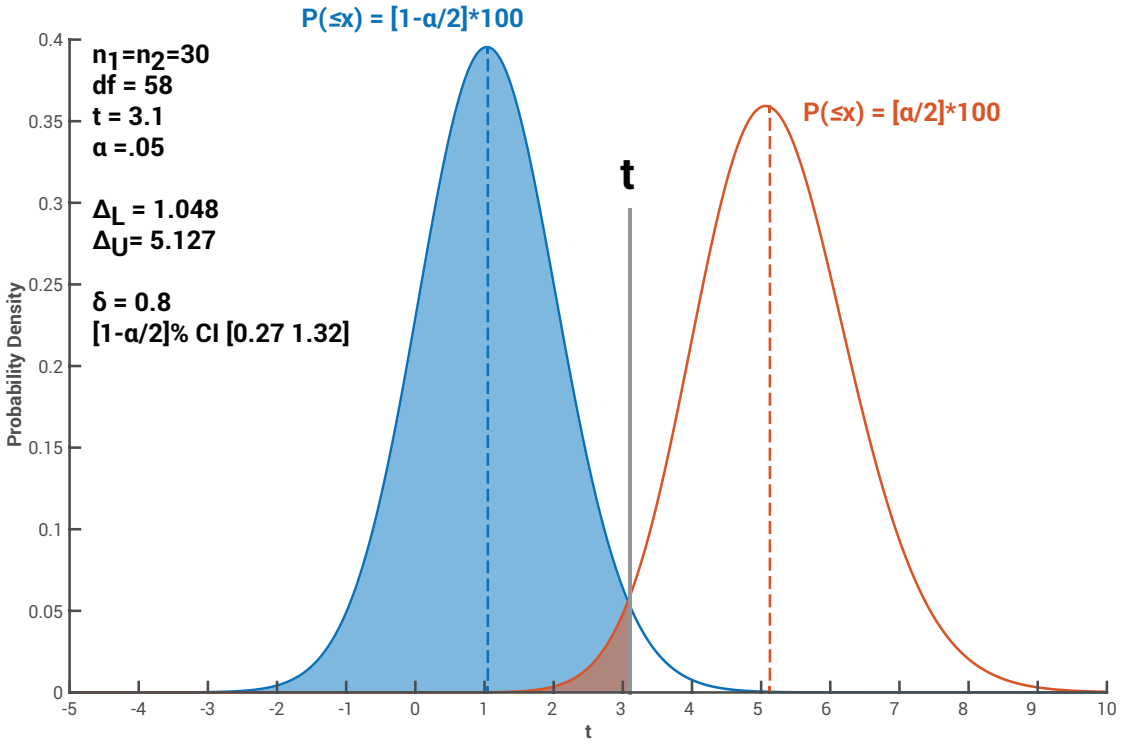

Figure 3A.B1. Finding the two non-central *t* distributions with best fitting non-centrality parameters (Δ_L and Δ_U). The blue *pdf* is the non-central t distribution with the best fitting Δ_L for which a cumulative density of [1-α/2]*100 falls below *t*. The orange distribution is the best fitting Δ_U for which a cumulative density of [α/2]*100 falls below *t*. Values taken from Kline (2004).

parameter (Δ). The non-centrality parameter reflects the degree to which the null hypothesis is false. If Δ = 0, the resulting distribution is a symmetrical central *t* distribution with the same *df*, while it will be positively skewed when Δ > 0 and negatively skewed when Δ < 0. In an independent samples design, the effect size between two sample means is related to the non-centrality parameter as follows:

$$\Delta = \delta\sqrt{\frac{n_1 n_2}{n_1 + n_2}} \qquad \textbf{Equation 3A.B1}$$

When building confidence intervals around an effect size for a dependent samples design, as we have done here, exact confidence intervals can only be defined when the mean difference is standardize by the standard deviation of the difference scores (s_D). Effect sizes standardized by the within-group pooled standard deviation or by the standard deviation of a single group are too complex and do not follow a central or non-central *t* distribution. In a dependent samples design, the effect size is related to the non-centrality parameter as follows:

$$\delta = \Delta\sqrt{\frac{2s_D^2}{n\left(s_1^2 + s_2^2\right)}} \qquad \textbf{Equation 3A.B2}$$

and the variance of the difference scores (s_D^2) is defined as

$$s_D^2 = s_1^2 + s_2^2 - 2\,\mathrm{cov}_{12}$$
$$\mathrm{cov}_{12} = r_{12}s_1 s_2 \qquad \textbf{Equation 3A.B3}$$

where cov_{12} is the covariance of the observed scores across conditions and is the product of the cross condition correlation and the within condition standard deviations.

As both the non-centrality parameter and effect size are linked, we can build confidence intervals around an effect size measure by first building a confidence interval for the non-centrality parameter and then transforming it into the effect size units. For a given *t* statistic ($t = m_1 - m_2 / s_{m_1 - m_2}$), we can search for the non-central *t* distribution with Δ such that [1-α/2]*100 falls below the *t* statistic (the lower limit, Δ_L) and conversely find the non-central *t* distribution with Δ such that [α/2]*100 falls below *t* (the upper limit, Δ_U). **Figure 3A.B1** illustrates this concept for an independent sample design with values taken from Kline (2004). When both the Δ_L and Δ_U have been found, they can easily be converted into effect size values (**equation 3A.B1** and **equation 3A.B2**).

Finding the appropriate non-central *t* distribution can easily be completed in MATLAB, using the *nctcdf* function (requires the statistics toolbox) to calculate the cumulative density of the non-central *t* distribution at a particular t statistic, for given *df* and Δ (see attached MATLAB code). Statistical software, including SAS and STATISTICA also include non-central *t* distribution calculators that allow building exact confidence intervals around an effect size, and the Real Statistics Excel Resource Pack (http://www.real-statistics.com/) also contains a non-central *t* distribution calculator. We strongly encourage the construction of confidence intervals around effect sizes, as the effect, just as any other statistics, will always be subject to estimation error.

Case-Level Analyses

Trans-cranial Direct Current Stimulation in human observers are subject to a variety of factors that include the skull density, and alignment of cortical gyri with the electrodes that will moderate the effects of stimulation and vary significantly between observers (Datta et al., 2009; Miranda et al., 2006; Sadleir et al., 2010). Furthermore, given the magnitude of the non-shunted direct current that enters cortex is several orders of magnitude less than what is required to elicit action potentials (Creutzfeldt, Fromm, & Kapp, 1962; Peterchev et al., 2012; Rahman et al., 2013), we expected contrast sensitivity values obtain during stimulation of have different variance than those obtain prior to stimulation (as some observers may respond more between observers receiving tDCS have predominantly focused on the removal of "non-responders" (observers that shown small or effects in the opposite direction typically reported for a tDCS polarity), we opted to implement case-level analyses, which allowed us to keep all observers that underwent tDCS in our data analysis. Case-level analyses can be particularly beneficial when the variance between two samples (here pre-stimulation and stimulation) is believed to differ significantly, but their central tendency may not. Case-level analyses are therefore ideally suited to quantify the effects of neuro-modulators, including tDCS, as the effects of stimulation are known to be small (Jacobson et al., 2012) at the level of central tendency, but may induce large effects in certain observers more susceptible to neuro-stimulation. There are many forms of case-level analyses (see Kline, 2004), however, given that our data showed large suppressive effects of a-tDCS, we opted to measure the Left-Tail Ratios for all stimulus dimensions presented in the results section. **Table 3A.B2** reports all left-tail ratios for this study.

Table 3A.B2. Left-Tail Ratios for all stimulus blocks

Stimulus Dimensions		Spatial Frequency (cycles/°) 0.5	4	8	12
45° Oblique					
Fixed Period					
	a-tDCS	2.509*	4.344	12.673	124.192
	c-tDCS	6.467	1.023*	1.655	16.4807
Fixed Size					
	a-tDCS	4.595	36.283	34.843	14.253
	c-tDCS	1.037	15.652	1.286*	2.366*
Horizontal					
Fixed Period					
	a-tDCS	1.744*	1.342*	1.226	3.394
	c-tDCS	2.559*	24.803	7.521	1.701
Fixed Size					
	a-tDCS	2.065	109.215	2.606	4.168
	c-tDCS	4.696*	1.051	1.598*	26.565

Note. Values marked with an asterisk (*) are ratios with the proportion of scores from the pre-stimulation distribution as the numerator.

A Left-tail ratio is the relative proportion of scores from two different groups (here contrast sensitivity collected prior to and during tDCS) that fall in the lower extreme (left-tail) of the combined frequency distribution. Tail ratios are always calculated with the largest value as the numerator and are therefore always larger than 1. We computed left-tail ratios based on a cut-off point relative to the mean (M_t) and standard deviation (s_T) of the combined distribution (pre-stimulation and stimulation) for each stimulus dimension presented to observers in this study. The mean and standard deviation of the combined distribution are calculated as follows.

$$M_T = \left[n_1 M_1 + n_2 M_2 \right]$$
$$SS_T = n_1 \left(M_1 - M_T \right)^2 + n_2 \left(M_2 - M_T \right)^2 + df\left(s_1^2 \right) + df\left(s_2^2 \right) \qquad \textbf{Equation 3A.B4}$$
$$s_T = \sqrt{\frac{SS_T}{df}}$$

The cut-point for left tail ratios is defined as one standard deviation below the grand mean. The distance between the cut-off score ($M_T - s_T$) and the mean of each sample is then converted into a z-score and the proportion of scores that fall below this z-score under the normal distribution is calculated. The left-tail ratio is then simply the ratio between both proportions, with the largest proportion always placed as the numerator.

$$z_1 = \frac{\left(M_T - s_T \right) - M_1}{s_1}$$
$$z_2 = \frac{\left(M_T - s_T \right) - M_2}{s_2} \qquad \textbf{Equation 3A.B5}$$
$$LTR = \frac{P(\geq z_1)}{P(\geq z_2)}$$